ISSN 1007-9327 (print)
ISSN 2219-2840 (online)

World Journal of *Gastroenterology*

World J Gastroenterol 2023 April 21; 29(15): 2222-2358

Published by Baishideng Publishing Group Inc

World Journal of Gastroenterology

Contents

Weekly Volume 29 Number 15 April 21, 2023

REVIEW

MINIREVIEWS

ORIGINAL ARTICLE

Basic Study

Case Control Study

Retrospective Study

ABOUT COVER

Editorial Board Member of *World Journal of Gastroenterology*, Hirayuki Enomoto, MD, PhD, Associate Professor, Division of Hepatobiliary and Pancreatic Disease, Department of Internal Medicine, Hyogo Medical University, Nishinomiya 663-8501, Hyogo, Japan. enomoto@hyo-med.ac.jp

AIMS AND SCOPE

The primary aim of *World Journal of Gastroenterology* (*WJG*, *World J Gastroenterol*) is to provide scholars and readers from various fields of gastroenterology and hepatology with a platform to publish high-quality basic and clinical research articles and communicate their research findings online. *WJG* mainly publishes articles reporting research results and findings obtained in the field of gastroenterology and hepatology and covering a wide range of topics including gastroenterology, hepatology, gastrointestinal endoscopy, gastrointestinal surgery, gastrointestinal oncology, and pediatric gastroenterology.

INDEXING/ABSTRACTING

The *WJG* is now abstracted and indexed in Science Citation Index Expanded (SCIE, also known as SciSearch®), Current Contents/Clinical Medicine, Journal Citation Reports, Index Medicus, MEDLINE, PubMed, PubMed Central, Scopus, Reference Citation Analysis, China National Knowledge Infrastructure, China Science and Technology Journal Database, and Superstar Journals Database. The 2022 edition of Journal Citation Reports® cites the 2021 impact factor (IF) for *WJG* as 5.374; IF without journal self cites: 5.187; 5-year IF: 5.715; Journal Citation Indicator: 0.84; Ranking: 31 among 93 journals in gastroenterology and hepatology; and Quartile category: Q2. The *WJG*'s CiteScore for 2021 is 8.1 and Scopus CiteScore rank 2021: Gastroenterology is 18/149.

RESPONSIBLE EDITORS FOR THIS ISSUE

Production Editor: *Yi-Xuan Cai*; **Production Department Director:** *Xiang Li*; **Editorial Office Director:** *Jia-Ru Fan.*

NAME OF JOURNAL
World Journal of Gastroenterology

ISSN
ISSN 1007-9327 (print) ISSN 2219-2840 (online)

LAUNCH DATE
October 1, 1995

FREQUENCY
Weekly

EDITORS-IN-CHIEF
Andrzej S Tarnawski

EDITORIAL BOARD MEMBERS
http://www.wjgnet.com/1007-9327/editorialboard.htm

PUBLICATION DATE
April 21, 2023

INSTRUCTIONS TO AUTHORS
https://www.wjgnet.com/bpg/gerinfo/204

GUIDELINES FOR ETHICS DOCUMENTS
https://www.wjgnet.com/bpg/GerInfo/287

GUIDELINES FOR NON-NATIVE SPEAKERS OF ENGLISH
https://www.wjgnet.com/bpg/gerinfo/240

PUBLICATION ETHICS
https://www.wjgnet.com/bpg/GerInfo/288

PUBLICATION MISCONDUCT
https://www.wjgnet.com/bpg/gerinfo/208

ARTICLE PROCESSING CHARGE
https://www.wjgnet.com/bpg/gerinfo/242

STEPS FOR SUBMITTING MANUSCRIPTS
https://www.wjgnet.com/bpg/GerInfo/239

ONLINE SUBMISSION
https://www.f6publishing.com

World Journal of Gastroenterology

Submit a Manuscript: https://www.f6publishing.com

World J Gastroenterol 2023 April 21; 29(15): 2222-2240

DOI: 10.3748/wjg.v29.i15.2222

ISSN 1007-9327 (print) ISSN 2219-2840 (online)

REVIEW

Intersections between innate immune response and gastric cancer development

Franz Villarroel-Espindola, Troy Ejsmentewicz, Roxana Gonzalez-Stegmaier, Roddy A Jorquera, Esteban Salinas

Specialty type: Biochemistry and molecular biology

Provenance and peer review: Invited article; Externally peer reviewed.

Peer-review model: Single blind

Peer-review report's scientific quality classification
Grade A (Excellent): A
Grade B (Very good): B
Grade C (Good): C, C
Grade D (Fair): 0
Grade E (Poor): 0

P-Reviewer: Jin C, China; Kanaoujiya R, India; Luo W, China; Zhao Q, China

Received: September 20, 2022
Peer-review started: September 20, 2022
First decision: October 20, 2022
Revised: November 7, 2022
Accepted: March 9, 2023
Article in press: March 9, 2023
Published online: April 21, 2023

Franz Villarroel-Espindola, Troy Ejsmentewicz, Roxana Gonzalez-Stegmaier, Roddy A Jorquera, Esteban Salinas, Translational Medicine Unit, Instituto Oncologico Fundacion Arturo Lopez Perez, Santiago 7500000, Metropolitan region, Chile

Corresponding author: Franz Villarroel-Espindola, PhD, Director, Translational Medicine Unit, Instituto Oncologico Fundacion Arturo Lopez Perez, Rancagua 878, Providencia, Santiago 7500000, Metropolitan region, Chile. franz.villarroel@falp.org

Abstract

Worldwide, gastric cancer (GC) is the fifth most commonly diagnosed malignancy. It has a reduced prevalence but has maintained its poor prognosis being the fourth leading cause of deaths related to cancer. The highest mortality rates occur in Asian and Latin American countries, where cases are usually diagnosed at advanced stages. Overall, GC is viewed as the consequence of a multifactorial process, involving the virulence of the *Helicobacter pylori* (*H. pylori*) strains, as well as some environmental factors, dietary habits, and host intrinsic factors. The tumor microenvironment in GC appears to be chronically inflamed which promotes tumor progression and reduces the therapeutic opportunities. It has been suggested that inflammation assessment needs to be measured qualitatively and quantitatively, considering cell-infiltration types, availability of receptors to detect damage and pathogens, and presence or absence of aggressive *H. pylori* strains. Gastrointestinal epithelial cells express several Toll-like receptors and determine the first defensive line against pathogens, and have been also described as mediators of tumorigenesis. However, other molecules, such as cytokines related to inflammation and innate immunity, including immune checkpoint molecules, interferon-gamma pathway and NETosis have been associated with an increased risk of GC. Therefore, this review will explore innate immune activation in the context of premalignant lesions of the gastric epithelium and established gastric tumors.

Key Words: Gastric cancer; Toll-like receptor; *Helicobacter pylori*; Nuclear factor kappa B; Neutrophils

Core Tip: Premalignant cascade of gastric cancer starts with a chronic gastritis, and evolves to atrophic gastritis, intestinal metaplasia, dysplasia and finally the carcinoma. During the process, different immune responses contribute to inflammation of the gastric epithelium. Our work compiles studies related to the innate immune response with a focus on molecular and cellular features such as, Toll-like receptors, neutrophils, cytokines and socioeconomic factors, as crucial players during the precancerous cascade and the cancer onset.

Citation: Villarroel-Espindola F, Ejsmentewicz T, Gonzalez-Stegmaier R, Jorquera RA, Salinas E. Intersections between innate immune response and gastric cancer development. *World J Gastroenterol* 2023; 29(15): 2222-2240
URL: https://www.wjgnet.com/1007-9327/full/v29/i15/2222.htm
DOI: https://dx.doi.org/10.3748/wjg.v29.i15.2222

INTRODUCTION

Globally, gastric cancer (GC) is the fifth most commonly diagnosed malignancy. Although there has been a reduction in its incidence, its poor prognosis makes it the fourth leading cause of cancer related deaths per year[1], and around 86% of all GC cases in 2018 occurred in countries with a high or very high Human Development Index, where 60% of the total cases occurred in Eastern and South-Eastern Asia[2]. GC development is a multistep process initiated by the transition of normal mucosa to non-atrophic gastritis. This superficial gastritis may progress to atrophic gastritis, then intestinal metaplasia and finally to dysplasia and adenocarcinoma[3]. Overall, GC is viewed as the consequence of a multifactorial process involving environmental factors (socioeconomic status, smoking and alcohol consumption), dietary habits (diets rich in salt and poor in antioxidants) and intrinsic factors (ethnicity, genetic background, age and sex)[4,5]. Recently, a meta-analysis and prospective cohort study demonstrated in the Chinese population, that healthy lifestyle factors such as abstention from smoking, non-consumption of alcohol, low consumption of preserved foods, and frequent intake of fresh fruits and vegetables and all of these factors in combination can significantly reduce the relative and absolute risk of incidence of GC. Although, the individual carries a high polygenic risk of GC based on the presence of 112 single-nucleotide polymorphisms[6]. This observation suggests that some intrinsic host factors, like the genetic background, may be secondary to external or environmental aspects during GC onset.

Most of the malignant gastric tumors correspond to the histological type of adenocarcinoma (approximately 90%), with a lower percentage of lymphomas of the mucosa-associated lymphoid tissue, leiomyosarcomas and other rarer tumors[7,8]. The adenocarcinomas have been divided classically into two histological subtypes: Diffuse and intestinal, each of which have differences in their presentations depending on the anatomic subsite, age when diagnosed, sex, race, demographical distribution and socio-economic situation[7-9]. More recent molecular and genomic classifications have defined four major genomic subtypes of GC: The Epstein-Barr virus (EBV) infected tumors; genomically stable tumors; chromosomally unstable tumors; and tumors with microsatellite instability (MSI)[5], all of which offer a poor prognosis and different molecular profiles.

It is very well documented that GC is strongly associated with infectious agents such as the bacterium *Helicobacter pylori* (*H. pylori*) and, recently, the EBV[5]. Approximately 15%–20% of human cancers are provoked by cancer-causing viruses[10]; however, the specific role of EBV in GC development is not clear as of yet. Although the World Health Organization has categorized *H. pylori* as a group 1 carcinogen[11], the role of other bacteria in causing cancer is controversial; studies have shown that some bacteria, such as *Fusobacterium nucleatum*[12], and *Porphyromonas spp.*[13,14] play a role in the development of colon, oral and other digestive cancers. Nevertheless, all those microorganisms can promote a local inflammatory status and a parallel activation of protumoral pathways.

Innate immunity represents the first barrier against pathogens, and epithelial cells of the gastric mucosa are the first line of immunity against, for example, an *H. pylori* infection. In response to an infection, many physiological adaptations are observed, such as an increase in vascular diameter and permeability along with an overexpression of cell-adhesion molecules on endothelial cells which promotes the extravasation of myeloid cells into the inflamed site of infection. The characteristics of an inflamed microenvironment are low levels of glucose and a scarcity of oxygen due to an altered metabolism, increased oxygen consumption by neutrophils, and a reduced oxygen supply due to disrupted perfusion[15]. It is within such a hypoxic microenvironment that immune cells kill and prevent the spread of invading microorganisms. Accumulating evidence suggests that chronic inflammation, either non-infectious such as in autoimmune disorders or, as a result of a pathogen infection, is connected to cancer development. At the same time, the crosstalk between innate and adaptive immunity is critical for the successful eradication of different pathogens and tumor cells.

The aim of this review is to provide an overview of innate immune activation in the context of gastrointestinal malignancies, focusing on the premalignant lesions of the epithelium and the gastric tumor microenvironment. During the transition from atrophic gastritis to the final carcinoma, some microorganisms will play a determinant role promoting the neoplastic transformation or contributing with a particular tumor phenotype. This work compiles studies related to Toll-like receptors (TLRs), neutrophils, cytokines and pathogens, as crucial players during the precancerous cascade and the cancer onset (Figure 1), allowing the correlation of those aspects with clinical and socioeconomic variables.

STARTERS AND MEDIATORS OF THE INNATE IMMUNE RESPONSE IN GASTRIC TISSUE

Gastro-intestinal epithelial cells express several TLRs that can respond to exogenous infectious ligands or pathogen-associated molecular patterns (PAMPs). TLRs are the most important class of pattern recognition receptors (PRRs). These transmembrane proteins present a distinctive Leucine-Rich Repeat extracellular domain that confers specificity to their ligands[16], and a cytoplasmic signaling domain homologous to that of the interleukin 1 receptor (IL-1R), termed the toll/IL-1R homology domain[17]. Up to now, the TLR family consists of ten (TLR1-TLR10) and twelve (TLR1-TLR9 and TLR11-TLR13) members identified in humans and mice respectively[18]. These receptors are expressed in various immune cells, including macrophages, Dendritic cells (DCs), B cells, specific types of T cells, and even in non-immune cells such as fibroblasts and epithelial cells; their activation leads to the induction of inflammatory cytokines, chemokines, antigen-presenting molecules, and costimulatory molecules[15,17,19].

Epithelial cells from the gastric mucosa are considered as the first line of innate immunity against gastrointestinal pathogens, including *H. pylori* infection, and the PRRs have shown a wide range of expression in normal and pathological tissue (Table 1).

Human gastric epithelial cells and tumor cells were found to express both TLR2 and TLR4 and both receptors are described as responsible for the *H. pylori* lipopolysaccharides (LPS) recognition. However, the results are contradictory and have not accurately probed the role of those receptors due both to the diversity of the host's immune system and the pathogenicity of the *H. pylori* strain[20,21]. TLR2 is the most extensively expressed gene among all the TLRs in gastric tumors and high levels of TLR4 are associated with a higher risk of GC[22-24].

On the other hand, TLR3 and TLR4 have been implicated in several disorders related to the gastroesophageal reflux disease spectrum and largely documented, including the expression of both receptors and expression of their downstream products, such as cyclooxygenase-2, IL-8, nuclear factor-κB (NF-κB), and nitric oxide in human tissue samples and *ex vivo* cell cultures from the esophagus, the esophageal-gastric junction and the stomach[25].

TLR5 is expressed within the esophageal epithelium and has been shown to increase in a stepwise manner with progression from normal to dysplastic and eventually neoplastic states[26]. In addition, it is well documented that TLR5 is present in both primary gastric epithelial cells and gastric tumor cell lines[22,24,27]; however, the role of TLR5 during the gastric precancerous cascade is not yet clear.

TLR5 is responsible for flagellin recognition. *H. pylori* flagellin seems to be a less potent stimulator compared with other flagellins[28] but has a significant role in long-term bacterial persistence. The lack of TLR5 activity in response to *H. pylori* flagellin is caused mainly by the amino acid residues variation R89, L93, and E114 described as hotspots for binding TLR5 which, replaced with threonine (R89T), lysine (L93K), and aspartate (E114D) in *H. pylori* flagellin, lead to receptor evasion[29]. TLR5 instead recognizes CagL and CagY, two proteins from the type IV secretion system (T4SS) of *H. pylori*, and both have immunoregulatory properties[30,31]. A high TLR5 expression has been suggested to have a better prognosis amongst young GC patients in an early stage of disease, and this better outcome may be associated with a non-distant metastasis and an intestinal-type cancer[32].

TLR9, the only TLR with both anti- and pro-inflammatory roles, is involved in the recognition of *H. pylori* DNA, and the promotion or suppression role of TLR9 will depend on the gastric environment [22]. TLR9 expression has been shown to be up-regulated in *H. pylori* infected gastric tissue compared with non-infected tissue, and it was not related to the presence of tumor cells, suggesting that increased TLR9 expression was specifically associated with *H. pylori* infection[33]. It is reported that TLR9 interaction with *H. pylori* and *H. pylori* DNA, triggers an IL-8 secretion response mediated by the NF-κB pathway[34].

The role of TLR9 in cancer is not absolutely clear, but patients with stage II of GC and a high TLR9 expression had a better prognosis than cases with lower levels[32].

Other TLRs have been described, TLR1, TLR7, TLR8, and TLR10, but further studies are required in order to understand their role in GC and in *H. pylori* infected individuals, as well as other pathogens[22,23,35]. However, high levels of TLR10 expression have been observed in gastric biopsy samples from subjects with *H. pylori* and, when NCI-N87 gastric cells were co-cultured with the bacteria, both TLR10 and TLR2 mRNA levels were upregulated[35]. Those results suggest that TLR10 is a functional receptor and that TLR2/TLR10 heterodimer functions in *H. pylori* LPS recognition[35].

Table 1 Expression of Toll-like receptors in esophageal and gastric epitheliums

PRR	Organ	Model	Method	Ligand	Observation	Reference
TLR1/2	Esophagus	Esophageal carcinoma and premalignant lesions	IHQ	Triacyl lipopeptide	Receptor upregulation in tumor and dysplasia	[22,171]
TLR2	Stomach; esophagus	Human ADC and premalignant lesions; *H. pylori* infection mice model and*in vitro* culture	IHQ; RT-qPCR	Microbial lipopeptide	Receptor upregulation in tumor cores. Increased tumorigenesis; constitutive expression in TE-1 cell line	[21,22,27,32,172-174]
TLR3	Stomach; esophagus	Human gastric and esophageal carcinoma	IHQ; RT-qPCR	dsRNA	Increased receptor levels correlate with poor prognosis; increased expression on EAC-derived cell lines	[25,174-176]
TLR4	Stomach; esophagus	Human ADC and premalignant lesions; *H. pylori* infection; esophageal carcinoma	IHQ; RT-qPCR	LPS	Upregulation in tumor cores; weak association with clinicopathologic variables; high expression correlates with poor prognosis; upregulation of IL-8 and COX-2 in BE	[21,24,25,27,32,171,173-179,182]
TLR5	Stomach; esophagus	Human ADC and premalignant lesions; *H pylori* infection	IHQ	Flagellin	Highly expressed; upregulation in tumor and older patients; association with necrosis and tumor growth in the stomach; overexpression in dysplastic lesions of BE; no association with EAC prognosis	[26,27,32,177]
TLR6	Esophagus	Esophageal carcinoma and human dysplasia	IHQ; IF	Diacyl lipopeptide	Upregulated in tumor tissue	[22,171]
TLR7	Stomach; esophagus	Human ADC and normal tissue	IHQ; WB; RT-qPCR	ssRNA	Downregulated in gastric tumors; high levels correlate with a better outcome in GC; constitutive expression in TE-1 cell line; association between expression and tumor grade in ESCC	[22,32,173,174,176,180,183]
TLR9	Stomach; esophagus	Human ADC	IHQ; RT-qPCR	ssDNA; dsDNA	Upregulated in early tumors; correlation with better prognosis in GC; association with histopathological grade in ESCC and dysplasia; high expression in EAC correlates with advanced tumor stage and metastasis	[24,25,32-34,173,175,176,181,184]
TLR10	Stomach	Human biopsy	RT-qPCR	ssDNA; dsDNA	Upregulated by *H. pylori*	[35]

ADC: Adenocarcinoma; BE: Barrett's esophagus; EAC: Esophageal adenocarcinoma; ESCC: Esophageal squamous cell carcinoma; GC: Gastric cancer; *H. pylori*: *Helicobacter pylori*; IF: Immunofluorescence; IHQ: Immunohistochemistry; PRR: Pattern recognition receptor; RT-qPCR: Reverse transcription and quantitative PCR; TE-1: Human cell line derived from esophageal cancer; TLR: Toll-like receptors; WB: Western blot.

From a cellular perspective, neutrophils are the most abundant white blood cells in human blood and also considered as part of the first line of defense against infections by pathogens[36]. These cells have the ability to capture and destroy invading microorganisms and participate as mediators of inflammation. Phagocytosis and formation of neutrophil extracellular traps are part of the cellular mechanisms for pathogen elimination, as well as granules releasing[36-38].

Neutrophils extracellular traps (NETs) formation, known as NETosis is a process of releasing extracellular web-like structures, and is described as a coat consisting of decondensed chromatin filaments, histones and antimicrobial proteins[39]. NETosis is a mechanism of innate immunity to contain and prevent microbial spread, and eliminate bacteria[40].

H. pylori can activate different cells of innate immunity, including neutrophils, and these activated cells recognize *H. pylori* infection through different receptors, such as TLR2, TLR4, and TLR9[34,41,42]. TLR5 has not been detected in neutrophils localized in the lamina propria during *H. pylori* gastritis[24]. The activation and recruitment of neutrophils is stimulated by *H. pylori* neutrophil-activating protein, or HP-NAP[37,43]. TLR2 interacts with HP-NAP for the secretion of IL-8[41]. However, the interaction between neutrophils and *H. pylori* appears to be complex and contradictory and shows the development of different mechanisms of immune evasion, including NET degradation, the increase in bacterial resistance mediated by the modification of proteins or surface polysaccharides, or the suppression of NET formation[44].

H. pylori has shown a selective alteration of neutrophils function mediated by the inactivation of NADPH Oxidase and superoxide release[45]. In addition, the bacterium performs lipid A modification mediated by lipid A phosphatases to resist the polymyxin, an antimicrobial peptide[46]. Another study remarked on the presence of an outer membrane-associated nuclease that can degrade extracellular DNA, where the ability to degrade exogenous DNA was originally proposed as a purine source uptake mechanism[47], but it could also have the potential role of degrading NETs[48].

Although NETosis was described as an antimicrobial process, it has been described in other pathologies, including cancer. The first study that provided evidence on NET in cancer was Berger-Achituv *et al*[49] studying the Ewing sarcoma. The authors proposed NET as a pro-tumor effect and the

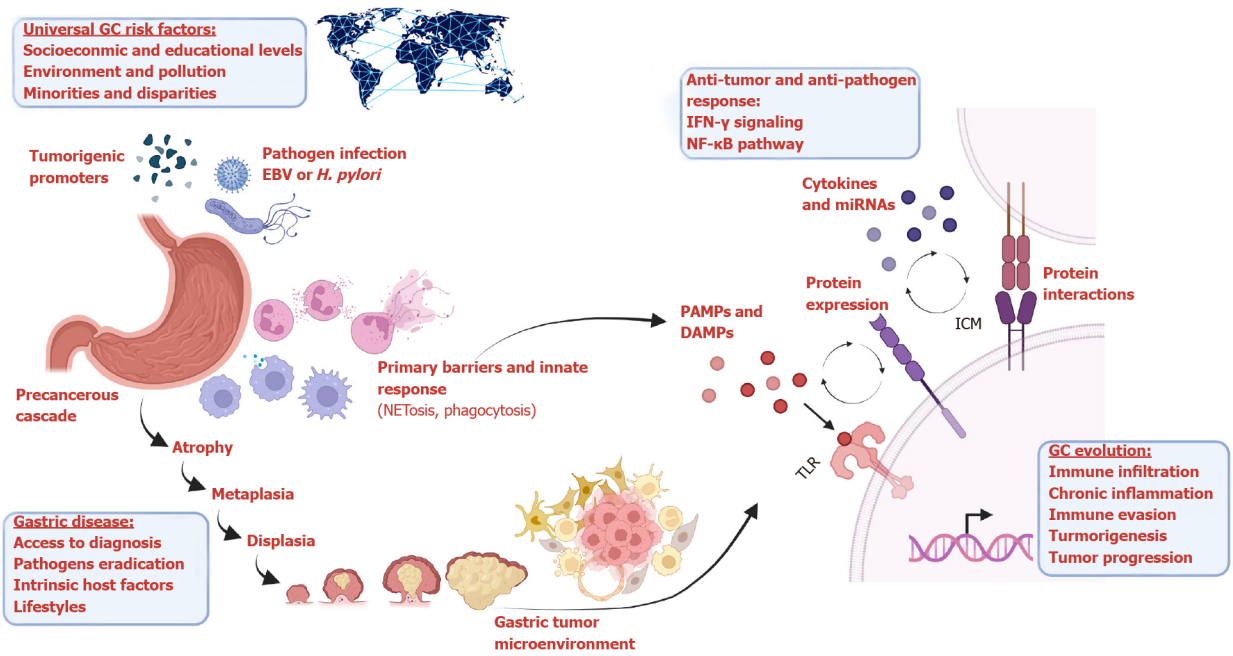

DOI: 10.3748/wjg.v29.i15.2222

Figure 1 Graphical abstract. Intersections between innate immune response and gastric cancer (GC) development is driven by common mediators, such as molecular pathways [nuclear factor-kappa B (NF-κB) and interferon-gamma (IFN-γ)], cellular processes (neutrophil and myeloid cells activation), and activators/inducers [pathogen-associated molecular patterns (PAMPs), damage-associated molecular patterns (DAMPs), tumor-antigens]. However, universal risk factors are identified affecting globally to any human being, which depending on extrinsic and intrinsic host factors might facilitate the progression of the precancerous cascade to GC. This image is created in BioRender.com. EBV: Epstein-Barr virus; *H. pylori*: *Helicobacter pylori*; ICM: Immune checkpoint molecule; TLR: Toll-like receptor.

possibility of using this parameter as a poor prognostic biomarker[49].

Regarding GC, the first study was reported by Yang *et al*[50]. The authors found the correlation of NET formation with TNM status and a significant increase in the formation of fibrin and thrombin, however, the focus was on peripheral circulation. More recently, the formation of NETs within the gastric tumor microenvironment including immunofluorescent staining of Neutrophil Elastase (NE) and citrullinated-histone 3[51,52] showed that NETs are more abundant in the tumor core than in the adjacent non-tumor tissue[51,52], and the plasma from GC patients revealed the capacity of NET formation *in vitro*[52]. NETs measured in peripheral blood have been shown to be significantly correlated with GC and staging, and its levels decrease after surgery[50-52].

A very recent report showed that abdominal infectious complications after gastrectomy would stimulate neutrophils to release NETs both in peripheral blood and the abdominal cavity, facilitating GC metastasis *in vitro* and *in vivo* dependent on transforming growth factor (TGF)-β signaling[53]. The formation of NETs has an important role in the epithelial-mesenchymal transition and gastric tumor progression, because NETosis may induce proliferation, invasion, migration, and a mesenchymal phenotype, in addition to its immune role, which makes it difficult to be therapeutically targeted.

ACCOMPLICE CELLS AND MEDIATORS OF AN ANTI-TUMOR RESPONSE

Additionally, the macrophages have been demonstrated to be important cells for the innate immune system in healthy and tumor tissue. Within the tumor microenvironment (TME), macrophages are known as tumor-associated macrophages (TAMs) and play a key role in the recognition and clearance of foreign and damaged cells, as well as in tumor development and the response to several cancer therapies.

Macrophages can infiltrate solid tumors modulating T cell activity within the TME, and often undergo phenotype polarization in response to stimuli or inhibitory factors, either to pro-inflammatory (M1) or anti-inflammatory (M2) subtypes, which cause immune response or immune escape of the tumors respectively[54-57]. The general consensus is that TAMs are usually pro-tumorigenic. These cells are recruited by tumor-derived chemokines and produce low levels of inflammatory cytokines, promote Th2-T cell response, favor wound healing, and increase angiogenesis and metastases[55,56].

IL-6 and tumor necrosis factor (TNF)-α are both pro-inflammatory cytokines, exerting pro-tumoral functions, including the promotion of angiogenesis and metastasis, and these molecules can be secreted by myeloid cells and leukocytes under different conditions and stimuli[54-56]. In parallel to classic

immunomodulators such as cytokines and chemokines, some microRNAs (miR) have shown a significant impact on macrophages activity[57]. miR-125b, miR-127, miR-155, miR-181 and miR-451 are significantly upregulated in M1 macrophages, whereas miR-125a-5p, miR-146a, miR-145-5p, miR-143-3p are highly expressed in M2 macrophages[58,59].

miR-155 directly targets the expression of the IL-13 receptor α1, thereby inhibiting STAT6 activation and promoting M1 polarization[59]. miR-155 knockdown in myeloid cells induces faster tumor growth, reduction of M1-macrophages and enrichment of pro-tumor cytokines within the TME[60]. In addition, miR-125b overexpression enhanced responsiveness to interferon (IFN)-γ, through the targeting of IRF4 and increased expression of pro-inflammatory cytokines[58,61].

miR-187, miR-146a, let-7e, and miR-92a are considered anti-inflammatory miRs because they downregulate IL-6 and TNF-α in human macrophages by targeting the TLRs signaling[57,62]. The NF-κB-dependent miR-146a expression is induced in monocytes and macrophages upon triggering of TLR4 to act as a modulator of the inflammatory response[61]. miR-155 is key to modulating genes related to M2/pro-Th2 phenotype in macrophages, and includes CCL18, SERPINE, CD23 and DC-SIGN[56]. In addition, other microRNAs will modulate directly or indirectly the NF-κB or TLR activity, such as miR9, miR-21, miR-29b, and those can be expressed and released by both TAMs and solid tumors in exosomes [57,62-65]. Due to the inflammatory microenvironment and oncogenic mutations, a significant number of human cancers have constitutive miRs deregulation affecting NF-κB activity, cytokine production and hallmarks of cancer such as apoptosis, proliferation and tumor survival[57,62,65].

Previous studies demonstrated that Gastric Epithelial Cells (GECs) function as antigen presenting cells by constitutively expressing MHC class II[66]. Interestingly, *H. pylori* infection induces up-regulation of costimulatory molecules (CD86 and CD80) among GECs[66], suggesting its potential to be used as a local bridge between innate and acquired immunity; however, the capacity to play a role secreting cytokines and polarizing macrophages requires further studies.

The inhibition of the polarization of pro-inflammatory macrophages can accelerate the development of precancerous lesions in GC[67]. In addition, when TAMs spread in the peritoneum of GC patients, these cells normally are polarized to an anti-inflammatory subtype (M2), which can promote the growth and progression of GC when the tumor exists[68]. In fact, high densities of TAMs are associated with poor survival in GC patients[68,69].

INTRINSIC AND EXTRINSIC MODULATORS OF INFLAMMATION AND PRECANCEROUS LESIONS

Currently, there is enough evidence based on epidemiological, molecular and pathological studies that persistent infection with *H. pylori* is a risk factor for the development of gastric adenocarcinoma[70-73], estimating an increment in the relative risk by 3–6 times in infected people which might represent over 80% of all distal GC cases and some with proximal gastric tumors[1,74,75]. The prevalence of *H. pylori* infection is extraordinarily high, infecting 50% of the world's population[1,76-78].

H. pylori is a Gram-negative bacterium which colonizes the human stomach and promotes a full immune response locally and sustainably[19,79,80]. Strains of *H. pylori* are grouped into two broad families tentatively named type I and type II, which are based on whether they express or not the vacuolating cytotoxin (VacA) and the CagA antigen (cytotoxin-associated gene A)[81].

One of the major determinants of *H. pylori*'s virulence is the cag pathogenicity island (cag PAI)[82-84]. This cagPAI is a 40-kb DNA region surrounding the *cagA* gene that contains about 27-31 genes that encode a bacterial type IV secretion system acting as a syringe-like structure, which allows for the delivery of bacterial effector molecules into host gastric epithelial cells[85]. During infection with *H. pylori*, CagA is translocated into epithelial cells, and it is tyrosine-phosphorylated in the EPIYA motifs by the proto-oncogene tyrosine-protein kinase Src and the members of the Abelson family of non-receptor tyrosine kinases[86,87], which results in the interaction with various intracellular signaling pathways, triggering changes in the cytoskeleton, in the morphology and in the mobility of the host cells [86,87].

Compared with cagA– strains, *H. pylori* cagA+ strains significantly increase the risk of developing severe gastritis, atrophic gastritis, peptic ulcer disease and distal GC. In fact, people infected with cagA+ strains have higher degrees of gastric inflammation and epithelial cell damage than people from whom cagA- strains have been isolated[88]. People infected with cagA+ *H. pylori* strains have an enhanced expression of IL-1α, IL-1β, and IL-8 in gastric biopsies compared to uninfected persons or patients infected with cagA- strains[89]. Keeping that consideration in mind, proinflammatory cytokines will be up-regulated by a local infection; however, the magnitude of that systemic response and the profile of released cytokines and chemokines will depend also on host factors.

Regarding host factors, many polymorphisms in genes related to inflammation and innate immunity, such as cytokines and MHC molecules, have been reported to be associated with an increased risk of GC [90-92]. Among the cytokines with polymorphisms that have been associated with GC are IL-1β, IL-1Rβ, IL-4, IL-6, IL-10, TNF-α, and TNF-β[93-97]. Based on ethnic backgrounds, two sets of haplotypes for IL-1 β and IL-10 have been related to increased risk for GC[93-95]; specifically, IL-1β-1464G/-511C/-31T and

IL-10-1082G/-819C/952C for Asians and IL-1β-1464C/-511T/-31C and IL-10-1082A/-819T/952T for Caucasians[95].

Canedo *et al*[96] found that IFN-γ receptor 1 -56C/T polymorphism is a relevant host susceptibility factor for GC development associated with *H. pylori* infection. Polymorphism in the promoter region of the gene coding for IL-10 and TGF-β has been also described in the Mexican population in relation to susceptibility to GC[97]. There is a need for extended studies in different populations and in larger patient groups, particularly in regions of Latin America where the burden of GC is more severe. In recent years, NF-κB has been widely studied in inflammation, immunity and cancer, but its roles are still unclear[98-100]. NF-κB is a master transcription factor activated downstream of the TLR and cytokines such as TNF-α and IL-1β[98]. In contrast to the canonical NF-κB pathway, the noncanonical NF-κB activation responds to specific stimuli, including ligands from the TNFR superfamily members such as LTβR, BAFFR, CD40 and RANK[99].

In GC, *H. pylori* is associated with increased expression of the proinflammatory NF-κB[101-104]. It has been shown that the induction of NF-κB mediated by *H. pylori* induces the expression of activation-induced cytidine deaminase, which has been demonstrated to induce nucleotide modifications in the *TP53* gene in gastric cell models[105] and suggests that the accumulation of those *TP53* gene alterations might contribute to the development of gastric neoplasia.

As an example, *in vitro* studies showed that programmed death (PD)-1 is increased among gastric epithelial cells after *H. pylori* infection and its immunosuppressive functions on T-cells may contribute to carcinogenesis[106]. Evidence from small studies observed an up-regulation of PD-1 and programmed cell death-ligand 1 (PD-L1) in human *H. pylori*-related gastric carcinoma[107].

In addition, *H. pylori* has shown other effects within the gastrointestinal epithelium not associated with inflammation but compromising the genome stability, for example, reduced levels of transcripts for DNA mismatch repair (MMR) proteins such as MutS, MutL RAD51, FEN1, POLD1, and LIG1[108-110], and this phenotype might be more severe in cases cagA+ *H. pylori*[110]. However, the deficiency MMR in gastric tumors was recently shown to predict clinical response to pembrolizumab[111], demonstrating also the expansion of antigen-specific T cells reactive to tumor-derived neoantigens, suggesting that further studies are required to understand the interaction between pathogens and genomic features as biomarkers.

CROSSTALK BETWEEN VIRAL INFECTION AND INNATE IMMUNITY ACTIVATION

The EBV is a ubiquitous virus and member of the subfamily of human Gammaherpesvirinae[112] and can infect several cell types, including B-lymphocytes, epithelial cells, and fibroblasts[113]. EBV is the main pathogenic factor for nasopharyngeal carcinoma. However, studies find that EBV infection is also associated with the development of T-cell lymphoma and EBV-associated GC[114]. Although the infection rate of EBV is extraordinarily high, reaching over 90% of the adult population worldwide[115, 116], the incidence rate of EBV-positive GC remains low, representing around 9% of characterized stomach adenocarcinomas[117], these EBV-positive tumors display recurrent PIK3CA mutations, extreme DNA hypermethylation, and amplification of JAK2 and both PD-L1 and PD-L2[5].

The EBV-positive GC has been characterized by an increased expression of PD-L1, and a sustained immune-infiltration, which is indicative of the presence of stable T-cells and supports the use of an immune checkpoint inhibitor for the treatment of this GC subtype[118,119]. In addition, most EBV-positive GCs show MSI which has also been associated with inflammation and local immune activation [120-123]. Previous groups have shown that high density of intra-tumoral or stromal CD8+ T cells with a high percentage of PD-L1 expression seems to be associated with a worse progression-free survival and overall survival[118,120,124]. However, a recent study demonstrated that EBV-positive GC patients treated with immunotherapy showed favorable responses[125], suggesting that viral status represents a potential predictive biomarker for using immune-checkpoint inhibitors; however, the balance between pro-inflammatory and immunosuppressive signals together with a concomitant viral infection requires more studies to clarify its role as a biomarker.

Type I and type II IFN are central to both combating virus infection and modulating the antiviral immune response[126]. The cytokine IFN-γ is mainly produced by T Cell CD4+ and natural killers to activate macrophages. The ligation to its receptor triggers an activation of the Janus-Activated kinases, JAK1 and JAK2, and subsequently the activation of STAT1 and interferon regulatory factor 1 (IRF1). STAT1 and IRF1 are activated by phosphorylation and translocated to the nucleus to regulate the *IFN-γ* gene expression[127].

Crucial to the induction of type I IFN is the recognition of viral PAMPs by PRRs, among which, the cyclic GMP-AMP synthase-stimulator of interferon genes modulates the antiviral response triggered by DNA viruses and retroviruses[128]. In addition, most viruses, including EBV, stimulate innate immune response during primary infection predominantly by activating the expression of TLRs, such as TLR2, TLR3, TLR4, TLR7, TLR8, and TLR9[129]. TLR2 is likely activated by EBV surface glycoprotein gp350 [130] and the nonstructural protein dUTPase[131], while EBV-encoded small RNAs released from EBV-infected cells are detected by TLR3[132]. Furthermore, EBV can activate monocytes and plasmacytoid

DCs through cooperative action of TLR9 and TLR2[133].

Activation of PRRs by EBV-PAMPs triggers JAK-STAT-mediated IFN response and different branches of innate immune signaling including NF-κB pathway; inflammasome activation; and programmed cell death such as apoptosis and necroptosis[134]. However, innate immunity is a double-edged sword as the induction of pro-inflammatory responses and activation of programmed cell death might release a burst of virions and may therefore facilitate the spread of infection[135].

Recently, IFN-γ has been the subject of studies due to its immune role in cancer development, especially in GC. There are several signaling pathways of innate immunity during GC development in which interferon is involved, such as in proliferation, metastasis, and advancement of GC through the upregulation of integrin β3-mediated NF-κB signaling[136]. Serum levels of IFN-γ are elevated in GC which may promote systemic and local responses[137] at the same time, for example: peroxisome proliferator-activated receptor delta, a ligand involved in physiologic processes in cell metabolism, proliferation, and inflammation[138] together with IFN-γ signaling creates an inflammatory tumor-promoting microenvironment enabling villin-expressing gastric progenitor cells transformation and gastric tumorigenesis[139]. Furthermore, natural killer (NK) cells play a role in innate immunity against cancer cells. Lee *et al*[140] reported that IFN-γ produced by the activated NK decreases in GC patients compared with healthy donors. This low level of IFN-γ-NK could be used as a non-invasive biomarker for carcinogenesis in GC[140].

Some reports including Latin American cohorts have shown that concentrations of IFN-γ and IL-10 are significantly higher in GC than in non-oncological cases, and within the GC group, IFN-γ levels are increased at the early stages (I/II) and remain higher in late stage (IV)[141]. Interestingly, increased levels of viral capsid antigen antibodies are significantly associated with elevated serum levels of IFN-γ, particularly in the intestinal type of GC[142]. Therefore, IFN-γ is suggested as a biomarker for assessing GC risk; however, this molecule is known to mediate gastric damage or immune antipathogen responses, as well as the expression of some negative immune checkpoint molecules.

The PD-L1 expression is activated by several cytokines, of which IFN-γ is the strongest[143]. In a melanoma cell line model, PD-L1 has shown to be mainly regulated by the type II interferon receptor signaling pathway through JAK1 and JAK2, several STATs including STAT1/STAT2/STAT3, to converge on the binding of IRF1 to the PD-L1 promoter[144]. Later, Chen *et al*[145] treated with IFN-γ thirty-four cultured human tumor lines, including 18 melanomas (MEL), 12 renal cell carcinomas (RCC), 3 squamous cell carcinomas of the head and neck (SCCHN), and 1 non-small-cell lung carcinoma, and as wildtype control the authors considered isolated peripheral blood monocytes. The results indicated that PD-L1 was constitutively expressed on 1/17 cultured MELs, 8/11 RCCs, 3/3 SCCHNs, and on monocytes; however, the inhibition of STAT1 but not STAT3 was more critical to reduce IFN-γ-induced PD-L1 protein expression on tumor cells[145]. Other authors have provided evidence of a crosstalk between JAK2-STAT1 and PI3K-AKT pathways in response to IFN-γ in lung adenocarcinoma[146]. Transcriptome analysis demonstrated that tumor tissues expressing IFN-γ display gene expression associated with suppressed cell cycle progression and expansion, which was not observed in PD-L1 negative tumors. In lung adenocarcinoma cells, IFN-γ induces the activation of JAK2-STAT1 and PI3K-AKT pathways, showing that the activation of JAK2-STAT1 is responsible for the anti-proliferative effect of IFN-γ, and the inhibition of PI3K downregulates PD-L1 expression and enhances the anti-proliferative effect of IFN-γ[146]. In addition to the cytokine regulation, a lncRNA (long non-coding RNA) named Interferon-stimulated non-coding RNA 1 (INCR1) has been described as a major regulator of IFN-γ signaling in tumors by post-transcriptional modulation of PD-L1 and JAK2 expression[147]. INCR1 is expressed as an antisense RNA from the PD-L1/PD-L2 locus and has been detected in human samples across multiple tumor types, and its levels increase after IFN-γ stimulation, correlating with PD-L1 but not PD-L2 expression[147].

Regarding GC, PD-L1 has shown a wide and very variable range of expression based on technique and cutoff, however, it seems to be absent in non-tumor gastric tissue[148-151]. Imai *et al*[152] showed IFN-γ treatments enhanced the expression of intracellular and membranous PD-L1 expression in GC cell lines. This upregulation of PD-L1 induced by IFN-γ was associated with the JAK-STAT but not the MAPK and PI3K-AKT pathway activation[152,153]. PD-L1 overexpression mediated by IFN-γ is also seen in GC with positive EBV[154]. Polymorphism in PD-L1 related to GC has also been described. PD-L1rs2297136 was positively correlated with a higher proportion of PD-L1 protein and could be employed as a tool of prognosis in GC patients[155,156].

A recent study suggested the role of ISG12a as a tumor suppressor in gastrointestinal tissue[157,158]. ISG12 or interferon alpha-inducible protein 27 promotes β-catenin proteasomal degradation by inhibiting the degradation of ubiquitinated Axin, thereby suppressing the canonical Wnt/β-catenin signaling pathway[158]. Reduced levels of ISG12a were observed in gastrointestinal cancer, such as hepatocellular cancer and GC, and it was associated with an immune-suppressive tumor microenvironment. The authors argue that β-catenin is a transcription factor for PD-L1, and the inhibition of the Wnt/β-catenin signaling by ISG12a makes tumor cells more sensitive to NK cell-mediated killing[157]. Therefore, the balance between the induction or suppression of IFN-stimulated genes[159], such as ISG12a, may accelerate the malignant transformation of cancer cells and lead to a poor prognosis in gastrointestinal cancer[157,160].

NON-BIOLOGICAL FEATURES AS IMMUNE AND PREMALIGNANT MODULATORS

GC is currently accepted as the consequence of a multifactorial process, involving pathogen infection and the virulence of some strains (as *H. pylori*), environmental factors, dietary habits, and host intrinsic factors, as we have discussed above; however, socioeconomic factors, such as education level and occupation, have shown to be determinant during the progression of the premalignant cascade of GC and the patient's outcome after the cancer onset[161-163].

Asia accounts for 71% of GC's worldwide, in which China's incidence is 44.1%. The high incidence in China is marked by the rural population, and their exposure to carcinogens through diet, the environment and the *H. pylori* infection *per se*[164]. The incidence of GC in Europe is heterogeneous; while the highest incidence is in Central and Eastern Europe, the lowest incidence is in Western and Northern Europe, which correlates with a higher detection of *H. pylori* in Eastern Europe compared to Western Europe[165], as well as an observed higher consumption of red and processed meat resulting in an increased risk of GC[166].

After Europe, Latin American countries have shown a high incidence of gastric malignancies. The associated risk factors are infection with *H. pylori*, diet and habits such as smoking, consumption of salt, alcohol and meat, as well as ethnicity and age[167]. Some authors have suggested that Latin America has a close correlation between GC incidence and altitude which is based on the presence of a mountainous geography, such as the Sierra Madre, Cordillera de Centroamerica and the Cordillera de los Andes[168]. However, the mortality and incidence rates for gastric malignancies in the Chilean population is statistically higher than the average rates in the rest of Latin America, becoming the second cause of death from cancer in Chile, affecting 11.6 per 100000 inhabitants and causing around 3000 deaths per year[1]. That incidence seems to correlate mainly with socioeconomic status, Mapuche ethnicity, and age at the primary *H. pylori* infection[169].

Surprisingly, most of the countries with the highest incidence of GC are not those with low incomes (Table 2). In fact, it seems that the vicious circle between precancerous lesions, inflammation and GC onset is caused by the low level of education within the population. A study performed within the Swedish population, that considered the economically active population, showed an increased risk factor of GC in workers engaged in manual-labor occupations and in industry. The statistics were standardized for categories of occupation and adjusted by age, period and region, and confirmed that overall manual-workers and farmers had the highest risk of GC, including male miners and quarry workers[162]. The European Prospective Investigation into Cancer and Nutrition cohort included about 520000 participants mostly aged 35–70 years and, after an average follow-up of 6.5 years, reported 268 cases with adenocarcinoma of the stomach. Higher education was significantly associated with a reduced risk of GC with a hazard ratio (HR) of 0.64 (95%CI: 0.43–0.98) and, as was expected from other reports, that effect was more pronounced for cancer of the cardia (HR: 0.42) as compared to non-cardia GC (HR: 0.66)[163].

A survey to address GC risk factors and endoscopic screening within the North American population showed that ethnicity, cultural habits and immigration patterns are potentially useful to identify high-risk persons from multicultural areas within the United States[170]. The authors identified that dietary habits during teenage years (15-18) and education below high school level may represent signs of risk for GC in older people of foreign birth[170]. Most recently, based on the previous research, a secondary analysis showed that education level was the single most reliable measure of GC risk among three variables of socioeconomic status including, education, income, and occupation, which are the most commonly used for health outcomes such as cancer survival[171]. Similar results were observed in a seroepidemiologic study in Japan where the *H. pylori* positive rate increased at 1% per year for people born after 1950 but was comparatively constant for people with birth dates before 1950[171]. Based on the authors, the apparent decreased prevalence of *H. pylori* post-war was accompanied by the Western-ization of the country and subsequently by a reduction in the frequency of atrophic gastritis and the incidence of gastric carcinoma during the most modern times[171,172].

The infection status in adults is considered to be influenced by socioeconomic status in childhood; however, given the massive improvement in hygiene and the economic environment around the world, it has contributed to the variation in the trends in incidence and death rates of GC among the countries mentioned above. Based on other authors, the education in *H. pylori* eradication and gastric malignancies is largely due to unplanned prevention caused by the widespread adoption of technology and improved manufacturing practices of the food industry. In a similar way, the prevalence of *H. pylori* infection may be reduced owing to improvements in sanitary and housing conditions based on education at early ages by primary schools and in adult life by primary health workers.

Where the intersection between education and immunity is not evident, by intuition a limited knowledge regarding gastrointestinal health and eradication of *H. pylori* infection might dramatically influence the development of GC. Therefore, the inflammatory process induced by a pathogen or even an incipient neoplasm may not receive enough attention, progressing finally to an advanced disease with limited therapeutic opportunities and uncertain outcome for the patient.

Table 2 Gastric cancer incidence and socioeconomic indicators per country

Country	Estimated cases	Crude rate	ASR, world[1]	Cum. risk	HDI classification
Japan	138470	109.5	31.6	9.35	Very high
Korea	28713	56	27.9	6.51	Very high
Brunei Darussalam	55	12.6	13.5	5.93	Very high
Russia	37364	25.6	13.5	3.29	Very high
Chile	4208	22	13.1	4.17	Very high
Lithuania	864	31.7	13	3.4	Very high
Estonia	379	28.6	12.3	3.2	Very high
Latvia	530	28.1	12	3.01	Very high
Portugal	2950	28.9	11	2.99	Very high
Slovakia	1210	22.2	10.7	3.12	Very high
Mongolia	860	26.2	32.5	7.71	High
China	478508	33.1	20.6	5.24	High
Iran	14656	17.4	17.5	6.58	High
Kazakhstan	3357	17.9	15.8	3.47	High
Belarus	2739	29	15.4	3.5	High
Peru	6300	19.1	15.2	5.16	High
Colombia	8214	16.1	12.8	3.61	High
Costa Rica	952	18.7	12.8	4.12	High
Samoa	20	10.1	12.8	3.75	High
Azerbaijan	1453	14.3	12.7	3.42	High
Tajikistan	1301	13.6	23.4	6.96	Medium
Kyrgyzstan	1027	15.7	19.7	5.01	Medium
Cabo Verde	82	14.7	18.4	5.88	Medium
Bhutan	118	15.3	17.7	3.88	Medium
Viet Nam	17906	18.4	15.5	3.57	Medium
Sao Tome and Principe	18	8.2	14.7	2.06	Medium
Myanmar	7235	13.3	13.7	3.58	Medium
Lao	675	9.3	12.9	3.17	Medium
Guatemala	1637	9.1	12.2	3.93	Medium
Turkmenistan	583	9.7	11.8	2.37	Medium
Haiti	1184	10.4	13.5	4.58	Low
Mali	1097	5.4	12.8	2.96	Low
Afghanistan	2149	5.5	12.4	3.18	Low
Zimbabwe	641	4.3	9.4	3.24	Low
Papua New Guinea	474	5.3	9.2	3.17	Low
Rwanda	587	4.5	8.1	1.61	Low
Yemen	966	3.2	7.1	2.68	Low
Senegal	597	3.6	7	1.66	Low
Benin	429	3.5	7	2.29	Low
Mauritania	143	3.1	5.6	1.46	Low

[1]Top 10 countries with the highest age-standardized incidence rates per 100000 inhabitants, per each human development index classification. Source: Globocan 2020, access by https://gco.iarc.fr. ASR: Age-standardized incidence rate; HDI: Human development index.

CONCLUSION

During the transition from premalignant lesions of the gastric epithelium to the final carcinoma, some microorganisms will play a determinant role promoting the neoplastic transformation or contributing with particular tumor phenotype and its heterogeneity, together with different mutagenic agents and genomic aberrations. This review provides an overview on innate immune activation in the context of gastrointestinal malignancies and compiles studies related to TLRs, neutrophils, cytokines and pathogens, as crucial players during the precancerous cascade and the cancer onset, allowing the correlation of those aspects with clinical and socioeconomic variables.

As shown in the graphical abstract, intersections between innate immune response and GC development is driven by common mediators, such as NF-κB and IFN-γ molecular pathways, cellular processes (neutrophil and myeloid cells activation), and activators/inducers (PAMP, damage-associated molecular patterns, tumor-antigens). However, universal risk factors are identified affecting globally any human being which, depending on extrinsic and intrinsic host factors, might facilitate the progression of the precancerous cascade to GC.

Modern therapies such as adoptive cell therapy, vaccines, and especially immunotherapy using checkpoint inhibitors, which have not been mentioned in this work, have shown in clinical trials the role of restoring the balance in favor of the immune system against GC. In the words of Dunn *et al*[173] the observed benefits in GC may be based on (1) Elimination: NK cells and T lymphocytes (helper and cytotoxic) secrete interferon IFN-γ leading to a reduction of angiogenesis and proliferation of cancerous cells; moreover, macrophages and DC secrete cytokines that activate immune cells to phagocytize dead tumor cells; (2) Equilibrium: Residual cancerous cells remain in a dormant state because DC and cytotoxic T cells secrete IFN-γ and inhibitory cytokines (IL-12) suppress them; and (3) Escape: Tumor cells change their features, up-regulating immune checkpoint pathways, which will be transmitted to the daughter cells, therefore escaping immunosuppression and proliferating, along with the apoptosis of the effector lymphocytes[173]. The success of those treatments relies on an efficient immune system, and of course an innate response able to promote priming and mobilization of newly activated immune cells; the presence of pathogens or their PAMPs, as well as molecules derived from the tumor itself will continuously modulate the tumor immune microenvironment. The shape of the tumor will also depend on the host background (genome stability, driver mutations and other gene variants) but in addition, the external environment shaped by the socioeconomic status of each person will determine the final outcome.

Innate immunity is the beginning, and certainly, will be part of the final response against tumors. All these observations require further investigation but it is clear that pathogens like *H. pylori* and EBV need to be assessed in GC based on their role as biomarkers and as potential mechanisms of resistance to therapy.

FOOTNOTES

Author contributions: Villarroel-Espíndola F contributed to the conceptualization, methodology, original draft preparation, writing, reviewing, editing, supervision and funding acquisition; Ejsmentewicz T and Salinas E contributed to the writing of the original draft; González-Stegmaier R contributed to the writing of the original draft, reviewing, editing and visualization; Jorquera R contributed to the writing, reviewing, editing and visualization.

Supported by Instituto Oncológico Fundación Arturo López Pérez, Santiago, Chile; National Research and Development Agency of Chile (ANID) and National Fund for Scientific and Technological Development (FONDECYT), No. 1221415 (to Villarroel-Espindola F).

Conflict-of-interest statement: Dr. F. Villarroel-Espindola has received compensation from Ilico SpA. and Gebrax-Chile for consulting services. Other authors declare having no conflict of interests, neither real nor perceivable, in relation to this article.

Country/Territory of origin: Chile

ORCID number: Franz Villarroel-Espindola 0000-0003-0080-2444; Roxana Gonzalez-Stegmaier 0000-0002-6345-7054.

Corresponding Author's Membership in Professional Societies: European Society for Medical Oncology, No. 529044.

S-Editor: Wang JL
L-Editor: Filipodia
P-Editor: Wang JL

REFERENCES

1 **Sung H**, Ferlay J, Siegel RL, Laversanne M, Soerjomataram I, Jemal A, Bray F. Global Cancer Statistics 2020: GLOBOCAN Estimates of Incidence and Mortality Worldwide for 36 Cancers in 185 Countries. *CA Cancer J Clin* 2021; **71**: 209-249 [PMID: 33538338 DOI: 10.3322/caac.21660]
2 **Thrift AP**, El-Serag HB. Burden of Gastric Cancer. *Clin Gastroenterol Hepatol* 2020; **18**: 534-542 [PMID: 31362118 DOI: 10.1016/j.cgh.2019.07.045]
3 **Peek RM Jr**, Blaser MJ. Helicobacter pylori and gastrointestinal tract adenocarcinomas. *Nat Rev Cancer* 2002; **2**: 28-37 [PMID: 11902583 DOI: 10.1038/nrc703]
4 **Waldum HL**, Fossmark R. Types of Gastric Carcinomas. *Int J Mol Sci* 2018; **19** [PMID: 30567376 DOI: 10.3390/ijms19124109]
5 **Cancer Genome Atlas Research Network**. Comprehensive molecular characterization of gastric adenocarcinoma. *Nature* 2014; **513**: 202-209 [PMID: 25079317 DOI: 10.1038/nature13480]
6 **Jin G**, Lv J, Yang M, Wang M, Zhu M, Wang T, Yan C, Yu C, Ding Y, Li G, Ren C, Ni J, Zhang R, Guo Y, Bian Z, Zheng Y, Zhang N, Jiang Y, Chen J, Wang Y, Xu D, Zheng H, Yang L, Chen Y, Walters R, Millwood IY, Dai J, Ma H, Chen K, Chen Z, Hu Z, Wei Q, Shen H, Li L. Genetic risk, incident gastric cancer, and healthy lifestyle: a meta-analysis of genome-wide association studies and prospective cohort study. *Lancet Oncol* 2020; **21**: 1378-1386 [PMID: 33002439 DOI: 10.1016/S1470-2045(20)30460-5]
7 **Röcken C**. Molecular classification of gastric cancer. *Expert Rev Mol Diagn* 2017; **17**: 293-301 [PMID: 28118758 DOI: 10.1080/14737159.2017.1286985]
8 **Carneiro F**, Lauwers G. Epithelial tumours of the stomach. In: Shepherd NA, Warren BF, Williams GT, Greenson JK, Lauwers GY, Novelli MR, editors. Morson and Dawson's Gastrointestinal Pathology. Wiley Online Library, 2013: 180-222 [DOI: 10.1002/9781118399668.ch13]
9 **Karimi P**, Islami F, Anandasabapathy S, Freedman ND, Kamangar F. Gastric cancer: descriptive epidemiology, risk factors, screening, and prevention. *Cancer Epidemiol Biomarkers Prev* 2014; **23**: 700-713 [PMID: 24618998 DOI: 10.1158/1055-9965.EPI-13-1057]
10 **Soto D**, Song C, McLaughlin-Drubin ME. Epigenetic Alterations in Human Papillomavirus-Associated Cancers. *Viruses* 2017; **9** [PMID: 28862667 DOI: 10.3390/v9090248]
11 **Crowe SE**. Helicobacter pylori Infection. *N Engl J Med* 2019; **380**: 1158-1165 [PMID: 30893536 DOI: 10.1056/NEJMcp1710945]
12 **Hashemi Goradel N**, Heidarzadeh S, Jahangiri S, Farhood B, Mortezaee K, Khanlarkhani N, Negahdari B. Fusobacterium nucleatum and colorectal cancer: A mechanistic overview. *J Cell Physiol* 2019; **234**: 2337-2344 [PMID: 30191984 DOI: 10.1002/jcp.27250]
13 **Nagy KN**, Sonkodi I, Szöke I, Nagy E, Newman HN. The microflora associated with human oral carcinomas. *Oral Oncol* 1998; **34**: 304-308 [PMID: 9813727]
14 **Michaud DS**. Role of bacterial infections in pancreatic cancer. *Carcinogenesis* 2013; **34**: 2193-2197 [PMID: 23843038 DOI: 10.1093/carcin/bgt249]
15 **Colotta F**, Allavena P, Sica A, Garlanda C, Mantovani A. Cancer-related inflammation, the seventh hallmark of cancer: links to genetic instability. *Carcinogenesis* 2009; **30**: 1073-1081 [PMID: 19468060 DOI: 10.1093/carcin/bgp127]
16 **Matsushima N**, Miyashita H, Mikami T, Kuroki Y. A nested leucine rich repeat (LRR) domain: the precursor of LRRs is a ten or eleven residue motif. *BMC Microbiol* 2010; **10**: 235 [PMID: 20825685 DOI: 10.1186/1471-2180-10-235]
17 **Akira S**, Uematsu S, Takeuchi O. Pathogen recognition and innate immunity. *Cell* 2006; **124**: 783-801 [PMID: 16497588 DOI: 10.1016/j.cell.2006.02.015]
18 **Behzadi P**, García-Perdomo HA, Karpiński TM. Toll-Like Receptors: General Molecular and Structural Biology. *J Immunol Res* 2021; **2021**: 9914854 [PMID: 34195298 DOI: 10.1155/2021/9914854]
19 **Smith SM**. Role of Toll-like receptors in Helicobacter pylori infection and immunity. *World J Gastrointest Pathophysiol* 2014; **5**: 133-146 [PMID: 25133016 DOI: 10.4291/wjgp.v5.i3.133]
20 **Amedei A**, Cappon A, Codolo G, Cabrelle A, Polenghi A, Benagiano M, Tasca E, Azzurri A, D'Elios MM, Del Prete G, de Bernard M. The neutrophil-activating protein of Helicobacter pylori promotes Th1 immune responses. *J Clin Invest* 2006; **116**: 1092-1101 [PMID: 16543949 DOI: 10.1172/JCI27177]
21 **Yokota S**, Ohnishi T, Muroi M, Tanamoto K, Fujii N, Amano K. Highly-purified Helicobacter pylori LPS preparations induce weak inflammatory reactions and utilize Toll-like receptor 2 complex but not Toll-like receptor 4 complex. *FEMS Immunol Med Microbiol* 2007; **51**: 140-148 [PMID: 17645528 DOI: 10.1111/j.1574-695X.2007.00288.x]
22 **Melit LE**, Mărginean CO, Mărginean CD, Mărginean MO. The Relationship between Toll-like Receptors and Helicobacter pylori-Related Gastropathies: Still a Controversial Topic. *J Immunol Res* 2019; **2019**: 8197048 [PMID: 30863783 DOI: 10.1155/2019/8197048]
23 **Uno K**, Kato K, Shimosegawa T. Novel role of toll-like receptors in Helicobacter pylori - induced gastric malignancy. *World J Gastroenterol* 2014; **20**: 5244-5251 [PMID: 24833854 DOI: 10.3748/wjg.v20.i18.5244]

24 **Schmausser B**, Andrulis M, Endrich S, Lee SK, Josenhans C, Müller-Hermelink HK, Eck M. Expression and subcellular distribution of toll-like receptors TLR4, TLR5 and TLR9 on the gastric epithelium in Helicobacter pylori infection. *Clin Exp Immunol* 2004; **136**: 521-526 [PMID: 15147355 DOI: 10.1111/j.1365-2249.2004.02464.x]

25 **Baghdadi J**, Chaudhary N, Pei Z, Yang L. Microbiome, innate immunity, and esophageal adenocarcinoma. *Clin Lab Med* 2014; **34**: 721-732 [PMID: 25439272 DOI: 10.1016/j.cll.2014.08.001]

26 **Helminen O**, Huhta H, Takala H, Lehenkari PP, Saarnio J, Kauppila JH, Karttunen TJ. Increased Toll-like receptor 5 expression indicates esophageal columnar dysplasia. *Virchows Arch* 2014; **464**: 11-18 [PMID: 24221343 DOI: 10.1007/s00428-013-1505-2]

27 **Smith MF Jr**, Mitchell A, Li G, Ding S, Fitzmaurice AM, Ryan K, Crowe S, Goldberg JB. Toll-like receptor (TLR) 2 and TLR5, but not TLR4, are required for Helicobacter pylori-induced NF-kappa B activation and chemokine expression by epithelial cells. *J Biol Chem* 2003; **278**: 32552-32560 [PMID: 12807870 DOI: 10.1074/jbc.M305536200]

28 **Andersen-Nissen E**, Smith KD, Strobe KL, Barrett SL, Cookson BT, Logan SM, Aderem A. Evasion of Toll-like receptor 5 by flagellated bacteria. *Proc Natl Acad Sci U S A* 2005; **102**: 9247-9252 [PMID: 15956202 DOI: 10.1073/PNAS.0502040102]

29 **Kim JH**, Namgung B, Jeon YJ, Song WS, Lee J, Kang SG, Yoon SI. Helicobacter pylori flagellin: TLR5 evasion and fusion-based conversion into a TLR5 agonist. *Biochem Biophys Res Commun* 2018; **505**: 872-878 [PMID: 30301528 DOI: 10.1016/j.bbrc.2018.09.179]

30 **Pachathundikandi SK**, Tegtmeyer N, Arnold IC, Lind J, Neddermann M, Falkeis-Veits C, Chattopadhyay S, Brönstrup M, Tegge W, Hong M, Sticht H, Vieth M, Müller A, Backert S. T4SS-dependent TLR5 activation by Helicobacter pylori infection. *Nat Commun* 2019; **10**: 5717 [PMID: 31844047 DOI: 10.1038/s41467-019-13506-6]

31 **Tegtmeyer N**, Neddermann M, Lind J, Pachathundikandi SK, Sharafutdinov I, Gutiérrez-Escobar AJ, Brönstrup M, Tegge W, Hong M, Rohde M, Delahay RM, Vieth M, Sticht H, Backert S. Toll-like Receptor 5 Activation by the CagY Repeat Domains of Helicobacter pylori. *Cell Rep* 2020; **32**: 108159 [PMID: 32937132 DOI: 10.1016/j.celrep.2020.108159]

32 **Kasurinen A**, Hagström J, Laitinen A, Kokkola A, Böckelman C, Haglund C. Evaluation of toll-like receptors as prognostic biomarkers in gastric cancer: high tissue TLR5 predicts a better outcome. *Sci Rep* 2019; **9**: 12553 [PMID: 31467388 DOI: 10.1038/s41598-019-49111-2]

33 **Tang K**, McLeod L, Livis T, West AC, Dawson R, Yu L, Balic JJ, Chonwerawong M, Wray-McCann G, Oshima H, Oshima M, Deswaerte V, Ferrero RL, Jenkins BJ. Toll-like Receptor 9 Promotes Initiation of Gastric Tumorigenesis by Augmenting Inflammation and Cellular Proliferation. *Cell Mol Gastroenterol Hepatol* 2022; **14**: 567-586 [PMID: 35716851 DOI: 10.1016/j.jcmgh.2022.06.002]

34 **Alvarez-Arellano L**, Cortés-Reynosa P, Sánchez-Zauco N, Salazar E, Torres J, Maldonado-Bernal C. TLR9 and NF-κB are partially involved in activation of human neutrophils by Helicobacter pylori and its purified DNA. *PLoS One* 2014; **9**: e101342 [PMID: 24987851 DOI: 10.1371/journal.pone.0101342]

35 **Nagashima H**, Iwatani S, Cruz M, Jiménez Abreu JA, Uchida T, Mahachai V, Vilaichone RK, Graham DY, Yamaoka Y. Toll-like Receptor 10 in Helicobacter pylori Infection. *J Infect Dis* 2015; **212**: 1666-1676 [PMID: 25977263 DOI: 10.1093/infdis/jiv270]

36 **Rosales C**. Neutrophil: A Cell with Many Roles in Inflammation or Several Cell Types? *Front Physiol* 2018; **9**: 113 [PMID: 29515456 DOI: 10.3389/fphys.2018.00113]

37 **Hakkim A**, Fuchs TA, Martinez NE, Hess S, Prinz H, Zychlinsky A, Waldmann H. Activation of the Raf-MEK-ERK pathway is required for neutrophil extracellular trap formation. *Nat Chem Biol* 2011; **7**: 75-77 [PMID: 21170021 DOI: 10.1038/nchembio.496]

38 **Stephan A**, Fabri M. The NET, the trap and the pathogen: neutrophil extracellular traps in cutaneous immunity. *Exp Dermatol* 2015; **24**: 161-166 [PMID: 25421224 DOI: 10.1111/exd.12599]

39 **Wang W**, Zhang J, Zheng N, Li L, Wang X, Zeng Y. The role of neutrophil extracellular traps in cancer metastasis. *Clin Transl Med* 2020; **10**: e126 [PMID: 32961033 DOI: 10.1002/ctm2.126]

40 **Brinkmann V**, Reichard U, Goosmann C, Fauler B, Uhlemann Y, Weiss DS, Weinrauch Y, Zychlinsky A. Neutrophil extracellular traps kill bacteria. *Science* 2004; **303**: 1532-1535 [PMID: 15001782 DOI: 10.1126/science.1092385]

41 **Wen SH**, Hong ZW, Chen CC, Chang HW, Fu HW. Helicobacter pylori Neutrophil-Activating Protein Directly Interacts with and Activates Toll-like Receptor 2 to Induce the Secretion of Interleukin-8 from Neutrophils and ATRA-Induced Differentiated HL-60 Cells. *Int J Mol Sci* 2021; **22** [PMID: 34768994 DOI: 10.3390/ijms222111560]

42 **Alvarez-Arellano L**, Camorlinga-Ponce M, Maldonado-Bernal C, Torres J. Activation of human neutrophils with Helicobacter pylori and the role of Toll-like receptors 2 and 4 in the response. *FEMS Immunol Med Microbiol* 2007; **51**: 473-479 [PMID: 17892476 DOI: 10.1111/j.1574-695X.2007.00327.x]

43 **Nishioka H**, Baesso I, Semenzato G, Trentin L, Rappuoli R, Del Giudice G, Montecucco C. The neutrophil-activating protein of Helicobacter pylori (HP-NAP) activates the MAPK pathway in human neutrophils. *Eur J Immunol* 2003; **33**: 840-849 [PMID: 12672049 DOI: 10.1002/EJI.200323726]

44 **Ríos-López AL**, González GM, Hernández-Bello R, Sánchez-González A. Avoiding the trap: Mechanisms developed by pathogens to escape neutrophil extracellular traps. *Microbiol Res* 2021; **243**: 126644 [PMID: 33199088 DOI: 10.1016/j.micres.2020.126644]

45 **Allen LA**, Beecher BR, Lynch JT, Rohner OV, Wittine LM. Helicobacter pylori disrupts NADPH oxidase targeting in human neutrophils to induce extracellular superoxide release. *J Immunol* 2005; **174**: 3658-3667 [PMID: 15749904 DOI: 10.4049/JIMMUNOL.174.6.3658]

46 **Tran AX**, Whittimore JD, Wyrick PB, McGrath SC, Cotter RJ, Trent MS. The lipid A 1-phosphatase of Helicobacter pylori is required for resistance to the antimicrobial peptide polymyxin. *J Bacteriol* 2006; **188**: 4531-4541 [PMID: 16740959 DOI: 10.1128/JB.00146-06]

47 **Liechti GW**, Goldberg JB. Helicobacter pylori salvages purines from extracellular host cell DNA utilizing the outer membrane-associated nuclease NucT. *J Bacteriol* 2013; **195**: 4387-4398 [PMID: 23893109 DOI: 10.1128/JB.00388-13]

48 **Honda M**, Kubes P. Neutrophils and neutrophil extracellular traps in the liver and gastrointestinal system. *Nat Rev Gastroenterol Hepatol* 2018; **15**: 206-221 [PMID: 29382950 DOI: 10.1038/nrgastro.2017.183]

49 **Berger-Achituv S**, Brinkmann V, Abed UA, Kühn LI, Ben-Ezra J, Elhasid R, Zychlinsky A. A proposed role for neutrophil extracellular traps in cancer immunoediting. *Front Immunol* 2013; **4**: 48 [PMID: 23508552 DOI: 10.3389/fimmu.2013.00048]

50 **Yang C**, Sun W, Cui W, Li X, Yao J, Jia X, Li C, Wu H, Hu Z, Zou X. Procoagulant role of neutrophil extracellular traps in patients with gastric cancer. *Int J Clin Exp Pathol* 2015; **8**: 14075-14086 [PMID: 26823721]

51 **Zhang Y**, Hu Y, Ma C, Sun H, Wei X, Li M, Wei W, Zhang F, Yang F, Wang H, Gu K. Diagnostic, Therapeutic Predictive, and Prognostic Value of Neutrophil Extracellular Traps in Patients With Gastric Adenocarcinoma. *Front Oncol* 2020; **10**: 1036 [PMID: 32714865 DOI: 10.3389/fonc.2020.01036]

52 **Zhu T**, Zou X, Yang C, Li L, Wang B, Li R, Li H, Xu Z, Huang D, Wu Q. Neutrophil extracellular traps promote gastric cancer metastasis by inducing epithelialmesenchymal transition. *Int J Mol Med* 2021; **48** [PMID: 34013374 DOI: 10.3892/IJMM.2021.4960]

53 **Xia X**, Zhang Z, Zhu C, Ni B, Wang S, Yang S, Yu F, Zhao E, Li Q, Zhao G. Neutrophil extracellular traps promote metastasis in gastric cancer patients with postoperative abdominal infectious complications. *Nat Commun* 2022; **13**: 1017 [PMID: 35197446 DOI: 10.1038/s41467-022-28492-5]

54 **Huang S**, DeGuzman A, Bucana CD, Fidler IJ. Nuclear factor-kappaB activity correlates with growth, angiogenesis, and metastasis of human melanoma cells in nude mice. *Clin Cancer Res* 2000; **6**: 2573-2581 [PMID: 10873114]

55 **Arlauckas SP**, Garren SB, Garris CS, Kohler RH, Oh J, Pittet MJ, Weissleder R. Arg1 expression defines immunosuppressive subsets of tumor-associated macrophages. *Theranostics* 2018; **8**: 5842-5854 [PMID: 30613266 DOI: 10.7150/thno.26888]

56 **Mantovani A**, Marchesi F, Malesci A, Laghi L, Allavena P. Tumour-associated macrophages as treatment targets in oncology. *Nat Rev Clin Oncol* 2017; **14**: 399-416 [PMID: 28117416 DOI: 10.1038/nrclinonc.2016.217]

57 **Curtale G**. MiRNAs at the Crossroads between Innate Immunity and Cancer: Focus on Macrophages. *Cells* 2018; **7** [PMID: 29419779 DOI: 10.3390/cells7020012]

58 **Chaudhuri AA**, So AY, Sinha N, Gibson WS, Taganov KD, O'Connell RM, Baltimore D. MicroRNA-125b potentiates macrophage activation. *J Immunol* 2011; **187**: 5062-5068 [PMID: 22003200 DOI: 10.4049/jimmunol.1102001]

59 **Zhang Y**, Zhang M, Zhong M, Suo Q, Lv K. Expression profiles of miRNAs in polarized macrophages. *Int J Mol Med* 2013; **31**: 797-802 [PMID: 23443577 DOI: 10.3892/ijmm.2013.1260]

60 **Banerjee S**, Xie N, Cui H, Tan Z, Yang S, Icyuz M, Abraham E, Liu G. MicroRNA let-7c regulates macrophage polarization. *J Immunol* 2013; **190**: 6542-6549 [PMID: 23667114 DOI: 10.4049/jimmunol.1202496]

61 **Taganov KD**, Boldin MP, Chang KJ, Baltimore D. NF-kappaB-dependent induction of microRNA miR-146, an inhibitor targeted to signaling proteins of innate immune responses. *Proc Natl Acad Sci U S A* 2006; **103**: 12481-12486 [PMID: 16885212 DOI: 10.1073/pnas.0605298103]

62 **Yang M**, Chen J, Su F, Yu B, Lin L, Liu Y, Huang JD, Song E. Microvesicles secreted by macrophages shuttle invasion-potentiating microRNAs into breast cancer cells. *Mol Cancer* 2011; **10**: 117 [PMID: 21939504 DOI: 10.1186/1476-4598-10-117]

63 **Zheng P**, Chen L, Yuan X, Luo Q, Liu Y, Xie G, Ma Y, Shen L. Exosomal transfer of tumor-associated macrophage-derived miR-21 confers cisplatin resistance in gastric cancer cells. *J Exp Clin Cancer Res* 2017; **36**: 53 [PMID: 28407783 DOI: 10.1186/s13046-017-0528-y]

64 **Bazzoni F**, Rossato M, Fabbri M, Gaudiosi D, Mirolo M, Mori L, Tamassia N, Mantovani A, Cassatella MA, Locati M. Induction and regulatory function of miR-9 in human monocytes and neutrophils exposed to proinflammatory signals. *Proc Natl Acad Sci U S A* 2009; **106**: 5282-5287 [PMID: 19289835 DOI: 10.1073/pnas.0810909106]

65 **Cekaite L**, Rantala JK, Bruun J, Guriby M, Agesen TH, Danielsen SA, Lind GE, Nesbakken A, Kallioniemi O, Lothe RA, Skotheim RI. MiR-9, -31, and -182 deregulation promote proliferation and tumor cell survival in colon cancer. *Neoplasia* 2012; **14**: 868-879 [PMID: 23019418 DOI: 10.1593/neo.121094]

66 **Ye G**, Barrera C, Fan X, Gourley WK, Crowe SE, Ernst PB, Reyes VE. Expression of B7-1 and B7-2 costimulatory molecules by human gastric epithelial cells: potential role in CD4+ T cell activation during Helicobacter pylori infection. *J Clin Invest* 1997; **99**: 1628-1636 [PMID: 9120006 DOI: 10.1172/JCI119325]

67 **Zhang QW**, Liu L, Gong CY, Shi HS, Zeng YH, Wang XZ, Zhao YW, Wei YQ. Prognostic significance of tumor-associated macrophages in solid tumor: a meta-analysis of the literature. *PLoS One* 2012; **7**: e50946 [PMID: 23284651 DOI: 10.1371/journal.pone.0050946]

68 **Yamaguchi T**, Fushida S, Yamamoto Y, Tsukada T, Kinoshita J, Oyama K, Miyashita T, Tajima H, Ninomiya I, Munesue S, Harashima A, Harada S, Yamamoto H, Ohta T. Tumor-associated macrophages of the M2 phenotype contribute to progression in gastric cancer with peritoneal dissemination. *Gastric Cancer* 2016; **19**: 1052-1065 [PMID: 26621525 DOI: 10.1007/s10120-015-0579-8]

69 **Rojas A**, Delgado-López F, Gonzalez I. Tumor-associated macrophages in gastric cancer: more than bystanders in tumor microenvironment. *Gastric Cancer* 2017; **20**: 215-216 [PMID: 26894296 DOI: 10.1007/s10120-016-0596-2]

70 **Asaka M**, Kimura T, Kato M, Kudo M, Miki K, Ogoshi K, Kato T, Tatsuta M, Graham DY. Possible role of Helicobacter pylori infection in early gastric cancer development. *Cancer* 1994; **73**: 2691-2694 [PMID: 8194007 DOI: 10.1002/1097-0142(19940601)73:11<2691::aid-cncr2820731107>3.0.co;2-2]

71 **Blaser MJ**, Parsonnet J. Parasitism by the "slow" bacterium Helicobacter pylori leads to altered gastric homeostasis and neoplasia. *J Clin Invest* 1994; **94**: 4-8 [PMID: 8040281 DOI: 10.1172/JCI117336]

72 **Sipponen P**, Hyvärinen H. Role of Helicobacter pylori in the pathogenesis of gastritis, peptic ulcer and gastric cancer. *Scand J Gastroenterol Suppl* 1993; **196**: 3-6 [PMID: 8341988 DOI: 10.3109/00365529309098333]

73 **Talley NJ**, Zinsmeister AR, Weaver A, DiMagno EP, Carpenter HA, Perez-Perez GI, Blaser MJ. Gastric adenocarcinoma and Helicobacter pylori infection. *J Natl Cancer Inst* 1991; **83**: 1734-1739 [PMID: 1770552 DOI: 10.1093/jnci/83.23.1734]

74 **Parsonnet J**, Friedman GD, Vandersteen DP, Chang Y, Vogelman JH, Orentreich N, Sibley RK. Helicobacter pylori infection and the risk of gastric carcinoma. *N Engl J Med* 1991; **325**: 1127-1131 [PMID: 1891020 DOI: 10.1056/NEJM199110173251603]

75 An international association between Helicobacter pylori infection and gastric cancer. The EUROGAST Study Group. *Lancet* 1993; **341**: 1359-1362 [PMID: 8098787 DOI: 10.1016/0140-6736(93)90938-D]

76 **Piazuelo MB**, Correa P. Gastric cáncer: Overview. *Colomb Med (Cali)* 2013; **44**: 192-201 [PMID: 24892619]

77 **Forman D**, Sitas F, Newell DG, Stacey AR, Boreham J, Peto R, Campbell TC, Li J, Chen J. Geographic association of Helicobacter pylori antibody prevalence and gastric cancer mortality in rural China. *Int J Cancer* 1990; **46**: 608-611 [PMID: 2210881 DOI: 10.1002/IJC.2910460410]

78 **Nomura A**, Stemmermann GN, Chyou PH, Kato I, Perez-Perez GI, Blaser MJ. Helicobacter pylori infection and gastric carcinoma among Japanese Americans in Hawaii. *N Engl J Med* 1991; **325**: 1132-1136 [PMID: 1891021 DOI: 10.1056/NEJM199110173251604]

79 **Correa P**. Is gastric carcinoma an infectious disease? *N Engl J Med* 1991; **325**: 1170-1171 [PMID: 1891027 DOI: 10.1056/NEJM199110173251611]

80 **Solnick JV**, Tompkins LS. Helicobacter pylori and gastroduodenal disease: pathogenesis and host-parasite interaction. *Infect Agents Dis* 1992; **1**: 294-309 [PMID: 1344668]

81 **Xiang Z**, Censini S, Bayeli PF, Telford JL, Figura N, Rappuoli R, Covacci A. Analysis of expression of CagA and VacA virulence factors in 43 strains of Helicobacter pylori reveals that clinical isolates can be divided into two major types and that CagA is not necessary for expression of the vacuolating cytotoxin. *Infect Immun* 1995; **63**: 94-98 [PMID: 7806390 DOI: 10.1128/iai.63.1.94-98.1995]

82 **Wroblewski LE**, Peek RM Jr, Wilson KT. Helicobacter pylori and gastric cancer: factors that modulate disease risk. *Clin Microbiol Rev* 2010; **23**: 713-739 [PMID: 20930071 DOI: 10.1128/CMR.00011-10]

83 **Torres J**, Pérez-Pérez GI, Leal-Herrera Y, Muñoz O. Infection with CagA+ Helicobacter pylori strains as a possible predictor of risk in the development of gastric adenocarcinoma in Mexico. *Int J Cancer* 1998; **78**: 298-300 [PMID: 9766561 DOI: 10.1002/(SICI)1097-0215(19981029)78:3<298::AID-IJC6>3.0.CO;2-Q]

84 **Censini S**, Lange C, Xiang Z, Crabtree JE, Ghiara P, Borodovsky M, Rappuoli R, Covacci A. cag, a pathogenicity island of Helicobacter pylori, encodes type I-specific and disease-associated virulence factors. *Proc Natl Acad Sci U S A* 1996; **93**: 14648-14653 [PMID: 8962108 DOI: 10.1073/pnas.93.25.14648]

85 **Varon C**, Mosnier JF, Lehours P, Matysiak-Budnik T, Mégraud F. Gastric carcinogenesis and Helicobacter pylori infection. *Methods Mol Biol* 2009; **511**: 237-265 [PMID: 19347300 DOI: 10.1007/978-1-59745-447-6_10]

86 **Stein M**, Bagnoli F, Halenbeck R, Rappuoli R, Fantl WJ, Covacci A. c-Src/Lyn kinases activate Helicobacter pylori CagA through tyrosine phosphorylation of the EPIYA motifs. *Mol Microbiol* 2002; **43**: 971-980 [PMID: 11929545 DOI: 10.1046/j.1365-2958.2002.02781.x]

87 **Poppe M**, Feller SM, Römer G, Wessler S. Phosphorylation of Helicobacter pylori CagA by c-Abl leads to cell motility. *Oncogene* 2007; **26**: 3462-3472 [PMID: 17160020 DOI: 10.1038/sj.onc.1210139]

88 **Crabtree JE**, Taylor JD, Wyatt JI, Heatley RV, Shallcross TM, Tompkins DS, Rathbone BJ. Mucosal IgA recognition of Helicobacter pylori 120 kDa protein, peptic ulceration, and gastric pathology. *Lancet* 1991; **338**: 332-335 [PMID: 1677696 DOI: 10.1016/0140-6736(91)90477-7]

89 **Peek RM**, Miller GG, Tham KT, Perez-Perez GI, Cover TL, Dunn D, Blaser MJ. Detection of cagA expression in vivo and demonstration of preferential cytokinc expression by cagA+ H. pylori strains in gastric mucosa. *Am J Gastroenterol* 1994; **89**: 1334

90 **Kamangar F**, Dawsey SM, Blaser MJ, Perez-Perez GI, Pietinen P, Newschaffer CJ, Abnet CC, Albanes D, Virtamo J, Taylor PR. Opposing risks of gastric cardia and noncardia gastric adenocarcinomas associated with Helicobacter pylori seropositivity. *J Natl Cancer Inst* 2006; **98**: 1445-1452 [PMID: 17047193 DOI: 10.1093/jnci/djj393]

91 **Sugimoto M**, Yamaoka Y, Furuta T. Influence of interleukin polymorphisms on development of gastric cancer and peptic ulcer. *World J Gastroenterol* 2010; **16**: 1188-1200 [PMID: 20222161 DOI: 10.3748/wjg.v16.i10.1188]

92 **Sugimoto M**, Furuta T, Yamaoka Y. Influence of inflammatory cytokine polymorphisms on eradication rates of Helicobacter pylori. *J Gastroenterol Hepatol* 2009; **24**: 1725-1732 [PMID: 20136959 DOI: 10.1111/j.1440-1746.2009.06047.x]

93 **Beales IL**, Calam J. Interleukin 1 beta and tumour necrosis factor alpha inhibit acid secretion in cultured rabbit parietal cells by multiple pathways. *Gut* 1998; **42**: 227-234 [PMID: 9536948 DOI: 10.1136/gut.42.2.227]

94 **El-Omar EM**, Carrington M, Chow WH, McColl KE, Bream JH, Young HA, Herrera J, Lissowska J, Yuan CC, Rothman N, Lanyon G, Martin M, Fraumeni JF Jr, Rabkin CS. Interleukin-1 polymorphisms associated with increased risk of gastric cancer. *Nature* 2000; **404**: 398-402 [PMID: 10746728 DOI: 10.1038/35006081]

95 **Kim J**, Kim Y, Lee KA. Ethnic differences in gastric cancer genetic susceptibility: allele flips of interleukin gene. *World J Gastroenterol* 2014; **20**: 4558-4565 [PMID: 24782608 DOI: 10.3748/wjg.v20.i16.4558]

96 **Canedo P**, Corso G, Pereira F, Lunet N, Suriano G, Figueiredo C, Pedrazzani C, Moreira H, Barros H, Carneiro F, Seruca R, Roviello F, Machado JC. The interferon gamma receptor 1 (IFNGR1) -56C/T gene polymorphism is associated with increased risk of early gastric carcinoma. *Gut* 2008; **57**: 1504-1508 [PMID: 18593809 DOI: 10.1136/gut.2007.143578]

97 **Martínez-Campos C**, Torres-Poveda K, Camorlinga-Ponce M, Flores-Luna L, Maldonado-Bernal C, Madrid-Marina V, Torres J. Polymorphisms in IL-10 and TGF-β gene promoter are associated with lower risk to gastric cancer in a Mexican population. *BMC Cancer* 2019; **19**: 453 [PMID: 31092242 DOI: 10.1186/s12885-019-5627-z]

98 **Liu T**, Zhang L, Joo D, Sun SC. NF-κB signaling in inflammation. *Signal Transduct Target Ther* 2017; **2**: 17023-17023 [PMID: 29158945 DOI: 10.1038/sigtrans.2017.23]

99 **Sun SC**. The non-canonical NF-κB pathway in immunity and inflammation. *Nat Rev Immunol* 2017; **17**: 545-558 [PMID: 28580957 DOI: 10.1038/nri.2017.52]

100 **Xia Y**, Shen S, Verma IM. NF-κB, an active player in human cancers. *Cancer Immunol Res* 2014; **2**: 823-830 [PMID: 25187272 DOI: 10.1158/2326-6066.CIR-14-0112]

101 **Peek RM Jr**. IV. Helicobacter pylori strain-specific activation of signal transduction cascades related to gastric inflammation. *Am J Physiol Gastrointest Liver Physiol* 2001; **280**: G525-G530 [PMID: 11254477 DOI: 10.1152/ajpgi.2001.280.4.G525]

102 **Soutto M**, Bhat N, Khalafi S, Zhu S, Poveda J, Garcia-Buitrago M, Zaika A, El-Rifai W. NF-kB-dependent activation of STAT3 by H. pylori is suppressed by TFF1. *Cancer Cell Int* 2021; **21**: 444 [PMID: 34419066 DOI: 10.1186/s12935-021-02140-2]

103 **Shibata W**, Hirata Y, Yoshida H, Otsuka M, Hoshida Y, Ogura K, Maeda S, Ohmae T, Yanai A, Mitsuno Y, Seki N, Kawabe T, Omata M. NF-kappaB and ERK-signaling pathways contribute to the gene expression induced by cag PAI-positive-Helicobacter pylori infection. *World J Gastroenterol* 2005; **11**: 6134-6143 [PMID: 16273640 DOI: 10.3748/wjg.v11.i39.6134]

104 **Shen L**, Zeng J, Ma L, Li S, Chen C, Jia J, Liang X. Helicobacter pylori Induces a Novel NF-kB/LIN28A/let-7a/hTERT Axis to Promote Gastric Carcinogenesis. *Mol Cancer Res* 2021; **19**: 74-85 [PMID: 33004623 DOI: 10.1158/1541-7786.MCR-19-0678]

105 **Matsumoto Y**, Marusawa H, Kinoshita K, Endo Y, Kou T, Morisawa T, Azuma T, Okazaki IM, Honjo T, Chiba T. Helicobacter pylori infection triggers aberrant expression of activation-induced cytidine deaminase in gastric epithelium. *Nat Med* 2007; **13**: 470-476 [PMID: 17401375 DOI: 10.1038/nm1566]

106 **Das S**, Suarez G, Beswick EJ, Sierra JC, Graham DY, Reyes VE. Expression of B7-H1 on gastric epithelial cells: its potential role in regulating T cells during Helicobacter pylori infection. *J Immunol* 2006; **176**: 3000-3009 [PMID: 16493058 DOI: 10.4049/jimmunol.176.5.3000]

107 **Lu B**, Chen L, Liu L, Zhu Y, Wu C, Jiang J, Zhang X. T-cell-mediated tumor immune surveillance and expression of B7 co-inhibitory molecules in cancers of the upper gastrointestinal tract. *Immunol Res* 2011; **50**: 269-275 [PMID: 21717068 DOI: 10.1007/s12026-011-8227-9]

108 **Kim JJ**, Tao H, Carloni E, Leung WK, Graham DY, Sepulveda AR. Helicobacter pylori impairs DNA mismatch repair in gastric epithelial cells. *Gastroenterology* 2002; **123**: 542-553 [PMID: 12145807 DOI: 10.1053/gast.2002.34751]

109 **Hardbower DM**, Peek RM Jr, Wilson KT. At the Bench: Helicobacter pylori, dysregulated host responses, DNA damage, and gastric cancer. *J Leukoc Biol* 2014; **96**: 201-212 [PMID: 24868089 DOI: 10.1189/jlb.4BT0214-099R]

110 **Kontizas E**, Tastsoglou S, Karamitros T, Karayiannis Y, Kollia P, Hatzigeorgiou AG, Sgouras DN. Impact of Helicobacter pylori Infection and Its Major Virulence Factor CagA on DNA Damage Repair. *Microorganisms* 2020; **8** [PMID: 33339161 DOI: 10.3390/microorganisms8122007]

111 **Le DT**, Durham JN, Smith KN, Wang H, Bartlett BR, Aulakh LK, Lu S, Kemberling H, Wilt C, Luber BS, Wong F, Azad NS, Rucki AA, Laheru D, Donehower R, Zaheer A, Fisher GA, Crocenzi TS, Lee JJ, Greten TF, Duffy AG, Ciombor KK, Eyring AD, Lam BH, Joe A, Kang SP, Holdhoff M, Danilova L, Cope L, Meyer C, Zhou S, Goldberg RM, Armstrong DK, Bever KM, Fader AN, Taube J, Housseau F, Spetzler D, Xiao N, Pardoll DM, Papadopoulos N, Kinzler KW, Eshleman JR, Vogelstein B, Anders RA, Diaz LA Jr. Mismatch repair deficiency predicts response of solid tumors to PD-1 blockade. *Science* 2017; **357**: 409-413 [PMID: 28596308 DOI: 10.1126/science.aan6733]

112 **Lange PT**, White MC, Damania B. Activation and Evasion of Innate Immunity by Gammaherpesviruses. *J Mol Biol* 2022; **434**: 167214 [PMID: 34437888 DOI: 10.1016/j.jmb.2021.167214]

113 **Epstein A**. Why and How Epstein-Barr Virus Was Discovered 50 Years Ago. *Curr Top Microbiol Immunol* 2015; **390**: 3-15 [PMID: 26424640 DOI: 10.1007/978-3-319-22822-8_1]

114 **Sun K**, Jia K, Lv H, Wang SQ, Wu Y, Lei H, Chen X. EBV-Positive Gastric Cancer: Current Knowledge and Future Perspectives. *Front Oncol* 2020; **10**: 583463 [PMID: 33381453 DOI: 10.3389/fonc.2020.583463]

115 **Lieberman PM**. Virology. Epstein-Barr virus turns 50. *Science* 2014; **343**: 1323-1325 [PMID: 24653027 DOI: 10.1126/science.1252786]

116 **Bocian J**, Januszkiewicz-Lewandowska D. [Epstein-Barr virus infection - life cycle, methods of diagnosis, associated diseases]. *Postepy Hig Med Dosw (Online)* 2011; **65**: 286-298 [PMID: 21677354 DOI: 10.5604/17322693.943104]

117 **Camargo MC**, Bowlby R, Chu A, Pedamallu CS, Thorsson V, Elmore S, Mungall AJ, Bass AJ, Gulley ML, Rabkin CS. Validation and calibration of next-generation sequencing to identify Epstein-Barr virus-positive gastric cancer in The Cancer Genome Atlas. *Gastric Cancer* 2016; **19**: 676-681 [PMID: 26095338 DOI: 10.1007/s10120-015-0508-x]

118 **Dong M**, Wang HY, Zhao XX, Chen JN, Zhang YW, Huang Y, Xue L, Li HG, Du H, Wu XY, Shao CK. Expression and prognostic roles of PIK3CA, JAK2, PD-L1, and PD-L2 in Epstein-Barr virus-associated gastric carcinoma. *Hum Pathol* 2016; **53**: 25-34 [PMID: 26980034 DOI: 10.1016/j.humpath.2016.02.007]

119 **Yang L**, Wang Y, Wang H. Use of immunotherapy in the treatment of gastric cancer. *Oncol Lett* 2019; **18**: 5681-5690 [PMID: 31788040 DOI: 10.3892/ol.2019.10935]

120 **Kim ST**, Cristescu R, Bass AJ, Kim KM, Odegaard JI, Kim K, Liu XQ, Sher X, Jung H, Lee M, Lee S, Park SH, Park JO, Park YS, Lim HY, Lee H, Choi M, Talasaz A, Kang PS, Cheng J, Loboda A, Lee J, Kang WK. Comprehensive molecular characterization of clinical responses to PD-1 inhibition in metastatic gastric cancer. *Nat Med* 2018; **24**: 1449-1458 [PMID: 30013197 DOI: 10.1038/s41591-018-0101-z]

121 **Lee HE**, Chae SW, Lee YJ, Kim MA, Lee HS, Lee BL, Kim WH. Prognostic implications of type and density of tumour-infiltrating lymphocytes in gastric cancer. *Br J Cancer* 2008; **99**: 1704-1711 [PMID: 18941457 DOI: 10.1038/sj.bjc.6604738]

122 **Wakatsuki K**, Sho M, Yamato I, Takayama T, Matsumoto S, Tanaka T, Migita K, Ito M, Hotta K, Nakajima Y. Clinical impact of tumor-infiltrating CD45RO$^+$ memory T cells on human gastric cancer. *Oncol Rep* 2013; **29**: 1756-1762 [PMID: 23440298 DOI: 10.3892/or.2013.2302]

123 **Coutzac C**, Pernot S, Chaput N, Zaanan A. Immunotherapy in advanced gastric cancer, is it the future? *Crit Rev Oncol Hematol* 2019; **133**: 25-32 [PMID: 30661655 DOI: 10.1016/j.critrevonc.2018.10.007]

124 **Thompson ED**, Zahurak M, Murphy A, Cornish T, Cuka N, Abdelfatah E, Yang S, Duncan M, Ahuja N, Taube JM, Anders RA, Kelly RJ. Patterns of PD-L1 expression and CD8 T cell infiltration in gastric adenocarcinomas and associated immune stroma. *Gut* 2017; **66**: 794-801 [PMID: 26801886 DOI: 10.1136/gutjnl-2015-310839]

125 **Xie T**, Liu Y, Zhang Z, Zhang X, Gong J, Qi C, Li J, Shen L, Peng Z. Positive Status of Epstein-Barr Virus as a Biomarker for Gastric Cancer Immunotherapy: A Prospective Observational Study. *J Immunother* 2020; **43**: 139-144 [PMID: 32134806 DOI: 10.1097/CJI.0000000000000316]

126 **Lee AJ**, Ashkar AA. The Dual Nature of Type I and Type II Interferons. *Front Immunol* 2018; **9**: 2061 [PMID: 30254639

DOI: 10.3389/fimmu.2018.02061]
127 **Ni L**, Lu J. Interferon gamma in cancer immunotherapy. *Cancer Med* 2018; **7**: 4509-4516 [PMID: 30039553 DOI: 10.1002/cam4.1700]
128 **Miao L**, Qi J, Zhao Q, Wu QN, Wei DL, Wei XL, Liu J, Chen J, Zeng ZL, Ju HQ, Luo HY, Xu RH. Targeting the STING pathway in tumor-associated macrophages regulates innate immune sensing of gastric cancer cells. *Theranostics* 2020; **10**: 498-515 [PMID: 31903134 DOI: 10.7150/thno.37745]
129 **Lünemann A**, Rowe M, Nadal D. Innate Immune Recognition of EBV. *Curr Top Microbiol Immunol* 2015; **391**: 265-287 [PMID: 26428378 DOI: 10.1007/978-3-319-22834-1_9]
130 **Gaudreault E**, Fiola S, Olivier M, Gosselin J. Epstein-Barr virus induces MCP-1 secretion by human monocytes *via* TLR2. *J Virol* 2007; **81**: 8016-8024 [PMID: 17522215 DOI: 10.1128/JVI.00403-07]
131 **Ariza ME**, Glaser R, Kaumaya PT, Jones C, Williams MV. The EBV-encoded dUTPase activates NF-kappa B through the TLR2 and MyD88-dependent signaling pathway. *J Immunol* 2009; **182**: 851-859 [PMID: 19124728 DOI: 10.4049/jimmunol.182.2.851]
132 **Iwakiri D**, Zhou L, Samanta M, Matsumoto M, Ebihara T, Seya T, Imai S, Fujieda M, Kawa K, Takada K. Epstein-Barr virus (EBV)-encoded small RNA is released from EBV-infected cells and activates signaling from Toll-like receptor 3. *J Exp Med* 2009; **206**: 2091-2099 [PMID: 19720839 DOI: 10.1084/jem.20081761]
133 **Fiola S**, Gosselin D, Takada K, Gosselin J. TLR9 contributes to the recognition of EBV by primary monocytes and plasmacytoid dendritic cells. *J Immunol* 2010; **185**: 3620-3631 [PMID: 20713890 DOI: 10.4049/jimmunol.0903736]
134 **Jangra S**, Yuen KS, Botelho MG, Jin DY. Epstein-Barr Virus and Innate Immunity: Friends or Foes? *Microorganisms* 2019; **7** [PMID: 31238570 DOI: 10.3390/microorganisms7060183]
135 **Pontejo SM**, Murphy PM, Pease JE. Chemokine Subversion by Human Herpesviruses. *J Innate Immun* 2018; **10**: 465-478 [PMID: 30165356 DOI: 10.1159/000492161]
136 **Xu YH**, Li ZL, Qiu SF. IFN-γ Induces Gastric Cancer Cell Proliferation and Metastasis Through Upregulation of Integrin β3-Mediated NF-κB Signaling. *Transl Oncol* 2018; **11**: 182-192 [PMID: 29306706 DOI: 10.1016/j.tranon.2017.11.008]
137 **Wu D**, Zhang P, Ma J, Xu J, Yang L, Xu W, Que H, Chen M, Xu H. Serum biomarker panels for the diagnosis of gastric cancer. *Cancer Med* 2019; **8**: 1576-1583 [PMID: 30873760 DOI: 10.1002/cam4.2055]
138 **Neels JG**, Grimaldi PA. Physiological functions of peroxisome proliferator-activated receptor β. *Physiol Rev* 2014; **94**: 795-858 [PMID: 24987006 DOI: 10.1152/physrev.00027.2013]
139 **Zuo X**, Deguchi Y, Xu W, Liu Y, Li HS, Wei D, Tian R, Chen W, Xu M, Yang Y, Gao S, Jaoude JC, Liu F, Chrieki SP, Moussalli MJ, Gagea M, Sebastian MM, Zheng X, Tan D, Broaddus R, Wang J, Ajami NJ, Swennes AG, Watowich SS, Shureiqi I. PPARD and Interferon Gamma Promote Transformation of Gastric Progenitor Cells and Tumorigenesis in Mice. *Gastroenterology* 2019; **157**: 163-178 [PMID: 30885780 DOI: 10.1053/j.gastro.2019.03.018]
140 **Lee J**, Park KH, Ryu JH, Bae HJ, Choi A, Lee H, Lim J, Han K, Park CH, Jung ES, Oh EJ. Natural killer cell activity for IFN-gamma production as a supportive diagnostic marker for gastric cancer. *Oncotarget* 2017; **8**: 70431-70440 [PMID: 29050291 DOI: 10.18632/oncotarget.19712]
141 **Sánchez-Zauco N**, Torres J, Gómez A, Camorlinga-Ponce M, Muñoz-Pérez L, Herrera-Goepfert R, Medrano-Guzmán R, Giono-Cerezo S, Maldonado-Bernal C. Circulating blood levels of IL-6, IFN-γ, and IL-10 as potential diagnostic biomarkers in gastric cancer: a controlled study. *BMC Cancer* 2017; **17**: 384 [PMID: 28558708 DOI: 10.1186/s12885-017-3310-9]
142 **Cárdenas-Mondragón MG**, Torres J, Sánchez-Zauco N, Gómez-Delgado A, Camorlinga-Ponce M, Maldonado-Bernal C, Fuentes-Pananá EM. Elevated Levels of Interferon-γ Are Associated with High Levels of Epstein-Barr Virus Reactivation in Patients with the Intestinal Type of Gastric Cancer. *J Immunol Res* 2017; **2017**: 7069242 [PMID: 29349089 DOI: 10.1155/2017/7069242]
143 **Zou W**, Wolchok JD, Chen L. PD-L1 (B7-H1) and PD-1 pathway blockade for cancer therapy: Mechanisms, response biomarkers, and combinations. *Sci Transl Med* 2016; **8**: 328rv4 [PMID: 26936508 DOI: 10.1126/scitranslmed.aad7118]
144 **Garcia-Diaz A**, Shin DS, Moreno BH, Saco J, Escuin-Ordinas H, Rodriguez GA, Zaretsky JM, Sun L, Hugo W, Wang X, Parisi G, Saus CP, Torrejon DY, Graeber TG, Comin-Anduix B, Hu-Lieskovan S, Damoiseaux R, Lo RS, Ribas A. Interferon Receptor Signaling Pathways Regulating PD-L1 and PD-L2 Expression. *Cell Rep* 2017; **19**: 1189-1201 [PMID: 28494868 DOI: 10.1016/j.celrep.2017.04.031]
145 **Chen S**, Crabill GA, Pritchard TS, McMiller TL, Wei P, Pardoll DM, Pan F, Topalian SL. Mechanisms regulating PD-L1 expression on tumor and immune cells. *J Immunother Cancer* 2019; **7**: 305 [PMID: 31730010 DOI: 10.1186/s40425-019-0770-2]
146 **Gao Y**, Yang J, Cai Y, Fu S, Zhang N, Fu X, Li L. IFN-γ-mediated inhibition of lung cancer correlates with PD-L1 expression and is regulated by PI3K-AKT signaling. *Int J Cancer* 2018; **143**: 931-943 [PMID: 29516506 DOI: 10.1002/ijc.31357]
147 **Mineo M**, Lyons SM, Zdioruk M, von Spreckelsen N, Ferrer-Luna R, Ito H, Alayo QA, Kharel P, Giantini Larsen A, Fan WY, Auduong S, Grauwet K, Passaro C, Khalsa JK, Shah K, Reardon DA, Ligon KL, Beroukhim R, Nakashima H, Ivanov P, Anderson PJ, Lawler SE, Chiocca EA. Tumor Interferon Signaling Is Regulated by a lncRNA INCR1 Transcribed from the PD-L1 Locus. *Mol Cell* 2020; **78**: 1207-1223.e8 [PMID: 32504554 DOI: 10.1016/j.molcel.2020.05.015]
148 **Wu C**, Zhu Y, Jiang J, Zhao J, Zhang XG, Xu N. Immunohistochemical localization of programmed death-1 ligand-1 (PD-L1) in gastric carcinoma and its clinical significance. *Acta Histochem* 2006; **108**: 19-24 [PMID: 16530813 DOI: 10.1016/j.acthis.2006.01.003]
149 **Wu P**, Wu D, Li L, Chai Y, Huang J. PD-L1 and Survival in Solid Tumors: A Meta-Analysis. *PLoS One* 2015; **10**: e0131403 [PMID: 26114883 DOI: 10.1371/journal.pone.0131403]
150 **Kulangara K**, Zhang N, Corigliano E, Guerrero L, Waldroup S, Jaiswal D, Ms MJ, Shah S, Hanks D, Wang J, Lunceford J, Savage MJ, Juco J, Emancipator K. Clinical Utility of the Combined Positive Score for Programmed Death Ligand-1 Expression and the Approval of Pembrolizumab for Treatment of Gastric Cancer. *Arch Pathol Lab Med* 2019; **143**: 330-337 [PMID: 30028179 DOI: 10.5858/arpa.2018-0043-OA]

151 **Ma J**, Li J, Qian M, Han W, Tian M, Li Z, Wang Z, He S, Wu K. PD-L1 expression and the prognostic significance in gastric cancer: a retrospective comparison of three PD-L1 antibody clones (SP142, 28-8 and E1L3N). *Diagn Pathol* 2018; **13**: 91 [PMID: 30463584 DOI: 10.1186/s13000-018-0766-0]

152 **Imai Y**, Chiba T, Kondo T, Kanzaki H, Kanayama K, Ao J, Kojima R, Kusakabe Y, Nakamura M, Saito T, Nakagawa R, Suzuki E, Nakamoto S, Muroyama R, Tawada A, Matsumura T, Nakagawa T, Kato J, Kotani A, Matsubara H, Kato N. Interferon-γ induced PD-L1 expression and soluble PD-L1 production in gastric cancer. *Oncol Lett* 2020; **20**: 2161-2168 [PMID: 32782533 DOI: 10.3892/ol.2020.11757]

153 **Mimura K**, Teh JL, Okayama H, Shiraishi K, Kua LF, Koh V, Smoot DT, Ashktorab H, Oike T, Suzuki Y, Fazreen Z, Asuncion BR, Shabbir A, Yong WP, So J, Soong R, Kono K. PD-L1 expression is mainly regulated by interferon gamma associated with JAK-STAT pathway in gastric cancer. *Cancer Sci* 2018; **109**: 43-53 [PMID: 29034543 DOI: 10.1111/cas.13424]

154 **Nakano H**, Saito M, Nakajima S, Saito K, Nakayama Y, Kase K, Yamada L, Kanke Y, Hanayama H, Onozawa H, Okayama H, Fujita S, Sakamoto W, Saze Z, Momma T, Mimura K, Ohki S, Goto A, Kono K. PD-L1 overexpression in EBV-positive gastric cancer is caused by unique genomic or epigenomic mechanisms. *Sci Rep* 2021; **11**: 1982 [PMID: 33479394 DOI: 10.1038/s41598-021-81667-w]

155 **Wu Y**, Cao D, Qu L, Cao X, Jia Z, Zhao T, Wang Q, Jiang J. PD-1 and PD-L1 co-expression predicts favorable prognosis in gastric cancer. *Oncotarget* 2017; **8**: 64066-64082 [PMID: 28969052 DOI: 10.18632/oncotarget.19318]

156 **Kim JG**, Chae YS, Sohn SK, Cho YY, Moon JH, Park JY, Jeon SW, Lee IT, Choi GS, Jun SH. Vascular endothelial growth factor gene polymorphisms associated with prognosis for patients with colorectal cancer. *Clin Cancer Res* 2008; **14**: 62-66 [PMID: 18172253 DOI: 10.1158/1078-0432.CCR-07-1537]

157 **Deng R**, Zuo C, Li Y, Xue B, Xun Z, Guo Y, Wang X, Xu Y, Tian R, Chen S, Liu Q, Chen J, Wang J, Huang X, Li H, Guo M, Yang M, Wu Z, Ma J, Hu J, Li G, Tang S, Tu Z, Ji H, Zhu H. The innate immune effector ISG12a promotes cancer immunity by suppressing the canonical Wnt/β-catenin signaling pathway. *Cell Mol Immunol* 2020; **17**: 1163-1179 [PMID: 32963356 DOI: 10.1038/s41423-020-00549-9]

158 **Rasmussen UB**, Wolf C, Mattei MG, Chenard MP, Bellocq JP, Chambon P, Rio MC, Basset P. Identification of a new interferon-alpha-inducible gene (p27) on human chromosome 14q32 and its expression in breast carcinoma. *Cancer Res* 1993; **53**: 4096-4101 [PMID: 8358738]

159 **Borden EC**. Interferons α and β in cancer: therapeutic opportunities from new insights. *Nat Rev Drug Discov* 2019; **18**: 219-234 [PMID: 30679806 DOI: 10.1038/s41573-018-0011-2]

160 **Xue B**, Yang D, Wang J, Xu Y, Wang X, Qin Y, Tian R, Chen S, Xie Q, Liu N, Zhu H. ISG12a Restricts Hepatitis C Virus Infection through the Ubiquitination-Dependent Degradation Pathway. *J Virol* 2016; **90**: 6832-6845 [PMID: 27194766 DOI: 10.1128/JVI.00352-16]

161 **Sarkar S**, Dauer MJ, In H. Socioeconomic Disparities in Gastric Cancer and Identification of a Single SES Variable for Predicting Risk. *J Gastrointest Cancer* 2022; **53**: 170-178 [PMID: 33404986 DOI: 10.1007/s12029-020-00564-z]

162 **Ji J**, Hemminki K. Socio-economic and occupational risk factors for gastric cancer: a cohort study in Sweden. *Eur J Cancer Prev* 2006; **15**: 391-397 [PMID: 16912567 DOI: 10.1097/00008469-200610000-00003]

163 **Nagel G**, Linseisen J, Boshuizen HC, Pera G, Del Giudice G, Westert GP, Bueno-de-Mesquita HB, Allen NE, Key TJ, Numans ME, Peeters PH, Sieri S, Siman H, Berglund G, Hallmans G, Stenling R, Martinez C, Arriola L, Barricarte A, Chirlaque MD, Quiros JR, Vineis P, Masala G, Palli D, Panico S, Tumino R, Bingham S, Boeing H, Bergmann MM, Overvad K, Boutron-Ruault MC, Clavel-Chapelon F, Olsen A, Tjonneland A, Trichopoulou A, Bamia C, Soukara S, Sabourin JC, Carneiro F, Slimani N, Jenab M, Norat T, Riboli E, González CA. Socioeconomic position and the risk of gastric and oesophageal cancer in the European Prospective Investigation into Cancer and Nutrition (EPIC-EURGAST). *Int J Epidemiol* 2007; **36**: 66-76 [PMID: 17227779 DOI: 10.1093/ije/dyl275]

164 **Yang L**, Ying X, Liu S, Lyu G, Xu Z, Zhang X, Li H, Li Q, Wang N, Ji J. Gastric cancer: Epidemiology, risk factors and prevention strategies. *Chin J Cancer Res* 2020; **32**: 695-704 [PMID: 33446993 DOI: 10.21147/j.issn.1000-9604.2020.06.03]

165 **Xie Y**, Shi L, He X, Luo Y. Gastrointestinal cancers in China, the USA, and Europe. *Gastroenterol Rep (Oxf)* 2021; **9**: 91-104 [PMID: 34026216 DOI: 10.1093/gastro/goab010]

166 **Agudo A**, Cayssials V, Bonet C, Tjønneland A, Overvad K, Boutron-Ruault MC, Affret A, Fagherazzi G, Katzke V, Schübel R, Trichopoulou A, Karakatsani A, La Vecchia C, Palli D, Grioni S, Tumino R, Ricceri F, Panico S, Bueno-de-Mesquita B, Peeters PH, Weiderpass E, Skeie G, Nøst TH, Lasheras C, Rodríguez-Barranco M, Amiano P, Chirlaque MD, Ardanaz E, Ohlsson B, Dias JA, Nilsson LM, Myte R, Khaw KT, Perez-Cornago A, Gunter M, Huybrechts I, Cross AJ, Tsilidis K, Riboli E, Jakszyn P. Inflammatory potential of the diet and risk of gastric cancer in the European Prospective Investigation into Cancer and Nutrition (EPIC) study. *Am J Clin Nutr* 2018; **107**: 607-616 [PMID: 29635497 DOI: 10.1093/ajcn/nqy002]

167 **Ruíz-García E**, Guadarrama-Orozco J, Vidal-Millán S, Lino-Silva LS, López-Camarillo C, Astudillo-de la Vega H. Gastric cancer in Latin America. *Scand J Gastroenterol* 2018; **53**: 124-129 [PMID: 29275643 DOI: 10.1080/00365521.2017.1417473]

168 **Torres J**, Correa P, Ferreccio C, Hernandez-Suarez G, Herrero R, Cavazza-Porro M, Dominguez R, Morgan D. Gastric cancer incidence and mortality is associated with altitude in the mountainous regions of Pacific Latin America. *Cancer Causes Control* 2013; **24**: 249-256 [PMID: 23224271 DOI: 10.1007/s10552-012-0114-8]

169 **Heise K**, Bertran E, Andia ME, Ferreccio C. Incidence and survival of stomach cancer in a high-risk population of Chile. *World J Gastroenterol* 2009; **15**: 1854-1862 [PMID: 19370783 DOI: 10.3748/WJG.15.1854]

170 **In H**, Langdon-Embry M, Gordon L, Schechter CB, Wylie-Rosett J, Castle PE, Margaret Kemeny M, Rapkin BD. Can a gastric cancer risk survey identify high-risk patients for endoscopic screening? *J Surg Res* 2018; **227**: 246-256 [PMID: 29622399 DOI: 10.1016/j.jss.2018.02.053]

171 **Asaka M**, Kimura T, Kudo M, Takeda H, Mitani S, Miyazaki T, Miki K, Graham DY. Relationship of Helicobacter pylori to serum pepsinogens in an asymptomatic Japanese population. *Gastroenterology* 1992; **102**: 760-766 [PMID: 1537513 DOI: 10.1016/0016-5085(92)90156-s]

172 **Inoue M**, Tsugane S. Epidemiology of gastric cancer in Japan. *Postgrad Med J* 2005; **81**: 419-424 [PMID: 15998815 DOI: 10.1136/pgmj.2004.029330]

173 **Dunn GP**, Old LJ, Schreiber RD. The three Es of cancer immunoediting. *Annu Rev Immunol* 2004; **22**: 329-360 [PMID: 15032581 DOI: 10.1146/annurev.immunol.22.012703.104803]

174 **Huhta H**, Helminen O, Lehenkari PP, Saarnio J, Karttunen TJ, Kauppila JH. Toll-like receptors 1, 2, 4 and 6 in esophageal epithelium, Barrett's esophagus, dysplasia and adenocarcinoma. *Oncotarget* 2016; **7**: 23658-23667 [PMID: 27008696 DOI: 10.18632/oncotarget.8151]

175 **Kennedy CL**, Najdovska M, Tye H, McLeod L, Yu L, Jarnicki A, Bhathal PS, Putoczki T, Ernst M, Jenkins BJ. Differential role of MyD88 and Mal/TIRAP in TLR2-mediated gastric tumourigenesis. *Oncogene* 2014; **33**: 2540-2546 [PMID: 23728346 DOI: 10.1038/onc.2013.205]

176 **Diakowska D**, Nienartowicz M, Grabowski K, Rosińczuk J, Krzystek-Korpacka M. Toll-like receptors TLR-2, TLR-4, TLR-7, and TLR-9 in tumor tissue and serum of the patients with esophageal squamous cell carcinoma and gastro-esophageal junction cancer. *Adv Clin Exp Med* 2019; **28**: 515-522 [PMID: 29968427 DOI: 10.17219/acem/87012]

177 **Uehara A**, Fujimoto Y, Fukase K, Takada H. Various human epithelial cells express functional Toll-like receptors, NOD1 and NOD2 to produce anti-microbial peptides, but not proinflammatory cytokines. *Mol Immunol* 2007; **44**: 3100-3111 [PMID: 17403538 DOI: 10.1016/j.molimm.2007.02.007]

178 **Fernandez-Garcia B**, Eiró N, González-Reyes S, González L, Aguirre A, González LO, Del Casar JM, García-Muñiz JL, Vizoso FJ. Clinical significance of toll-like receptor 3, 4, and 9 in gastric cancer. *J Immunother* 2014; **37**: 77-83 [PMID: 24509170 DOI: 10.1097/CJI.0000000000000016]

179 **Sheyhidin I**, Nabi G, Hasim A, Zhang RP, Ainiwaer J, Ma H, Wang H. Overexpression of TLR3, TLR4, TLR7 and TLR9 in esophageal squamous cell carcinoma. *World J Gastroenterol* 2011; **17**: 3745-3751 [PMID: 21990957 DOI: 10.3748/wjg.v17.i32.3745]

180 **Pimentel-Nunes P**, Afonso L, Lopes P, Roncon-Albuquerque R Jr, Gonçalves N, Henrique R, Moreira-Dias L, Leite-Moreira AF, Dinis-Ribeiro M. Increased expression of toll-like receptors (TLR) 2, 4 and 5 in gastric dysplasia. *Pathol Oncol Res* 2011; **17**: 677-683 [PMID: 21455638 DOI: 10.1007/s12253-011-9368-9]

181 **Chen G**, Xu M, Chen J, Hong L, Lin W, Zhao S, Zhang G, Dan G, Liu S. Clinicopathological Features and Increased Expression of Toll-Like Receptor 4 of Gastric Cardia Cancer in a High-Risk Chinese Population. *J Immunol Res* 2018; **2018**: 7132868 [PMID: 29670922 DOI: 10.1155/2018/7132868]

182 **Verbeek RE**, Siersema PD, Ten Kate FJ, Fluiter K, Souza RF, Vleggaar FP, Bus P, van Baal JW. Toll-like receptor 4 activation in Barrett's esophagus results in a strong increase in COX-2 expression. *J Gastroenterol* 2014; **49**: 1121-1134 [PMID: 23955118 DOI: 10.1007/s00535-013-0862-6]

183 **Jiang J**, Dong L, Qin B, Shi H, Guo X, Wang Y. Decreased expression of TLR7 in gastric cancer tissues and the effects of TLR7 activation on gastric cancer cells. *Oncol Lett* 2016; **12**: 631-636 [PMID: 27347192 DOI: 10.3892/ol.2016.4617]

184 **Takala H**, Kauppila JH, Soini Y, Selander KS, Vuopala KS, Lehenkari PP, Saarnio J, Karttunen TJ. Toll-like receptor 9 is a novel biomarker for esophageal squamous cell dysplasia and squamous cell carcinoma progression. *J Innate Immun* 2011; **3**: 631-638 [PMID: 21876325 DOI: 10.1159/000329115]

World Journal of Gastroenterology

Submit a Manuscript: https://www.f6publishing.com

World J Gastroenterol 2023 April 21; 29(15): 2241-2260

DOI: 10.3748/wjg.v29.i15.2241

ISSN 1007-9327 (print) ISSN 2219-2840 (online)

REVIEW

Emerging role of non-invasive and liquid biopsy biomarkers in pancreatic cancer

Akash Bararia, Prosenjeet Chakraborty, Paromita Roy, Bitan Kumar Chattopadhay, Amlan Das, Aniruddha Chatterjee, Nilabja Sikdar

Specialty type: Gastroenterology and hepatology

Provenance and peer review: Invited article; Externally peer reviewed.

Peer-review model: Single blind

Peer-review report's scientific quality classification
Grade A (Excellent): A
Grade B (Very good): B
Grade C (Good): 0
Grade D (Fair): 0
Grade E (Poor): 0

P-Reviewer: Białek Ł, Poland; Wang XB, China

Received: November 28, 2022
Peer-review started: November 28, 2022
First decision: January 11, 2023
Revised: February 2, 2023
Accepted: March 15, 2023
Article in press: March 15, 2023
Published online: April 21, 2023

Akash Bararia, Nilabja Sikdar, Human Genetics Unit, Indian Statistical Institute, Kolkata 700108, India

Prosenjeet Chakraborty, Department of Molecular Biosciences, SVYASA School of Yoga and Naturopathy, Bangalore 560105, India

Paromita Roy, Department of Pathology, Tata Medical Center, Kolkata 700160, India

Bitan Kumar Chattopadhay, Department of General Surgery, IPGMER & SSKM Hospital, Kolkata 700020, India

Amlan Das, Department of Biochemistry, Royal Global University, Assam 781035, India

Aniruddha Chatterjee, Department of Pathology, Dunedin School of Medicine, University of Otago, Dunedin 9061, New Zealand

Aniruddha Chatterjee, School of Health Sciences and Technology, University of Petroleum and Energy Studies, Dehradun 248007, India

Corresponding author: Nilabja Sikdar, PhD, Research Scientist, Doctor, Human Genetics Unit, Indian Statistical Institute, 203, B.T. Road, Kolkata 700108, India. snilabja@isical.ac.in

Abstract

A global increase in the incidence of pancreatic cancer (PanCa) presents a major concern and health burden. The traditional tissue-based diagnostic techniques provided a major way forward for molecular diagnostics; however, they face limitations based on diagnosis-associated difficulties and concerns surrounding tissue availability in the clinical setting. Late disease development with asymptomatic behavior is a drawback in the case of existing diagnostic procedures. The capability of cell free markers in discriminating PanCa from autoimmune pancreatitis and chronic pancreatitis along with other precancerous lesions can be a boon to clinicians. Early-stage diagnosis of PanCa can be achieved only if these biomarkers specifically discriminate the non-carcinogenic disease stage from malignancy with respect to tumor stages. In this review, we comprehensively described the non-invasive disease detection approaches and why these approaches are gaining popularity for their early-stage diagnostic capability and associated clinical feasibility.

Key Words: Non-invasive biomarkers; Cell free biomarkers; Proteomic biomarkers; Liquid biopsy-based diagnostics; Pancreatic cancer biomarkers

Core Tip: Considering the limited commercial availability of cell free nucleic acids and secreted proteome-based non-invasive biomarkers it is crucial to summarize them for the proper diagnosis of pancreatic cancer and distinguish it from other benign pancreatic diseases. We also highlighted the clinical use of these non-invasive biomarkers in diagnostics. This review will successfully guide readers to address the current issues and aid in the cutting-edge development of biomarkers with higher sensitivity and specificity.

Citation: Bararia A, Chakraborty P, Roy P, Chattopadhay BK, Das A, Chatterjee A, Sikdar N. Emerging role of non-invasive and liquid biopsy biomarkers in pancreatic cancer. *World J Gastroenterol* 2023; 29(15): 2241-2260
URL: https://www.wjgnet.com/1007-9327/full/v29/i15/2241.htm
DOI: https://dx.doi.org/10.3748/wjg.v29.i15.2241

INTRODUCTION

The global population is severely burdened by the increase in multiple types of cancer. Cancer-related incidence and its associated mortality have emerged as a major threat to global health in developed countries, like the United States, European countries, Canada, and Australia, and developing as well as under-developed countries including India and Southeast Asian countries. Pancreatic cancer (PanCa) is a deadly and emerging type of cancer because of its associated poor survival. Only 20% of patients are eligible for surgery due to the physiologically deep-rooted location and the generalized symptoms caused by the close proximity to crucial vessels. In 2022, the estimated new incidences in the United States alone are 62210 (male) and 32970 (female), and the estimated deaths associated with PanCa are 25970 males and 23860 females.

Per the GLOBACON 2020 data, PanCa is the 12th most common cause of cancer with 495000 new cases across the globe with approximately 47% of the new cases registered in Asia and another major proportion of 28% in Europe. There might be an increase in the incidence by 70% by the end of 2022, which translates into approximately 844000 new cases per year. As documented in the United States population, PanCa-related mortality has relatively increased in men than in women. In the United Kingdom, PanCa is the tenth most frequent cancer type, and it ranks fifth in terms of cancer-related deaths per year. Some risk factors associated with PanCa apart from genetic predisposition include obesity, diet and smoking. PanCa-associated surgery has a high mortality risk making it a more life-threatening disease[1-4]. Based on the demography and ethnicity of patients, the profile of biomarkers and predisposition to particular risk factors can vary[4,5].

LIQUID BIOPSY AND ITS ROLE IN PANCA DIAGNOSIS

Liquid biopsy (also known as a fluid biopsy) is an approach to identify markers released from tumors in the blood or associated body fluids. It includes but is not limited to cell-free DNA (cfDNA), cell-free RNA (cfRNA), cell-free proteins, circulating tumor cells and exosomes[6-8]. Liquid biopsy is rapidly developing and has a highly emerging market with an estimated $5 billion (USD) turnover globally by 2023[9]. DNA is the most dominant approach in terms of biomarker identification from plasma or serum and in terms of availability for clinical practices, which makes cfDNA a lucrative option.

There are multiple factors that make liquid biopsy an attractive option in comparison to tissue biopsy. A major reason is that traditional tissue biopsy fails to identify tissue heterogeneity in depth whereas liquid biopsy does that more efficiently[10]. The reason behind this is based on the concept that various categories of tumor materials are released in the blood irrespective of tumor heterogeneity. Therefore, making the liquid biopsy samples, such as plasma or serum, a cocktail that has tumor markers irrespective of cell type is not present in the case of the traditional biopsy technique. In addition, the exponential growth of next generation sequencing technologies enables the identification of cell free nucleic acids with high sensitivity, which is of great clinical application.

Moreover, traditional tissue biopsy is not applicable in the case of patients that are in an early stage and have not developed a tumor of significant size[11]. Early-stage PanCa is usually asymptomatic, and no operative options are available to examine the tumor, making traditional tissue biopsy non-

functional in this context. For early or advanced diagnosis and disease assessment, liquid biopsy can be a major step forward toward cancer prevention and screening of populations. APAPTEST was the first cancer blood-based test done to identify markers in the case of cervical cancer[12]. Disease-targeted liquid biopsy-based biomarkers can detect patients who have an intermediate chance of developing PanCa such as those having chronic pancreatitis (CP), diabetes or a genetic predisposition to PanCa. It can also distinguish between PanCa and pancreatic diseases that are immune system modulated in their origin.

A crucial requirement is distinguishing autoimmune pancreatitis (AIP) from PanCa. AIP diagnosis, which is an autoimmune disease based on the rise in IgG4 levels in serum, is based on a liquid biopsy-based approach for identification and differentiation from malignancies such as PanCa. Upregulation of IgG4-positive plasma cells in organ tissues followed by increased IgG4 levels in the serum is usually defined as type 1 AIP. On the contrary, type 2 AIP has no connection with IgG4. It demonstrates features in the pancreatic ducts resembling granulocytic epithelial lesions. Type 1 AIP also acts as a pancreatic lesion related to IgG4-related disease[13]. Since both type I AIP and type II AIP are based on identification using non-invasive approaches, the development of these techniques is urgent to support cases where invasive approaches are a less viable option. This approach acts as a powerful alternative to existing diagnostic methods and will be highly beneficial for the identification of cases with aggressive tumor biology and support clinicians to make proper individualized targeted therapy[13-17].

The methylation status alteration in cancer cells is also an important point to consider for disease diagnosis. The nature of methylation based alterations discriminates itself from genetic changes based on tumor tissue type specificity, which is crucial in the case of methylation alterations apart from being more pervasive and prevalent in terms of occurrences[18,19]. Aberrant DNA methylation alterations mostly occur in CpG islands and play a vital role in activating tumor suppressor genes and oncogenes, thereby modulating the genome[20-23]. The approach to identifying cfDNA-based methylation changes is a growing area of interest because invasive approaches are not always feasible and proactive in terms of clinical diagnostics[24,25]. Various reports claimed that in the case of pancreatic ductal adenocarcinoma (PDAC) an altered methylation signature has been observed when tumor tissues were compared with normal tissues, hence directing its implications in biomarker development[26,27].

The neoplastic tendency of the pancreas needs to be identified, and specific non-invasive markers discriminating PanCa from CP or other pancreatic precursor lesions such as pancreatic intraepithelial neoplasia (PanIN), intrapapillary mucinous neoplasia (IPMN) and mucinous cystic neoplasm need to be developed[28]. Luo *et al*[29] documented that cg10673833, a circulating tumor DNA (ctDNA) methylation marker was found to be very sensitive (89.7%) and specific (86.8%) for the detection of colorectal cancer and its associated pre-cancerous lesions. SEPT9 was the first blood-based screening test that the Food and Drug Administration approved for colorectal cancer. Cancer-seek was developed by Tivey *et al*[30]. It is a blood test that detects circulatory protein and cfDNA biomarkers. It is capable of detecting eight cancer types, mostly in their respective advanced stages, with a specificity of 99% and a sensitivity of 69%-98%, which varied based on cancer type[12,20].

PANCA AND ITS ASSOCIATED BENIGN DISEASES

Systemic approaches to develop biomarkers to distinguish PDAC from other precancerous lesions are of great importance as they will also support the early diagnosis of PDAC and substantially improve outcomes. Single gene analysis has its limitation in early detection because it has been observed that the specificity and sensitivity of biomarkers in combination increase more than single biomarkers. Traditional serum-based biomarkers like CA19-9, CA125, and carcinoembryonic antigen (CEA) for PanCa diagnostics are of immense importance, but there is a need for the development of more sensitive and specific non-invasive biomarkers. The sensitivity and specificity of detection are usually much higher when the above three biomarkers are used jointly instead of individually[21,31]. In addition, varied combinations of DNA methylation-based biomarkers are being developed to better understand the complexity of the diseases including both the initiation and neoplastic stages. Concurrently addressing the contribution of immune cells in the cfDNA pool and its associated methylation or hydroxyl-methylation pattern is of great importance as it can be obtained from plasma samples[32-35].

Almost 50 of 100000 people are affected by CP worldwide with an increasing trend, and a CP-associated prolonged inflammatory state enhances tissue conversion to neoplasia. Pancreatic tumor (PT) formation is also increasing along with CP worldwide. Mortality due to PTs is close to 6%. After a diagnosis of CP, it takes almost 10 years before tumor symptoms appear, which is a long latency period with sufficient time for early diagnosis and treatment *via* non-invasive approaches. *PENK* DNA methylation has been observed broadly in precancerous lesions of various grades including extraductal and intraductal PTs and CP along with PanIN, IPMN and mucinous cystic neoplasm. *PENK* methylation alterations increased as the neoplastic tissue grade increased but was absent in the case of AIP and adjacent normal pancreatic tissue[36].

In a study of an 87 gene panel, 6 genes, namely *PRKC, IKZF1, CD1D, KCNK12, CLEC11A* and *NDRG4*, were shown to have clinical ability and potential as a cfDNA diagnostic biomarker for PanCa[37]. In this

study using pancreatic juice taken from PanCa, CP and healthy patients, the authors documented that most of the biomarkers were successful in discriminating patients with PanCa from healthy patients, but only *CD1D* was successful in discriminating patients with CP from PanCa with a sensitivity of 84%[37,38]. A remarkable change in methylation status was documented by Liggett *et al*[39], where they showcased that hypomethylated genes in CP converted to hypermethylated genes in PanCa, suggesting that altered methylation is also a driving reason for neoplasia development in the case of PTs.

A total of 14 genes, namely *CCND2, CDKN2B, DAPK1, MUC2, MYOD1,* promoter A of *MLH1, CDKN1C, ESR1, MGMT PGK1*, the proximal region of the *PGR* promoter, *RARB, RB1* and *SYK*, were successful in distinguishing CP from PanCa based on cfDNA DNA methylation profiling with 91% sensitivity and specificity[38,39]. In a study to identify cell death specific to tissue type by Lehmann-Werman *et al*[40], they observed that *CUX2* and *REG1A* are specific to pancreas tissue type. They also found these genes to be hypomethylated in plasma in both PanCa and CP, but the levels were lowered in other lower neoplastic grade lesions. *CUX2* was more hypomethylated in the case of PanCa and *REG1A* was higher in CP, which gives the ability to discriminate CP from PanCa based on tissue death irrespective of etiology[38,40].

In a study using pancreatic juice samples collected from PanCa and other associated precancerous lesions, six genes were demonstrated to be differentially methylated between CP and PanCa[41]. The six genes, *TFPI2, NPTX2, FOXE1, p16, ppENK* and *CyclinD2*, were able to successfully distinguish between CP and PanCa as CP had lower levels of methylation than PanCa. Similarly, the levels differed amongst healthy tissue and high-risk patients creating a gradient of altered methylation across various stages starting from healthy to precancerous to PanCa samples. It was also able to distinguish between IPMN and PanCa based on cfDNA methylation from pancreatic juice samples. Further, the study also attempted to address the limitations of IPMN diagnostics, which cytology mostly fails[42]. Promoter DNA methylation of the *CDO1* gene was identified to be involved in early-stage PanCa based on cytological experiments. cfDNA methylation analysis of *CDO1* from PanCa, CP and AIP patients showed that significant promoter methylation was associated with PanCa but was absent in CP and AIP [43]. In another study, *CD1D* showed cfDNA methylation when analyzed in pancreatic juice samples of PanCa [area under the curve (AUC): 0.92], but no methylation was documented in benign diseases[21,43]. In a study by Humeau *et al*[44], they reported that urine and sputum are also suitable alternatives to plasma for cell-free nucleic acid biomarker development. The utility of other material such as urine as a source of non-invasive testing needs further data and investigation.

MicroRNA (miRNA), namely hsa-miR-23a and hsa-miR-23b, have been documented to be overexpressed in IPMN patient saliva, which makes it a suitable precancerous lesion biomarker. It was also observed that hsa-miR-210 along with let-7c signals may be leveraged from saliva in distinguishing CP from healthy subjects[32,44]. Su *et al*[45] concurrently conducted a study using serum as a sample source and observed that miR-877, miR-3201, miR-890, miR-602 and miR-16-2-3p were successful in distinguishing low-risk and high-risk PDAC[32,45]. Irrespective of this development, there is still a hindrance in using miRNAs in clinical diagnostics due to reproducibility issues and variable expression of miRNAs. However, substantial work is ongoing in this area[32].

In a study to differentiate PDAC from CP by Bosch *et al*[46], it was documented that the the presence of a high level of soluble AXL (sAXL) was associated with lower overall survival in the case of PDAC. When identified from plasma, a higher level of sAXL was documented in PDAC than in CP and healthy controls, and they concluded that it is a potential biomarker for discriminating CP from PDAC and useful in identifying the onset of PDAC by its increasing level during monitoring. The findings were also validated in murine models. sAXL was also found to be overexpressed in IPMN, which is a pre-PDAC stage[46].

Weeks *et al*[47] conducted research where they studied the urine proteome differences amongst PDAC, CP and healthy individuals. They noticed 101 proteins that were significantly altered in PanCa and CP. S100A9 was found to be downregulated in PanCa but overexpressed in CP. Annexin A2, CD59 and gelsolin proteins were also found to be dysregulated in PDAC samples[47]. An isotope-coded affinity tag tended to successfully distinguish between PanCa and CP based on quantitative protein expression[41]. In this review, we documented the important cell free biomarkers that are vital in the early-stage detection of PanCa and are able to distinguish PanCa from its non-malignant precursors.

CFDNA AND ITS ASSOCIATED SECRETED PROTEOME

cfDNA in PanCa and its association with benign pancreatic diseases

First reported in 1948 by Mandel and Meta[48], cfDNA is undoubtedly the most dominant form among the liquid biopsy-based approaches and when released by tumor is also a ctDNA. Leon *et al*[49] in 1977 introduced cfDNA levels, which were found to be notably more advanced in malignancies than in healthy individuals thereby showcasing its role in carcinogenesis. Similar observations were made in 1983 with PDAC patients, and it was noted that cfDNA levels were higher in PDAC patients than in CP and acute pancreatitis[50]. The origin of cfDNA in the blood can be due to release from tumors, apoptosis or necrosis and other active cellular secretions. A major factor leading to the rise in cfDNA

studies in cancer management is the half-life of cfDNA, which is around 16 min-2.5 h, and that it can be monitored for overall disease progression and associated clinical prognosis with medical treatment (Table 1)[12,49,51].

Cancer diagnosis and treatment face a major setback from recurrence of the malignancy that cannot be ideally monitored using traditional techniques due to the lack of proper tumor formation and its associated diagnostic techniques. Postoperative or post-chemotherapeutic analysis of ctDNA in the blood can also be referred to as minimal residual disease (MRD) analysis. Minimal residual disease analysis cannot be ideally performed using imaging and traditional biopsy techniques, and the analysis using cfDNA/ctDNA is a great advance to measure tumor recurrence (Table 1)[12,52].

In terms of aberrant DNA methylation, which is also a common observation in PDAC patients, it has been documented that a change in methylation levels has been observed in various stages of dysplasia [53,54]. This indicates that the level of cfDNA methylation across various pre-PanCa lesions to PDAC is altered providing a candidate opportunity to track PDAC progression. In 2009, Melnikov *et al*[55] established the use of cfDNA methylation in PDAC diagnosis from 30 plasma samples. This was completed using microarray technology where they identified that the promoter region was hypomethylated in five genes with a sensitivity and specificity of 76% and 59%, respectively[55]. A crucial step in PanCa treatment is staging as that provides a proper clinical treatment approach and is associated with DNA promoter hypermethylation. Henriksen *et al*[56] reported that the use of cfDNA promoter hypermethylation as a prognostic biomarker in PDAC staging, which is based on the hypothesis that cfDNA methylation is stage-specific, can help in stage classification. Henriksen *et al*[56] analyzed a set of 28 genes in PDAC plasma samples. They developed the first prognostic prediction model using cfDNA hypermethylation targeting PDAC staging. They separated cluster cases with and without distant metastasis. The researchers were also able to document significantly higher numbers of hypermethylated genes clustering in stage IV PDAC than in earlier stages amongst which *BNC1* was the most significant gene of interest (Table 1)[25,27,56].

A crucial challenge in cell free nucleosome identification for the differentiation of benign pancreatic disease from PanCa is a nonspecific rise of cell free nucleosome levels in the serum of patients while quantifying the cell free nucleosome. Bauden *et al*[36] identified the cell free nucleosome epigenetic alterations specific to disease type and stages by isolating intact nucleosomes and then quantifying them using an enzyme-linked immunosorbent assay. They were successful in quantifying five serum cell free nucleosome diagnostic biomarkers with an AUC of 0.95, which differentiated PanCa from a healthy pancreas. The epigenetic profiles of cell free nucleosomes often differ between individual patient serum samples based on cancer and healthy populations. Understanding that the epigenetic changes usually occur at the onset of the neoplastic transformation stages, those already in pre-neoplastic stages may represent cell free nucleosome profiles that can act as possible cell free biomarkers for the early detection of cancer (Table 1)[36].

Role of cfDNA as a diagnostic and therapeutic biomarker

Tumors in the pancreas can occur in tissues that are hard to isolate due to their depth of location and also small tumor size can be a limitation. Therefore, in this context blood-based cell free biomarkers are of high clinical importance[56]. Melnikov *et al*[55] investigated that they developed the MethDet56 test which contained screening of 56 gene promoters from PDAC plasma samples that identified five promoters namely *CCND2, SOCS1, THBS1, PLAU* and *VHL* with significant aberrant DNA methylation and with sensitivity and specificity of 76% and 59% respectively. These are initial biomarker development work showcasing that blood-based biomarkers could be highly valuable in diagnosis and prognosis if further studied and developed[55]. In a study by Sato *et al*[57], three out of six genes, namely *CLDN5, SFRP1* and *NPTX2*, previously validated in tissue samples were found to be differentially methylated in pancreatic juice samples collected from PTs[38,57]. However, Matsubayashi *et al*[42] concluded that five genes that were previously validated by solid biopsy failed were not replicated in liquid biopsy. Although the genes *TFPI2*, *PENK, CCND2, NPTX2* and *FOXE1* were successfully able to discriminate PanCa from healthy tissue, the analysis failed to discriminate CP from PanCa or healthy tissue based on cfDNA methylation (Table 1)[42,55].

Yi *et al*[58] interestingly found the use of *BNC1* and *ADAMTS1* as novel serum-based biomarkers for early PanCa detection. The same research group concluded that low frequencies of these two genes were observed in pancreatitis, and there was a significant methylation difference between PanINs and PanCa. *BNC1* could still be detected in PanIN-1, but *ADAMTS1* could only be detected significantly in invasive PanCas[58]. Li *et al*[59] reported in an analogous study that *BNC1* and *SEPT9* were found to be highly methylated in PanCa and were suggested to have a significant role in PanCa diagnostic cfDNA biomarker development from plasma. A limitation of the study was that cfDNA methylation level in plasma was also found to be elevated in other benign diseases such as CP, acute pancreatitis and other lesions as these are risk factors leading to PT formation. This suggests a possible role of methylation changes in driving the progression of benign lesions to metastatic PanCa[60].

Global epigenetic alterations in 5-methylcytosine (5mC) and 5-hydroxymethylcytosine (5hmC) work as standalone entities in carcinogenesis[61]. Cao *et al*[62] concluded in this context that 5mC as well as 5hmC work as effective cfDNA in PDAC diagnostics and that when 5mC-5hmC work as an integrated system it provides an enhanced diagnostic power. As reported by Guler *et al*[33], PanCa early detection

Table 1 Cell free DNA involved in pancreatic cancer diagnostic and prognostics

Target candidate	Up/down	Sample	Potential value
CEA mRNA	Up	Whole blood	D
EGFR mRNA	Up	Serum	D
4GnT mRNA	Up	Whole blood	D
COL6A3 mRNA	Up	Serum	D/P
Mir-155	Up	Plasma	D
miR-196a	Up	Plasma	D
miR-21	Up	Plasma	D
miR-210	Up	Plasma	D
miR-155	Up	Pancreatic juice	D
miR-21	Up	Plasma	D
miR-196a	Up	Serum	D/P
miR-200a	Up	Serum	D
miR-200b	Up	Plasma	D
miR-210	Up	Plasma	D
miR-18a	Up	Plasma	D/T
miR-16	Up	Plasma	D
miR-196a	Up	Plasma	D
miR-185	Up	Serum	D
miR-191	Up	Serum	D
miR-20a	Up	Serum	D
miR-21	Up	Serum	D/P
miR-24	Up	Serum	D
miR-25	Up	Serum	D
miR-99a	Up	Serum	D
miR-1290	Up	Serum	D
miR-221	Up	Plasma	D/T/P
miR-375	Down	Plasma	D/T/P
miR-375	Up	Plasma	D
miR-27a3p	Up	Whole blood	D
miR-196a	Up	Serum	D
miR-196b	Up	Serum	D
miR-205	Up	Pancreatic juice	D/P
miR-210	Up	Saliva	D/P
miR-492	Up	Plasma	D/P
miR-1427	Up	Plasma	D/P
miR-22	Up	Plasma	D
miR-642b	Up	Plasma	D
miR-885-5p	Up	Plasma	D
Multigene index	Up	Whole blood	D
miR-483-3p	Up	Plasma	D
MIR-21	Up	Serum	D

MIR-210	Down	Serum	D
MIR-155	Up	Serum	D
miR-222	Down	Serum	D
miR-203	Down	Serum	D
miR-132	Down	Serum	D
miR-212	Down	Serum	D
miR-96	Down	Serum	D
mi-126	Down	Serum	D
mi-217	Down	Serum	D
Let-7	Down	Serum	D
miR-144	Down	Serum	D
miR-148	Down	Serum	D
miR-34a	Down	Serum	D
miR-3548	Up	Serum	D

CEA: Carcinoembryonic antigen; D: Diagnostic; P: Prognostic; T: Therapeutic; miR: MicroRNA.

is suitable using 5hmC-based detection techniques, and a regression model showed an AUC of 0.919 encompassing a highly variable gene set. The low cfDNA methylation observation in the case of PDAC was consistent with other studies, and it corresponded to *KRAS* mutation increase in malignancy. PDAC 5-hmC increase was observed at the transcription start site and 3' untranslated region, but a decrease was seen in the promoters[33]. cfDNA-based *KRAS* mutation identification is usually a good indicator of neoplasia though with limited specificity. *KRAS* remains a widely used gene for the early stage detection of PanCa. Other gene mutations, such as *DNMT3A, TP53, GNAS, JAK2* and *BCORL1*, remain alternative ctDNA-based biomarkers[24,63-65]. However, it is clear that analysis of somatic genes in ctDNA provides limited sensitivity in detecting early-stage tumors (Table 1).

Cell free protein (secreted proteome) in PanCa and its associated benign pancreatic diseases

The secreted proteome often acts as a suitable diagnostic biomarker, but currently only CA19-9 is a Food and Drug Administration-approved biomarker for PDAC diagnosis. It has substantial drawbacks and lacks a proper proteomic dataset for PanCa. Often false negative CA19-9 results are given by patients with *FUT3* mutations, and false positives are also observed in non-malignant CP patients as CA19-9 is usually very highly overexpressed[46].

The plasma-free amino acids (PFAAs) index is growing in popularity as a suitable approach for the diagnosis of PanCa. A study to compare the PFAAs index between PanCa and healthy controls by Fukutake *et al*[66] found PFAAs as a significant biomarker capable of distinguishing PDAC. The receiver operating curve AUC developed index was demonstrated to suitably discriminate PanCa from controls. PFAAs are modulated by metabolic changes, in particular in organ systems based on disease induction. As a result, most metabolomic studies consider the analysis of the PFAAs index[66]. Sources of protein biomarker analysis are usually blood and pancreatic juice, but it can also be validated from tissue samples. Wu *et al*[21] documented that altered levels of proteins, namely GPC1, PFAA, OPNT + TIMP-1, CPA4, MUC5AC and C4BPA, were observed in the serum of PanCa patients. They also documented that GPC1 level was significantly higher in PanCa patients than in patients with benign pancreatic diseases such as CP or AIP. It was also documented that serum levels of cell free CPA4 were significantly higher in PanCa than in healthy controls with a parallel observation that C4BPA was comparatively more sensitive than CA19-9. A crucial observation was based on PFAA where it was revealed that PFAA levels correlated with PanCa staging and that can be used for pathological PanCa staging. A significantly high level of serine in plasma was also documented along with a significant decrease in threonine levels in PanCa patient plasma (Table 2)[21,66,67].

Proteomic techniques are gaining a lot of attention for studying protein expression in PanCa. Urine as a source for the non-invasive analysis of biomarkers has gained attention. Advantages of using urine are: (1) Common proteins such as albumin are less abundant; (2) Sample processing is simpler (the plasma secreted proteome (secretome) is much more complex than the urine proteome); (3) Urine is more thermostable; and (4) 49% of proteins are soluble products in urine obtained from glomerular filtration of lymphatic fluids (indicates that various external sources contribute towards the pool of the urine proteome and its protein components). Similar studies have been completed in breast and ovarian cancers; and it is likely to remain an active area of investigation (Table 2)[47,68,69].

Table 2 Cell free protein (secreted proteome) involved in pancreatic cancer diagnostic and prognostics

Target candidate	Up/down	Sample	Target	Pathway	Potential value
ADAMTS1	Up	Plasma	ADAMTS1	Methylation	D
BNC1	Up	Plasma	BNC1	Methylation	D
CDKN1C	Up	Plasma	CDKN1C	Methylation	D
MLH1	Down	Plasma	MLH1	Mutation	D
PGR (prox)	Up	Plasma	PGR	Cell signaling	D
SYK	Up	Plasma	SYK protein, mRNA	Cell signaling	D
CCND2	Up	Plasma	Cyclin D2	Cell signaling	D
ALX4	Up	Plasma	Transcription factor	Mutation	P
APC	Down	Plasma	APC	Mutation	P
BMP3	Up	Plasma	TGFβ	Cell signaling	P
BNC1	Up	Plasma	BNC1	Cell signaling	P
BRCA1	Up	Plasma	BRCA1	Mutation	P
CDKN2B	Up	Plasma	Ink4, p16, p14	Cell signaling	P
CHFR	Up	Plasma	E3 Ubiquitin-protein	Cell signaling, check point	P
ESR1	Up	Plasma	ESR1, Transcription factor	Cell signaling	P
EYA2	Up	Plasma	EYA2	Cell cycle	P
GSTP1	Up	Plasma	GSTP1	Cell signaling	P
HIC1	Up	Plasma	HIC ZBTB TRANSCRIPTIONAL RECEPTOR 1	Cell signaling	P
MEST1v2	Up	Plasma	Alpha/Beta hydrolase superfamily	Cell signaling	P
Foxe1	Down	Pancreatic juice	Foxe1	Methylation	D
MGMT	Up	Plasma	MGMT	Methylation	P
MLH1	Up	Plasma	MLH1	Mutation	P
NPTX2	Up	Pancreatic juice	NP, synaptic proteins	Cell signaling	P
NEUROG1	Up	Plasma	NEUROG1	Cell signaling, regulatory network	P
RARB	Up	Plasma	RARB	Cell signaling	P
RASSF1A	Down	Plasma	RAS effector protein	Methylation	P
SFRP2	Up	Plasma	SFRP2	Wnt signaling	P
SEPT9v2	Up	Plasma	Septin9	Cell cycle	P
CDID	Up	Pancreatic juice	CDID	Methylation	D
PRKC	Up	Pancreatic juice	PRKC	Methylation	D
IKZF1	Up	Pancreatic juice	IKZF1	Methylation	D
KCNK12	Up	Pancreatic juice	KCNK12	Methylation	D
CLEC11A	Up	Pancreatic juice	CLEC11A	Methylation	D/P
NDRG4	Up	Pancreatic juice	*NDRG4* promoter	Methylation	D
SST	Up	Plasma	SST	Downstream signaling, transcriptional regulation	P

TFPI2	Up	Pancreatic juice	TFPI2	Gene silencing, cell adhesion plasmin signaling	P
TAC1	Up	Plasma	TAC1	Gpcr downstream, signal transduction	P
VIM	Up	Plasma	Vimentin	Cell signaling	P
WNT5A	Up	Plasma	WNT5A	Wnt signaling	P
PENK	Up	Pancreatic juice	Proenkephalin	Apoptotic, downstream signaling	
DCC	Down	Plasma	Netrin-1 Receptor	Mutation	D
P16	Down	Pancreatic juice	CDKN2A	Mutation, cell cycle regulation	D
P14	Down	Plasma	CDKN2A	Cell cycle	D
DNMT1	Up	Plasma	DNMT1	Mutation	D
DNMT3A	Up	Plasma	DNMT3A	Methylation	D
DNMT3B	Up	Plasma	DNA	Methylation	D

D: Diagnostic; P: Prognostic.

Role of secretome as a diagnostic and therapeutic biomarker

Cell free nucleic acid alone or combined with the secretome is likely to enhance sensitivity in PanCa diagnosis, and it remains an area of high interest in the field. Research often claims that patients with some signature of circulating proteins ideally overlap with circulating DNA. The main issue is that cfDNA and cell free proteins are most often seen in advanced stages than in early stages[63]. A secretome study to identify cell free proteins as biomarkers in PanCa is usually dominated by the urine proteome. In a study by Poruk *et al*[70], the researchers validated a pair of biomarkers to distinguish between PDAC and healthy controls as well as distinguishing it from CP. This group also focused on the ability of the biomarker to identify the early onset of the disease. The pair of biomarkers were OPN and TIMP-1, and they were found to be uniformly overexpressed in the case of PDAC. Due to their tendency to be available as the secretome in blood, they were easy to detect and were shown to be a useful tool for diagnosis. OPN particularly acts as a more advanced prognostic biomarker by itself[70-72]. Urine samples are also a reliable source of cell free biomarker isolation and identification.

A three-protein biomarker panel was developed from urine samples of PDAC patients and were assayed using GeLC/mass spectroscopy (MS)/MS and validated using an enzyme-linked immunosorbent assay. The candidate protein biomarkers were namely LYVE-1, TFF1 and REG1A, and they provided an AUC of 0.89. These biomarkers were able to distinguish between early-stage PDAC and advanced-stage PDAC and were almost consistent with CA-19 levels that were documented in regard to every PDAC stage. The panel was also able to distinguish between PDAC and CP based on the higher levels of biomarkers in PDAC than in CP as well as PDAC stage I-II. The concentrations of these proteins were significantly higher than CP, which generated a clear demarcation between these groups [73].

Kaur *et al*[74] reported MUC5AC as a suitable biomarker candidate for PanCa diagnosis based on its capability to differentiate between PanCa, CP and AIP. Another urine-based diagnosis study claimed that neutrophil gelatinase-associated lipocalin can provide valuable information on the onset of PanCa identification[21,74]. Considering that pancreatic juice collection is an invasive process, the parallel study was completed studying the role of ARG2 as PanCa biomarker, which was specific in targeting the bile component for PanCa early-stage detection. sLR11, which is present in the bile of PanCa cases, was able to discriminate between PanCa and healthy controls[75]. A panel of CA19-9, CA 242, CA 125 and CEA obtained from serum showed a sensitivity and specificity of 90% and 94%, respectively[76,77]. A novel nucleosome marker panel developed by Bauden *et al*[36] showed better sensitivity than CA19-9 in discriminating PanCa from a healthy control. The markers were *H3K4Me2, H2AZ, H2AK119Ub, H2A1.1* and 5mC[36]. Additionally, as documented by Melo *et al*[78], the absolute prediction (AUC = 1.0) of PanCa using glypican 1 on exosomes identified by MS showed utility as a biomarker (Table 2).

cfRNA in PanCa and its association with benign pancreatic diseases

Amidst the traditional serum-based biomarkers like CA19-9, CA125 and CEA for PanCa diagnostics, there is an immense need for the development of more sensitive and specific non-invasive biomarkers. Sensitivity and specificity are usually higher when the three are used jointly (Table 3)[21,31].

Uncontrolled proliferating cancer has a high mortality rate, and treatment and diagnosis are also difficult due to the lack of screening imaging modalities and specific biomarkers. Emerging evidence of biomarkers generated from tumor cells contains a high quantity of RNA in the bloodstream that block

Table 3 Cell-free RNA involved in pancreatic cancer diagnostic and prognostics

Target candidate	Up/down	Sample	Target	Pathway	Potential value
ERBB2	Up	Plasma	Ch 12, *KRAS*	Mutation	D
CDKN2A	Down	Plasma	Gene, Ch 9p21	Mutation	D
SMAD4	Down	Plasma	TGFβ	Cell signaling	D
TP53	Down	Plasma	P53 protein	Mutation/cell signaling	D
EGFR	Up	Plasma	Exon 19, 21	Cell signaling/mutation	D
PBRM1	Down	Plasma	SWI/SNF ch remodeling comp	Mutation, immune checkpoint blockade	D
KMT2D	Down	Plasma	FOX1-miR-1224, HIF/GATA5-miR-133a	Mutation	D
RNF43	Down	Plasma	RNF43PROTEIN	Wnt signaling	D
TP63	Down	Plasma	P63 protein	Cell signaling	D
MTOR	Up	Plasma	mTOR	mTOR signaling	D
NRAS	Up	Plasma	*NRAS*	Mutation	D
HRAS	Up	Plasma	*HRAS*	Mutation	D
BRCA1	Down	Plasma	BRCA1	Signaling	D
BRCA2	Down	Plasma	BRCA2	Signaling	D
PALB2	Up	Plasma	PALB2	Signaling/mutation	D
GPC1	Up	Serum	MAPK, PI3K-AKT-mTOR, Hedgehog signaling	Cell signaling	D
PFAA	Up	Serum	MAPK, PI3K-AKT-mTOR, Hedgehog signaling	Cell signaling	D
OPNT+TIMP-1	Up	Serum	MAPK, PI3K-AKT-mTOR, signaling	Cell signaling	D
CPA4	Up	Serum	MAPK, mTOR, Hedgehog signaling	Cell signaling	D
MUC5 AC	Up	Urine/pancreatic juice	MAPK, PI3K-AKT-mTOR, Hedgehog signaling	Cell signaling	D/P
C4BPA	Up	Serum	MAPK, PI3K-AKT-mTOR, Hedgehog signaling	Cell signaling	D
OPN	Up	Serum	OPN	Cell signaling	P
TIMP-1	Up	Serum	TIMP-1	Cell signaling	D
NGAL	Up	Urine	Receptor binding protein	Cell signaling	D
ARG2	Down	Pancreatic juice	Beta cell function	Cell signaling	D
LYVE-1	Up	Urine	Receptor binding glycoprotein		D
TFF1	Up	Urine	Regulation of transcription factor	Promoter modeling	D
REG1A	Up	Urine	REG1A protein	Cell signaling	D

NGAL: Neutrophil gelatinase-associated lipocalin; miR: MicroRNA; D: Diagnostic; P: Prognostic.

RNases in blood. They also showcase sufficient levels for quantitative analyses[79]. Living cells consistently release RNA, which is encapsulated inside big lipoprotein complexes, namely exosomes/microvesicles (MVs). RNA that is obtained from dead or dying cells found from blood is connected with apoptotic bodies and protein complexes[80].

Exosomes range from 40-140 nm in diameter and are made of lipoprotein membranous vesicles of endocytic origin. They are formed from the fusion of multivesicular bodies with the plasma membrane. They are released into extracellular spaces thereafter[81]. MVs are much larger than exosomes and have a diameter ranging from 100-1000 nm. They have heterogeneous morphologies, and they originate from the plasma membrane by budding with the extracellular space.

Apoptotic bodies are morphologically MVs that are heterogeneous in shape, spanning 50-500 nm in diameter, and contain organelles. They are released *via* outward protrusion from the plasma membrane

during the late phase of apoptosis[82]. Several studies have demonstrated that tumors specifically secrete exosomes or MVs, which contain specific miRNAs. However, Arroyo *et al*[83] stated that miRNAs in circulation are principally found in the Ago2 ribonucleoprotein complex and not vesicles. This indicates that detected miRNAs are derived mostly from apoptotic and necrotic processes, which occur frequently in tumor cells. These circulating RNAs are found in the plasma or serum of patients and are upregulated when compared to healthy patients.

A significant amount of RNA biomarkers have been shown to be circulating miRNAs and are mostly tissue specific. Some reports found tumor-specific upregulation of various types of small noncoding RNAs (ncRNAs), such as small nuclear RNAs, Piwi-interacting RNAs and long ncRNAs (lncRNAs) like HOTAIR and MALAT1. They act as diagnostic and prognostic markers in the serum or plasma of cancer patients[84,85]. Amidst that, some have reported alterations in gene expression according to disease progression, which discriminates between a chronic inflammatory state and carcinoma (Table 3)[86,87].

Funaki *et al*[88] detected *CEA* mRNA by real-time reverse transcription PCR in the whole blood of PanCa patients. Clarke *et al*[89] also detected *EGFR* mRNA in the serum and detected alpha 1,4-N-acetylglucosaminyltransferase mRNA in the mononuclear cell fraction of peripheral blood from PanCa patients. Kang *et al*[90] further demonstrated that serum-type collagen mRNA acts as good marker of PanCa. It undergoes tumor-specific alternative splicing, which is expected to result in high specificity (Table 3).

In PanCa, the tumor suppressor genes *p53*, *p16* and *SMAD4* are rendered inactive by the miRNAs, which are produced only in tumor tissues[91]. In pancreatic cell lines and tissue, miR-21 is increased, which drastically lowers the survival rate. In the *KRAS* (G12D) animal model, it has been reported that miR-21 overexpression is the lesion onset point that leads to tumor growth. miR-155 is also overexpressed in PanCa. This aids in the development of tumors. Decreasing the expression of miR-155, *MT1-MMP, KRAS,* and *EGFR* inhibits cell growth. miR-221 is also upregulated in PanCa and promotes distant metastasis as well as unresectable tumors[92]. In approximately 50%-70% of cases of PanCa in humans, the *p53* gene has a point mutation. Hypoxia with malnutrition trigger stress signaling in cells that upregulates *p53*, which increases the expression of numerous genes, including *MIR-107*, *MIR-34a/b/c* and *MIR-34* (Table 3)[15,65,86].

Role of cfRNA as a diagnostic and therapeutic biomarker

According to some reports, miRNA dysregulation has been reported in feces, urine and saliva, which are easy to obtain by non-invasive methods. The levels of miR-143, miR-223 and miR-30 were seen to be higher in the urine of patients with stage I disease. The combination of miR-143 with miR-30 showed very high sensitivity and specificity of 83.3% and 96.2%, respectively. Yang *et al*[93] reported that the levels of miR-21 and miR-155 were much higher in PanCa patient stool when compared with healthy controls. Recently studies revealed that salivary miRNAs were stable because of the protection of exosomes or protein complexes, thus highlighting promising roles as diagnostic markers. *SNHG15* serum expression exerts an average diagnostic value (Table 3)[94].

Liao *et al*[95] found that plasma snoRNA *SNORD33/66/76* might serve as a diagnostic biomarker for non-small cell lung cancer (NSCLC) using comprehensive next generation sequencing analysis. Wang *et al*[96] detected the expression of miRNAs in the plasma of patients with PDAC and identified miRs-21, miR-210, miR-155 and miR-196a. They are upregulated in PanCa tissue and cell lines as candidate biomarkers, and miR-200a/b, miR-18a, miR-221 and miR-196a/b have been found to be upregulated in the serum/plasma in parallel with cancer tissues by comprehensive sequence and microarray analysis (Table 3)[96,97].

Kishikawa *et al*[86] suggested that some miRNAs, such as miR-16, miR-223 and let-7, are highly and constantly expressed in the serum/plasma and are correlated with the number of blood cells. Tang *et al*[98] found higher levels of three lncRNAs, long intergenic non protein-coding RNA 1627 (LINC01627), LINC01628 and ERICH1 antisense RNA 1 (ERICH1-AS1; also known as DLGAP2), in the plasma from patients with NSCLC than in samples from healthy individuals after microarray assay. They proposed a potential diagnostic signature for NSCLC based on these lncRNAs. Anfossi *et al*[99,100] suggested that urine levels of miR-148a and miR-375 have been found to be significantly downregulated and upregulated, respectively, in patients with prostate cancer and enabled patients with prostate cancer to be distinguished from healthy individuals (Table 3).

Higher levels of expression of hsa-miR-106a, hsa-miR-125a-5p, hsa-miR-129-3p, hsa-miR-375, hsa-miR-205, hsa-miR-29b, hsa-miR-21 and hsa-miR-7 in histopathology as well as in cytology samples using real-time reverse transcription PCR act as valuable diagnostic biomarkers in different types of cancer[101]. Also, miR-21, miR-210, miR-155 and miR-196a, which have been upregulated in PanCa tissue and cell lines, have been identified by Wang *et al*[96] as candidate biomarkers. A possible diagnostic biomarker for malignant melanoma is miR-221. Li *et al*[103] found that patients with high serum miR-221 levels had significantly worse 5-year relapse-free survival (12.5% *vs* 45.2%; $P = 0.008$). Increased circulating levels of miR-221 allowed patients with melanoma to be discriminated from healthy individuals ($P = 0.0001$) (Table 3)[103].

Rac1 downregulation leads to the switching of the MKK4-JNK-c-Jun pathway, which silences miR-124. In response to TGF, miR-200a and miR-205 are downregulated in PDAC during epithelial-mesenchymal transformation (EMT), while miR-21 overexpression is identified as the lesion initiator

that drives tumor growth in a *KRAS* (G12D) animal model. miR-155, which is elevated in PanCa, aids in the development of tumors.

Karandish *et al*[104] suggested that stress signaling in cells induced by hypoxia and starvation upregulate *p53* and activate the expression of several genes, such as *MIR-107*, *MIR-34a/b/c* and *MIR-34*. Mutation of *p53* mediates transcription of *MIR-130b* and *MIR-155*, which modifies the expression of the corresponding target genes (*ZEB1* and *ZNF652*). This leads to cell proliferation and invasion in several cancers. *ZEB1* has been shown by Wellner *et al*[106] to control the activation of EMT in pancreatic cancer stem cells and to suppress the production of the miR-200 family[104]. In addition, *p53* mutation impairs the maturation of miR-145 and miR-16-1 causing cell proliferation, invasion and migration in PDAC (Table 3).

As a long intergenic non-protein coding RNA, *p53* induced transcript (Linc-pint) is ubiquitously expressed in humans and acts as a direct *p53* transcriptional target. Plasma lncRNA Linc-pint was significantly decreased in patients with PanCa, carcinoma of the ampulla of Vater and cholangiocarcinoma compared with healthy volunteers[108]. Therefore, Linc-pint might be used for identifying the cause of malignant obstructive jaundice and helping to trace the origin of the cancer. Some of these results indicate that low plasma Linc-pint expression could serve as a minimally invasive biomarker for early PanCa detection and that low Linc-pint levels in PanCa tumors could be used for predicting patient prognosis(Table 3)[103].

Prior studies revealed that upregulation of chromatin-interacting lncRNA along with MEG3 inhibited PanCa cell proliferation with the activation of *p53*. Additionally, lncRNA-NUTF2P3-001 contributed to PanCa proliferation and invasion by activating the miR-3923/KRAS signaling pathway. Moreover, LOC389641 promoted the progression of PDAC and increased cell invasion by regulating E-cadherin with the possible involvement of *TNFRSF10A* (Table 3)[109].

The d-signature comprises eight extracellular vesicle long RNAs, including *FGA, KRT19, HIST1H2BK, ITIH2, MARCH2, CLDN1, MAL2* and *TIMP1*, for PDAC detection, and the d-signature could distinguish between CA19-9 negative PDAC cases and healthy controls, thus complementing the use of CA19-9 in PDAC detection. It could also distinguish PDAC from CP with high accuracy. Circ-LDLRAD3 was found to be increased in PanCa tissues as well as in plasma samples. It was markedly related to lymphatic invasion, along with venous invasion and metastasis. Circ-LDLRAD3 has not been reported as an ideal standalone biomarker but may be in combination with CA19-9[110].

The circRNAs *PDE8A* and *IARS* are present in the plasma exosome. They were upregulated along with a concurrent association with prognosis and progression of PanCa. They were also likely to be promising biomarkers in the detection of early-stage PanCa. When compared with the healthy controls, circ-001569 levels were higher. Aberrant levels of *CPA4, PFAA, MUC5AC, GPANCA1, OPNT* + *TIMP-1* and *C4BPA* were frequently reported in serum samples of PanCa patients. In pancreatic juice samples, the higher regulation of ARG2 signifies its role as a biomarker for PanCa diagnosis. Neutrophil gelatinase-associated lipocalin in urine also provides some clue for early diagnosis of PanCa (Table 3)[111,112].

Role of immunological treatments in PanCa and non-malignant diseases

The lack of immune and targeted molecular therapies is a reason for treatment failure and lower survival rates[113]. The reason behind less efficient immune therapies in PanCa is unclear. Usually, PTs are surrounded by thick desmoplastic stroma making targeted treatments less effective. Other reasons of immune therapy failure are chemokine-initiated barring of T cells followed by comparatively faulty antigenicity when compared to other solid tumors[114]. A model states that the systemic progression of PDAC development initiates from PanIN1 to PanIN3 and finally leads to invasive PDAC. This occurs when high progressive deposition of desmoplastic stroma and alteration of leucocyte infiltration happens[115].

The lower mutation burden in PDAC is partially due to poor antigenicity of the tumor microenvironment (TME). The abundant immunosuppressive TME plays a crucial role in blocking T cell activation, which further leads to lower immune therapy efficiency[116]. A significantly increased level of the *TH17* and *Th1* genes acts as an inflammatory immune marker[117]. A variety of immune biomarkers have been reported in PDAC. Those with sound prognostic capability are *CD3, CD4, CD8* and *CD20*. In contrast, increased expression of *CD163, FOXP3, CD204, CD68* and *CD66b* leads to poorer outcomes[114,118].

Interestingly, the presence of T cells has no clinical correlation with PDAC. Tumor-infiltrating CD3+ T cells have been identified in isolated PDAC tumors. However, due to the lack of CD3 zeta expression, the capability to activate T cell-associated receptor signaling has been lost and is under functioning [119]. The tumor immune microenvironment and TME of PDAC is peculiar when compared with other solid tumors because immune therapy does not yield significant results in PanCa treatment. PD-L1, CTLA-4 and PD-1 targeting antibodies are part of immune checkpoints, and inhibition of these targets has been successful in other malignancies but have failed in curative treatment of PanCa[120]. Of note, PD-L1 and PD-1 expression is significantly lower in PDAC than in other tumors. PD-L1 has high expression in almost 30%-40% of PanCa cases, which is correlated with CD8+ cells, thereby indicating a poor prognosis[120,121].

Table 4 Cell-free biomarkers involved in distinguishing pancreatic cancer from other pancreatic benign diseases

Biomarkers	CP	AIP	PanIN	IPMN	MCN
PENK DNA	Yes	No	Yes	Yes	Yes
CUX2	Yes	No	No	No	No
REGIA	Yes	No	No	No	No
TFP12	Yes	No	Yes	Yes	Yes
FOXE1	Yes	No	Yes	Yes	Yes
P16	Yes	No	Yes	Yes	Yes
NPTX2	Yes	No	Yes	Yes	Yes
PENK	Yes	No	Yes	Yes	Yes
CYCLIN D2	Yes	No	Yes	Yes	Yes
CDO1	No	Yes	No	No	No
HAS-mIR-23a	No	No	No	Yes	No
HAS-mIR-23b	No	No	No	Yes	No
HAS-mIR-210	Yes	No	No	No	No
Let-7c	Yes	No	No	No	No
S100A9	Yes	No	No	No	No
BNCI	No	No	Yes	No	No
ADAMTS1	No	No	No	No	No
BNC1	No	No	No	No	No
9-Sep	No	No	No	No	No
GPC1	No	No	No	No	No
PFAA	No	No	No	No	No
OPNT + TIMP-1	No	No	No	No	No
CPA4	No	No	No	No	No
MUC5 AC	No	No	No	No	No
C4BPA	No	No	No	No	No

AIP: Autoimmune pancreatitis; CP: Chronic pancreatitis; IPMN: Intrapapillary mucinous neoplasia; MCN: Mucinous cystic neoplasm; PanCa: Pancreatic cancer; PanIN: Pancreatic intraepithelial neoplasia.

CONCLUSION

Currently, a variety of specimens have emerged as possible sources for liquid biopsy analysis for diagnostic applications. Apart from plasma or serum, urine and sputum have also produced promising disease diagnostic results[44,122]. Liquid biopsies are ideally non-invasive or minimally invasive for sample collection, minimizing patient stress and discomfort. Non-invasive approaches can significantly aid clinical research and utility. Even the recurrence and metastasis of the disease can be potentially monitored based on the cfDNA methods (Table 4).

Therefore, in this review we highlighted the current development in tools for PanCa early diagnosis and prognosis. We demonstrated that useful data can be obtained based on DNA methylation signatures and mutations. The heterogeneity in the pool of cfDNA isolated from a suitable source, such as plasma, contains cfDNA molecules obtained from various origins, and various outcomes, such as DNA methylation or gene mutations, could be obtained from such material. The process of properly understanding the disease source and cfDNA origin has been facilitated significantly by advancements in technologies, such as single cell-based techniques[40]. These advancements can further facilitate liquid biopsy research associated with PanCa biomarker discovery. This also showcases that aberrant DNA methylation signatures harness a significant capability to guide PanCa disease management[32,51]. Approximately 300 clinical trials are currently ongoing that target the use of cfDNA biomarkers in the diagnosis of malignancies. Limitations include cfDNA isolation and sample processing and understanding the biology of ctDNA based on its release from tumors.

The outcome of the secretome can also support PanCa diagnosis significantly. Premalignant lesions such as PanIN are still facing detection challenges because no PanIN-specific protein has been clinically approved. The alterations in cell free nucleic acids does not always manifest into protein changes that can be clinically validated and utilized. However, the secretome in PanCa and secretome biomarkers specific to premalignant lesions are yet to be identified for clinical use but are likely to be highly useful in the future. Validation of biomarkers based on cfDNA alterations and subsequent protein expression can substantially help in the early diagnosis of PanCa and other pancreatic-associated diseases[51,123].

ACKNOWLEDGEMENTS

First, we would like to thank all the authors and clinicians whose valuable work has supported us in writing this review. Second, we also acknowledge clinicians from Tata Medical Center namely Dr. Sudeep Banerjee and Dr. Paromita Roy along with clinicians from Apollo Multispecialty Hospital namely Dr. Sumit Gulati and Dr. Supriyo Ghatak. Dr. Aniruddha Chatterjee would like to thank Rutherford Discovery Fellowship from the Royal Society of New Zealand and University of Otago, Dunedin, New Zealand for their support. The authors specifically thank and acknowledge Mr. Saraswan Sikdar.

FOOTNOTES

Author contributions: Bararia A and Chakraborty P wrote the first draft of the paper and constructed the flow chart and tables; Chatterjee A, Roy P, Chattopadhay B K, Das A and Sikdar N provided valuable input, suggestions, comments and guidance while writing the review manuscript and contributed to proofreading and editing; Sikdar N constructed, wrote, conceptualized, and edited the review manuscript.

Supported by the Department of Biotechnology, Government of India Grant Sanction, Ramalingaswami Re-entry Fellowship, No. RLS/BT/Re-entry/05/2012.

Conflict-of-interest statement: The authors declare no conflicts of interest.

Country/Territory of origin: India

ORCID number: Nilabja Sikdar 0000-0003-4465-472X.

S-Editor: Zhang H
L-Editor: Filipodia
P-Editor: Zhang H

REFERENCES

1 **Sharma S**, Tapper WJ, Collins A, Hamady ZZR. Predicting Pancreatic Cancer in the UK Biobank Cohort Using Polygenic Risk Scores and Diabetes Mellitus. *Gastroenterology* 2022; **162**: 1665-1674.e2 [PMID: 35065983 DOI: 10.1053/j.gastro.2022.01.016]

2 **Siegel RL**, Miller KD, Fuchs HE, Jemal A. Cancer statistics, 2022. *CA Cancer J Clin* 2022; **72**: 7-33 [PMID: 35020204 DOI: 10.3322/caac.21708]

3 **Kavaliauskas P**, Dulskas A, Kildusiene I, Arlauskas R, Stukas R, Smailyte G. Trends in Pancreatic Cancer Incidence and Mortality in Lithuania, 1998-2015. *Int J Environ Res Public Health* 2022; **19** [PMID: 35055770 DOI: 10.3390/ijerph19020949]

4 **Sikdar N**, Saha G, Dutta A, Ghosh S, Shrikhande SV, Banerjee S. Genetic Alterations of Periampullary and Pancreatic Ductal Adenocarcinoma: An Overview. *Curr Genomics* 2018; **19**: 444-463 [PMID: 30258276 DOI: 10.2174/1389202919666180221160753]

5 **Saha G**, Singh R, Mandal A, Das S, Chattopadhyay E, Panja P, Roy P, DeSarkar N, Gulati S, Ghatak S, Ghosh S, Banerjee S, Roy B, Chaudhuri D, Arora N, Biswas NK, Sikdar N. A novel hotspot and rare somatic mutation p.A138V, at TP53 is associated with poor survival of pancreatic ductal and periampullary adenocarcinoma patients. *Mol Med* 2020; **26**: 59 [PMID: 32552660 DOI: 10.1186/s10020-020-00183-1]

6 **Vasantharajan SS**, Eccles MR, Rodger EJ, Pattison S, McCall JL, Gray ES, Calapre L, Chatterjee A. The Epigenetic landscape of Circulating tumour cells. *Biochim Biophys Acta Rev Cancer* 2021; **1875**: 188514 [PMID: 33497709 DOI:

10.1016/j.bbcan.2021.188514]
7 **Kilgour E**, Rothwell DG, Brady G, Dive C. Liquid Biopsy-Based Biomarkers of Treatment Response and Resistance. *Cancer Cell* 2020; **37**: 485-495 [PMID: 32289272 DOI: 10.1016/j.ccell.2020.03.012]
8 **Krebs MG**, Metcalf RL, Carter L, Brady G, Blackhall FH, Dive C. Molecular analysis of circulating tumour cells-biology and biomarkers. *Nat Rev Clin Oncol* 2014; **11**: 129-144 [PMID: 24445517 DOI: 10.1038/nrclinonc.2013.253]
9 **Chen D**, Xu T, Wang S, Chang H, Yu T, Zhu Y, Chen J. Liquid Biopsy Applications in the Clinic. *Mol Diagn Ther* 2020; **24**: 125-132 [PMID: 31919754 DOI: 10.1007/s40291-019-00444-8]
10 **Qi ZH**, Xu HX, Zhang SR, Xu JZ, Li S, Gao HL, Jin W, Wang WQ, Wu CT, Ni QX, Yu XJ, Liu L. The Significance of Liquid Biopsy in Pancreatic Cancer. *J Cancer* 2018; **9**: 3417-3426 [PMID: 30271504 DOI: 10.7150/jca.24591]
11 **Siravegna G**, Mussolin B, Venesio T, Marsoni S, Seoane J, Dive C, Papadopoulos N, Kopetz S, Corcoran RB, Siu LL, Bardelli A. How liquid biopsies can change clinical practice in oncology. *Ann Oncol* 2019; **30**: 1580-1590 [PMID: 31373349 DOI: 10.1093/annonc/mdz227]
12 **Liu S**, Wang J. Current and Future Perspectives of Cell-Free DNA in Liquid Biopsy. *Curr Issues Mol Biol* 2022; **44**: 2695-2709 [PMID: 35735625 DOI: 10.3390/cimb44060184]
13 **Yokode M**, Shiokawa M, Kodama Y. Review of Diagnostic Biomarkers in Autoimmune Pancreatitis: Where Are We Now? *Diagnostics (Basel)* 2021; **11** [PMID: 33923064 DOI: 10.3390/diagnostics11050770]
14 **Henriksen SD**, Thorlacius-Ussing O. Cell-Free DNA Methylation as Blood-Based Biomarkers for Pancreatic Adenocarcinoma-A Literature Update. *Epigenomes* 2021; **5** [PMID: 34968295 DOI: 10.3390/epigenomes5020008]
15 **Minaga K**, Watanabe T, Hara A, Kamata K, Omoto S, Nakai A, Otsuka Y, Sekai I, Yoshikawa T, Yamao K, Takenaka M, Chiba Y, Kudo M. Identification of serum IFN-α and IL-33 as novel biomarkers for type 1 autoimmune pancreatitis and IgG4-related disease. *Sci Rep* 2020; **10**: 14879 [PMID: 32938972 DOI: 10.1038/s41598-020-71848-4]
16 **Kawa S**, Kamisawa T, Notohara K, Fujinaga Y, Inoue D, Koyama T, Okazaki K. Japanese Clinical Diagnostic Criteria for Autoimmune Pancreatitis, 2018: Revision of Japanese Clinical Diagnostic Criteria for Autoimmune Pancreatitis, 2011. *Pancreas* 2020; **49**: e13-e14 [PMID: 31856100 DOI: 10.1097/MPA.0000000000001443]
17 **Kamisawa T**, Chari ST, Lerch MM, Kim MH, Gress TM, Shimosegawa T. Recent advances in autoimmune pancreatitis: type 1 and type 2. *Gut* 2013; **62**: 1373-1380 [PMID: 23749606 DOI: 10.1136/gutjnl-2012-304224]
18 **Chatterjee A**, Bararia A, Ganguly D, Mondal PK, Roy P, Banerjee S, Ghosh S, Gulati S, Ghatak S, Chattopadhay BK, Basu P, Chatterjee A, Sikdar N. DNA methylome in pancreatic cancer identified novel promoter hyper-methylation in NPY and FAIM2 genes associated with poor prognosis in Indian patient cohort. *Cancer Cell Int* 2022; **22**: 334 [PMID: 36329447 DOI: 10.1186/s12935-022-02737-1]
19 **Bararia A**, Dey S, Gulati S, Ghatak S, Ghosh S, Banerjee S, Sikdar N. Differential methylation landscape of pancreatic ductal adenocarcinoma and its precancerous lesions. *Hepatobiliary Pancreat Dis Int* 2020; **19**: 205-217 [PMID: 32312637 DOI: 10.1016/j.hbpd.2020.03.010]
20 **Cohen JD**, Li L, Wang Y, Thoburn C, Afsari B, Danilova L, Douville C, Javed AA, Wong F, Mattox A, Hruban RH, Wolfgang CL, Goggins MG, Dal Molin M, Wang TL, Roden R, Klein AP, Ptak J, Dobbyn L, Schaefer J, Silliman N, Popoli M, Vogelstein JT, Browne JD, Schoen RE, Brand RE, Tie J, Gibbs P, Wong HL, Mansfield AS, Jen J, Hanash SM, Falconi M, Allen PJ, Zhou S, Bettegowda C, Diaz LA Jr, Tomasetti C, Kinzler KW, Vogelstein B, Lennon AM, Papadopoulos N. Detection and localization of surgically resectable cancers with a multi-analyte blood test. *Science* 2018; **359**: 926-930 [PMID: 29348365 DOI: 10.1126/science.aar3247]
21 **Wu H**, Ou S, Zhang H, Huang R, Yu S, Zhao M, Tai S. Advances in biomarkers and techniques for pancreatic cancer diagnosis. *Cancer Cell Int* 2022; **22**: 220 [PMID: 35761336 DOI: 10.1186/s12935-022-02640-9]
22 **Banerjee R**, Smith J, Eccles MR, Weeks RJ, Chatterjee A. Epigenetic basis and targeting of cancer metastasis. *Trends Cancer* 2022; **8**: 226-241 [PMID: 34952829 DOI: 10.1016/j.trecan.2021.11.008]
23 **Smith J**, Sen S, Weeks RJ, Eccles MR, Chatterjee A. Promoter DNA Hypermethylation and Paradoxical Gene Activation. *Trends Cancer* 2020; **6**: 392-406 [PMID: 32348735 DOI: 10.1016/j.trecan.2020.02.007]
24 **Galardi F**, Luca F, Romagnoli D, Biagioni C, Moretti E, Biganzoli L, Leo AD, Migliaccio I, Malorni L, Benelli M. Cell-Free DNA-Methylation-Based Methods and Applications in Oncology. *Biomolecules* 2020; **10** [PMID: 33334040 DOI: 10.3390/biom10121677]
25 **Liu MC**, Oxnard GR, Klein EA, Swanton C, Seiden MV; CCGA Consortium. Sensitive and specific multi-cancer detection and localization using methylation signatures in cell-free DNA. *Ann Oncol* 2020; **31**: 745-759 [PMID: 33506766 DOI: 10.1016/j.annonc.2020.02.011]
26 **Manoochehri M**, Wu Y, Giese NA, Strobel O, Kutschmann S, Haller F, Hoheisel JD, Moskalev EA, Hackert T, Bauer AS. SST gene hypermethylation acts as a pan-cancer marker for pancreatic ductal adenocarcinoma and multiple other tumors: toward its use for blood-based diagnosis. *Mol Oncol* 2020; **14**: 1252-1267 [PMID: 32243066 DOI: 10.1002/1878-0261.12684]
27 **Luo H**, Wei W, Ye Z, Zheng J, Xu RH. Liquid Biopsy of Methylation Biomarkers in Cell-Free DNA. *Trends Mol Med* 2021; **27**: 482-500 [PMID: 33500194 DOI: 10.1016/j.molmed.2020.12.011]
28 **Huang Y**, Huang C, Jiang X, Yan Y, Zhuang K, Liu F, Li P, Wen Y. Exploration of Potential Roles of m5C-Related Regulators in Colon Adenocarcinoma Prognosis. *Front Genet* 2022; **13**: 816173 [PMID: 35281843 DOI: 10.3389/fgene.2022.816173]
29 **Luo H**, Zhao Q, Wei W, Zheng L, Yi S, Li G, Wang W, Sheng H, Pu H, Mo H, Zuo Z, Liu Z, Li C, Xie C, Zeng Z, Li W, Hao X, Liu Y, Cao S, Liu W, Gibson S, Zhang K, Xu G, Xu RH. Circulating tumor DNA methylation profiles enable early diagnosis, prognosis prediction, and screening for colorectal cancer. *Sci Transl Med* 2020; **12** [PMID: 31894106 DOI: 10.1126/scitranslmed.aax7533]
30 **Tivey A**, Church M, Rothwell D, Dive C, Cook N. Circulating tumour DNA - looking beyond the blood. *Nat Rev Clin Oncol* 2022; **19**: 600-612 [PMID: 35915225 DOI: 10.1038/s41571-022-00660-y]
31 **Goonetilleke KS**, Siriwardena AK. Systematic review of carbohydrate antigen (CA 19-9) as a biochemical marker in the diagnosis of pancreatic cancer. *Eur J Surg Oncol* 2007; **33**: 266-270 [PMID: 17097848 DOI: 10.1016/j.ejso.2006.10.004]
32 **Brancaccio M**, Natale F, Falco G, Angrisano T. Cell-Free DNA Methylation: The New Frontiers of Pancreatic Cancer

Biomarkers' Discovery. *Genes (Basel)* 2019; **11** [PMID: 31877923 DOI: 10.3390/genes11010014]

33 **Guler GD**, Ning Y, Ku CJ, Phillips T, McCarthy E, Ellison CK, Bergamaschi A, Collin F, Lloyd P, Scott A, Antoine M, Wang W, Chau K, Ashworth A, Quake SR, Levy S. Detection of early stage pancreatic cancer using 5-hydroxymethylcytosine signatures in circulating cell free DNA. *Nat Commun* 2020; **11**: 5270 [PMID: 33077732 DOI: 10.1038/s41467-020-18965-w]

34 **Moss J**, Magenheim J, Neiman D, Zemmour H, Loyfer N, Korach A, Samet Y, Maoz M, Druid H, Arner P, Fu KY, Kiss E, Spalding KL, Landesberg G, Zick A, Grinshpun A, Shapiro AMJ, Grompe M, Wittenberg AD, Glaser B, Shemer R, Kaplan T, Dor Y. Comprehensive human cell-type methylation atlas reveals origins of circulating cell-free DNA in health and disease. *Nat Commun* 2018; **9**: 5068 [PMID: 30498206 DOI: 10.1038/s41467-018-07466-6]

35 **Chhatriya B**, Mukherjee M, Ray S, Saha B, Lahiri S, Halder S, Ghosh I, Khamrui S, Das K, Bhattacharjee S, Mohapatra SK, Goswami S. Transcriptome analysis identifies putative multi-gene signature distinguishing benign and malignant pancreatic head mass. *J Transl Med* 2020; **18**: 420 [PMID: 33160365 DOI: 10.1186/s12967-020-02597-1]

36 **Bauden M**, Pamart D, Ansari D, Herzog M, Eccleston M, Micallef J, Andersson B, Andersson R. Circulating nucleosomes as epigenetic biomarkers in pancreatic cancer. *Clin Epigenetics* 2015; **7**: 106 [PMID: 26451166 DOI: 10.1186/s13148-015-0139-4]

37 **Kisiel JB**, Raimondo M, Taylor WR, Yab TC, Mahoney DW, Sun Z, Middha S, Baheti S, Zou H, Smyrk TC, Boardman LA, Petersen GM, Ahlquist DA. New DNA Methylation Markers for Pancreatic Cancer: Discovery, Tissue Validation, and Pilot Testing in Pancreatic Juice. *Clin Cancer Res* 2015; **21**: 4473-4481 [PMID: 26023084 DOI: 10.1158/1078-0432.CCR-14-2469]

38 **Natale F**, Vivo M, Falco G, Angrisano T. Deciphering DNA methylation signatures of pancreatic cancer and pancreatitis. *Clin Epigenetics* 2019; **11**: 132 [PMID: 31492175 DOI: 10.1186/s13148-019-0728-8]

39 **Liggett T**, Melnikov A, Yi QL, Replogle C, Brand R, Kaul K, Talamonti M, Abrams RA, Levenson V. Differential methylation of cell-free circulating DNA among patients with pancreatic cancer versus chronic pancreatitis. *Cancer* 2010; **116**: 1674-1680 [PMID: 20143430 DOI: 10.1002/cncr.24893]

40 **Lehmann-Werman R**, Neiman D, Zemmour H, Moss J, Magenheim J, Vaknin-Dembinsky A, Rubertsson S, Nellgård B, Blennow K, Zetterberg H, Spalding K, Haller MJ, Wasserfall CH, Schatz DA, Greenbaum CJ, Dorrell C, Grompe M, Zick A, Hubert A, Maoz M, Fendrich V, Bartsch DK, Golan T, Ben Sasson SA, Zamir G, Razin A, Cedar H, Shapiro AM, Glaser B, Shemer R, Dor Y. Identification of tissue-specific cell death using methylation patterns of circulating DNA. *Proc Natl Acad Sci U S A* 2016; **113**: E1826-E1834 [PMID: 26976580 DOI: 10.1073/pnas.1519286113]

41 **Chen R**, Pan S, Yi EC, Donohoe S, Bronner MP, Potter JD, Goodlett DR, Aebersold R, Brentnall TA. Quantitative proteomic profiling of pancreatic cancer juice. *Proteomics* 2006; **6**: 3871-3879 [PMID: 16739137 DOI: 10.1002/pmic.200500702]

42 **Matsubayashi H**, Canto M, Sato N, Klein A, Abe T, Yamashita K, Yeo CJ, Kalloo A, Hruban R, Goggins M. DNA methylation alterations in the pancreatic juice of patients with suspected pancreatic disease. *Cancer Res* 2006; **66**: 1208-1217 [PMID: 16424060 DOI: 10.1158/0008-5472.CAN-05-2664]

43 **Nishizawa N**, Harada H, Kumamoto Y, Kaizu T, Katoh H, Tajima H, Ushiku H, Yokoi K, Igarashi K, Fujiyama Y, Okuwaki K, Iwai T, Watanabe M, Yamashita K. Diagnostic potential of hypermethylation of the cysteine dioxygenase 1 gene (CDO1) promoter DNA in pancreatic cancer. *Cancer Sci* 2019; **110**: 2846-2855 [PMID: 31325200 DOI: 10.1111/cas.14134]

44 **Humeau M**, Vignolle-Vidoni A, Sicard F, Martins F, Bournet B, Buscail L, Torrisani J, Cordelier P. Salivary MicroRNA in Pancreatic Cancer Patients. *PLoS One* 2015; **10**: e0130996 [PMID: 26121640 DOI: 10.1371/journal.pone.0130996]

45 **Su Q**, Zhu EC, Qu YL, Wang DY, Qu WW, Zhang CG, Wu T, Gao ZH. Serum level of co-expressed hub miRNAs as diagnostic and prognostic biomarkers for pancreatic ductal adenocarcinoma. *J Cancer* 2018; **9**: 3991-3999 [PMID: 30410604 DOI: 10.7150/jca.27697]

46 **Martínez-Bosch N**, Cristóbal H, Iglesias M, Gironella M, Barranco L, Visa L, Calafato D, Jiménez-Parrado S, Earl J, Carrato A, Manero-Rupérez N, Moreno M, Morales A, Guerra C, Navarro P, García de Frutos P. Soluble AXL is a novel blood marker for early detection of pancreatic ductal adenocarcinoma and differential diagnosis from chronic pancreatitis. *EBioMedicine* 2022; **75**: 103797 [PMID: 34973624 DOI: 10.1016/j.ebiom.2021.103797]

47 **Weeks ME**, Hariharan D, Petronijevic L, Radon TP, Whiteman HJ, Kocher HM, Timms JF, Lemoine NR, Crnogorac-Jurcevic T. Analysis of the urine proteome in patients with pancreatic ductal adenocarcinoma. *Proteomics Clin Appl* 2008; **2**: 1047-1057 [PMID: 21136905 DOI: 10.1002/prca.200780164]

48 **Bettegowda C**, Sausen M, Leary RJ, Kinde I, Wang Y, Agrawal N, Bartlett BR, Wang H, Luber B, Alani RM, Antonarakis ES, Azad NS, Bardelli A, Brem H, Cameron JL, Lee CC, Fecher LA, Gallia GL, Gibbs P, Le D, Giuntoli RL, Goggins M, Hogarty MD, Holdhoff M, Hong SM, Jiao Y, Juhl HH, Kim JJ, Siravegna G, Laheru DA, Lauricella C, Lim M, Lipson EJ, Marie SK, Netto GJ, Oliner KS, Olivi A, Olsson L, Riggins GJ, Sartore-Bianchi A, Schmidt K, Shih lM, Oba-Shinjo SM, Siena S, Theodorescu D, Tie J, Harkins TT, Veronese S, Wang TL, Weingart JD, Wolfgang CL, Wood LD, Xing D, Hruban RH, Wu J, Allen PJ, Schmidt CM, Choti MA, Velculescu VE, Kinzler KW, Vogelstein B, Papadopoulos N, Diaz LA Jr. Detection of circulating tumor DNA in early- and late-stage human malignancies. *Sci Transl Med* 2014; **6**: 224ra24 [PMID: 24553385 DOI: 10.1126/scitranslmed.3007094]

49 **Leon SA**, Shapiro B, Sklaroff DM, Yaros MJ. Free DNA in the serum of cancer patients and the effect of therapy. *Cancer Res* 1977; **37**: 646-650 [PMID: 837366]

50 **Shapiro B**, Chakrabarty M, Cohn EM, Leon SA. Determination of circulating DNA levels in patients with benign or malignant gastrointestinal disease. *Cancer* 1983; **51**: 2116-2120 [PMID: 6188527 DOI: 10.1002/1097-0142(19830601)51:11<2116::aid-cncr2820511127>3.0.co;2-s]

51 **Chang S**, Hur JY, Choi YL, Lee CH, Kim WS. Current status and future perspectives of liquid biopsy in non-small cell lung cancer. *J Pathol Transl Med* 2020; **54**: 204-212 [PMID: 32460474 DOI: 10.4132/jptm.2020.02.27]

52 **Thakral D**, Das N, Basnal A, Gupta R. Cell-free DNA for genomic profiling and minimal residual disease monitoring in Myeloma- are we there yet? *Am J Blood Res* 2020; **10**: 26-45 [PMID: 32685257]

53 **Chatterjee A**, Stockwell PA, Ahn A, Rodger EJ, Leichter AL, Eccles MR. Genome-wide methylation sequencing of

paired primary and metastatic cell lines identifies common DNA methylation changes and a role for EBF3 as a candidate epigenetic driver of melanoma metastasis. *Oncotarget* 2017; **8**: 6085-6101 [PMID: 28030832 DOI: 10.18632/oncotarget.14042]

54 **Chatterjee A**, Rodger EJ, Eccles MR. Epigenetic drivers of tumourigenesis and cancer metastasis. *Semin Cancer Biol* 2018; **51**: 149-159 [PMID: 28807546 DOI: 10.1016/j.semcancer.2017.08.004]

55 **Melnikov AA**, Scholtens D, Talamonti MS, Bentrem DJ, Levenson VV. Methylation profile of circulating plasma DNA in patients with pancreatic cancer. *J Surg Oncol* 2009; **99**: 119-122 [PMID: 19065635 DOI: 10.1002/jso.21208]

56 **Henriksen SD**, Madsen PH, Larsen AC, Johansen MB, Pedersen IS, Krarup H, Thorlacius-Ussing O. Promoter hypermethylation in plasma-derived cell-free DNA as a prognostic marker for pancreatic adenocarcinoma staging. *Int J Cancer* 2017; **141**: 2489-2497 [PMID: 28857158 DOI: 10.1002/ijc.31024]

57 **Sato N**, Fukushima N, Maitra A, Matsubayashi H, Yeo CJ, Cameron JL, Hruban RH, Goggins M. Discovery of novel targets for aberrant methylation in pancreatic carcinoma using high-throughput microarrays. *Cancer Res* 2003; **63**: 3735-3742 [PMID: 12839967]

58 **Yi JM**, Guzzetta AA, Bailey VJ, Downing SR, Van Neste L, Chiappinelli KB, Keeley BP, Stark A, Herrera A, Wolfgang C, Pappou EP, Iacobuzio-Donahue CA, Goggins MG, Herman JG, Wang TH, Baylin SB, Ahuja N. Novel methylation biomarker panel for the early detection of pancreatic cancer. *Clin Cancer Res* 2013; **19**: 6544-6555 [PMID: 24088737 DOI: 10.1158/1078-0432.CCR-12-3224]

59 **Li S**, Yuan Y, Xiao H, Dai J, Ye Y, Zhang Q, Zhang Z, Jiang Y, Luo J, Hu J, Chen C, Wang G. Discovery and validation of DNA methylation markers for overall survival prognosis in patients with thymic epithelial tumors. *Clin Epigenetics* 2019; **11**: 38 [PMID: 30832724 DOI: 10.1186/s13148-019-0619-z]

60 **Li XB**, Ma J, Liu ZW, He WF, Li ZZ, Cui M, Hao H, Zhou GP, You L, Wang J, Han XL, Zhao YP. Non-invasive detection of pancreatic cancer by measuring DNA methylation of Basonuclin 1 and Septin 9 in plasma. *Chin Med J (Engl)* 2019; **132**: 1504-1506 [PMID: 31205116 DOI: 10.1097/CM9.0000000000000257]

61 **Rodger EJ**, Chatterjee A, Morison IM. 5-hydroxymethylcytosine: a potential therapeutic target in cancer. *Epigenomics* 2014; **6**: 503-514 [PMID: 25431943 DOI: 10.2217/epi.14.39]

62 **Cao F**, Wei A, Hu X, He Y, Zhang J, Xia L, Tu K, Yuan J, Guo Z, Liu H, Xie D, Li A. Integrated epigenetic biomarkers in circulating cell-free DNA as a robust classifier for pancreatic cancer. *Clin Epigenetics* 2020; **12**: 112 [PMID: 32703318 DOI: 10.1186/s13148-020-00898-2]

63 **Cohen JD**, Javed AA, Thoburn C, Wong F, Tie J, Gibbs P, Schmidt CM, Yip-Schneider MT, Allen PJ, Schattner M, Brand RE, Singhi AD, Petersen GM, Hong SM, Kim SC, Falconi M, Doglioni C, Weiss MJ, Ahuja N, He J, Makary MA, Maitra A, Hanash SM, Dal Molin M, Wang Y, Li L, Ptak J, Dobbyn L, Schaefer J, Silliman N, Popoli M, Goggins MG, Hruban RH, Wolfgang CL, Klein AP, Tomasetti C, Papadopoulos N, Kinzler KW, Vogelstein B, Lennon AM. Combined circulating tumor DNA and protein biomarker-based liquid biopsy for the earlier detection of pancreatic cancers. *Proc Natl Acad Sci U S A* 2017; **114**: 10202-10207 [PMID: 28874546 DOI: 10.1073/pnas.1704961114]

64 **Kim JE**, Lee KT, Lee JK, Paik SW, Rhee JC, Choi KW. Clinical usefulness of carbohydrate antigen 19-9 as a screening test for pancreatic cancer in an asymptomatic population. *J Gastroenterol Hepatol* 2004; **19**: 182-186 [PMID: 14731128 DOI: 10.1111/j.1440-1746.2004.03219.x]

65 **Mohan S**, Ayub M, Rothwell DG, Gulati S, Kilerci B, Hollebecque A, Sun Leong H, Smith NK, Sahoo S, Descamps T, Zhou C, Hubner RA, McNamara MG, Lamarca A, Valle JW, Dive C, Brady G. Analysis of circulating cell-free DNA identifies KRAS copy number gain and mutation as a novel prognostic marker in Pancreatic cancer. *Sci Rep* 2019; **9**: 11610 [PMID: 31406261 DOI: 10.1038/s41598-019-47489-7]

66 **Fukutake N**, Ueno M, Hiraoka N, Shimada K, Shiraishi K, Saruki N, Ito T, Yamakado M, Ono N, Imaizumi A, Kikuchi S, Yamamoto H, Katayama K. A Novel Multivariate Index for Pancreatic Cancer Detection Based On the Plasma Free Amino Acid Profile. *PLoS One* 2015; **10**: e0132223 [PMID: 26133769 DOI: 10.1371/journal.pone.0132223]

67 **Sun L**, Burnett J, Guo C, Xie Y, Pan J, Yang Z, Ran Y, Sun D. CPA4 is a promising diagnostic serum biomarker for pancreatic cancer. *Am J Cancer Res* 2016; **6**: 91-96 [PMID: 27073726]

68 **Barratt J**, Topham P. Urine proteomics: the present and future of measuring urinary protein components in disease. *CMAJ* 2007; **177**: 361-368 [PMID: 17698825 DOI: 10.1503/cmaj.061590]

69 **Schaub S**, Wilkins J, Weiler T, Sangster K, Rush D, Nickerson P. Urine protein profiling with surface-enhanced laser-desorption/ionization time-of-flight mass spectrometry. *Kidney Int* 2004; **65**: 323-332 [PMID: 14675066 DOI: 10.1111/j.1523-1755.2004.00352.x]

70 **Poruk KE**, Firpo MA, Scaife CL, Adler DG, Emerson LL, Boucher KM, Mulvihill SJ. Serum osteopontin and tissue inhibitor of metalloproteinase 1 as diagnostic and prognostic biomarkers for pancreatic adenocarcinoma. *Pancreas* 2013; **42**: 193-197 [PMID: 23407481 DOI: 10.1097/MPA.0b013e31825e354d]

71 **Zhivkova-Galunska M**, Adwan H, Eyol E, Kleeff J, Kolb A, Bergmann F, Berger MR. Osteopontin but not osteonectin favors the metastatic growth of pancreatic cancer cell lines. *Cancer Biol Ther* 2010; **10**: 54-64 [PMID: 20495387 DOI: 10.4161/cbt.10.1.12161]

72 **Fahrmann JF**, Bantis LE, Capello M, Scelo G, Dennison JB, Patel N, Murage E, Vykoukal J, Kundnani DL, Foretova L, Fabianova E, Holcatova I, Janout V, Feng Z, Yip-Schneider M, Zhang J, Brand R, Taguchi A, Maitra A, Brennan P, Max Schmidt C, Hanash S. A Plasma-Derived Protein-Metabolite Multiplexed Panel for Early-Stage Pancreatic Cancer. *J Natl Cancer Inst* 2019; **111**: 372-379 [PMID: 30137376 DOI: 10.1093/jnci/djy126]

73 **Radon TP**, Massat NJ, Jones R, Alrawashdeh W, Dumartin L, Ennis D, Duffy SW, Kocher HM, Pereira SP, Guarner posthumous L, Murta-Nascimento C, Real FX, Malats N, Neoptolemos J, Costello E, Greenhalf W, Lemoine NR, Crnogorac-Jurcevic T. Identification of a Three-Biomarker Panel in Urine for Early Detection of Pancreatic Adenocarcinoma. *Clin Cancer Res* 2015; **21**: 3512-3521 [PMID: 26240291 DOI: 10.1158/1078-0432.CCR-14-2467]

74 **Kaur S**, Smith LM, Patel A, Menning M, Watley DC, Malik SS, Krishn SR, Mallya K, Aithal A, Sasson AR, Johansson SL, Jain M, Singh S, Guha S, Are C, Raimondo M, Hollingsworth MA, Brand RE, Batra SK. A Combination of MUC5AC and CA19-9 Improves the Diagnosis of Pancreatic Cancer: A Multicenter Study. *Am J Gastroenterol* 2017; **112**: 172-183 [PMID: 27845339 DOI: 10.1038/ajg.2016.482]

75 **Terai K**, Jiang M, Tokuyama W, Murano T, Takada N, Fujimura K, Ebinuma H, Kishimoto T, Hiruta N, Schneider WJ, Bujo H. Levels of soluble LR11/SorLA are highly increased in the bile of patients with biliary tract and pancreatic cancers. *Clin Chim Acta* 2016; **457**: 130-136 [PMID: 27079357 DOI: 10.1016/j.cca.2016.04.010]

76 **Ansari D**, Torén W, Zhou Q, Hu D, Andersson R. Proteomic and genomic profiling of pancreatic cancer. *Cell Biol Toxicol* 2019; **35**: 333-343 [PMID: 30771135 DOI: 10.1007/s10565-019-09465-9]

77 **Gu YL**, Lan C, Pei H, Yang SN, Liu YF, Xiao LL. Applicative Value of Serum CA19-9, CEA, CA125 and CA242 in Diagnosis and Prognosis for Patients with Pancreatic Cancer Treated by Concurrent Chemoradiotherapy. *Asian Pac J Cancer Prev* 2015; **16**: 6569-6573 [PMID: 26434876 DOI: 10.7314/apjcp.2015.16.15.6569]

78 **Melo SA**, Luecke LB, Kahlert C, Fernandez AF, Gammon ST, Kaye J, LeBleu VS, Mittendorf EA, Weitz J, Rahbari N, Reissfelder C, Pilarsky C, Fraga MF, Piwnica-Worms D, Kalluri R. Glypican-1 identifies cancer exosomes and detects early pancreatic cancer. *Nature* 2015; **523**: 177-182 [PMID: 26106858 DOI: 10.1038/nature14581]

79 **Tsui NB**, Ng EK, Lo YM. Stability of endogenous and added RNA in blood specimens, serum, and plasma. *Clin Chem* 2002; **48**: 1647-1653 [PMID: 12324479]

80 **Ma R**, Jiang T, Kang X. Circulating microRNAs in cancer: origin, function and application. *J Exp Clin Cancer Res* 2012; **31**: 38 [PMID: 22546315 DOI: 10.1186/1756-9966-31-38]

81 **Samos J**, García-Olmo DC, Picazo MG, Rubio-Vitaller A, García-Olmo D. Circulating nucleic acids in plasma/serum and tumor progression: are apoptotic bodies involved? *Ann N Y Acad Sci* 2006; **1075**: 165-173 [PMID: 17108207 DOI: 10.1196/annals.1368.022]

82 **Sato-Kuwabara Y**, Melo SA, Soares FA, Calin GA. The fusion of two worlds: non-coding RNAs and extracellular vesicles--diagnostic and therapeutic implications (Review). *Int J Oncol* 2015; **46**: 17-27 [PMID: 25338714 DOI: 10.3892/ijo.2014.2712]

83 **Arroyo JD**, Chevillet JR, Kroh EM, Ruf IK, Pritchard CC, Gibson DF, Mitchell PS, Bennett CF, Pogosova-Agadjanyan EL, Stirewalt DL, Tait JF, Tewari M. Argonaute2 complexes carry a population of circulating microRNAs independent of vesicles in human plasma. *Proc Natl Acad Sci U S A* 2011; **108**: 5003-5008 [PMID: 21383194 DOI: 10.1073/pnas.1019055108]

84 **Ji P**, Diederichs S, Wang W, Böing S, Metzger R, Schneider PM, Tidow N, Brandt B, Buerger H, Bulk E, Thomas M, Berdel WE, Serve H, Müller-Tidow C. MALAT-1, a novel noncoding RNA, and thymosin beta4 predict metastasis and survival in early-stage non-small cell lung cancer. *Oncogene* 2003; **22**: 8031-8041 [PMID: 12970751 DOI: 10.1038/sj.onc.1206928]

85 **Saha B**, Chhatriya B, Pramanick S, Goswami S. Bioinformatic Analysis and Integration of Transcriptome and Proteome Results Identify Key Coding and Noncoding Genes Predicting Malignancy in Intraductal Papillary Mucinous Neoplasms of the Pancreas. *Biomed Res Int* 2021; **2021**: 1056622 [PMID: 34790815 DOI: 10.1155/2021/1056622]

86 **Kishikawa T**, Otsuka M, Ohno M, Yoshikawa T, Takata A, Koike K. Circulating RNAs as new biomarkers for detecting pancreatic cancer. *World J Gastroenterol* 2015; **21**: 8527-8540 [PMID: 26229396 DOI: 10.3748/wjg.v21.i28.8527]

87 **Chhatriya B**, Mukherjee M, Ray S, Sarkar P, Chatterjee S, Nath D, Das K, Goswami S. Comparison of tumour and serum specific microRNA changes dissecting their role in pancreatic ductal adenocarcinoma: a meta-analysis. *BMC Cancer* 2019; **19**: 1175 [PMID: 31795960 DOI: 10.1186/s12885-019-6380-z]

88 **Funaki NO**, Tanaka J, Kasamatsu T, Ohshio G, Hosotani R, Okino T, Imamura M. Identification of carcinoembryonic antigen mRNA in circulating peripheral blood of pancreatic carcinoma and gastric carcinoma patients. *Life Sci* 1996; **59**: 2187-2199 [PMID: 8950323 DOI: 10.1016/s0024-3205(96)00576-0]

89 **Clarke LE**, Leitzel K, Smith J, Ali SM, Lipton A. Epidermal growth factor receptor mRNA in peripheral blood of patients with pancreatic, lung, and colon carcinomas detected by RT-PCR. *Int J Oncol* 2003; **22**: 425-430 [PMID: 12527944]

90 **Kang CY**, Wang J, Axell-House D, Soni P, Chu ML, Chipitsyna G, Sarosiek K, Sendecki J, Hyslop T, Al-Zoubi M, Yeo CJ, Arafat HA. Clinical significance of serum COL6A3 in pancreatic ductal adenocarcinoma. *J Gastrointest Surg* 2014; **18**: 7-15 [PMID: 24002763 DOI: 10.1007/s11605-013-2326-y]

91 **Chang TC**, Wentzel EA, Kent OA, Ramachandran K, Mullendore M, Lee KH, Feldmann G, Yamakuchi M, Ferlito M, Lowenstein CJ, Arking DE, Beer MA, Maitra A, Mendell JT. Transactivation of miR-34a by p53 broadly influences gene expression and promotes apoptosis. *Mol Cell* 2007; **26**: 745-752 [PMID: 17540599 DOI: 10.1016/j.molcel.2007.05.010]

92 **Habbe N**, Koorstra JB, Mendell JT, Offerhaus GJ, Ryu JK, Feldmann G, Mullendore ME, Goggins MG, Hong SM, Maitra A. MicroRNA miR-155 is a biomarker of early pancreatic neoplasia. *Cancer Biol Ther* 2009; **8**: 340-346 [PMID: 19106647 DOI: 10.4161/cbt.8.4.7338]

93 **Yang JY**, Sun YW, Liu DJ, Zhang JF, Li J, Hua R. MicroRNAs in stool samples as potential screening biomarkers for pancreatic ductal adenocarcinoma cancer. *Am J Cancer Res* 2014; **4**: 663-673 [PMID: 25520858]

94 **Jiang P**, Yin Y, Wu Y, Sun Z. Silencing of long non-coding RNA SNHG15 suppresses proliferation, migration and invasion of pancreatic cancer cells by regulating the microRNA-345-5p/RAB27B axis. *Exp Ther Med* 2021; **22**: 1273 [PMID: 34594410 DOI: 10.3892/etm.2021.10708]

95 **Liao J**, Yu L, Mei Y, Guarnera M, Shen J, Li R, Liu Z, Jiang F. Small nucleolar RNA signatures as biomarkers for non-small-cell lung cancer. *Mol Cancer* 2010; **9**: 198 [PMID: 20663213 DOI: 10.1186/1476-4598-9-198]

96 **Wang H**, Yin F, Yuan F, Men Y, Deng M, Liu Y, Li Q. Pancreatic cancer differential methylation atlas in blood, peri-carcinomatous and diseased tissue. *Transl Cancer Res* 2020; **9**: 421-431 [PMID: 35117387 DOI: 10.21037/tcr.2019.11.26]

97 **Liu J**, Gao J, Du Y, Li Z, Ren Y, Gu J, Wang X, Gong Y, Wang W, Kong X. Combination of plasma microRNAs with serum CA19-9 for early detection of pancreatic cancer. *Int J Cancer* 2012; **131**: 683-691 [PMID: 21913185 DOI: 10.1002/ijc.26422]

98 **Tang Q**, Ni Z, Cheng Z, Xu J, Yu H, Yin P. Three circulating long non-coding RNAs act as biomarkers for predicting NSCLC. *Cell Physiol Biochem* 2015; **37**: 1002-1009 [PMID: 26393913 DOI: 10.1159/000430226]

99 **Anfossi S**, Babayan A, Pantel K, Calin GA. Clinical utility of circulating non-coding RNAs - an update. *Nat Rev Clin Oncol* 2018; **15**: 541-563 [PMID: 29784926 DOI: 10.1038/s41571-018-0035-x]

100 **Anfossi S**, Giordano A, Gao H, Cohen EN, Tin S, Wu Q, Garza RJ, Debeb BG, Alvarez RH, Valero V, Hortobagyi GN,

Calin GA, Ueno NT, Woodward WA, Reuben JM. High serum miR-19a levels are associated with inflammatory breast cancer and are predictive of favorable clinical outcome in patients with metastatic HER2+ inflammatory breast cancer. *PLoS One* 2014; **9**: e83113 [PMID: 24416156 DOI: 10.1371/journal.pone.0083113]

101 **Kamińska K**, Nalejska E, Kubiak M, Wojtysiak J, Żołna Ł, Kowalewski J, Lewandowska MA. Prognostic and Predictive Epigenetic Biomarkers in Oncology. *Mol Diagn Ther* 2019; **23**: 83-95 [PMID: 30523565 DOI: 10.1007/s40291-018-0371-7]

102 **Akamatsu M**, Makino N, Ikeda Y, Matsuda A, Ito M, Kakizaki Y, Saito Y, Ishizawa T, Kobayashi T, Furukawa T, Ueno Y. Specific MAPK-Associated MicroRNAs in Serum Differentiate Pancreatic Cancer from Autoimmune Pancreatitis. *PLoS One* 2016; **11**: e0158669 [PMID: 27380024 DOI: 10.1371/journal.pone.0158669]

103 **Li L**, Zhang GQ, Chen H, Zhao ZJ, Chen HZ, Liu H, Wang G, Jia YH, Pan SH, Kong R, Wang YW, Sun B. Plasma and tumor levels of Linc-pint are diagnostic and prognostic biomarkers for pancreatic cancer. *Oncotarget* 2016; **7**: 71773-71781 [PMID: 27708234 DOI: 10.18632/oncotarget.12365]

104 **Karandish F**, Mallik S. Biomarkers and Targeted Therapy in Pancreatic Cancer. *Biomark Cancer* 2016; **8**: 27-35 [PMID: 27147897 DOI: 10.4137/BiC.s34414]

105 **Jia X**, Wang X, Guo X, Ji J, Lou G, Zhao J, Zhou W, Guo M, Zhang M, Li C, Tai S, Yu S. MicroRNA-124: An emerging therapeutic target in cancer. *Cancer Med* 2019; **8**: 5638-5650 [PMID: 31389160 DOI: 10.1002/cam4.2489]

106 **Wellner U**, Schubert J, Burk UC, Schmalhofer O, Zhu F, Sonntag A, Waldvogel B, Vannier C, Darling D, zur Hausen A, Brunton VG, Morton J, Sansom O, Schüler J, Stemmler MP, Herzberger C, Hopt U, Keck T, Brabletz S, Brabletz T. The EMT-activator ZEB1 promotes tumorigenicity by repressing stemness-inhibiting microRNAs. *Nat Cell Biol* 2009; **11**: 1487-1495 [PMID: 19935649 DOI: 10.1038/ncb1998]

107 **Wang P**, Chen L, Zhang J, Chen H, Fan J, Wang K, Luo J, Chen Z, Meng Z, Liu L. Methylation-mediated silencing of the miR-124 genes facilitates pancreatic cancer progression and metastasis by targeting Rac1. *Oncogene* 2014; **33**: 514-524 [PMID: 23334332 DOI: 10.1038/onc.2012.598]

108 **Marín-Béjar O**, Marchese FP, Athie A, Sánchez Y, González J, Segura V, Huang L, Moreno I, Navarro A, Monzó M, García-Foncillas J, Rinn JL, Guo S, Huarte M. Pint lincRNA connects the p53 pathway with epigenetic silencing by the Polycomb repressive complex 2. *Genome Biol* 2013; **14**: R104 [PMID: 24070194 DOI: 10.1186/gb-2013-14-9-r104]

109 **Zheng S**, Chen H, Wang Y, Gao W, Fu Z, Zhou Q, Jiang Y, Lin Q, Tan L, Ye H, Zhao X, Luo Y, Li G, Ye L, Liu Y, Li W, Li Z, Chen R. Long non-coding RNA LOC389641 promotes progression of pancreatic ductal adenocarcinoma and increases cell invasion by regulating E-cadherin in a TNFRSF10A-related manner. *Cancer Lett* 2016; **371**: 354-365 [PMID: 26708505 DOI: 10.1016/j.canlet.2015.12.010]

110 **Yu S**, Li Y, Liao Z, Wang Z, Qian L, Zhao J, Zong H, Kang B, Zou WB, Chen K, He X, Meng Z, Chen Z, Huang S, Wang P. Plasma extracellular vesicle long RNA profiling identifies a diagnostic signature for the detection of pancreatic ductal adenocarcinoma. *Gut* 2020; **69**: 540-550 [PMID: 31562239 DOI: 10.1136/gutjnl-2019-318860]

111 **Rong Z**, Xu J, Shi S, Tan Z, Meng Q, Hua J, Liu J, Zhang B, Wang W, Yu X, Liang C. Circular RNA in pancreatic cancer: a novel avenue for the roles of diagnosis and treatment. *Theranostics* 2021; **11**: 2755-2769 [PMID: 33456571 DOI: 10.7150/thno.56174]

112 **Hogendorf P**, Durczyński A, Skulimowski A, Kumor A, Poznańska G, Strzelczyk J. Neutrophil Gelatinase-Associated Lipocalin (NGAL) concentration in urine is superior to CA19-9 and Ca 125 in differentiation of pancreatic mass: Preliminary report. *Cancer Biomark* 2016; **16**: 537-543 [PMID: 27002756 DOI: 10.3233/CBM-160595]

113 **Park WG**, Li L, Appana S, Wei W, Stello K, Andersen DK, Hughes SJ, Whitcomb DC, Brand RE, Yadav D, Habtezion A; Consortium for the Study of Chronic Pancreatitis, Diabetes, and Pancreatic Cancer. Unique circulating immune signatures for recurrent acute pancreatitis, chronic pancreatitis and pancreatic cancer: A pilot study of these conditions with and without diabetes. *Pancreatology* 2020; **20**: 51-59 [PMID: 31791885 DOI: 10.1016/j.pan.2019.11.008]

114 **Lee B**, Gibbs P. Inflammation, Biomarkers and Immuno-Oncology Pathways in Pancreatic Cancer. *J Pers Med* 2019; **9** [PMID: 31035449 DOI: 10.3390/jpm9020020]

115 **Brosens LA**, Hackeng WM, Offerhaus GJ, Hruban RH, Wood LD. Pancreatic adenocarcinoma pathology: changing "landscape". *J Gastrointest Oncol* 2015; **6**: 358-374 [PMID: 26261723 DOI: 10.3978/j.issn.2078-6891.2015.032]

116 **Alexandrov LB**, Nik-Zainal S, Wedge DC, Aparicio SA, Behjati S, Biankin AV, Bignell GR, Bolli N, Borg A, Børresen-Dale AL, Boyault S, Burkhardt B, Butler AP, Caldas C, Davies HR, Desmedt C, Eils R, Eyfjörd JE, Foekens JA, Greaves M, Hosoda F, Hutter B, Ilicic T, Imbeaud S, Imielinski M, Jäger N, Jones DT, Jones D, Knappskog S, Kool M, Lakhani SR, López-Otín C, Martin S, Munshi NC, Nakamura H, Northcott PA, Pajic M, Papaemmanuil E, Paradiso A, Pearson JV, Puente XS, Raine K, Ramakrishna M, Richardson AL, Richter J, Rosenstiel P, Schlesner M, Schumacher TN, Span PN, Teague JW, Totoki Y, Tutt AN, Valdés-Mas R, van Buuren MM, van 't Veer L, Vincent-Salomon A, Waddell N, Yates LR; Australian Pancreatic Cancer Genome Initiative; ICGC Breast Cancer Consortium; ICGC MMML-Seq Consortium; ICGC PedBrain, Zucman-Rossi J, Futreal PA, McDermott U, Lichter P, Meyerson M, Grimmond SM, Siebert R, Campo E, Shibata T, Pfister SM, Campbell PJ, Stratton MR. Signatures of mutational processes in human cancer. *Nature* 2013; **500**: 415-421 [PMID: 23945592 DOI: 10.1038/nature12477]

117 **Thorsson V**, Gibbs DL, Brown SD, Wolf D, Bortone DS, Ou Yang TH, Porta-Pardo E, Gao GF, Plaisier CL, Eddy JA, Ziv E, Culhane AC, Paull EO, Sivakumar IKA, Gentles AJ, Malhotra R, Farshidfar F, Colaprico A, Parker JS, Mose LE, Vo NS, Liu J, Liu Y, Rader J, Dhankani V, Reynolds SM, Bowlby R, Califano A, Cherniack AD, Anastassiou D, Bedognetti D, Mokrab Y, Newman AM, Rao A, Chen K, Krasnitz A, Hu H, Malta TM, Noushmehr H, Pedamallu CS, Bullman S, Ojesina AI, Lamb A, Zhou W, Shen H, Choueiri TK, Weinstein JN, Guinney J, Saltz J, Holt RA, Rabkin CS; Cancer Genome Atlas Research Network, Lazar AJ, Serody JS, Demicco EG, Disis ML, Vincent BG, Shmulevich I. The Immune Landscape of Cancer. *Immunity* 2018; **48**: 812-830.e14 [PMID: 29628290 DOI: 10.1016/j.immuni.2018.03.023]

118 **Tewari N**, Zaitoun AM, Arora A, Madhusudan S, Ilyas M, Lobo DN. The presence of tumour-associated lymphocytes confers a good prognosis in pancreatic ductal adenocarcinoma: an immunohistochemical study of tissue microarrays. *BMC Cancer* 2013; **13**: 436 [PMID: 24063854 DOI: 10.1186/1471-2407-13-436]

119 **Ryschich E**, Nötzel T, Hinz U, Autschbach F, Ferguson J, Simon I, Weitz J, Fröhlich B, Klar E, Büchler MW, Schmidt J. Control of T-cell-mediated immune response by HLA class I in human pancreatic carcinoma. *Clin Cancer Res* 2005; **11**:

498-504 [PMID: 15701833]

120 **Di Federico A**, Mosca M, Pagani R, Carloni R, Frega G, De Giglio A, Rizzo A, Ricci D, Tavolari S, Di Marco M, Palloni A, Brandi G. Immunotherapy in Pancreatic Cancer: Why Do We Keep Failing? *Cancers (Basel)* 2022; **14** [PMID: 35626033 DOI: 10.3390/cancers14102429]

121 **Karamitopoulou E**, Andreou A, Pahud de Mortanges A, Tinguely M, Gloor B, Perren A. PD-1/PD-L1-Associated Immunoarchitectural Patterns Stratify Pancreatic Cancer Patients into Prognostic/Predictive Subgroups. *Cancer Immunol Res* 2021; **9**: 1439-1450 [PMID: 34526323 DOI: 10.1158/2326-6066.CIR-21-0144]

122 **Fernández-Carballo BL**, Broger T, Wyss R, Banaei N, Denkinger CM. Toward the Development of a Circulating Free DNA-Based In Vitro Diagnostic Test for Infectious Diseases: a Review of Evidence for Tuberculosis. *J Clin Microbiol* 2019; **57** [PMID: 30404942 DOI: 10.1128/JCM.01234-18]

123 **Sitek B**, Sipos B, Alkatout I, Poschmann G, Stephan C, Schulenborg T, Marcus K, Lüttges J, Dittert DD, Baretton G, Schmiegel W, Hahn SA, Klöppel G, Meyer HE, Stühler K. Analysis of the pancreatic tumor progression by a quantitative proteomic approach and immunhistochemical validation. *J Proteome Res* 2009; **8**: 1647-1656 [PMID: 19714807 DOI: 10.1021/pr800890j]

World Journal of Gastroenterology

Submit a Manuscript: https://www.f6publishing.com

World J Gastroenterol 2023 April 21; 29(15): 2261-2271

DOI: 10.3748/wjg.v29.i15.2261

ISSN 1007-9327 (print) ISSN 2219-2840 (online)

MINIREVIEWS

Immunotherapy for recurrent hepatocellular carcinoma

Ahan Bhatt, Jennifer Wu

Specialty type: Gastroenterology and hepatology

Provenance and peer review: Invited article; Externally peer reviewed.

Peer-review model: Single blind

Peer-review report's scientific quality classification

Grade A (Excellent): 0
Grade B (Very good): B, B
Grade C (Good): C
Grade D (Fair): 0
Grade E (Poor): 0

P-Reviewer: Al-Haggar M, Egypt; Chen T, China; Rajer M, Slovenia

Received: September 15, 2022
Peer-review started: September 15, 2022
First decision: January 3, 2023
Revised: January 25, 2023
Accepted: March 14, 2023
Article in press: March 14, 2023
Published online: April 21, 2023

Ahan Bhatt, Jennifer Wu, Division of Hematology and Oncology, Perlmutter Cancer Center of NYU Langone Health, NYU School of Medicine, New York, NY 10016, United States

Corresponding author: Jennifer Wu, MD, Associate Professor, Attending Doctor, Division of Hematology and Oncology, Perlmutter Cancer Center of NYU Langone Health, NYU School of Medicine, 462 First Ave, BCD556, New York, NY 10016, United States.
jennifer.wu@nyulangone.org

Abstract

Hepatocellular carcinoma (HCC) is presented frequently in late stages that are not amenable for curative treatment. Even for patients who can undergo resection for curative treatment of HCC, up to 50% recur. For patients who were not exposed to systemic therapy prior to recurrence, recurrence frequently cannot be subjected to curative therapy or local treatments. Such patients have several options of immunotherapy (IO). This includes programmed cell death protein 1 (PD-1) and cytotoxic T- lymphocyte associated protein 4 treatment, combination of PD-1 and vascular endothelial growth factor inhibitor or single agent PD-1 therapy when all other options are deemed inappropriate. There are also investigational therapies in this area that explore either PD-1 and tyrosine kinase inhibitors or a novel agent in addition to PD-1 with vascular endothelial growth factor inhibitors. This mini-review explored IO options for patients with recurrent HCC who were not exposed to systemic therapy at the initial diagnosis. We also discussed potential IO options for patients with recurrent HCC who were exposed to first-line therapy with curative intent at diagnosis.

Key Words: Liver neoplasms; Immune checkpoint blockade; Combination drug therapy; PD-1- PD-L1 blockade; CTLA-4 inhibitor.

Core Tip: Immunotherapy (IO) has made strong headway in the management of hepatocellular carcinoma (HCC). For patients who recur on local therapy, IO has become the standard of care treatment option for unresectable HCC. The role of IO agents is still not explored in patients who progress on prior IO. This mini-review highlighted the various treatment options available in clinical practice as well as upcoming novel management strategies in recurrent HCC.

Citation: Bhatt A, Wu J. Immunotherapy for recurrent hepatocellular carcinoma. *World J Gastroenterol* 2023; 29(15): 2261-2271
URL: https://www.wjgnet.com/1007-9327/full/v29/i15/2261.htm
DOI: https://dx.doi.org/10.3748/wjg.v29.i15.2261

INTRODUCTION

Hepatocellular carcinoma (HCC) is one of the most common cancers worldwide, with more than 900000 new cases in 2020. HCC accounts for the third most cancer deaths, next only to lung cancer and colorectal cancer. It occurs twice as frequently in males compared to females and is more common in Eastern Asian countries compared to Europe[1]. In the United States (US), there is a shift in the incidence and mortality of HCC from predominantly Asians/Pacific Islanders to African American and Hispanic communities[2]. Such change is most likely due to the successful implementation of hepatitis B virus control measures such as vaccination and effective anti-viral therapy (hepatitis B virus is the main cause of HCC in Eastern Asian populations)[3,4]. On the other hand, nonalcoholic steatohepatitis (NASH) is another common cause of HCC in the Western world and is quickly becoming a key contributor to increasing HCC cases[5]. Between the period of 2010 to 2019, NASH has seen the fastest growth in HCC-associated deaths globally[6]. In the US, NASH is viewed as the most common risk factor (59%), followed by hepatitis C (22%)[7]. Chronic alcohol consumption continues to be a leading cause of HCC as well in the US and other Western countries[8].

Managing patients with early-stage HCC includes local therapy using transplantation, hepatic resection, ablation or transarterial chemoembolization (TACE), but there is always a chance of recurrence. The rate of recurrence was found to be 16% with liver transplantations for HCC, which is the lowest among all local therapy approaches. Thus, for patients eligible for liver transplantation, it is the best treatment option for patients with early HCC[9]. In patients treated with surgical resection, recurrence is seen in > 50% of the patients[10]. Radiofrequency ablation showed recurrence in more than 80% of the patients, either locally or distant at the 5-year follow-up[11]. Surgical resection when compared to ablation for HCC did not show significant improvement in overall survival (OS); however, the disease-free survival period was significantly better for surgical resection[12]. Therefore, resection is often preferred over ablation in HCC. TACE is traditionally used as a bridge to transplantation. For patients who cannot proceed with transplantation, TACE can still provide effective local control. In a large study of 681 patients, of which 287 were treated in the first-line therapy with TACE, recurrence was seen in 43.2% of the patients that achieved complete response (CR)[13].

If HCC recurs, patients can be candidates again for local therapy as described above. However, if they are not amenable to local therapy, systemic therapy is used. There are two types of systemic therapies: (1) Immunotherapy (IO) based; and (2) Non-Immunotherapy based. In this review, we focused on the IO-based systemic approaches.

IMMUNOTHERAPY BASED APPROACHES IN THE FIRST-LINE SETTING

Atezolizumab with bevacizumab

Atezolizumab (Atezo), a programmed death ligand 1 (PD-L1) inhibitor, and bevacizumab (Bev), a vascular endothelial growth factor receptor (VEGF) inhibitor were initially tested in a phase Ib study to evaluate their role for the management of untreated, advanced HCC patients[14-16]. Atezo acts by preventing T cell suppression and selectively inhibiting PD-L1 from attaching to programmed cell death protein 1 (PD-1)receptors[14]. Bev inhibits VEGF, which is commonly associated with progression and development of liver cancer[17]. It acts by inhibiting angiogenesis and tumor growth[18]. The combination of Atezo and Bev can act by reversing VEGF mediated immunosuppression and increased T cell infiltration in the tumor microenvironment, which can be efficacious in treating cancer[19,20].

The IMBRAVE150 study established Atezo in combination with Bev as the standard of care for advanced HCC patients[21] (Table 1). The IMBRAVE 150 (NCT03434379) was a large multicenter, open label phase III randomized study that evaluated the safety and efficacy of Atezo in combination with Bev in comparison to sorafenib in the first-line setting for systemic therapy naïve patients with unresectable HCC[22]. At the time of the first analysis at data cutoff, the OS rate at 12 months (mo) was 67.2% [95% confidence interval (CI): 61.3-73.1] with Atezo + Bev and 54.6% (95%CI: 45.2-64.0) with sorafenib. Median OS (mOS) was not reached for the Atezo + Bev arm and was 13.2 mo (95%CI: 10.4-not reached) for the sorafenib arm. The study had shown median progression-free survival (mPFS) of 6.8 mo (95%CI: 5.7-8.3) for the Atezo + Bev arm and 4.3 mo (95%CI: 4.0 to 5.6) for the sorafenib arm. Thus, the OS and PFS were significantly improved compared to the tyrosine kinase inhibitor (TKI) sorafenib. The Atezo + Bev arm in the study demonstrated a superior overall response rate (ORR) of 27.3% (95%CI: 22.5-32.5) when compared to the sorafenib arm of 11.9% (95%CI: 7.4-18.0), per response evaluation

Table 1 Immunotherapy regimens for first-line use in patients with advanced hepatocellular carcinoma with no prior systemic therapy

Immunotherapy regimen	IMBRAVE150 (NCT03434379)	HIMALAYA (NCT03298451)
Drugs	Atezolizumab, Bevacizumab	Durvalumab, Tremelimumab
Drug class combination	PD-L1 inhibitor, VEGF inhibitor	PD-1 inhibitor, CTLA-4 inhibitor
Study population	Child-Pugh A, ECOG score 0/1, no prior systemic therapy	Child-Pugh A, ECOG score 0/1, BCLC B or C, no prior systemic therapy
Key difference	Portal vein thrombosis patients included	Portal vein thrombosis patients excluded
EGD required?	Yes	No
Overall survival	19.2 mo (95%CI: 17.0-23.7)	16.4 mo (95%CI: 14.2-19.6)
Median progression free survival	6.8 mo (95%CI: 5.7-8.3) *vs* 4.3 (95%CI: 4.0-5.6)	3.8 mo (95%CI: 3.7-5.3)
Overall response rate	27.3% (95%CI: 22.5-32.5)	STRIDE arm: 20.1%
Long-term survival data	Not available	Available

BCLC: Barcelona Clinic Liver Cancer; CI: Confidence interval; CTLA-4: Cytotoxic T lymphocyte associated protein-4; ECOG: Eastern Cooperative Oncology Group; EGD: Esophagogastroduodenoscopy; FDA: Food and Drug Administration; PD-1: Programmed cell death protein-1; PD-L1: Programmed death- ligand 1; STRIDE: Single Tremelimumab Regular Interval Durvalumab; VEGF: Vascular endothelial growth factor.

criteria in solid tumors 1.1 (RECIST 1.1) (P <0.001).

The Atezo+Bev is the only first-line combination regimen involving IO that evaluated high risk patients having Vp4 thrombus, bile duct invasion or liver infiltration > 50%. The improved OS, mPFS and ORR compared to sorafenib regardless of patient etiology and disease risk stamped its role in first-line management of treatment naïve unresectable HCC. The only caveat is that the trial required a pretreatment evaluation of esophageal varices because of its increased complications with cirrhosis and HCC and due to the side effect profile of Bev. Varices, if present, also needed to be treated otherwise the patients were excluded from the trial. Hence, the trial selectively looked at patients who had preserved liver function (Child-Pugh class A) and a decreased risk of variceal bleeding.

At the American Society of Clinical Oncology (ASCO) Gastrointestinal Cancers Symposium 2021, additional data was presented. After a median 15.6mo (range: 0-28.6) follow-up, the mOS was 19.2 mo (95%CI: 17.0-23.7) in the Atezo + Bev arm and 13.4 mo (95%CI: 11.4-16.9) in the sorafenib arm, whereas the mPFS and ORR were similar to the original presented data[23]. The updated data showed 8% of the patients achieving CR with Atezo + Bev compared to < 1% with sorafenib. Moreover, data for a PD-L1 negative patient subgroup did not reveal a meaningful difference in OS, thus suggesting treatment efficacy regardless of PD-L1 expression.

Durvalumab and tremelimumab

Durvalumab (Durva), a PD-L1 inhibitor, and tremelimumab (Treme), a cytotoxic T lymphocyte associated protein 4 (CTLA-4) inhibitor, based on their additive and complementary immunostimulatory activity, were combined in the treatment of HCC[24-26]. At the ASCO 2022 Gastrointestinal Cancers Symposium, the HIMALAYA study was presented. HIMALAYA is an open-label, multicenter, phase III study evaluating the IO combination of Treme+ Durva *vs* sorafenib. Patients with newly diagnosed unresected HCC not amenable to local therapy were initially randomized to the Single Treme Regular Interval Durva (STRIDE regimen) or Durva or sorafenib in a 1:1:1 ratio[27]. The study met the primary endpoint of improved OS in the Treme + Durva arm (STRIDE regimen) when compared to sorafenib. This was also the first study to evaluate long-term OS, with a median follow-up duration of more than 30 mo.

OS was significantly improved for STRIDE *vs* sorafenib [hazard ratio (HR): 0.78; 95%CI: 0.65-0.92; P = 0.0035). The mOS for STRIDE was 16.4 mo (95%CI: 14.1-19.5) *vs*13.7 mo (95%CI: 12.2-16.1) for sorafenib. The mPFS was 3.8 mo (95%CI: 3.7-5.3) in the STRIDE arm and 4.1 mo (95%CI: 3.8-5.5) in the sorafenib arm. Despite a similar PFS for STRIDE and sorafenib, more patients remained progression free at the time of data cutoff for the STRIDE arm. Patients also continued on treatment with STRIDE (46.9%) for at least one cycle compared to sorafenib (36%) past disease progression, which would suggest that more patients derived clinical benefit from this combination. The STRIDE regimen showed superiority in ORR (20.1%) compared to sorafenib (5.1%). In addition, Durva met the objective of OS non-inferiority to sorafenib (HR: 0.86; 95%CI: 0.73-1.03). The ORR was higher for Durva (17.0%) than for sorafenib (5.1%).

In contrast to the IMBRAVE150 study, the HIMALAYA study did not include Vp4 thrombus patients, which is considered a high risk patient group. The subgroup analyses are not available yet[22,27]. The STRIDE regimen was not associated with an increased risk of bleeding with esophageal varices, thus eliminating the need for esophagogastroduodenoscopy for evaluation, as is required for the Atezo+ Bev combination. Therefore, STRIDE can be a very good option for patients who are contraindicated to Bev

(commonly fistula, recent bleeding, high grade varices, severe hypertension and proteinuria).

Even though benefits were seen with the STRIDE regimen, it only involved a single dose of Treme, a CTLA-4 inhibitor, which drives the majority of the toxicities in the IO combination and was seen in this study as well. STRIDE is a proposed treatment regimen for patients who are treatment naïve and have unresectable disease. The treatment was approved for first-line use in October 2022 by the Food and Drug Administration (FDA)[28]. The OS non-inferiority of Durva to sorafenib, along with higher ORR and lower toxicity profile, makes Durva a very attractive option compared to sorafenib. Durva is not FDA approved yet for HCC.

Tislelizumab

The RATIONALE 301 study is a phase III randomized, open label study that evaluated tislelizumab, a PD-1 inhibitor, *vs* sorafenib as first-line treatment for unresectable HCC[29]. The primary objective of the study is to compare OS. The patients have unresectable HCC with no prior systemic therapy, Child-Pugh A class and Eastern Cooperative Oncology Group (ECOG) score 0 or 1. The patients are randomized 1:1 and received either tislelizumab or sorafenib. The study reported non-inferiority of tislelizumab to sorafenib in terms of OS, with a favorable safety profile (mOS: 15.9 mo for tislelizumab *vs* 14.1 mo for sorafenib; stratified HR: 0.85; 95%CI: 0.712-1.019)[30]. Based on the results of this study, single agent tislelizumab can be a potential first-line option for the management of HCC.

Ipilimumab + nivolumab

Checkmate 9DW is another phase III trial evaluating ipilimumab and nivolumab *vs* standard of care TKIs sorafenib or lenvatinib in patients with unresectable HCC who have not received systemic therapy [31]. The primary objective is to measure OS, and the secondary objective is to measure ORR and duration of response.

SRF388

SRF388 is another agent that is being used in combination with Atezo and Bev in the frontline setting for patients with advanced HCC. SRF388 is an inhibitor of interleukin-27 (IL-27), and as a single agent has reduced HCC growth in mouse models[32]. HCC development is suppressed if IL-27 is inhibited in NASH-induced HCC models. Higher levels of IL-27 have also been shown to reduce survival in HCC. IL-27 upregulates PD-L1 expression, lymphocyte activation gene 3 (LAG-3), T cell immunoglobulin and mucin-domain containing protein 3 and T cell immunoglobulin and ITIM domain (TIGIT). Thus, combining PD1 therapy with SRF388 increases cytokines such as tumor necrosis factor- alpha and interferon-gamma, which can potentially help in reducing tumor growth.

The preliminary results from a phase I study showed that there were no significant drug-related toxicities (grade > 3 or higher or dose limiting toxicity) and achieved a response similar to preclinical mouse models in humans[33]. Phase II of the study, SRF388-201 study, is currently open and actively recruiting patients who are newly diagnosed with no prior systemic therapy, Child class A, not eligible for TACE and have ECOG 0 or 1. The patients will be randomized 1:1 and will either receive SRF388 or placebo in combination with Atezo and Bev.

CHILD-PUGH SCORE B GROUP

All currently approved therapies are based on studies that exclude Child-Pugh score B patients. There is no prospective data evaluating this group of patients in a first-line setting. A retrospective study evaluated 27 advanced HCC patients with Child-Pugh score B after treatment with Atezo + Bev[34]. The study compared these patients with 130 patients with Child-Pugh score A. Modest activity of the Atezo + Bev combination was seen with an ORR of 14.8% in the Child-Pugh score B group compared to 32.3% for Child-Pugh score A group. mPFS and OS were 3 mo (95%CI: 1.6-4.3) and 6 mo(95%CI: 4.9-7.0), respectively, for Child-Pugh score B compared to mPFS of 6 mo and mOS not reached for Child-Pugh score A group. More grade 3/4 adverse events were observed, with thrombocytopenia and aspartate transaminase elevation being the most common. A higher discontinuation rate was seen in the Child-Pugh score B group.

Similar retrospective studies have also shown that nivolumab and pembrolizumab have a limited role in the management of advanced HCC for Child-Pugh score B/C patients previously treated with other therapies. Poor outcomes were associated with high Child-Pugh score, portal vein thrombosis and diuretic refractory ascites[35,36]. Wong *et al*[36] demonstrated a superior response in Child-Pugh score B7 patients compared to Child-Pughscore B ≥ 8. A trial is currently open that is prospectively evaluating Atezo + Bev combination in HCC patients with Child-Pugh score B7 with no prior systemic therapy[37].

IMMUNOTHERAPY BASED APPROACHES IN SECOND-LINE SETTING

For patients exposed to non-immunotherapeutic agents in first-line

Current strategies involve using immunotherapeutic or non-immunotherapeutic agents in the first-line setting for advanced HCC. For patients who recur following non-immunotherapeutic agents like sorafenib or lenvatinib, several agents are currently approved by the FDA.

Nivolumab +ipilimumab

The Checkmate 040 study was an open label phase I/II dose escalation and expansion trial evaluating single agent nivolumab, a PD-1 inhibitor, in advanced HCC[38] (Table 2). The drug received accelerated approval for use in HCC in patients who progressed on sorafenib. The Checkmate 459 study evaluated nivolumab *vs* sorafenib for HCC. The study did not show significant improvement in OS with single agent nivolumab, which later resulted in the withdrawal of the drug[39,40].

Nivolumab in combination with ipilimumab, a CTLA-4 inhibitor, was also studied in patients with HCC after progression or intolerance to prior therapy in the randomized phase II portion Checkmate 040 study[41]. Majority of the patients received prior sorafenib and included patients who received up to three lines of prior systemic therapy. The study involved three arms with 1:1:1 randomization using different dose combinations of ipilimumab and nivolumab. Arm A had nivolumab 1 mg/kg plus ipilimumab 3 mg/kg (Ipi3 + Nivo1), administered every 3 weeks for four doses, followed by nivolumab 240 mg every 2 weeks. Arm B had nivolumab 3 mg/kg plus ipilimumab 1 mg/kg (Ipi1 + Nivo3), administered every 3 weeks for four doses, followed by nivolumab 240 mg every 2 weeks. Arm C had nivolumab 3 mg/kg every 2 weeks plus ipilimumab 1 mg/kg every 6 weeks.

A total of 148 patients were enrolled. The ORR was 32%, 27% and 29%, respectively, for the three arms. Time to response occurred early and was similar across all treatment arms, regardless of PD-L1 status or baseline alpha-fetoprotein (AFP) levels. The duration of response was also similar. However, mOS were 22.8mo (95%CI: 9.4-not reached), 12.5mo (95%CI: 7.6-16.4) and 12.7mo (95%CI: 7.4-33.0) for Arms A, B and C respectively. Arm A reported higher grade 3/4 treatment-related adverse events (53%) (TRAEs) and higher immune-mediated events compared to Arms B (29%) and C (31%), most likely correlative of the higher dose of ipilimumab. Rash, hepatitis and hypothyroidism were the most common immune-related AEs.

Amongst the three arms, arm A achieved the highest CR rate (8%) with the best OS at 30 mo (44%) and the longest mOS of 22 mo. This treatment of Ipi3 + Nivo1, followed by nivolumab single agent received accelerated approval by the FDA for second-line use in advanced HCC. At the ASCO 2021 Gastrointestinal Cancers Symposium, the 44 mo survival data was presented and continues to show promising results regarding long-term survival and safety profile[42]. A few caveats of the study were that it was an open label phase I/II study without a standard of care control arm and a small number of patients in each arm. The patients were also not stratified per risk factors. However, the study included high risk patients with extrahepatic spread and elevated AFP levels and multiple lines of prior systemic therapy.

Ipilimumab + nivolumab is the standard of care treatment option for patients who progressed or are intolerant to first-line non-immunotherapeutic agents such as sorafenib or lenvatinib.

Pembrolizumab

Keynote 224 is a single arm phase II study of pembrolizumab, a PD-1 inhibitor, in patients with advanced HCC who had progressed on or were intolerant to sorafenib[43]. In total, 104 participants received 200mg of pembrolizumab intravenously every 3 weeks for 2 years or until disease progression, toxicity or withdrawal from the trial. The primary objective of the study was ORR (17%). The mPFS was 4.9 mo (95%CI: 3.4-7.2), and mOS was 12.9 mo (95%CI: 9.7-15.5). TRAEs were observed in 73% of the patients, and 15% of the patients had serious TRAEs. Grade 3/4 TRAEs occurred in about 25% of the patients, with increased alanine transferase, increased aspartate transferase and fatigue being the most common. Immune-mediated grade 3/4 AEs were seen in only 4% of the patients, with adrenal insufficiency being the most common. Based on the data, pembrolizumab is an effective and tolerable option for patients previously treated with sorafenib.

The study also suggested that PD-L1 expression based on combined positive score using tumor and immune cells was correlative of anti PD-1 activity with pembrolizumab. This association was not significant when correlated to tumor positivity score alone. The limitations of the study were that it was a single arm study and did not compare pembrolizumab with a control arm.

Keynote 240 was a phase III global study that tested the efficacy of pembrolizumab with best supportive care (BSC) *vs* placebo with BSC in the second-line setting following progression or intolerance to sorafenib. However, there was no statistical difference seen in mOS or mPFS[44]. The mOS was 13.9 mo (95%CI: 11.6-16.0 mo) for pembrolizumab *vs* 10.6 mo (95%CI: 8.3-13.5 mo) for placebo (HR: 0.78; 95%CI: 0.61-0.99; P = 0.024). mPFS for pembrolizumab was 3.0 mo (95%CI: 2.8-4.1 mo) *vs* 2.8 mo (95%CI: 1.6-3.0 mo) for placebo at the final analysis (HR: 0.72; 95%CI: 0.57-0.90; P = 0.002). The ORR was 18.4%, which was similar to the ORR seen in Keynote 224.

Table 2 Current Food and Drug Administration-approved immunotherapy agents in second-line use post-progression on sorafenib in advanced hepatocellular carcinoma

Immunotherapy agent	Checkmate 040 (NCT01658878)	Keynote 224 (NCT02702414)
Drugs	Ipilimumab, nivolumab	Pembrolizumab
Drug class combination	CTLA-4 inhibitor, PD-1 inhibitor	PD-1 inhibitor
Study population	Child-Pugh A, ECOG score 0/1, prior systemic therapy with sorafenib or intolerance to sorafenib	Child-Pugh A, ECOG score 0/1, prior systemic therapy with sorafenib or intolerance to sorafenib
Overall survival	22.8mo (95%CI: 9.4-not reached)	12.9 mo (95%CI: 9.7-15.5)
Median progression free survival	3.9 mo (95%CI: 2.6-8.3)	4.9 mo (95%CI: 3.4-7.2)
Overall response rate	32%	18%
Most common treatment related AE	Rash, hepatitis, hypothyroidism	Hypothyroidism, hepatitis, adrenal insufficiency
Child-Pugh score B group studied	No data available	Retrospective data available
FDA approval	Yes	Yes

CI: Confidence interval; CTLA-4: Cytotoxic T lymphocyte associated protein-4; ECOG: Eastern cooperative oncology group; FDA: Food and drug administration; PD-1: Programmed cell death protein- 1.

Keynote 394 is another phase III randomized study evaluating pembrolizumab + BSC *vs* placebo + BSC, specifically in Asian patients with advanced HCC with progression on or intolerance to sorafenib or oxaliplatin chemotherapy. Early results were presented at ASCO 2022, and they showed that pembrolizumab with BSC improves OS, PFS and ORR in Asian patients[44]. At the final analysis, pembrolizumab significantly improved mOS *vs* placebo. mOS was noted to be 14.6 mo (95%CI: 12.6-18.0) for pembrolizumab *vs* 13.0 mo (95%CI: 10.5-15.1) for placebo. According to the protocol, if OS was superior, PFS and ORR at the second interim analysis were studied. Pembrolizumab significantly improved PFS (HR: 0.74; 95%CI: 0.6-0.9; P = 0.003) and ORR (estimated difference: 11.4%; 95%CI: 6.7-16.0; P = 0.00004).

Based on these studies, PD-1 single agent may have a differential benefit according to various pharmacodynamic changes amongst ethnic groups. Pembrolizumab therefore could be a better tolerated option for patients with progression or intolerance to first-line non-IO based agents, particularly in Asian patients.

For patients exposed to immunotherapeutic agents in first-line

There is no prospective data for any therapy in patients who recur following first-line IO. Clinical trials are currently underway exploring this space.

Wong *et al*[46] performed a retrospective analysis of 25 patients who had previously progressed on prior immune checkpoint inhibitor (ICI) monotherapy or combined therapy. Patients received ipilimumab in combination with either nivolumab or pembrolizumab. The 3-year follow-up data revealed that ORR was 16%, and CR rate was 12%. Overall, 40% of the patients achieved clinical benefit with this regimen, with a median duration of response of 11.5 mo (2.7-30.3 mo), and mOS were 10.9 mo. The drugs had an acceptable safety profile.

In clinical practice, when patients desire second-line IO after progression on first-line IO, we can potentially use agents that have not been tried in the first-line setting. Treme and Durva, which is an IO+IO combination can be tried after progression on Atezo and Bev, which is an IO + VEGF combination. The reverse order can also be offered for patients who are offered IO+ IO combination first. Further clinical trials in this space are also required to evaluate the role of these agents post-progression.

COMBINATION THERAPY TRIALS WITH SYSTEMIC THERAPY

Several non-immunotherapeutic agents have been approved by the FDA for use in the management of advanced HCC, either in first-line or second-line settings post-progression. Trials are ongoing in this space to evaluate their potential role in combination with an immunotherapeutic agent (Table 3).

Camrelizumab, an anti PD-1 inhibitor, in combination with rivoceranib, an anti-VEGF receptor type 2 TKI (apatinib), is the first phase III study to show positive survival benefits with a PD-1/PD-L1 inhibitor and anti-angiogenic TKI for unresectable HCC[47]. In this randomized, open-label, phase III trial, 543

Table 3 Possible treatment regimens for patients with advanced hepatocellular carcinoma who have recurred on local therapy

Patient group	Treatment	Status
Advanced HCC patients with no prior systemic therapy	Atezolizumab + bevacizumab	FDA approved for first-line use (no contraindications to atezolizumab/bevacizumab or both)
	Durvalumab + tremelimumab	Contraindications to atezolizumab or bevacizumab or both; FDA approved for first-line use
	Single agent immunotherapy	Poor ECOG 3-4
Advanced HCC with prior systemic therapy with TKIs like sorafenib or lenvatinib	Ipilimumab + nivolumab	FDA approved for second-line use
	Pembrolizumab	FDA approved for second-line use; High risk subgroups: Asian patients, poor ECOG
	Atezolizumab + bevacizumab	Warrants further evaluation
	Durvalumab + tremelimumab	
	Clinical trials	
HCC patients with prior IO based systemic therapy	Partner switching from currently available first-line options	Using drugs with different mechanism of action in comparison to first line IO therapy
	Pembrolizumab	Warrants further evaluation
	Ipilimumab + nivolumab	
	Clinical trials	

ECOG: Eastern cooperative oncology group; FDA: Food and drug administration; HCC: Hepatocellular carcinoma; IO: Immunotherapy; TKI: Tyrosine kinase inhibitor.

patients were randomized 1:1 to receive camrelizumab (C) + rivoceranib (R) /apatinib or sorafenib. Patients were stratified by macrovascular invasion and/or extrahepatic metastases, geographical region (Asia *vs* non-Asia) and baseline serum AFP (< 400 *vs* ≥ 400 ng/mL). The primary endpoints were PFS as well as OS. With a median follow-up time of 7.8 mo, PFS was significantly improved with C + R *vs* sorafenib [median 5.6 mo (95%CI: 5.5-6.3) *vs* 3.7 mo(2.8-3.7); HR: 0.52;95%CI: 0.41-0.65; $P < 0.0001$]. With a median follow-up of 14.5 mo, OS was significantly prolonged with C + R *vs* sorafenib [median 22.1 mo (95%CI: 19.1-27.2) *vs* 15.2 mo (13.0-18.5); HR: 0.62; 95%CI: 0.49-0.80; 1-sided $P < 0.0001$]. ORR, disease control rate and duration of response were also better with C+R *vs* sorafenib. Grade ≥3 TRAEs occurred in 80.9% with C + R and 52.4% with sorafenib. TRAE led to discontinuation of any treatment in 24.3% (of both agents in 3.7%) with C + R and 4.5% with sorafenib.

Keynote 524 was a phase Ib study to assess the antitumor activity of lenvatinib in combination with pembrolizumab. The initial data showed that the combination was safe for use with no drug limiting toxicities, and Grade ≥ 3 toxicities were seen in 67% of the patients. The ORR was 36% per RECIST 1.1, with 1 patient having CR. Median duration of response was 12.6 mo, and the ORR findings were consistent for subgroups with poor prognostic features. The time to treatment response was less than 2.0 mo, with mPFS of 8.6 mo and mOS of 22.0 mo[48].

Based on this promising activity, a phase III study, LEAP-002, tested pembrolizumab + lenvatinib as a combination therapy[49]. Patients (n = 794) were randomized 1:1 for lenvatinib + pembrolizumab *vs* lenvatinib + placebo. The dual primary endpoints of the study were OS and PFS. After the follow-up, the authors observed 17.6 mo for the final PFS and 32.1 mo for the final OS. The primary endpoints of OS and PFS did not meet pre-specified statistical significance. The mOS with lenvatinib + pembrolizumab was 21.2 mo *vs* 19.0 mo with lenvatinib, and the HR was 0.840 (95%CI: 0.708-0.997; $P = 0.0227$). mPFS at final analysis was 8.2 mo for lenvatinib + pembrolizumab *vs* 8 mo for the lenvatinib alone arm. HR for PFS at interim analysis 1 was 0.867 (95%CI: 0.734-1.024; $P = 0.04660$. ORR at final analysis was 26.1% for lenvatinib + pembrolizumab *vs* 17.5% for lenvatinib. Grade 3-5 TRAEs were 62.5% in the lenvatinib + pembrolizumab arm and 57.5% in the lenvatinib arm (grade 5). Notably, in the LEAP-002 trial, OS with lenvatinib monotherapy was the longest observed with a TKI (19.0 mo), which was much longer than the mOS of Lenvatinib (13.6 mo) shown in the REFLECT trial[50]. Based on the data, a meaningful difference in activity was not seen with lenvatinib + pembrolizumab *vs* lenvatinib monotherapy alone.

Cosmic 312 is a phase III trial comparing cabozantinib plus Atezo *vs* sorafenib as first-line systemic treatment for advanced HCC[51]. Patients with tumors invading the main portal vein were not excluded from the trial. Patients were randomly assigned (2:1:1) to cabozantinib 40 mg orally once daily plus Atezo 1200 mg q3 weeks, sorafenib 400 mg orally BID or single agent cabozantinib 60 mg orally once daily. Primary endpoints for the study were PFS in the first 372 patients in the intention to treat patient population and OS for all patients. mPFS was 6.8 mo (95%CI: 5.6-8.3) in the combination treatment

group *vs* 4.2 mo (95%CI: 2.8-7.0) in the sorafenib group (HR: 0.63; 95%CI: 0.44-0.91; $P = 0.0012$). mOS (interim analysis) was 15.4 mo (95%CI: 13.7-17.7) in the combination treatment group *vs* 15.5 mo (12.1-not estimable) in the sorafenib group (HR: 0.90; 95%CI: 0.69-1.18; $P = 0.44$).

NOVEL AGENTS

Several novel IO-based agents are currently in development that could have a potential role in the management of HCC.

LAG-3 inhibitors are potential agents in development and are currently being tested in their role in HCC. LAG-3 inhibition leads to the activation of exhausted T cells. Relatlimab, a LAG-3 inhibitor, is currently being tested with nivolumab for potential use in patients who have progressed on first-line TKIs, like sorafenib, and are IO naïve[52]. The agent is also being investigated in combination with nivolumab and Bev in treatment naïve unresectable HCC patients[53].

A novel therapy targeting glypican-3 (GPC-3) using chimeric antigen receptor T cells is underway in advanced HCC. Early results from two phase I studies have demonstrated their safety, with 2 patients out of 13 showing partial response[54]. Glypican-3 expression has been associated with a worse prognosis in HCC[55]. There are several trials underway in this space. Natural killer cell activity has also been potentially linked to an increased risk of recurrence following curative treatment of HCC[56]. FT500 and FATE NK-100 are some of the natural killer cell IO trials currently in development for their potential role in HCC[57,58].

CONCLUSION

The scope of IO in the management of HCC is indeed promising. We have moved beyond sorafenib, the standard of care in the first-line management of advanced HCC for the past decade[59]. Atezo in combination with Bev, based on the IMBRAVE150 study, can now be considered the new standard of care for patients who have a recurrence of disease and are not amenable to local therapy. The STRIDE regimen, based on the HIMALAYA study, can also be considered a potential option if a patient is not a good candidate for the IMBRAVE regimen. For patients previously treated with sorafenib and recur or progress, ipilimumab + nivolumab or pembrolizumab are currently identified agents in the second-line setting. In their study, Wong *et al*[46] have shown that continuing to use IO agents in the second-line setting post-progression on prior ICI is certainly protective. Clinical trials to evaluate the role of ICIs in this space are undoubtedly necessary. Partner switching such as using PD-1/PD-L1 inhibitors, VEGF-inhibitors or CTLA-4 inhibitors based on the currently approved therapies should also be evaluated in the second-line setting. The role of these agents in patients with Child-Pugh score B also needs further evaluation. We are also looking at emerging combinations of non-immunotherapeutic agents like lenvatinib and cabozantinib with immunotherapeutic agents, based on the LEAP-002 and COSMIC-312 trials. Further clinical trials are warranted to assess these agents' roles in managing HCC.

With the increasing use of immunotherapeutic agents in the neoadjuvant and adjuvant setting for early-stage HCC, we will see patients exposed to IO agents before recurrence and require systemic therapy. These patients may recur while still being on treatment with an IO agent or can recur after completion of treatment. The scope of immunotherapeutic agents in this setting will further need exploration. There is an unmet need for clinical trials to evaluate treatments involving HCC. Further immunotherapeutic agents are already being developed to improve the existing agents in the first-line setting.

FOOTNOTES

Author contributions: Bhatt A drafted the manuscript, coordinated all the authors' efforts and provided the final revisions; Wu J provided the concept of the manuscript, established the structure of the manuscript and revised the drafts.

Conflict-of-interest statement: All authors report having no relevant conflicts of interest for this article.

Country/Territory of origin: United States

ORCID number: Ahan Bhatt 0000-0003-1396-1735; Jennifer Wu 0000-0002-1714-0021.

S-Editor: Liu GL
L-Editor: Filipodia
P-Editor: Liu GL

REFERENCES

1 **Sung H**, Ferlay J, Siegel RL, Laversanne M, Soerjomataram I, Jemal A, Bray F. Global Cancer Statistics 2020: GLOBOCAN Estimates of Incidence and Mortality Worldwide for 36 Cancers in 185 Countries. *CA Cancer J Clin* 2021; **71**: 209-249 [PMID: 33538338 DOI: 10.3322/caac.21660]
2 **Altekruse SF**, Henley SJ, Cucinelli JE, McGlynn KA. Changing hepatocellular carcinoma incidence and liver cancer mortality rates in the United States. *Am J Gastroenterol* 2014; **109**: 542-553 [PMID: 24513805 DOI: 10.1038/ajg.2014.11]
3 **Ashtari S**, Pourhoseingholi MA, Sharifian A, Zali MR. Hepatocellular carcinoma in Asia: Prevention strategy and planning. *World J Hepatol* 2015; **7**: 1708-1717 [PMID: 26140091 DOI: 10.4254/wjh.v7.i12.1708]
4 **Arbuthnot P**, Kew M. Hepatitis B virus and hepatocellular carcinoma. *Int J Exp Pathol* 2001; **82**: 77-100 [PMID: 11454100 DOI: 10.1111/j.1365-2613.2001.iep0082-0077-x]
5 **Anstee QM**, Reeves HL, Kotsiliti E, Govaere O, Heikenwalder M. From NASH to HCC: current concepts and future challenges. *Nat Rev Gastroenterol Hepatol* 2019; **16**: 411-428 [PMID: 31028350 DOI: 10.1038/s41575-019-0145-7]
6 **Huang DQ**, Singal AG, Kono Y, Tan DJH, El-Serag HB, Loomba R. Changing global epidemiology of liver cancer from 2010 to 2019: NASH is the fastest growing cause of liver cancer. *Cell Metab* 2022; **34**: 969-977.e2 [PMID: 35793659 DOI: 10.1016/j.cmet.2022.05.003]
7 **Sanyal A**, Poklepovic A, Moyneur E, Barghout V. Population-based risk factors and resource utilization for HCC: US perspective. *Curr Med Res Opin* 2010; **26**: 2183-2191 [PMID: 20666689 DOI: 10.1185/03007995.2010.506375]
8 **Morgan TR**, Mandayam S, Jamal MM. Alcohol and hepatocellular carcinoma. *Gastroenterology* 2004; **127**: S87-S96 [PMID: 15508108 DOI: 10.1053/j.gastro.2004.09.020]
9 **de'Angelis N**, Landi F, Carra MC, Azoulay D. Managements of recurrent hepatocellular carcinoma after liver transplantation: A systematic review. *World J Gastroenterol* 2015; **21**: 11185-11198 [PMID: 26494973 DOI: 10.3748/wjg.v21.i39.11185]
10 **Shah SA**, Cleary SP, Wei AC, Yang I, Taylor BR, Hemming AW, Langer B, Grant DR, Greig PD, Gallinger S. Recurrence after liver resection for hepatocellular carcinoma: risk factors, treatment, and outcomes. *Surgery* 2007; **141**: 330-339 [PMID: 17349844 DOI: 10.1016/j.surg.2006.06.028]
11 **N'Kontchou G**, Mahamoudi A, Aout M, Ganne-Carrié N, Grando V, Coderc E, Vicaut E, Trinchet JC, Sellier N, Beaugrand M, Seror O. Radiofrequency ablation of hepatocellular carcinoma: long-term results and prognostic factors in 235 Western patients with cirrhosis. *Hepatology* 2009; **50**: 1475-1483 [PMID: 19731239 DOI: 10.1002/hep.23181]
12 **Wang JH**, Wang CC, Hung CH, Chen CL, Lu SN. Survival comparison between surgical resection and radiofrequency ablation for patients in BCLC very early/early stage hepatocellular carcinoma. *J Hepatol* 2012; **56**: 412-418 [PMID: 21756858 DOI: 10.1016/j.jhep.2011.05.020]
13 **Jeong SO**, Kim EB, Jeong SW, Jang JY, Lee SH, Kim SG, Cha SW, Kim YS, Cho YD, Kim HS, Kim BS, Kim YJ, Goo DE, Park SY. Predictive Factors for Complete Response and Recurrence after Transarterial Chemoembolization in Hepatocellular Carcinoma. *Gut Liver* 2017; **11**: 409-416 [PMID: 28208001 DOI: 10.5009/gnl16001]
14 **Herbst RS**, Soria JC, Kowanetz M, Fine GD, Hamid O, Gordon MS, Sosman JA, McDermott DF, Powderly JD, Gettinger SN, Kohrt HE, Horn L, Lawrence DP, Rost S, Leabman M, Xiao Y, Mokatrin A, Koeppen H, Hegde PS, Mellman I, Chen DS, Hodi FS. Predictive correlates of response to the anti-PD-L1 antibody MPDL3280A in cancer patients. *Nature* 2014; **515**: 563-567 [PMID: 25428504 DOI: 10.1038/nature14011]
15 **Ferrara N**, Hillan KJ, Novotny W. Bevacizumab (Avastin), a humanized anti-VEGF monoclonal antibody for cancer therapy. *Biochem Biophys Res Commun* 2005; **333**: 328-335 [PMID: 15961063 DOI: 10.1016/j.bbrc.2005.05.132]
16 **Lee M**, Ryoo BY, Hsu CH, Numata K, Stein S, Verret W, Hack S, Spahn J, Liu B, Abdullah H, He R, Lee KH. LBA39 - Randomised efficacy and safety results for atezolizumab (Atezo) + bevacizumab (Bev) in patients (pts) with previously untreated, unresectable hepatocellular carcinoma (HCC). *Annals of Oncology* 2019; **30**: v875 [DOI: 10.1093/annonc/mdz394.030]
17 **Morse MA**, Sun W, Kim R, He AR, Abada PB, Mynderse M, Finn RS. The Role of Angiogenesis in Hepatocellular Carcinoma. *Clin Cancer Res* 2019; **25**: 912-920 [PMID: 30274981 DOI: 10.1158/1078-0432.CCR-18-1254]
18 **Finn RS**, Bentley G, Britten CD, Amado R, Busuttil RW. Targeting vascular endothelial growth factor with the monoclonal antibody bevacizumab inhibits human hepatocellular carcinoma cells growing in an orthotopic mouse model. *Liver Int* 2009; **29**: 284-290 [PMID: 18482274 DOI: 10.1111/j.1478-3231.2008.01762.x]
19 **Fukumura D**, Kloepper J, Amoozgar Z, Duda DG, Jain RK. Enhancing cancer immunotherapy using antiangiogenics: opportunities and challenges. *Nat Rev Clin Oncol* 2018; **15**: 325-340 [PMID: 29508855 DOI: 10.1038/nrclinonc.2018.29]
20 **Wallin JJ**, Bendell JC, Funke R, Sznol M, Korski K, Jones S, Hernandez G, Mier J, He X, Hodi FS, Denker M, Leveque V, Cañamero M, Babitski G, Koeppen H, Ziai J, Sharma N, Gaire F, Chen DS, Waterkamp D, Hegde PS, McDermott DF. Atezolizumab in combination with bevacizumab enhances antigen-specific T-cell migration in metastatic renal cell carcinoma. *Nat Commun* 2016; **7**: 12624 [PMID: 27571927 DOI: 10.1038/ncomms12624]
21 **Food and Drug Administration**. FDA approves atezolizumab plus bevacizumab for unresectable hepatocellular carcinoma. Available from: https://www.fda.gov/drugs/resources-information-approved-drugs/fda-approves-atezolizumab-plus-bevacizumab-unresectable-hepatocellular-carcinoma

22 **Finn RS**, Qin S, Ikeda M, Galle PR, Ducreux M, Kim TY, Kudo M, Breder V, Merle P, Kaseb AO, Li D, Verret W, Xu DZ, Hernandez S, Liu J, Huang C, Mulla S, Wang Y, Lim HY, Zhu AX, Cheng AL; IMbrave150 Investigators. Atezolizumab plus Bevacizumab in Unresectable Hepatocellular Carcinoma. *N Engl J Med* 2020; **382**: 1894-1905 [PMID: 32402160 DOI: 10.1056/NEJMoa1915745]

23 **Cheng AL**, Qin S, Ikeda M, Galle PR, Ducreux M, Kim TY, Lim HY, Kudo M, Breder V, Merle P, Kaseb AO, Li D, Verret W, Ma N, Nicholas A, Wang Y, Li L, Zhu AX, Finn RS. Updated efficacy and safety data from IMbrave150: Atezolizumab plus bevacizumab vs. sorafenib for unresectable hepatocellular carcinoma. *J Hepatol* 2022; **76**: 862-873 [PMID: 34902530 DOI: 10.1016/j.jhep.2021.11.030]

24 **Stewart R**, Morrow M, Hammond SA, Mulgrew K, Marcus D, Poon E, Watkins A, Mullins S, Chodorge M, Andrews J, Bannister D, Dick E, Crawford N, Parmentier J, Alimzhanov M, Babcook JS, Foltz IN, Buchanan A, Bedian V, Wilkinson RW, McCourt M. Identification and Characterization of MEDI4736, an Antagonistic Anti-PD-L1 Monoclonal Antibody. *Cancer Immunol Res* 2015; **3**: 1052-1062 [PMID: 25943534 DOI: 10.1158/2326-6066.CIR-14-0191]

25 **Tarhini AA**, Kirkwood JM. Tremelimumab (CP-675,206): a fully human anticytotoxic T lymphocyte-associated antigen 4 monoclonal antibody for treatment of patients with advanced cancers. *Expert Opin Biol Ther* 2008; **8**: 1583-1593 [PMID: 18774925 DOI: 10.1517/14712598.8.10.1583]

26 **Kudo M**. Scientific Rationale for Combination Immunotherapy of Hepatocellular Carcinoma with Anti-PD-1/PD-L1 and Anti-CTLA-4 Antibodies. *Liver Cancer* 2019; **8**: 413-426 [PMID: 32479569 DOI: 10.1159/000503254]

27 **Abou-Alfa GK**, Chan SL, Kudo M, Lau G, Kelley RK, Furuse J, Sukeepaisarnjaroen W, Kang YK, Dao TV, De Toni EN, Rimassa L, Breder VV, Vasilyev A, Heurgue A, Tam V, Mody K, Thungappa SC, He P, Negro A, Sangro B. Phase 3 randomized, open-label, multicenter study of tremelimumab (T) and durvalumab (D) as first-line therapy in patients (pts) with unresectable hepatocellular carcinoma (uHCC): HIMALAYA. *Journal of Clinical Oncology* 2022; **40**: 379-379 [DOI: 10.1200/jco.2022.40.4_suppl.379]

28 **Kudo M**. Durvalumab Plus Tremelimumab: A Novel Combination Immunotherapy for Unresectable Hepatocellular Carcinoma. *Liver Cancer* 2022; **11**: 87-93 [PMID: 35634425 DOI: 10.1159/000523702]

29 **Qin S**, Finn RS, Kudo M, Meyer T, Vogel A, Ducreux M, Macarulla TM, Tomasello G, Boisserie F, Hou J, Li X, Song J, Zhu AX. RATIONALE 301 study: tislelizumab *vs* sorafenib as first-line treatment for unresectable hepatocellular carcinoma. *Future Oncol* 2019; **15**: 1811-1822 [PMID: 30969136 DOI: 10.2217/fon-2019-0097]

30 **Qin S**, Kudo M, Meyer T, Finn RS, Vogel A, Bai Y, Guo Y, Meng Z, Zhang T, Satoh T, Hiraoka A, Marino D, Assenat E, Wyrwicz L, Campos MC, Hsing-Tao K, Boisserie F, Li S, Chen Y, Zhu AX. LBA36 Final analysis of RATIONALE-301: Randomized, phase III study of tislelizumab*vs*sorafenib as first-line treatment for unresectable hepatocellular carcinoma. *Annals of Oncology* 2022; **33**: S1402-S3 [DOI: 10.1016/j.annonc.2022.08.033]

31 A Study of Nivolumab in Combination With Ipilimumab in Participants With Advanced Hepatocellular Carcinoma (CheckMate 9DW). [Internet] [cited31 July 2019]. Available from: https://clinicaltrials.gov/ct2/show/NCT04039607

32 **Rausch M**, Hua J, Moodley D, White KF, Walsh KH, Miller CE, Tan G, Lee BH, Cousineau I, Lattouf J-B, Stagg J, Palombella VJ, Holland PM, Hill JA. Abstract 4550: Increased IL-27 is associated with poor prognosis in renal cell carcinoma and supports use of SRF388, a first-in-class IL-27p28 blocking antibody, to counteract IL-27-mediated immunosuppression in this setting. *Cancer Research* 2020; **80** (16_suppl): 4550 [DOI: 10.1158/1538-7445.AM2020-4550]

33 **Naing A**, Mantia C, Morgensztern D, Kim T-Y, Li D, Kang Y-K, Marron TU, Tripathi A, George S, Rini BI, El-Khoueiry AB, Vaishampayan UN, Kelley RK, Ornstein MC, Appleman LJ, Harshman LC, Lee B, Tannir NM, Hammers HJ, Patnaik A. First-in-human study of SRF388, a first-in-class IL-27 targeting antibody, as monotherapy and in combination with pembrolizumab in patients with advanced solid tumors. *Journal of Clinical Oncology* 2022; **40** (16_suppl): 2501 [DOI: 10.1200/jco.2022.40.16_suppl.2501]

34 **Kim H**, Cheon J, Ha Y, Kim HS, Kim CG, Kim I, Kim C, Jung S-h, Chon HJ. Atezolizumab plus bevacizumab in Child-Pugh B advanced hepatocellular carcinoma patients. *Journal of Clinical Oncology* 2022; **40** (4_suppl): 397 [DOI: 10.1200/jco.2022.40.4_suppl.397]

35 **Choi WM**, Lee D, Shim JH, Kim KM, Lim YS, Lee HC, Yoo C, Park SR, Ryu MH, Ryoo BY, Choi J. Effectiveness and Safety of Nivolumab in Child-Pugh B Patients with Hepatocellular Carcinoma: A Real-World Cohort Study. *Cancers (Basel)* 2020; **12** [PMID: 32698355 DOI: 10.3390/cancers12071968]

36 **Wong JSL**, Kwok GW, Tang V, Li B, Leung RC-Y, Chiu JWY, Ma KW, She W-H, Tsang WYJ, Cheung TT, Yau T. Nivolumab/pembrolizumab in Child-Pugh grade B/C patients with advanced HCC. *Journal of Clinical Oncology* 2021; **39(15_suppl)**: e16184 [DOI: 10.1200/jco.2021.39.15_suppl.e16184]

37 A Study of Atezolizumab and Bevacizumab in Hepatocellular Carcinoma (AB7). Available from: https://clinicaltrials.gov/ct2/show/NCT04829383 [DOI: 10.1200/jco.2022.40.4_suppl.tps493]

38 **El-Khoueiry AB**, Sangro B, Yau T, Crocenzi TS, Kudo M, Hsu C, Kim TY, Choo SP, Trojan J, Welling TH Rd, Meyer T, Kang YK, Yeo W, Chopra A, Anderson J, Dela Cruz C, Lang L, Neely J, Tang H, Dastani HB, Melero I. Nivolumab in patients with advanced hepatocellular carcinoma (CheckMate 040): an open-label, non-comparative, phase 1/2 dose escalation and expansion trial. *Lancet* 2017; **389**: 2492-2502 [PMID: 28434648 DOI: 10.1016/S0140-6736(17)31046-2]

39 **Yau T**, Park JW, Finn RS, Cheng AL, Mathurin P, Edeline J, Kudo M, Harding JJ, Merle P, Rosmorduc O, Wyrwicz L, Schott E, Choo SP, Kelley RK, Sieghart W, Assenat E, Zaucha R, Furuse J, Abou-Alfa GK, El-Khoueiry AB, Melero I, Begic D, Chen G, Neely J, Wisniewski T, Tschaika M, Sangro B. Nivolumab *vs* sorafenib in advanced hepatocellular carcinoma (CheckMate 459): a randomised, multicentre, open-label, phase 3 trial. *Lancet Oncol* 2022; **23**: 77-90 [PMID: 34914889 DOI: 10.1016/S1470-2045(21)00604-5]

40 **Bristol Myers Squibb**. Bristol Myers Squibb Statement on Opdivo® (nivolumab) Monotherapy Post-Sorafenib Hepatocellular Carcinoma U.S. Indication.Available from: https://news.bms.com/news/details/2021/Bristol-Myers-Squibb-Statement-on-Opdivo-nivolumab-Monotherapy-Post-Sorafenib-Hepatocellular-Carcinoma-U.S.-Indication/default.aspx#:~:text=In%20consultation%20with%20the%20U.S.,sorafenib%20from%20the%20U.S.%20market

41 **Yau T**, Kang YK, Kim TY, El-Khoueiry AB, Santoro A, Sangro B, Melero I, Kudo M, Hou MM, Matilla A, Tovoli F, Knox JJ, Ruth He A, El-Rayes BF, Acosta-Rivera M, Lim HY, Neely J, Shen Y, Wisniewski T, Anderson J, Hsu C. Efficacy and Safety of Nivolumab Plus Ipilimumab in Patients With Advanced Hepatocellular Carcinoma Previously

Treated With Sorafenib: The CheckMate 040 Randomized Clinical Trial. *JAMA Oncol* 2020; **6**: e204564 [PMID: 33001135 DOI: 10.1001/jamaoncol.2020.4564]

42 **El-Khoueiry AB**, Yau T, Kang YK, Kim TY, Santoro A, Sangro B, Melero I, Kudo M, Hou MM, Matilla A, Tovoli F, Knox JJ, He AR, El-Rayes BF, Acosta-Rivera M, Lim HY, Memaj A, Sama AR, Hsu C. Nivolumab (NIVO) plus ipilimumab (IPI) combination therapy in patients (Pts) with advanced hepatocellular carcinoma (aHCC): Long-term results from CheckMate 040. *Journal of Clinical Oncology* 2021; **39**: 269 [DOI: 10.1200/jco.2021.39.3_suppl.269]

43 **Zhu AX**, Finn RS, Edeline J, Cattan S, Ogasawara S, Palmer D, Verslype C, Zagonel V, Fartoux L, Vogel A, Sarker D, Verset G, Chan SL, Knox J, Daniele B, Webber AL, Ebbinghaus SW, Ma J, Siegel AB, Cheng AL, Kudo M; KEYNOTE-224 investigators. Pembrolizumab in patients with advanced hepatocellular carcinoma previously treated with sorafenib (KEYNOTE-224): a non-randomised, open-label phase 2 trial. *Lancet Oncol* 2018; **19**: 940-952 [PMID: 29875066 DOI: 10.1016/S1470-2045(18)30351-6]

44 **Finn RS**, Ryoo BY, Merle P, Kudo M, Bouattour M, Lim HY, Breder V, Edeline J, Chao Y, Ogasawara S, Yau T, Garrido M, Chan SL, Knox J, Daniele B, Ebbinghaus SW, Chen E, Siegel AB, Zhu AX, Cheng AL; KEYNOTE-240 investigators. Pembrolizumab As Second-Line Therapy in Patients With Advanced Hepatocellular Carcinoma in KEYNOTE-240: A Randomized, Double-Blind, Phase III Trial. *J Clin Oncol* 2020; **38**: 193-202 [PMID: 31790344 DOI: 10.1200/JCO.19.01307]

45 **Qin SK**, Chen ZD, Fang WJ, Ren ZG, Xu RC, Ryoo BY, Meng ZQ, Bai YX, Chen XM, Liu XF, Xiao JX, Ho GF, Mao YM, Ye X, Ying JE, Li JF, Zhong WY, Zhou Y, Siegel AB, Hao CY. Pembrolizumab plus best supportive care *vs* placebo plus best supportive care as second-line therapy in patients in Asia with advanced hepatocellular carcinoma (HCC): Phase 3 KEYNOTE-394 study. *Journal of Clinical Oncology* 2022; **40**: 383 [DOI: 10.1200/jco.2022.40.4_suppl.383]

46 **Wong JSL**, Kwok GGW, Tang V, Li BCW, Leung R, Chiu J, Ma KW, She WH, Tsang J, Lo CM, Cheung TT, Yau T. Ipilimumab and nivolumab/pembrolizumab in advanced hepatocellular carcinoma refractory to prior immune checkpoint inhibitors. *J Immunother Cancer* 2021; **9** [PMID: 33563773 DOI: 10.1136/jitc-2020-001945]

47 **Qin S**, Chan LS, Gu S, Bai Y, Ren Z, Lin X, Chen Z, Jia W, Jin Y, Guo Y, Sultanbaev AV, Pazgan-Simon M, Pisetska M, Liang X, Chen C, Nie Z, Wang L, Cheng AL, Kaseb A, Vogel A. LBA35 Camrelizumab (C) plus rivoceranib (R) vs. sorafenib (S) as first-line therapy for unresectable hepatocellular carcinoma (uHCC): A randomized, phase III trial. *Annals of Oncology* 2022; **33**: S1401-S2 [DOI: 10.1016/j.annonc.2022.08.032]

48 **Finn RS**, Ikeda M, Zhu AX, Sung MW, Baron AD, Kudo M, Okusaka T, Kobayashi M, Kumada H, Kaneko S, Pracht M, Mamontov K, Meyer T, Kubota T, Dutcus CE, Saito K, Siegel AB, Dubrovsky L, Mody K, Llovet JM. Phase Ib Study of Lenvatinib Plus Pembrolizumab in Patients With Unresectable Hepatocellular Carcinoma. *J Clin Oncol* 2020; **38**: 2960-2970 [PMID: 32716739 DOI: 10.1200/JCO.20.00808]

49 **Finn RS**, Kudo M, Merle P, Meyer T, Qin S, Ikeda M, Xu R, Edeline J, Ryoo BY, Ren Z, Cheng AL, Galle PR, Kaneko S, Kumada H, Wang A, Mody K, Dubrovsky L, Siegel AB, Llovet J. LBA34 Primary results from the phase III LEAP-002 study: Lenvatinib plus pembrolizumab*vs*lenvatinib as first-line (1L) therapy for advanced hepatocellular carcinoma (aHCC). *Annals of Oncology* 2022; **33**: S1401 [DOI: 10.1016/j.annonc.2022.08.031]

50 **Kudo M**, Finn RS, Qin S, Han KH, Ikeda K, Piscaglia F, Baron A, Park JW, Han G, Jassem J, Blanc JF, Vogel A, Komov D, Evans TRJ, Lopez C, Dutcus C, Guo M, Saito K, Kraljevic S, Tamai T, Ren M, Cheng AL. Lenvatinib *vs* sorafenib in first-line treatment of patients with unresectable hepatocellular carcinoma: a randomised phase 3 non-inferiority trial. *Lancet* 2018; **391**: 1163-1173 [PMID: 29433850 DOI: 10.1016/S0140-6736(18)30207-1]

51 **Kelley RK**, Rimassa L, Cheng AL, Kaseb A, Qin S, Zhu AX, Chan SL, Melkadze T, Sukeepaisarnjaroen W, Breder V, Verset G, Gane E, Borbath I, Rangel JDG, Ryoo BY, Makharadze T, Merle P, Benzaghou F, Banerjee K, Hazra S, Fawcett J, Yau T. Cabozantinib plus atezolizumab *vs* sorafenib for advanced hepatocellular carcinoma (COSMIC-312): a multicentre, open-label, randomised, phase 3 trial. *Lancet Oncol* 2022; **23**: 995-1008 [PMID: 35798016 DOI: 10.1016/S1470-2045(22)00326-6]

52 A Phase 2, Randomized, Open-label Study of Relatlimab in Combination With Nivolumab in Participants With Advanced Hepatocellular Carcinoma Who Are Naive to IO Therapy But Progressed on Tyrosine Kinase Inhibitors (RELATIVITY-073). [Internet] [cited 28 September 2020]. Available from: https://clinicaltrials.gov/ct2/show/NCT04567615

53 A Study of Nivolumab and Relatlimab in Combination With Bevacizumab in Advanced Liver Cancer (RELATIVITY-106).[Internet] [cited 20 April 2022]. Available from: https://clinicaltrials.gov/ct2/show/NCT05337137

54 **Shi D**, Shi Y, Kaseb AO, Qi X, Zhang Y, Chi J, Lu Q, Gao H, Jiang H, Wang H, Yuan D, Ma H, Li Z, Zhai B. Chimeric Antigen Receptor-Glypican-3 T-Cell Therapy for Advanced Hepatocellular Carcinoma: Results of Phase I Trials. *Clin Cancer Res* 2020; **26**: 3979-3989 [PMID: 32371538 DOI: 10.1158/1078-0432.CCR-19-3259]

55 **Shirakawa H**, Suzuki H, Shimomura M, Kojima M, Gotohda N, Takahashi S, Nakagohri T, Konishi M, Kobayashi N, Kinoshita T, Nakatsura T. Glypican-3 expression is correlated with poor prognosis in hepatocellular carcinoma. *Cancer Sci* 2009; **100**: 1403-1407 [PMID: 19496787 DOI: 10.1111/j.1349-7006.2009.01206.x]

56 **Lee HA**, Goh HG, Lee YS, Jung YK, Kim JH, Yim HJ, Lee MG, An H, Jeen YT, Yeon JE, Byun KS, Seo YS. Natural killer cell activity is a risk factor for the recurrence risk after curative treatment of hepatocellular carcinoma. *BMC Gastroenterol* 2021; **21**: 258 [PMID: 34118869 DOI: 10.1186/s12876-021-01833-2]

57 FT500 as Monotherapy and in Combination With Immune Checkpoint Inhibitors in Subjects With Advanced Solid Tumors. [Internet] [cited15 February 2019]. Available from: https://clinicaltrials.gov/ct2/show/NCT03841110

58 FATE-NK100 as Monotherapy and in Combination With Monoclonal Antibody in Subjects With Advanced Solid Tumors. [Internet] [cited24 October 2017]. Available from: https://clinicaltrials.gov/ct2/show/NCT03319459

59 **Llovet JM**, Ricci S, Mazzaferro V, Hilgard P, Gane E, Blanc JF, de Oliveira AC, Santoro A, Raoul JL, Forner A, Schwartz M, Porta C, Zeuzem S, Bolondi L, Greten TF, Galle PR, Seitz JF, Borbath I, Häussinger D, Giannaris T, Shan M, Moscovici M, Voliotis D, Bruix J; SHARP Investigators Study Group. Sorafenib in advanced hepatocellular carcinoma. *N Engl J Med* 2008; **359**: 378-390 [PMID: 18650514 DOI: 10.1056/NEJMoa0708857]

World Journal of Gastroenterology

Submit a Manuscript: https://www.f6publishing.com

World J Gastroenterol 2023 April 21; 29(15): 2272-2282

DOI: 10.3748/wjg.v29.i15.2272

ISSN 1007-9327 (print) ISSN 2219-2840 (online)

MINIREVIEWS

Intestinal ultrasound as a non-invasive tool to monitor inflammatory bowel disease activity and guide clinical decision making

Michael T Dolinger, Maia Kayal

Specialty type: Gastroenterology and hepatology

Provenance and peer review: Invited article; Externally peer reviewed.

Peer-review model: Single blind

Peer-review report's scientific quality classification

Grade A (Excellent): 0
Grade B (Very good): B
Grade C (Good): C
Grade D (Fair): 0
Grade E (Poor): 0

P-Reviewer: Giannetti A, Italy; Zhou W, China

Received: October 26, 2022
Peer-review started: October 26, 2022
First decision: December 12, 2022
Revised: January 19, 2023
Accepted: March 31, 2023
Article in press: March 31, 2023
Published online: April 21, 2023

Michael T Dolinger, Department of Pediatric Gastroenterology, Icahn School of Medicine at Mount Sinai, New York, NY 10029, United States

Maia Kayal, Department of Medicine, Division of Gastroenterology, Icahn School of Medicine at Mount Sinai, New York, NY 10029, United States

Corresponding author: Maia Kayal, MD, MS, Assistant Professor, Department of Medicine, Division of Gastroenterology, Icahn School of Medicine at Mount Sinai, One Gustave L. Levy Place Box 1069, New York, NY 10029, United States. maia.kayal@mountsinai.org

Abstract

Intestinal ultrasound (IUS) is a non-invasive, real-time, cross-sectional imaging tool that can be used at the point-of-care to assess disease activity in patients with Crohn's disease or ulcerative colitis. IUS promotes quick and impactful treatment decisions that can modify disease progression and enhance patient compliance. This review will summarize the technical aspects of IUS, the evidence to support the use of IUS in disease activity monitoring, the comparison of IUS to current standard of care monitoring modalities such as colonoscopy and calprotectin, and the optimal positioning of IUS in a tight-control monitoring strategy.

Key Words: Crohn's disease; Ulcerative colitis; Disease monitoring; Intestinal ultrasound

Core Tip: Intestinal ultrasound (IUS) is a non-invasive, real-time, cross-sectional imaging tool that is currently underutilized for direct disease activity monitoring in Crohn's disease (CD) and ulcerative colitis (UC). IUS is the optimal point-of-care method to monitor disease activity in patients with CD or UC with excellent patient compliance and comparison to such traditional monitoring modalities as calprotectin, colonoscopy, and magnetic resonance enterography.

Citation: Dolinger MT, Kayal M. Intestinal ultrasound as a non-invasive tool to monitor inflammatory bowel disease activity and guide clinical decision making. *World J Gastroenterol* 2023; 29(15): 2272-2282
URL: https://www.wjgnet.com/1007-9327/full/v29/i15/2272.htm
DOI: https://dx.doi.org/10.3748/wjg.v29.i15.2272

INTRODUCTION

The current conventional approach to inflammatory bowel disease (IBD) monitoring in the United States includes routine patient visits to the gastroenterology clinic every 3-6 mo with more urgent or frequent visits based on symptomatology. During these visits, an assessment of the patient's current disease status is undertaken *via* history and physical examination. After the visit, the evaluation typically continues with biomarkers such as C-reactive protein and fecal calprotectin (FC), colonoscopy, and magnetic resonance enterography (MRE) though results are often delayed and compliance rates low. This traditional, fragmented model of IBD monitoring is not well suited to detect subclinical inflammation or prevent disease progression, and has contributed to a therapeutic effectiveness ceiling of 30%[1].

Intestinal ultrasound (IUS) is a non-invasive, real-time, cross-sectional imaging tool that is currently underutilized for direct disease activity monitoring in Crohn's disease (CD) and ulcerative colitis (UC)[2]. Use of IUS at the point-of-care in a tight monitoring model can add significant value to the routine clinic visit by allowing the treating gastroenterologist to accurately and immediately assess disease activity and treatment responsiveness, something that is sorely lacking in the current traditional IBD care model. Furthermore, IUS allows for the easy assessment of transmural healing (TH), a target beyond simple mucosal healing (MH) that may impact long-term disease outcomes.

In this review, we discuss key concepts to understand how IUS utilization will impact care delivery for patients with IBD and achieve disease modification. We will review the technical aspects of IUS, evidence for detection of disease activity and treatment responsiveness, comparison to current standard of care management tools such as MRE, FC, and ileo colonoscopy, impact on shared understanding and real-time decision making, optimal utilization, and future applications.

TECHNICAL ASPECTS OF IUS

Basic ultrasound machine requirements

Use of IUS as a cross-sectional tool for disease activity monitoring starts with a minimum requirement of a modern ultrasound machine available for regular use. Two probes are needed with ability to assess color Doppler signal (CDS) - a lower-frequency convex array probe (3-5 MHz) for global evaluation of the entire bowel and assessment of complications with ability for deeper penetration, and a higher-frequency linear array probe (5-15 MHz) for visualization of the five bowel wall layers and measurement of bowel wall thickness (BWT) to the level of 0.1 millimeters (mm)[3].

Patient preparation and the role of contrast

Fasting or bowel preparation prior to IUS is unnecessary for optimal visualization of the bowel and the examination can be performed without any prior planning. Intravenous [Contrast Enhanced Ultrasound (CEUS)] or oral contrast [Small Intestinal Contrast Ultrasound (SICUS)] are not beneficial during point-of-care evaluation in IBD activity monitoring and treatment response assessment. The value of CEUS and SICUS, based on local availability and expertise, is in the assessment of suspected complications. CEUS is a valuable tool in the detection of and differentiation of phlegmon and abscesses compared to traditional non-contrast IUS[4]. SICUS adds further value over IUS in the evaluation of proximal small bowel (proximal ileal and jejunal) lesions and detection of stenoses, but the ingestion of oral contrast leads to extended time for completion of the examination that is no longer suitable for use as a point-of-care assessment tool[5,6].

IUS examination

IUS examination should begin with an initial assessment of the distal sigmoid colon using the convex probe beginning in the left lower quadrant of the abdomen or left suprapubic region with identification of the iliac vessels and left iliopsoas muscle, fanning the probe up with the use of graded compression to identify air within the lumen of the distal sigmoid colon and visualization of the subsequent bowel wall layers (Figure 1).

The colon should then be tracked proximally visualizing the retroperitoneal descending colon to the left inferior border of the intercostals or just below to denote the splenic flexure, then to identify the transverse colon utilizing the thick wall of the stomach as an anatomical landmark, then to the hepatic flexure, downward toward the right lateral hemiabdomen to visualize the ascending colon, cecum, and

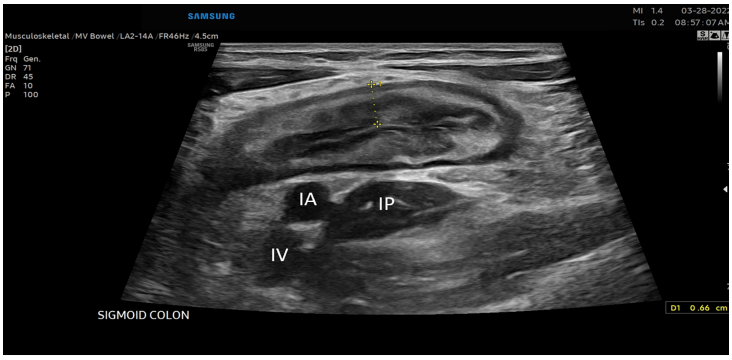

DOI: 10.3748/wjg.v29.i15.2272

Figure 1 Inflamed sigmoid colon located super to the iliac vessels and iliopsoas muscle in the left lower quadrant of the abdomen. IA: Iliac artery; IV: Iliac vein; IP: Iliopsoas muscle.

ultimately to the right lower quadrant of the abdomen and/or right suprapubic region to identify the ileocecal valve, and terminal ileum, again using the right lower quadrant iliac vessels and iliopsoas muscle as a landmark for proper identification of the terminal ileum superior. The remainder of the proximal small intestine should be scanned in a "lawn-mower" technique, sweeping up and down over the mid-abdomen, to visualize the remaining proximal small bowel. Differentiation of the large intestine and small intestine from one another during this process is essential and done easily based on the hypermotility and movement of intestinal contents within the small bowel compared to that of the colon. Once the global initial assessment of the bowel is complete with a convex probe, careful repeat assessment of the entire colon and small bowel should be performed for IBD activity assessment with the linear high-frequency probe. Measurements for BWT should be performed for each segment in both longitudinal and transverse planes, with an average of measurements taken at least 1 cm apart denoting the thickness between the lumen-mucosal interface and the muscularis-serosal interface (Figure 2). CDS assessment of the bowel wall for hyperemia should be performed in each segment with use of the modified Limberg score (Figure 3). The other two parameters that should be assessed in each segment are inflammatory fat (iFat) and the presence or loss of bowel wall layer stratification.

Bowel segments for IUS activity monitoring

The primary bowel segments assessed during every IUS examination are the sigmoid colon, descending colon, transverse colon, ascending colon, cecum, and terminal ileum[7]. Visualization of the rectum can be challenging and typically only performed with adequate resolution for disease activity assessment in patients with lower body mass indices and full bladders at the time of examination. Even with visualization of the rectum, normal values are not well defined, thus making it even harder for use at the point-of-care for disease activity assessment without benchmark with another non-invasive biomarker such as FC or a recent endoscopic evaluation. Additionally, the proximal small bowel beyond 30 cm of the ileum remains challenging and even an expert utilizing the proper technique may miss proximal ileal or jejunal inflammation relying on evaluation with IUS alone (Table 1).

MONITORING DISEASE ACTIVITY AND TREATMENT RESPONSE

Features of disease activity

IUS assessment of BWT is the primary and most important measure of disease activity in both CD and UC and has been shown to correlate with endoscopic inflammation[8]. In adults, a BWT cut-off > 3 mm in any segment is the most consistent individual IUS parameter that correlates with active endoscopic disease, with a sensitivity and specificity of 88%-89% and 93%-96% respectively[9,10]. When assessing the colonic bowel segments in patients with IBD, the per patient sensitivity and specificity of IUS to detect disease activity is 90% and 96% respectively[11]. UC is a transmural disease and thus IUS is an excellent option to monitor disease activity non-invasively and assess disease extension in patients with ulcerative proctitis[12]. In a retrospective study of patients with UC, BWT alone was shown to correlate with the Mayo endoscopic score[13]. In children, there is no agreed upon cut-off for BWT that correlates with endoscopic activity, however a BWT < 2 mm is almost always normal[14].

After BWT, hyperemia assessed by CDS is the next most important measure of disease activity. Assessment of CDS alone has been shown to correlate with CD clinical activity[15-17]. When combined with increased BWT, increased hyperemia is almost always representative of active disease. In fact, in development of both CD and UC IUS scores with endoscopy, multivariable analysis demonstrates that often the only independent predictors of endoscopic activity are BWT and hyperemia[18-20]. Additional

Table 1 Optimal and limited bowel segments for intestinal ultrasound disease activity monitoring

Optimal bowel segments	Limited bowel segments
Sigmoid colon	Rectum
Descending colon	Splenic flexure
Transverse colon	Proximal ileum
Ascending colon	Jejunum
Ileocecal valve	
Terminal ileum	

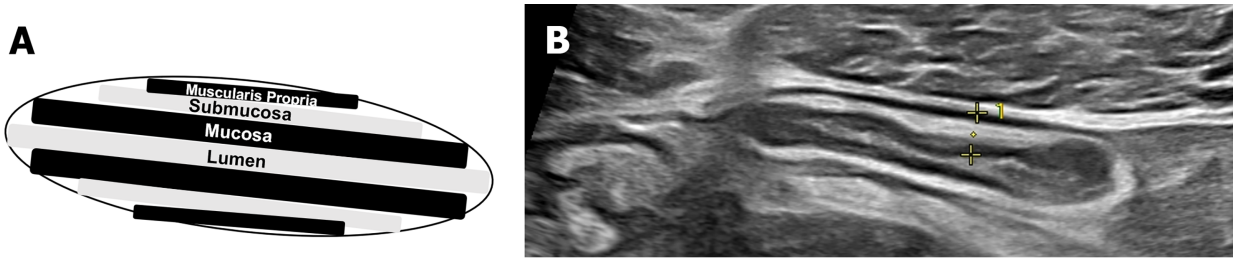

DOI: 10.3748/wjg.v29.i15.2272 **Copyright** ©The Author(s) 2023.

Figure 2 Measurements for bowel wall thickness. A: Schematic of bowel wall layers; B: Bowel wall thickness measurement in the inflamed terminal ileum, yellow lines indicate the measurement of bowel wall thickness from the lumen-mucosa interface to the muscularis propria-serosal interact.

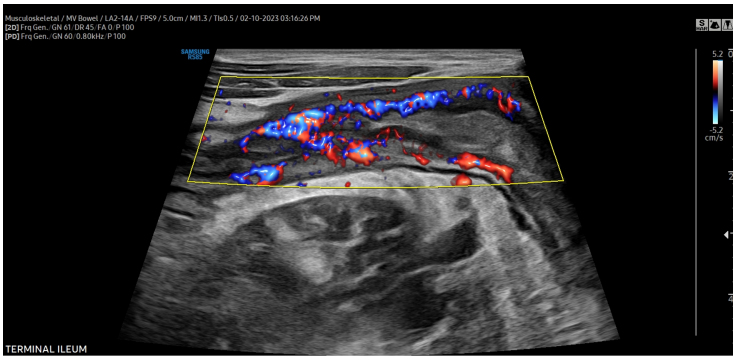

DOI: 10.3748/wjg.v29.i15.2272 **Copyright** ©The Author(s) 2023.

Figure 3 Severe hyperemia assessed by color Doppler signal. Color Doppler signal graded by the modified Limberg score. Shown here is a modified Limberg score of 3 in the terminal ileum. A score of 0 = absent signal. A score of 1: Short signals inside the bowel. A score of 2: Long signals inside the bowel, and a score of 3: Long signals inside and outside of the bowel.

characteristics of inflammation in IBD are focal disruption of the bowel wall layers, and hypoechoic or hyperechoic changes in the layers representing a loss of bowel wall stratification. Inflammatory mesenteric fat wrapping is seen, appearing hyperechoic encasing the inflamed bowel.

IUS activity scores

There have been more than twenty IUS activity scores developed for adults with CD and UC, with the most common and important parameters being BWT, followed by both hyperemia and bowel wall stratification[21]. Only a few recently developed IUS scores have been validated with a standardized endoscopic score. They are simple and can be used at the point-of-care for clinical decision making without significant time for calculation (Table 2)[19,20,22-24]. Only two scores specific to children with IBD have been developed, one CD and one UC, and only the UC score is validated with an endoscopic score[24,25]. A novel IUS score recently developed by a group of international experts, the International Bowel Ultrasound Group (IBUS)-SAS (score 0-100), is yet to be validated and is more complex. Although its clinical utility may be limited, it may serve as a novel score for disease monitoring and treatment response in clinical trials[26].

Table 2 Interpretation of validated and simple intestinal ultrasound activity scores for Crohn's disease and ulcerative colitis

IUS scoring system	BWT (mm)	iFAT	Modified LS	LBWS	Other
Crohn's disease indices					
SUS-CD (0-5)[19]	0: < 3.0 1: 3.0-4.9 2: 5.0-7.9 3: ≥ 8.0		0: LS 0 1: LS 1-2 2: LS 3		
Simple US score[20]	0.957 (BWT)		0.859 (LS)		
Ulcerative colitis indices					
MUC[21,24]	1.4 (BWT)		0: LS 0 2: LS 1-3		
UC-IUS (0-7)[25]	0: ≤ 2 1: 2.1-3.0 2: 3.1-4.0 3: > 4	0: Absent 1: Present	0: LS 0 1: LS 1 2: LS 2-3	0: No loss 1: Loss is present	
Civitelli UC index (0-4)[26] (pediatric)	0: ≤ 3 1: > 3		0: LS 0 2: LS 1-3	0: No loss 1: Loss is present	Abnormal haustrations (0: Normal, 1: Abnormal)

IUS: Intestinal ultrasound; BWT: Bowel wall thickness; iFat: Inflammatory fat; LS: Limberg Score; LBWS: Loss of bowel wall stratification; UC: Ulcerative colitis; CD: Crohn's disease.

Monitoring treatment response in CD and UC

IUS is a reliable tool to monitor treatment response in both CD and UC. Improvement in all IUS parameters (BWT, hyperemia, iFat, bowel wall stratification) can be seen within 12 wk of treatment initiation, with faster changes seen in certain patients and in the colon as compared to the ileum. (30) How to interpret these changes, including defining transmural remission, and the timing of repeat IUS assessments remains an evolving concept.

In patients with CD prescribed anti-inflammatory IBD therapy, a large multicenter German study demonstrated that improvement in all IUS measures can be seen at both 3 and 12 mo[27]. TH, defined as a BWT ≤ 3 mm and absent hyperemia by CDS, has been shown to be achievable in approximately 25%-31% of adult patients with CD after 2 years of treatment[28-32]. The STARDUST sub-study recently evaluated the effect of ustekinumab on TH monitored by IUS and demonstrated increasing TH rates to a total of 24.1% by week 48[33]. In 40 adult patients with endoscopically active CD initiating anti-tumor necrosis factor therapy, an 18% decrease in BWT 4-8 wk post-induction predicted endoscopic response [area under the receiver operating characteristic curve (AUROC) =0.77, odds ratio (OR) = 10.80, P = 0.012] and a BWT cut-off of 3.2 mm was accurate to detect endoscopic remission (AUROC = 0.94, OR = 39.42, P < 0.0001) at weeks 12-32[34]. Lastly, a recent multicenter Italian study of adult patients with CD treated with various biologic therapies demonstrated higher rates of TH (defined as normalization of all IUS parameters) with improvement in IUS in 53% at 3 mo and 64% by 1 year with a number needed to treat of 3.6 patients in order to achieve TH. Compared to MH alone, TH is associated with improved outcomes and a decreased risk of long-term disease progression[29,30,35,36].

Similarly, there is evidence in patients with UC to support the use of IUS as a monitoring tool of treatment response, and in fact, changes on IUS may be seen quicker in patients with UC compared to those with ileal CD. Evidence comes from a large multicenter German study of patients with UC who experienced clinical relapse and were treated with anti-inflammatory therapies; there was improvement in the colon BWT as early as 2 wk and BWT improvement continued 12 wk after treatment initiation [37]. In a study of 74 patients with UC, those who did not have a significant treatment response on IUS by 3 mo, measured by a significantly increased BWT to > 6 mm and presence of hyperemia, were at increased risk of continued severe endoscopic activity at 15 mo[38]. In 27 patients with UC treated with tofacitinib, BWT correlated with Mayo score (r = 0.68, P < 0.0001) and UC Endoscopic Index for Severity (r = 0.73, P < 0.0001) at induction and week 8 after treatment initiation. A decrease in BWT was more pronounced in patients with endoscopic response with a decrease in BWT of 32% from baseline being accurate for endoscopic response (AUROC = 0.87) and a BWT cut-off of 2.8 mm being the most accurate value to detect endoscopic remission (AUROC = 0.87)[39]. Utilizing IUS at baseline in patients with UC can also predict disease course. A Milan Ultrasound Criteria score > 6.2 at baseline in a study of 98

patients with UC was predictive of a negative disease course (need for corticosteroids, change in therapy, hospitalization, or colectomy) at 1.6 years after treatment initiation[40].

Utility for monitoring in pregnancy

While it is critical to control IBD activity during pregnancy, the tools for tight control disease activity monitoring are limited. IUS provides significant value for the precise monitoring of disease activity in the colon throughout all three trimesters and in the terminal ileum during the first two trimesters. In an Australian cohort of 90 pregnant women with IBD, 127 IUS examinations were performed. Adequate ileal views for disease activity assessment were obtained in 93% of patients at less than 20 wk gestational age, but in only 56% of patients at 20-26 wk. In contrast, adequate colonic views were obtained in 91% of all IUS examinations[41]. In this cohort, BWT was compared to FC as the current reference standard for disease activity monitoring during pregnancy and BWT was found to positively correlate with FC (r = 0.26, P = 0.03) and had a sensitivity of 74%, specificity of 83% and negative predictive value of 90%. Similarly, in a small Dutch cohort of 38 pregnant women with IBD, 27 of whom were followed with serial IUS examinations during pregnancy, feasibility to assess the terminal ileum significantly decreased from 91.3% in the first trimester to 21.7% in the third trimester (P < 0.0001). When compared to FC and clinical activity combined, IUS was able to distinguish active from quiescent disease with 84% sensitivity and 98% specificity[42].

Utility for monitoring in pediatrics

In children, use of IUS as a non-invasive tool to monitor disease activity is of even more importance than in adults, as younger children often require sedation for MRE and there is a need to reduce the risk of radiation exposure from repeated CT scans. As previously stated, there is a clear consensus that a cut-off value for normal BWT in children is not 3 mm, but more likely to be in the range of 2-2.5 mm[14]. Similar to adults, IUS can be used to monitor treatment response in children with CD treated with infliximab. In a study of 28 children with newly diagnosed ileal CD, BWT, hyperemia and involved segment length all significantly decreased as early as 2 wk after infliximab initiation and there was a strong correlation between CDS and FC (r = 0.71, P < 0.0001). Linear mixed models from this study demonstrated that BWT, hyperemia, and involved segment length continue to decrease over the course of 6 mo after infliximab initiation[43]. In a small pilot study of 13 children with small bowel CD undergoing infliximab induction, bowel wall hyperemia decreased in all but one patient post-induction (P = 0.01), indicating that hyperemia assessed by CDS may be the earliest IUS measure to normalize post-induction[44].

Utility for monitoring postoperative CD recurrence

IUS is an accurate tool for monitoring postoperative CD recurrence in the neo-terminal ileum after ileocolic resection. BWT greater than 3-3.5 mm is accurate to detect recurrence based on ileocolonoscopy with a sensitivity of 90%-100%[45]. In a study using both traditional IUS and CEUS to assess CD recurrence, 90 patients, 62 of which had severe recurrence (Rutgeerts score i3 or i4), underwent IUS, CEUS, and endoscopy. A BWT > 5 mm, without any additional parameters, demonstrated 100% specificity to detect recurrence and a BWT > 6 mm was 95.7% specific to detect severe recurrence. The addition of bowel wall contrast enhancement ≥ 70% to either BWT ≥ 5 or 6 mm was the most accurate to the Rutgeerts score with an AUROC of 0.89 for detecting recurrence[46].

COMPARISON WITH OTHER CROSS-SECTIONAL IMAGING MODALITIES

Overall IUS, MRE, and CTE have similar accuracy for the diagnosis of CD complications such as strictures, abscesses, and fistulae[47]. In the largest study to date, the prospective multi-center METRIC trial included 284 patients, 233 of which had small bowel CD, and demonstrated that IUS and MRE are comparable for detection of disease in the terminal ileum. IUS had a sensitivity and specificity of 92% and 84% while MRE had a sensitivity and specificity of 97% and 96%. MRE was superior to IUS for the detection of small bowel disease extent with a sensitivity of 80% compared to 70% for IUS. Similarly, in a multicenter Italian study of 234 adult patients with CD, IUS and MRE had comparable accuracy with a sensitivity and specificity to detect inflammation of 96% and 97% for IUS and 96% and 94% for MRE. MRE was more accurate than IUS to define small bowel disease extension (r = 0.69) and detect fistulae (k = 0.67), but comparable for detection of strictures (k = 0.82) and abscesses (k = 0.88)[48]. As such, the updated guidelines from the European Crohn's and Colitis Organization (ECCO)-European Society for Gastrointestinal and Abdominal Radiology and ECCO-European Society for Pediatric Gastroenterology, Hepatology, and Nutrition now propose the use of IUS in the diagnostic evaluation for adult and pediatric CD[49,50].

Follow-up analysis from the METRIC trial for observer agreement demonstrated that IUS and MRE are similar, with IUS performing slightly better than MRE numerically. Interobserver agreement for MRE was modest for new diagnosis [68% (k = 0.36)] and relapsed patients [78% (k = 0.56)] and only slight for colonic assessment for new diagnosis [61% (k = 0.21)] and relapsed patients [60% (k = 0.20)]

[51]. Interobserver agreement for IUS was higher than MRE in the small bowel for new diagnosis [82% (k = 0.64)] and for relapsed patients [81% (k = 0.63)] and in the colon for new diagnosis [64% (k = 0.27)] and relapsed patients [78% (k = 0.56)][52]. Furthermore, a retrospective study in children with IBD demonstrated that MRE is not accurate for the assessment of colonic disease, with the simplified Magnetic Resonance Index of Activity unable to identify severe lesions in colonic segments[53].

IMPACT ON PATIENT MANAGEMENT AND SHARED DECISION MAKING

When determining the optimal tight control monitoring tool, perhaps the most important aspect to consider is patient preference and compliance. IUS is one of the most preferred monitoring tool by patients with IBD. In a survey of 121 Australian patients with a formal diagnosis of IBD, IUS scored highly acceptable for disease activity monitoring (mean 9.20 ± 1.37) compared to colonoscopy (7.94 ± 2.30), FC (8.17 ± 1.96), serum sampling (8.87 ± 1.62) and alternative forms of cross-sectional imaging (8.67 ± 1.60)[54].

Beyond preference, use of IUS for IBD monitoring enhances shared understanding and increases the ability of providers to make major treatment decisions during routine clinic visits. In a study of patients randomized to ultrasound-driven IBD care *vs* non-ultrasound driven IBD care, patients who underwent IUS reported better understanding of all aspects of their disease and symptoms, and were more confident in their ability to make informed decisions about managing their disease[55]. Furthermore, gastroenterologists altered management by changing medications in 47% of patients in the ultrasound group compared to just 22% in the non-ultrasound group (P = 0.002). Based on disease activity, providers were more likely to change therapy when patients had an IUS compared to when they did not (P = 0.024).

POSITIONING ALGORITHM AT THE POINT OF CARE IN THE CLINIC

Debate over the timing and utilization of IUS for tight control monitoring, as well as the definition of treatment response and remission, is ongoing. Multiple studies demonstrate a decrease in BWT by week 4 after therapy initiation, but the longitudinal effect of response reassessment at this early timepoint is still unclear[43,56]. A panel of gastroenterologists from the IBUS developed an expert consensus statement and defined: (1) IUS response as a decrease in BWT by 25% from baseline or 2.0 mm, or greater than 1.0 mm with a decrease in CDS by the modified Limberg score of one grade; and (2) IUS remission as a BWT ≤ 3 mm and normal CDS or absence of hyperemia[57].

Here we propose a practical tight control monitoring algorithm based on IUS (Figure 4). IUS should be repeated post-induction at week eight, regardless of biologic therapy, to assess change in BWT and hyperemia by CDS. If there is no change or an increase in BWT and/or hyperemia, optimization of therapy (dose or interval escalation) should be considered. Repeat IUS should then occur again in eight weeks to reassess response. If again there is no change or worsening, repeat ileocolonoscopy assessment and subsequent therapy discontinuation and switch should be considered. If there is IUS response (as defined above), then the interval to repeat IUS should be extended to 12 wk. Repeat IUS should be performed then every 12 wk until one year and if complete IUS transmural remission is achieved, then IUS can be performed every 6 mo for subsequent monitoring and confirmation of sustained transmural remission.

FUTURE APPLICATIONS

Eventually, the use of IUS at the point-of-care may be able to quantify the proportion of active *vs* chronic inflammation in patients with IBD. This will aid in treatment decision making, guiding choices toward either an anti-inflammatory or anti-fibrotic therapy, with or without surgery. In a study of 35 CD patients who underwent sheer wave elastography (SWE) within 1 wk of surgical resection, a cut-off value of 22.5 kPa was 69.6% sensitive and 91.7% specific with an AUROC of 0.82 to discriminate between mild/moderate and severe fibrosis based on histopathology[58]. Future studies validating cut-offs to discriminate degrees of fibrosis and active inflammation are still needed, but in the future provides will be able to personalize management for patients based on where they fall on the active inflammation *vs* fibrosis pathway utilizing SWE[59,60]. Additionally, use of hand-held IUS in combination with artificial intelligence will be able to help patients monitor both their active inflammation and fibrosis remotely for further tight control in the future[61].

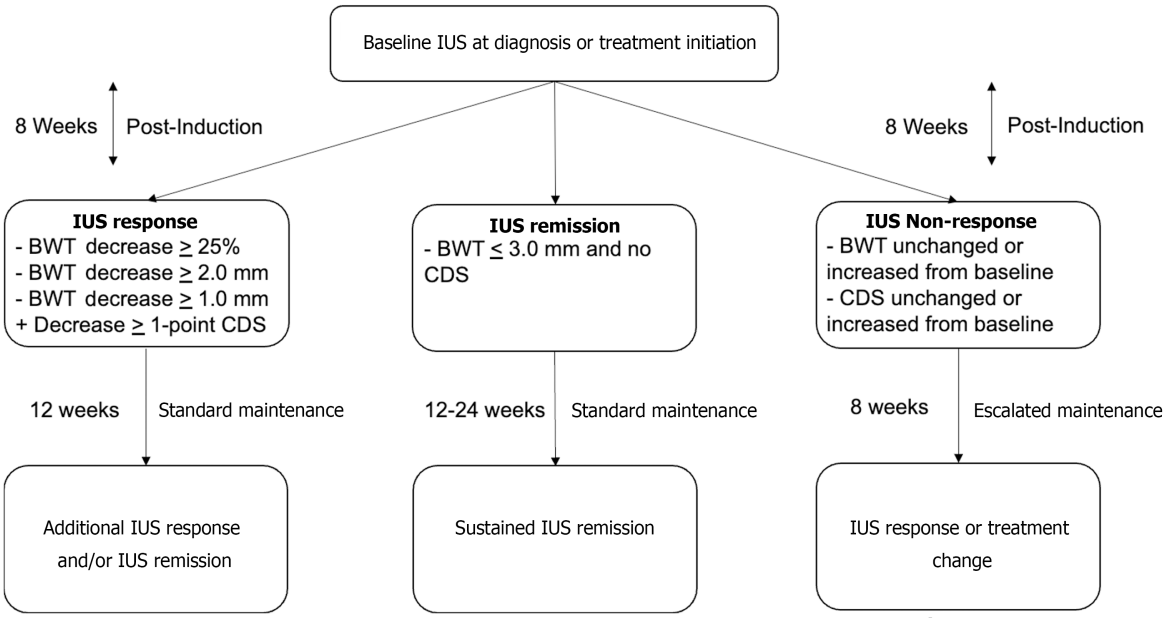

DOI: 10.3748/wjg.v29.i15.2272

Figure 4 Intestinal ultrasound-based tight control monitoring algorithm. IUS: Intestinal ultrasound; BWT: Bowel wall thickness; CDS: Color Doppler signal.

CONCLUSION

IUS is an accurate, non-invasive cross-sectional imaging tool to assess IBD activity in real time. Incorporation of IUS into a tight control monitoring strategy promotes quick and impactful treatment decisions that can modify disease progression and enhance patient compliance. Specific populations of patients with IBD, especially children and pregnant women, would benefit significantly from the increased use of IUS for disease monitoring. Continued advances in technology will likely allow for enhanced stratification of active *vs* chronic inflammation at the point-of-care and enable remote monitoring for even tighter control. Ultimately, an IUS-based tight control monitoring algorithm and prediction tool may be used for early treatment decisions to achieve sustained deep remission and disease modification.

FOOTNOTES

Author contributions: Dolinger MT and Kayal M contributed to the conception of the manuscript, Dolinger MT drafted manuscript; Kayal M edited the manuscript.

Conflict-of-interest statement: All the authors report no relevant conflicts of interest for this article.

Country/Territory of origin: United States

ORCID number: Maia Kayal 0000-0002-9640-950X.

S-Editor: Wang JJ
L-Editor: A
P-Editor: Cai YX

REFERENCES

1 **Kayal M**, Ungaro RC, Bader G, Colombel JF, Sandborn WJ, Stalgis C. Net Remission Rates with Biologic Treatment in

Crohn's Disease: A Reappraisal of the Clinical Trial Data. *Clin Gastroenterol Hepatol* 2022 [PMID: 35245701 DOI: 10.1016/j.cgh.2022.02.044]

2 **Bryant RV**, Friedman AB, Wright EK, Taylor KM, Begun J, Maconi G, Maaser C, Novak KL, Kucharzik T, Atkinson NSS, Asthana A, Gibson PR. Gastrointestinal ultrasound in inflammatory bowel disease: an underused resource with potential paradigm-changing application. *Gut* 2018; **67**: 973-985 [PMID: 29437914 DOI: 10.1136/gutjnl-2017-315655]

3 **Kucharzik T**, Kannengiesser K, Petersen F. The use of ultrasound in inflammatory bowel disease. *Ann Gastroenterol* 2017; **30**: 135-144 [PMID: 28243033 DOI: 10.20524/aog.2016.0105]

4 **Ripollés T**, Martínez-Pérez MJ, Paredes JM, Vizuete J, García-Martínez E, Jiménez-Restrepo DH. Contrast-enhanced ultrasound in the differentiation between phlegmon and abscess in Crohn's disease and other abdominal conditions. *Eur J Radiol* 2013; **82**: e525-e531 [PMID: 23838329 DOI: 10.1016/j.ejrad.2013.05.043]

5 **Calabrese E**, Maaser C, Zorzi F, Kannengiesser K, Hanauer SB, Bruining DH, Iacucci M, Maconi G, Novak KL, Panaccione R, Strobel D, Wilson SR, Watanabe M, Pallone F, Ghosh S. Bowel Ultrasonography in the Management of Crohn's Disease. A Review with Recommendations of an International Panel of Experts. *Inflamm Bowel Dis* 2016; **22**: 1168-1183 [PMID: 26958988 DOI: 10.1097/MIB.0000000000000706]

6 **Parente F**, Greco S, Molteni M, Anderloni A, Sampietro GM, Danelli PG, Bianco R, Gallus S, Bianchi Porro G. Oral contrast enhanced bowel ultrasonography in the assessment of small intestine Crohn's disease. A prospective comparison with conventional ultrasound, x ray studies, and ileocolonoscopy. *Gut* 2004; **53**: 1652-1657 [PMID: 15479688 DOI: 10.1136/gut.2004.041038]

7 **Parente F**, Greco S, Molteni M, Cucino C, Maconi G, Sampietro GM, Danelli PG, Cristaldi M, Bianco R, Gallus S, Bianchi Porro G. Role of early ultrasound in detecting inflammatory intestinal disorders and identifying their anatomical location within the bowel. *Aliment Pharmacol Ther* 2003; **18**: 1009-1016 [PMID: 14616167 DOI: 10.1046/j.1365-2036.2003.01796.x]

8 **Maconi G**, Nylund K, Ripolles T, Calabrese E, Dirks K, Dietrich CF, Hollerweger A, Sporea I, Saftoiu A, Maaser C, Hausken T, Higginson AP, Nürnberg D, Pallotta N, Romanini L, Serra C, Gilja OH. EFSUMB Recommendations and Clinical Guidelines for Intestinal Ultrasound (GIUS) in Inflammatory Bowel Diseases. *Ultraschall Med* 2018; **39**: 304-317 [PMID: 29566419 DOI: 10.1055/s-0043-125329]

9 **Fraquelli M**, Colli A, Casazza G, Paggi S, Colucci A, Massironi S, Duca P, Conte D. Role of US in detection of Crohn disease: meta-analysis. *Radiology* 2005; **236**: 95-101 [PMID: 15987966 DOI: 10.1148/radiol.2361040799]

10 **Dong J**, Wang H, Zhao J, Zhu W, Zhang L, Gong J, Li Y, Gu L, Li J. Ultrasound as a diagnostic tool in detecting active Crohn's disease: a meta-analysis of prospective studies. *Eur Radiol* 2014; **24**: 26-33 [PMID: 23921767 DOI: 10.1007/s00330-013-2973-0]

11 **Horsthuis K**, Bipat S, Bennink RJ, Stoker J. Inflammatory bowel disease diagnosed with US, MR, scintigraphy, and CT: meta-analysis of prospective studies. *Radiology* 2008; **247**: 64-79 [PMID: 18372465 DOI: 10.1148/radiol.2471070611]

12 **Torres J**, Billioud V, Sachar DB, Peyrin-Biroulet L, Colombel JF. Ulcerative colitis as a progressive disease: the forgotten evidence. *Inflamm Bowel Dis* 2012; **18**: 1356-1363 [PMID: 22162423 DOI: 10.1002/ibd.22839]

13 **Antonelli E**, Giuliano V, Casella G, Villanacci V, Baldini V, Baldoni M, Morelli O, Bassotti G. Ultrasonographic assessment of colonic wall in moderate-severe ulcerative colitis: comparison with endoscopic findings. *Dig Liver Dis* 2011; **43**: 703-706 [PMID: 21482208 DOI: 10.1016/j.dld.2011.02.019]

14 **van Wassenaer EA**, de Voogd FAE, van Rijn RR, van der Lee JH, Tabbers MM, van Etten-Jamaludin FS, Kindermann A, de Meij TGJ, Gecse KB, D'Haens GR, Benninga MA, Koot BGP. Bowel ultrasound measurements in healthy children - systematic review and meta-analysis. *Pediatr Radiol* 2020; **50**: 501-508 [PMID: 31838567 DOI: 10.1007/s00247-019-04567-2]

15 **Yekeler E**, Danalioglu A, Movasseghi B, Yilmaz S, Karaca C, Kaymakoglu S, Acunas B. Crohn disease activity evaluated by Doppler ultrasonography of the superior mesenteric artery and the affected small-bowel segments. *J Ultrasound Med* 2005; **24**: 59-65 [PMID: 15615929 DOI: 10.7863/jum.2005.24.1.59]

16 **Sjekavica I**, Barbarić-Babić V, Krznarić Z, Molnar M, Cuković-Cavka S, Stern-Padovan R. Assessment of Crohn's disease activity by doppler ultrasound of superior mesenteric artery and mural arteries in thickened bowel wall: cross-sectional study. *Croat Med J* 2007; **48**: 822-830 [PMID: 18074417 DOI: 10.3325/cmj.2007.6.822]

17 **Karoui S**, Nouira K, Serghini M, Ben Mustapha N, Boubaker J, Menif E, Filali A. Assessment of activity of Crohn's disease by Doppler sonography of superior mesenteric artery flow. *J Crohns Colitis* 2010; **4**: 334-340 [PMID: 21122523 DOI: 10.1016/j.crohns.2009.12.011]

18 **Sævik F**, Eriksen R, Eide GE, Gilja OH, Nylund K. Development and Validation of a Simple Ultrasound Activity Score for Crohn's Disease. *J Crohns Colitis* 2021; **15**: 115-124 [PMID: 32504533 DOI: 10.1093/ecco-jcc/jjaa112]

19 **Ripollés T**, Poza J, Suarez Ferrer C, Martínez-Pérez MJ, Martín-Algíbez A, de Las Heras Paez B. Evaluation of Crohn's Disease Activity: Development of an Ultrasound Score in a Multicenter Study. *Inflamm Bowel Dis* 2021; **27**: 145-154 [PMID: 32507880 DOI: 10.1093/ibd/izaa134]

20 **Allocca M**, Fiorino G, Bonovas S, Furfaro F, Gilardi D, Argollo M, Magnoni P, Peyrin-Biroulet L, Danese S. Accuracy of Humanitas Ultrasound Criteria in Assessing Disease Activity and Severity in Ulcerative Colitis: A Prospective Study. *J Crohns Colitis* 2018; **12**: 1385-1391 [PMID: 30085066 DOI: 10.1093/ecco-jcc/jjy107]

21 **Goodsall TM**, Nguyen TM, Parker CE, Ma C, Andrews JM, Jairath V, Bryant RV. Systematic Review: Gastrointestinal Ultrasound Scoring Indices for Inflammatory Bowel Disease. *J Crohns Colitis* 2021; **15**: 125-142 [PMID: 32614386 DOI: 10.1093/ecco-jcc/jjaa129]

22 **Allocca M**, Filippi E, Costantino A, Bonovas S, Fiorino G, Furfaro F, Peyrin-Biroulet L, Fraquelli M, Caprioli F, Danese S. Milan ultrasound criteria are accurate in assessing disease activity in ulcerative colitis: external validation. *United European Gastroenterol J* 2021; **9**: 438-442 [PMID: 33349199 DOI: 10.1177/2050640620980203]

23 **Bots S**, Nylund K, Löwenberg M, Gecse K, D'Haens G. Intestinal Ultrasound to Assess Disease Activity in Ulcerative Colitis: Development of a novel UC-Ultrasound Index. *J Crohns Colitis* 2021; **15**: 1264-1271 [PMID: 33411887 DOI: 10.1093/ecco-jcc/jjab002]

24 **Civitelli F**, Di Nardo G, Oliva S, Nuti F, Ferrari F, Dilillo A, Viola F, Pallotta N, Cucchiara S, Aloi M. Ultrasonography of

the colon in pediatric ulcerative colitis: a prospective, blind, comparative study with colonoscopy. *J Pediatr* 2014; **165**: 78-84.e2 [PMID: 24725581 DOI: 10.1016/j.jpeds.2014.02.055]

25 **Kellar A**, Wilson S, Kaplan G, DeBruyn J, Tanyingoh D, Novak KL. The Simple Pediatric Activity Ultrasound Score (SPAUSS) for the Accurate Detection of Pediatric Inflammatory Bowel Disease. *J Pediatr Gastroenterol Nutr* 2019; **69**: e1-e6 [PMID: 31232886 DOI: 10.1097/MPG.0000000000002298]

26 **Novak KL**, Nylund K, Maaser C, Petersen F, Kucharzik T, Lu C, Allocca M, Maconi G, de Voogd F, Christensen B, Vaughan R, Palmela C, Carter D, Wilkens R. Expert Consensus on Optimal Acquisition and Development of the International Bowel Ultrasound Segmental Activity Score [IBUS-SAS]: A Reliability and Inter-rater Variability Study on Intestinal Ultrasonography in Crohn's Disease. *J Crohns Colitis* 2021; **15**: 609-616 [PMID: 33098642 DOI: 10.1093/ecco-jcc/jjaa216]

27 **Kucharzik T**, Wittig BM, Helwig U, Börner N, Rössler A, Rath S, Maaser C; TRUST study group. Use of Intestinal Ultrasound to Monitor Crohn's Disease Activity. *Clin Gastroenterol Hepatol* 2017; **15**: 535-542.e2 [PMID: 27856365 DOI: 10.1016/j.cgh.2016.10.040]

28 **Castiglione F**, Testa A, Rea M, De Palma GD, Diaferia M, Musto D, Sasso F, Caporaso N, Rispo A. Transmural healing evaluated by bowel sonography in patients with Crohn's disease on maintenance treatment with biologics. *Inflamm Bowel Dis* 2013; **19**: 1928-1934 [PMID: 23835441 DOI: 10.1097/MIB.0b013e31829053ce]

29 **Castiglione F**, Imperatore N, Testa A, De Palma GD, Nardone OM, Pellegrini L, Caporaso N, Rispo A. One-year clinical outcomes with biologics in Crohn's disease: transmural healing compared with mucosal or no healing. *Aliment Pharmacol Ther* 2019; **49**: 1026-1039 [PMID: 30854708 DOI: 10.1111/apt.15190]

30 **Fernandes SR**, Rodrigues RV, Bernardo S, Cortez-Pinto J, Rosa I, da Silva JP, Gonçalves AR, Valente A, Baldaia C, Santos PM, Correia L, Venâncio J, Campos P, Pereira AD, Velosa J. Transmural Healing Is Associated with Improved Long-term Outcomes of Patients with Crohn's Disease. *Inflamm Bowel Dis* 2017; **23**: 1403-1409 [PMID: 28498158 DOI: 10.1097/MIB.0000000000001143]

31 **Paredes JM**, Ripollés T, Cortés X, Martínez MJ, Barrachina M, Gómez F, Moreno-Osset E. Abdominal sonographic changes after antibody to tumor necrosis factor (anti-TNF) alpha therapy in Crohn's Disease. *Dig Dis Sci* 2010; **55**: 404-410 [PMID: 19267199 DOI: 10.1007/s10620-009-0759-7]

32 **Paredes JM**, Moreno N, Latorre P, Ripollés T, Martinez MJ, Vizuete J, Moreno-Osset E. Clinical Impact of Sonographic Transmural Healing After Anti-TNF Antibody Treatment in Patients with Crohn's Disease. *Dig Dis Sci* 2019; **64**: 2600-2606 [PMID: 30874986 DOI: 10.1007/s10620-019-05567-w]

33 **Kucharzik T**, Wilkens R, D'Agostino MA, Maconi G, Le Bars M, Lahaye M, Bravatà I, Nazar M, Ni L, Ercole E, Allocca M, Machková N, de Voogd FAE, Palmela C, Vaughan R, Maaser C; STARDUST Intestinal Ultrasound study group. Early Ultrasound Response and Progressive Transmural Remission After Treatment With Ustekinumab in Crohn's Disease. *Clin Gastroenterol Hepatol* 2023; **21**: 153-163.e12 [PMID: 35842121 DOI: 10.1016/j.cgh.2022.05.055]

34 **de Voogd F**, Bots S, Gecse K, Gilja OH, D'Haens G, Nylund K. Intestinal Ultrasound Early on in Treatment Follow-up Predicts Endoscopic Response to Anti-TNFα Treatment in Crohn's Disease. *J Crohns Colitis* 2022; **16**: 1598-1608 [PMID: 35639823 DOI: 10.1093/ecco-jcc/jjac072]

35 **Bachour SP**, Shah RS, Lyu R, Nakamura T, Shen M, Li T, Dane B, Barnes EL, Rieder F, Cohen B, Qazi T, Lashner B, Achkar JP, Philpott J, Holubar SD, Lightner AL, Regueiro M, Axelrad J, Baker ME, Click B. Test Characteristics of Cross-sectional Imaging and Concordance With Endoscopy in Postoperative Crohn's Disease. *Clin Gastroenterol Hepatol* 2022; **20**: 2327-2336.e4 [PMID: 34968729 DOI: 10.1016/j.cgh.2021.12.033]

36 **Vaughan R**, Tjandra D, Patwardhan A, Mingos N, Gibson R, Boussioutas A, Ardalan Z, Al-Ani A, Gibson PR, Christensen B. Toward transmural healing: Sonographic healing is associated with improved long-term outcomes in patients with Crohn's disease. *Aliment Pharmacol Ther* 2022; **56**: 84-94 [PMID: 35343603 DOI: 10.1111/apt.16892]

37 **Maaser C**, Petersen F, Helwig U, Fischer I, Roessler A, Rath S, Lang D, Kucharzik T; German IBD Study Group and the TRUST&UC study group; German IBD Study Group and TRUST&UC study group. Intestinal ultrasound for monitoring therapeutic response in patients with ulcerative colitis: results from the TRUST&UC study. *Gut* 2020; **69**: 1629-1636 [PMID: 31862811 DOI: 10.1136/gutjnl-2019-319451]

38 **Parente F**, Molteni M, Marino B, Colli A, Ardizzone S, Greco S, Sampietro G, Gallus S. Bowel ultrasound and mucosal healing in ulcerative colitis. *Dig Dis* 2009; **27**: 285-290 [PMID: 19786753 DOI: 10.1159/000228562]

39 **de Voogd F**, van Wassenaer EA, Mookhoek A, Bots S, van Gennep S, Löwenberg M, D'Haens GR, Gecse KB. Intestinal Ultrasound Is Accurate to Determine Endoscopic Response and Remission in Patients With Moderate to Severe Ulcerative Colitis: A Longitudinal Prospective Cohort Study. *Gastroenterology* 2022; **163**: 1569-1581 [PMID: 36030056 DOI: 10.1053/j.gastro.2022.08.038]

40 **Allocca M**, Dell'Avalle C, Craviotto V, Furfaro F, Zilli A, D'Amico F, Bonovas S, Peyrin-Biroulet L, Fiorino G, Danese S. Predictive value of Milan ultrasound criteria in ulcerative colitis: A prospective observational cohort study. *United European Gastroenterol J* 2022; **10**: 190-197 [PMID: 35233934 DOI: 10.1002/ueg2.12206]

41 **Flanagan E**, Wright EK, Begun J, Bryant RV, An YK, Ross AL, Kiburg KV, Bell SJ. Monitoring Inflammatory Bowel Disease in Pregnancy Using Gastrointestinal Ultrasonography. *J Crohns Colitis* 2020; **14**: 1405-1412 [PMID: 32343768 DOI: 10.1093/ecco-jcc/jjaa082]

42 **De Voogd F**, Joshi H, Van Wassenaer E, Bots S, D'Haens G, Gecse K. Intestinal Ultrasound to Evaluate Treatment Response During Pregnancy in Patients With Inflammatory Bowel Disease. *Inflamm Bowel Dis* 2022; **28**: 1045-1052 [PMID: 34525186 DOI: 10.1093/ibd/izab216]

43 **Dillman JR**, Dehkordy SF, Smith EA, DiPietro MA, Sanchez R, DeMatos-Maillard V, Adler J, Zhang B, Trout AT. Defining the ultrasound longitudinal natural history of newly diagnosed pediatric small bowel Crohn disease treated with infliximab and infliximab-azathioprine combination therapy. *Pediatr Radiol* 2017; **47**: 924-934 [PMID: 28421251 DOI: 10.1007/s00247-017-3848-3]

44 **Dolinger MT**, Choi JJ, Phan BL, Rosenberg HK, Rowland J, Dubinsky MC. Use of Small Bowel Ultrasound to Predict Response to Infliximab Induction in Pediatric Crohn's Disease. *J Clin Gastroenterol* 2021; **55**: 429-432 [PMID: 32453126 DOI: 10.1097/MCG.0000000000001367]

45 **Rispo A**, Imperatore N, Testa A, Nardone OM, Luglio G, Caporaso N, Castiglione F. Diagnostic Accuracy of Ultrasonography in the Detection of Postsurgical Recurrence in Crohn's Disease: A Systematic Review with Meta-analysis. *Inflamm Bowel Dis* 2018; **24**: 977-988 [PMID: 29688470 DOI: 10.1093/ibd/izy012]

46 **Martínez MJ**, Ripollés T, Paredes JM, Moreno-Osset E, Pazos JM, Blanc E. Intravenous Contrast-Enhanced Ultrasound for Assessing and Grading Postoperative Recurrence of Crohn's Disease. *Dig Dis Sci* 2019; **64**: 1640-1650 [PMID: 30604372 DOI: 10.1007/s10620-018-5432-6]

47 **Panés J**, Bouzas R, Chaparro M, García-Sánchez V, Gisbert JP, Martínez de Guereñu B, Mendoza JL, Paredes JM, Quiroga S, Ripollés T, Rimola J. Systematic review: the use of ultrasonography, computed tomography and magnetic resonance imaging for the diagnosis, assessment of activity and abdominal complications of Crohn's disease. *Aliment Pharmacol Ther* 2011; **34**: 125-145 [PMID: 21615440 DOI: 10.1111/j.1365-2036.2011.04710.x]

48 **Castiglione F**, Mainenti PP, De Palma GD, Testa A, Bucci L, Pesce G, Camera L, Diaferia M, Rea M, Caporaso N, Salvatore M, Rispo A. Noninvasive diagnosis of small bowel Crohn's disease: direct comparison of bowel sonography and magnetic resonance enterography. *Inflamm Bowel Dis* 2013; **19**: 991-998 [PMID: 23429465 DOI: 10.1097/MIB.0b013e3182802b87]

49 **Maaser C**, Sturm A, Vavricka SR, Kucharzik T, Fiorino G, Annese V, Calabrese E, Baumgart DC, Bettenworth D, Borralho Nunes P, Burisch J, Castiglione F, Eliakim R, Ellul P, González-Lama Y, Gordon H, Halligan S, Katsanos K, Kopylov U, Kotze PG, Krustinš E, Laghi A, Limdi JK, Rieder F, Rimola J, Taylor SA, Tolan D, van Rheenen P, Verstockt B, Stoker J; European Crohn's and Colitis Organisation [ECCO] and the European Society of Gastrointestinal and Abdominal Radiology [ESGAR]. ECCO-ESGAR Guideline for Diagnostic Assessment in IBD Part 1: Initial diagnosis, monitoring of known IBD, detection of complications. *J Crohns Colitis* 2019; **13**: 144-164 [PMID: 30137275 DOI: 10.1093/ecco-jcc/jjy113]

50 **van Rheenen PF**, Aloi M, Assa A, Bronsky J, Escher JC, Fagerberg UL, Gasparetto M, Gerasimidis K, Griffiths A, Henderson P, Koletzko S, Kolho KL, Levine A, van Limbergen J, Martin de Carpi FJ, Navas-López VM, Oliva S, de Ridder L, Russell RK, Shouval D, Spinelli A, Turner D, Wilson D, Wine E, Ruemmele FM. The Medical Management of Paediatric Crohn's Disease: an ECCO-ESPGHAN Guideline Update. *J Crohns Colitis* 2020 [PMID: 33026087 DOI: 10.1093/ecco-jcc/jjaa161]

51 **Bhatnagar G**, Mallett S, Quinn L, Beable R, Bungay H, Betts M, Greenhalgh R, Gupta A, Higginson A, Hyland R, Ilangovan R, Lambie H, Mainta E, Patel U, Pilcher J, Plumb A, Porté F, Sidhu H, Slater A, Tolan D, Zealley I, Halligan S, Taylor S. Interobserver variation in the interpretation of magnetic resonance enterography in Crohn's disease. *Br J Radiol* 2022; **95**: 20210995 [PMID: 35195444 DOI: 10.1259/bjr.20210995]

52 **Bhatnagar G**, Quinn L, Higginson A, Plumb A, Halligan S, Tolan D, Lapham R, Mallett S, Taylor SA; METRIC study investigators. Observer agreement for small bowel ultrasound in Crohn's disease: results from the METRIC trial. *Abdom Radiol (NY)* 2020; **45**: 3036-3045 [PMID: 32037466 DOI: 10.1007/s00261-020-02405-w]

53 **Lepus CA**, Moote DJ, Bao S, Mosha MH, Hyams JS. Simplified Magnetic Resonance Index of Activity Is Useful for Terminal Ileal but not Colonic Disease in Pediatric Crohn Disease. *J Pediatr Gastroenterol Nutr* 2022; **74**: 610-616 [PMID: 35149649 DOI: 10.1097/MPG.0000000000003412]

54 **Rajagopalan A**, Sathananthan D, An YK, Van De Ven L, Martin S, Fon J, Costello SP, Begun J, Bryant RV. Gastrointestinal ultrasound in inflammatory bowel disease care: Patient perceptions and impact on disease-related knowledge. *JGH Open* 2020; **4**: 267-272 [PMID: 32280776 DOI: 10.1002/jgh3.12268]

55 **Friedman AB**, Asthana A, Knowles SR, Robbins A, Gibson PR. Effect of point-of-care gastrointestinal ultrasound on decision-making and management in inflammatory bowel disease. *Aliment Pharmacol Ther* 2021; **54**: 652-666 [PMID: 34157157 DOI: 10.1111/apt.16452]

56 **Ripollés T**, Martínez MJ, Barrachina MM. Crohn's disease and color Doppler sonography: response to treatment and its relationship with long-term prognosis. *J Clin Ultrasound* 2008; **36**: 267-272 [PMID: 18067121 DOI: 10.1002/jcu.20423]

57 **Ilvemark JFKF**, Hansen T, Goodsall TM, Seidelin JB, Al-Farhan H, Allocca M, Begun J, Bryant RV, Carter D, Christensen B, Dubinsky MC, Gecse KB, Kucharzik T, Lu C, Maaser C, Maconi G, Nylund K, Palmela C, Wilson SR, Novak K, Wilkens R. Defining Transabdominal Intestinal Ultrasound Treatment Response and Remission in Inflammatory Bowel Disease: Systematic Review and Expert Consensus Statement. *J Crohns Colitis* 2022; **16**: 554-580 [PMID: 34614172 DOI: 10.1093/ecco-jcc/jjab173]

58 **Chen YJ**, Mao R, Li XH, Cao QH, Chen ZH, Liu BX, Chen SL, Chen BL, He Y, Zeng ZR, Ben-Horin S, Rimola J, Rieder F, Xie XY, Chen MH. Real-Time Shear Wave Ultrasound Elastography Differentiates Fibrotic from Inflammatory Strictures in Patients with Crohn's Disease. *Inflamm Bowel Dis* 2018; **24**: 2183-2190 [PMID: 29718309 DOI: 10.1093/ibd/izy115]

59 **Dillman JR**, Stidham RW, Higgins PD, Moons DS, Johnson LA, Keshavarzi NR, Rubin JM. Ultrasound shear wave elastography helps discriminate low-grade from high-grade bowel wall fibrosis in ex vivo human intestinal specimens. *J Ultrasound Med* 2014; **33**: 2115-2123 [PMID: 25425367 DOI: 10.7863/ultra.33.12.2115]

60 **Lu C**, Gui X, Chen W, Fung T, Novak K, Wilson SR. Ultrasound Shear Wave Elastography and Contrast Enhancement: Effective Biomarkers in Crohn's Disease Strictures. *Inflamm Bowel Dis* 2017; **23**: 421-430 [PMID: 28129289 DOI: 10.1097/MIB.0000000000001020]

61 **Rispo A**, de Sire R, Mainenti PP, Imperatore N, Testa A, Maurea S, Ricciolino S, Nardone OM, Olmo O, Castiglione F. David Against Goliath: Direct Comparison of Handheld Bowel Sonography and Magnetic Resonance Enterography for Diagnosis of Crohn's Disease. *Inflamm Bowel Dis* 2023; **29**: 563-569 [PMID: 35666249 DOI: 10.1093/ibd/izac116]

World Journal of Gastroenterology

Submit a Manuscript: https://www.f6publishing.com

World J Gastroenterol 2023 April 21; 29(15): 2283-2293

DOI: 10.3748/wjg.v29.i15.2283

ISSN 1007-9327 (print) ISSN 2219-2840 (online)

MINIREVIEWS

Mechanisms of gastrointestinal barrier dysfunction in COVID-19 patients

Weijie Xue, Masaki Honda, Taizo Hibi

Specialty type: Gastroenterology and hepatology

Provenance and peer review: Invited article; Externally peer reviewed.

Peer-review model: Single blind

Peer-review report's scientific quality classification

Grade A (Excellent): 0
Grade B (Very good): B
Grade C (Good): C
Grade D (Fair): 0
Grade E (Poor): 0

P-Reviewer: Liakina V, Lithuania; Xin YN, China

Received: December 29, 2022
Peer-review started: December 29, 2022
First decision: February 1, 2023
Revised: February 13, 2023
Accepted: March 29, 2023
Article in press: March 29, 2023
Published online: April 21, 2023

Weijie Xue, Masaki Honda, Taizo Hibi, Department of Transplantation and Pediatric Surgery, Kumamoto University, Kumamoto 860-8556, Japan

Corresponding author: Masaki Honda, MD, PhD, Assistant Professor, Department of Transplantation and Pediatric Surgery, Kumamoto University, 1-1-1 Honjo, Chuo-ku, Kumamoto 860-8556, Japan. honda.masaki@kuh.kumamoto-u.ac.jp

Abstract

Coronavirus disease 2019 (COVID-19) caused by the novel severe acute respiratory syndrome coronavirus 2 (SARS-CoV-2) has become a major global public health event, resulting in a significant social and economic burden. Although COVID-19 was initially characterized as an upper respiratory and pulmonary infection, recent evidence suggests that it is a complex disease including gastrointestinal symptoms, such as diarrhea, nausea, and vomiting. Moreover, it remains unclear whether the gastrointestinal symptoms are caused by direct infection of the gastrointestinal tract by SARS-CoV-2 or are the result of systemic immune activation and subsequent dysregulation of homeostatic mechanisms. This review provides a brief overview of the mechanisms by which SARS-CoV-2 disrupts the integrity of the gastrointestinal barrier including the mechanical barrier, chemical barrier, microbial barrier, and immune barrier.

Key Words: Gastrointestinal barrier dysfunction; SARS-CoV-2; COVID-19; Angiotensin-converting enzyme 2; Microbiome; Immune cells

Core Tip: Coronavirus disease 2019 (COVID-19) has become a major global public health event, resulting in a significant social and economic burden. Although COVID-19 was initially characterized as an upper respiratory and pulmonary infection, recent evidence suggests that it is a complex disease including gastrointestinal symptoms. Moreover, it remains unclear whether the gastrointestinal symptoms are caused by direct infection of the gastrointestinal tract by severe acute respiratory syndrome coronavirus 2 (SARS-CoV-2) or are the result of systemic immune activation and subsequent dysregulation of homeostatic mechanisms. This review provides a brief overview of the mechanisms by which SARS-CoV-2 disrupts gastrointestinal barrier integrity.

Citation: Xue W, Honda M, Hibi T. Mechanisms of gastrointestinal barrier dysfunction in COVID-19 patients. *World J Gastroenterol* 2023; 29(15): 2283-2293
URL: https://www.wjgnet.com/1007-9327/full/v29/i15/2283.htm
DOI: https://dx.doi.org/10.3748/wjg.v29.i15.2283

INTRODUCTION

Since the advent of coronavirus disease 2019 (COVID-19), the disease has spread globally and had a profound impact on the lives and health of people around the world[1]. The virus that causes COVID-19, severe acute respiratory syndrome coronavirus 2 (SARS-CoV-2), replicates and matures once it enters cells through the angiotensin-converting enzyme 2 (ACE2) receptor. SARS-CoV-2 can trigger an inflammatory response that involves the activation of immune cells by a variety of cytokines[2,3]. ACE2 receptors are present in multiple cell types throughout the body, including the oral and nasal mucosa, lung, and gastrointestinal tract, indicating that SARS-CoV-2 can cause multi-organ damage[4,5].

The intestinal tract is the digestive organ of the body, but also has endocrine and immune functions, and is the first line of defense against non-specific infections. However, the intestine is also the largest reservoir of bacteria and endotoxins in the body and is, therefore, a hidden source of infection. While digesting and absorbing nutrients, the intestine contains bacteria and their metabolites, and the gastrointestinal barrier plays a very important role in preventing systemic absorption of harmful microbes and substances[6,7]. The gastrointestinal barrier is composed of the intestinal epithelial cell layer, mucus layer, normal intestinal flora, intestinal immune system, and intestine-hepatic axis, which together perform the functions of mechanical barrier, chemical barrier, microbial barrier, and immune barrier (Figure 1). This barrier plays an important role in homeostasis by preventing harmful substances and pathogens in the gastrointestinal tract from entering the internal environment of the body[8]. In this review, we describe the pathophysiological mechanisms of gastrointestinal barrier dysfunction in COVID-19 patients (Figure 2).

MECHANISMS OF THE GASTROINTESTINAL BARRIER

Mechanical barrier

The intestinal mechanical barrier consists of intestinal mucosal epithelial cells, tight junctions (TJs) between epithelial cells, and a layer of bacteria and mucous on the surface of epithelial cells. TJs are the most important component of the intestinal mechanical barrier[9] and are composed of four transmembrane proteins: Zonula occludens (ZO); occludin; claudins, and junctional adhesion molecules (JAMs). TJs form an important barrier against the translocation of bacteria and toxins in the intestine [10]. The TJs between cells close the gaps between adjacent intestinal epithelial cells, preventing bacteria and antigens in the intestinal lumen from entering the lamina propria and activating immune cells in the lamina propria. Therefore, TJs maintain the stability of the intestinal mucosal barrier and prevent abnormal immune reactions in the mucosa. Moreover, the TJs between intestinal epithelial cells play an important role in maintaining the morphological structure of epithelial cells, regulating the differentiation and repair of epithelial cells and intercellular material transport, and maintaining the barrier function of the intestinal mucosa and intestinal mucosal permeability[10-12].

Chemical barrier

The intestinal chemical barrier, also called the mucus layer, is a general term for the antimicrobial substances produced by the resident intestinal bacteria and host cells *e.g.,* Paneth cells and the chemicals that inhibit bacterial adhesion and colonization, such as gastric acid, digestive enzymes, lysozyme, and mucin[13,14]. The mucus layer, which is mainly composed of mucins and secretory mucin MUC2, limits the contact of gastrointestinal tissues with the microbiota[15,16]. Therefore, the mucus layer separates bacteria from intestinal epithelial cells in the intestinal lumen while allowing nutrient absorption[17]. It also lubricates the luminal contents to prevent degradation of the gastrointestinal tissues[18,19]. Gastric acid acts mainly at the beginning of the small intestine to inactivate bacteria and other pathogenic microorganisms. Lysozyme exerts bactericidal and antibacterial effects on the intestinal epithelial surface and in the intestinal lumen[20,21]. Moreover, bile is an important chemical barrier to endotoxins, as bile salts bind to endotoxins in the intestine and prevent absorption from the intestine into the portal vein[22].

Microbial barrier

The normal intestine is inhabited by a large number of bacteria, with at least 500 different species, most of which are anaerobic[23]. Under normal conditions, the normal flora maintain a relatively stable proportional relationship with each other. They combine with the intestinal mucosa to form a micro-

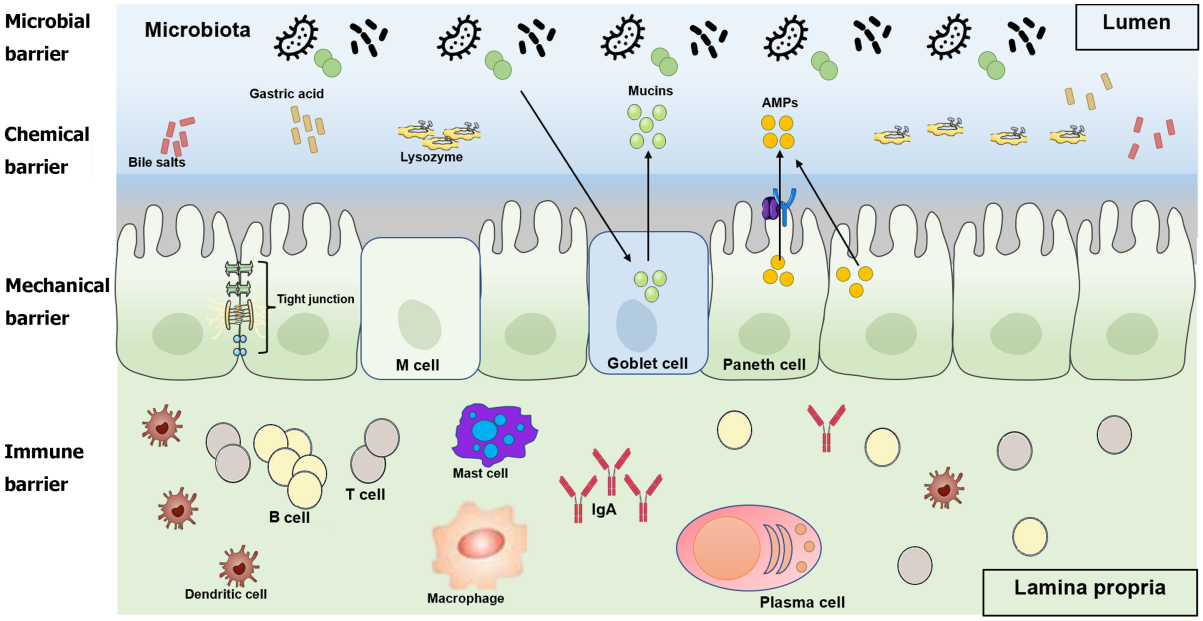

DOI: 10.3748/wjg.v29.i15.2283

Figure 1 Schematic diagram of the intestinal barrier. The intestinal barrier is composed of biological, chemical, mechanical, and immune barriers. The intestinal lumen contains antimicrobial peptides, mucins, gastric acid, bile salts, lysozyme, and commensal bacteria, which together provide a protective barrier effect and inhibit pathogen colonization. The epithelial layer consists of a single layer of epithelial cells with tight junctions that prevent paracellular passage. In addition, this layer also harbors M cells, Goblet cells, and Paneth cells. The lamina propria contains a large number of immune cells, including B cells, T cells, plasma cells, macrophages, dendritic cells, and mast cells.

ecosystem that is both interdependent and interactive with the micro-spatial structure of the host and this micro-ecosystem forms the microbial barrier of the intestine[24]. Under normal microecological conditions, the dominant replication of non-pathogenic intestinal flora can hinder the survival of pathogenic bacteria. At the same time, non-pathogenic flora also secrete some antibacterial and antimicrobial substances, such as lactic acid and bacteriocins, which can interfere with and inhibit the vitality and function of pathogenic bacteria[25-27].

Immune barrier

The intestine is both a digestive organ and the largest immune organ in the body and is, therefore, an important part of the systemic immune system. The intestine is constantly exposed to antigenic substances, such as microbial antigens and food antigens, but the gastrointestinal barrier, including the immune barrier, can effectively prevent the penetration of these antigens. The intestinal immune defense system is mainly composed of gut-associated lymphoid tissue (GALT) in the intestinal wall and secreted IgA, IgM, and IgE. GALT is the site of induction and activation of the immune response, mainly in the Peyer's patches that are distributed throughout the small intestine[28,29]. Most of the IgA in intestinal secretions is secretory IgA (sIgA), which is the most secreted immunoglobulin in the body and the main immunoglobulin on the intestinal mucosal surface. sIgA plays a leading role in humoral immunity and is the first line of defense against the adhesion and colonization of pathogens in the intestinal mucosa[30,31]. Furthermore, perivascular macrophages in the lamina propria constitute an anatomical barrier that functions to prevent bacterial translocation[32]. Also, neutrophils play an important role in capturing and killing pathogens in enterocolitis[33].

FACTORS CONTRIBUTING TO THE GASTROINTESTINAL BARRIER DYSFUNCTION CAUSED BY SARS-COV-2

SARS-CoV-2 and the mechanical barrier

Damage to the gastrointestinal mechanical barrier can be caused by direct infection of intestinal cells with SARS-CoV-2. The spike protein of SARS-CoV-2 has a high affinity for ACE2, which is widely expressed in intestinal epithelial cells. SARS-CoV-2 enters target cells mainly through the ACE2 receptor thus causing primary damage to the intestine by altering the expression and function of TJ-related proteins, leading to disruption of the paracellular barrier function[34-37]. A study by Sun *et al*[38] that compared differentially enriched proteins in the stools of COVID-19 patients and normal participants found evidence of intestinal infection and intestinal damage caused by SARS-CoV-2. For example,

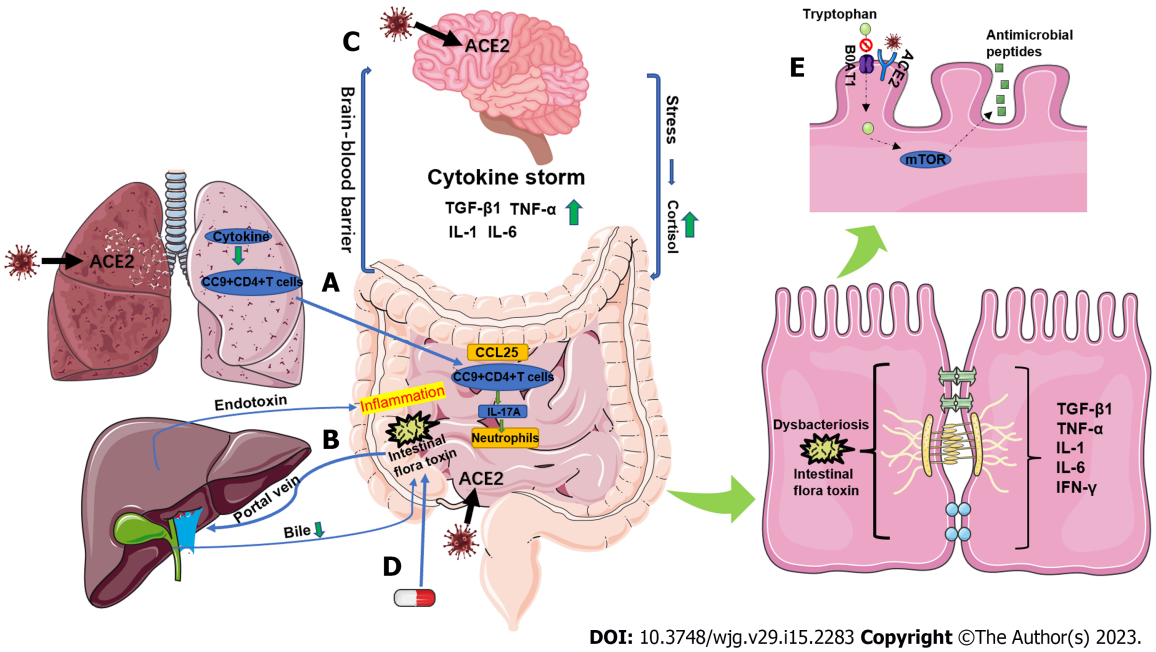

DOI: 10.3748/wjg.v29.i15.2283

Figure 2 Mechanisms of gastrointestinal barrier dysfunction in coronavirus disease 2019 patients. A: Severe acute respiratory syndrome coronavirus 2 (SARS-CoV-2) binds with angiotensin-converting enzyme 2 (ACE2) to enter the lung and, through the CCL25-CCR9 axis, mediate the recruitment of lung-derived effector CD4$^+$ T cells to the small intestine. This promotes the in-situ polarization of small intestinal Th17 cells and production of IL-17A leading to neutrophil aggregation and injuring the intestine; B: The intestinal flora is transferred to the liver through the portal vein, affecting liver function and leading to a decrease in endotoxin inactivation. Endotoxins enter the systemic circulation and induce an inflammatory response. In addition, decreased liver function also leads to reduced bile secretion and decreased inhibition of intestinal flora; C: The SARS-CoV-2 attack on cerebral neurons produces a large amount of pro-inflammatory cytokines that activate the systemic immune system, leading to damage of the gastrointestinal barrier. In addition, neurological damage activates the hypothalamic–pituitary–adrenal axis, which causes an increase in adrenal cortisol secretion, impairing the gastrointestinal barrier; D: The use of antibacterial or antiviral drugs may cause dysbiosis or immune suppression resulting in gastrointestinal barrier disorders; E: Competitive binding of ACE2 receptors by the SARS-CoV-2 virus inhibits tryptophan absorption through the B0AT1/ACE2 transport pathway in enterocytes, thus impairing regulation of antimicrobial peptide expression and causing dysbiosis of the flora, which disrupts the gastrointestinal barrier. ACE2: Angiotensin-converting enzyme 2.

certain protein components of human immunoglobulins and hemoglobin were upregulated in COVID-19 patients, suggesting an enhanced immune response and potential bleeding in the intestine.

Studies have also shown that ZO-1 interacts with: (1) Occludin, claudins, and JAM; (2) molecular components of intracellular TJ plaques, such as ZO-2, ZO-3, and cingulin; and (3) the actin cytoskeleton [39]. Thus, ZO-1 plays a key role in the structural and functional integrity of the paracellular barrier[39]. Furthermore, the cytoskeletal and barrier biomarkers KRT19 and ZO1 were respectively enriched in stool and blood samples from COVID-19 patients, suggesting increased intestinal paracellular permeability and injury[38,40]. Another group showed that the microbial metabolite d-lactate and the TJ regulator zonulin were increased in the serum of patients with severe COVID-19 and in COVID-19 patients with secondary infections[41]. These data suggest that biomarkers of intestinal permeability may also be early biomarkers for a fatal outcome. Indeed, treatment with larazotide, a zonulin inhibitor, significantly improved time-to-resolution of gastrointestinal symptoms and time-to-clearance of spike antigenemia in pediatric COVID-19 patients[42,43].

In addition, apoptosis of intestinal epithelial cells in COVID-19 patients is another important factor affecting the integrity of the gastrointestinal mechanical barrier. A study by Lehmann *et al*[44] demonstrated a significant increase in the number of apoptotic epithelial cells in COVID-19 patients by using immunohistochemistry to detect cleaved caspase-3. They also examined the histomorphological changes of epithelial cells and found apoptosis and subsequent regenerative proliferation of epithelial cells in the small intestine of COVID-19 patients[44].

In addition, infection of lung and small intestinal epithelial cells with SARS-CoV-2 stimulates secretion of large amounts of pro-inflammatory cytokines (chemokine-1, TGF-β1, TNF-α, IL-1, and IL-6) causing a cytokine storm and damage to the small intestine that disrupts the integrity of the gastrointestinal barrier[45]. Interestingly, this phenomenon was confirmed using human induced pluripotent stem (iPS)-derived intestinal epithelium, suggesting that iPSC could be a useful *in vitro* model for evaluating COVID-19 pathology in gastrointestinal barrier dysfunction[46].

SARS-CoV-2 and the chemical barrier

Many COVID-19 patients have a significantly reduced appetite, and severely affected patients, such as those dependent on mechanical ventilation, may not be able to eat, resulting in reduced secretion of gastric acid and bile. Under normal conditions, the intestinal epithelial surface is less susceptible to

damage by harmful substances due to the mucus cover, which plays an important role in the gastrointestinal barrier. Studies have shown that in rats receiving total parenteral nutrition, glands atrophy, the intestinal mucus layer is damaged and thinned, intestinal permeability increases, and the gastrointestinal barrier is disrupted[47,48]. In standard total parenteral nutrition, no food passes through the intestine in the loading state and certain essential intestinal nutrients such as glutamine are lacking. Numerous subsequent studies have confirmed that parenteral nutrition tends to damage the intestinal epithelial mucus layer, leading to disruption of the gastrointestinal barrier[49,50].

SARS-CoV-2 is known to be neuroinvasive, and when the body is infected with SARS-CoV-2, a cytokine storm is generated and the release of large amounts of pro-inflammatory cytokines leads to blood-brain barrier damage[51,52]. In addition, lipopolysaccharide (LPS) is recognized by Toll-like receptors, which transduce signals that stimulate release of inflammatory cytokines[53-55]. ACE2 is expressed in certain regions of the human brain as well as in neurons and SARS-CoV-2 can directly damage these target organs[56]. After SARS-CoV-2 infection, impairment of the gastrointestinal barrier causes leaky gut and increased translocation of bacterial metabolic components and toxins into the bloodstream, which activates the immune response and leads to systemic inflammation[57-59]. This can promote neuronal degeneration and the development of psychiatric and neurodegenerative disorders [60]. Furthermore, neurological damage can affect the gastrointestinal barrier *via* the neuroendocrine pathway; this occurs mainly through the hypothalamic–pituitary–adrenal (HPA) axis[61-63]. Stress activates the HPA axis, which ultimately leads to the release of glucocorticoids such as cortisol from the adrenal cortex. Cortisol can alter gastrointestinal dynamics, increase intestinal permeability, and affect the intestinal microbiota[61].

SARS-CoV-2 and the microbial barrier

When the microbial balance in the intestine is altered, pathogenic bacteria adhere to the intestinal epithelium and grow dominantly to replace the normal flora[64]. Pathogenic bacteria can directly damage the microvillous membrane proteins of the intestinal epithelium by producing bacterial proteases. Furthermore, pathogenic bacteria can alter biochemical reactions in the intestinal epithelium, leading to damage, blunting, fusion, or obliteration of the villi[65]. In addition, pathogenic bacteria can produce various toxins or other metabolites that inhibit protein synthesis in the intestinal epithelium, thereby damaging the intestinal mucosal barrier. Some opportunistic pathogens can also produce proteases that degrade IgA, which can weaken or eliminate the immune function provided by sIgA and promote bacterial translocation, leading to bacteremia and endotoxemia, thereby further damaging gastrointestinal barrier integrity[66].

A study by Sun *et al*[38] using metagenomic and metaproteomic methods showed significant changes in the composition of the gut microbiome in COVID-19 patients, characterized by a decrease in commensal species and an increase in opportunistic pathogenic species. Moreover, other studies have shown that the microbiota of COVID-19 patients is enriched with opportunistic pathogens, compared with healthy individuals[64,67-69]. Furthermore, the plasma concentration of the gut permeability marker FABP2 and gut microbial antigens PGN and LPS were significantly elevated in COVID-19 patients in comparison to healthy controls[70].

Hashimoto *et al*[71] found that ACE2 acts as a binding partner of amino acid transporter B0AT1 (SLC6A19) in the intestine and plays an important role in amino acid transport. Tryptophan is mainly absorbed through the B0AT1/ACE2 transport pathway in enterocytes, which activates the mammalian target of the rapamycin (mTOR) pathway to regulate the expression of antimicrobial peptides. These antimicrobial peptides affect the composition of the intestinal microbiota[71]. Competitive binding of ACE2 receptors by the SARS-CoV-2 virus prevents the absorption of tryptophan through the B0AT1/ACE2 transport pathway in enterocytes, impairs the regulation of antimicrobial peptide expression, and causes an intestinal dysbiosis, leading to disruption of the gastrointestinal barrier.

In addition, when patients with COVID-19 are admitted to hospital for treatment, changes in gastrointestinal barrier dysfunction are often induced by bacterial translocation and gut microbiome dysbiosis as a result of early and heavy use of antimicrobial drugs, such as macrolides, fluoroquinolones, or cephalosporin antibiotics[72-74]. Wu *et al*[75] reported that washed microbiota transplantation can improve the intestinal mucosal barrier function, inflammatory response, and immunity. Therefore, this treatment is expected to be an efficacious and safe therapeutic option for the treatment of COVID-19 patients with gut microbiota dysbiosis[75].

SARS-CoV-2 and the immune barrier

After binding to ACE2 receptors expressed on intestinal epithelial cells, SARS-CoV-2 is transported to the nuclear endosome and releases its RNA[76,77]. Toll-like receptors recognize viral RNA and signal downstream mediators, which induce IFN-α and -β production and then activate the transcription factor NF-κB to produce pro-inflammatory cytokines[78]. During SARS-CoV-2 infection, small intestinal tissue and feces show increased pro-inflammatory markers, including neutrophil and monocyte accumulation, increased chemokine-1, TGF-β1, IL-1, IL-6, IL-8, and IFN-γ expression and decreased levels of the anti-inflammatory cytokine IL-10[45,79,80]. IFN-γ is produced by several types of immune cells, especially T helper type 1 (Th1) cells. IFN-γ acts as a major inducer of the cell-mediated response to infection by activating macrophages, enhancing antigen presentation and T cell differentiation[81], and interacting

directly with epithelial cells, leading to chemokine expression and antimicrobial peptide secretion[82, 83]. In addition, mucosal $CD4^+$ and $CD8^+$ T cells, Th17 cells, neutrophils, dendritic cells, and macrophages were activated and T regulatory cells were reduced after intestinal epithelial cells were infected by SARS-CoV-2. Therefore, SARS-CoV-2 infection promotes an over-activated immune response that further damages intestinal epithelium[84-86]. Interestingly, one study found that SARS-CoV-2 was not always measurable in the stools of COVID-19 patients with gastrointestinal symptoms. These data further suggest that the gastrointestinal barrier dysfunction may not be a direct result of viral infection of intestinal mucosal epithelial cells, but rather a result of the immune response[87].

CCL25 is expressed in enterocytes and the CCL25-CCR9 axis mediates recruitment of lung-derived effector $CD4^+$ T cells to the small intestine[88]. $CCR9^+CD4^+$ T cells disrupt homeostasis of the intestinal flora, thereby promoting the in-situ polarization of small intestinal Th17 cells and the production of IL-17A, leading to neutrophil aggregation and ultimately mediating intestinal immune-mediated injury[88, 89]. Moreover, damage to the intestinal mucosa and bacterial imbalance can lead to harmful metabolites in the intestine being transferred to the liver through the portal vein, affecting liver function[90]. With impaired liver function, endotoxin inactivation is reduced, resulting in endotoxin entering the systemic circulation[91-94]. This induces an inflammatory response, damages intestinal mucosa, and causes bacterial translocation and bacteremia, inducing a systemic inflammatory response and thus forming a vicious cycle[95].

Furthermore, antiviral drugs can also cause gastrointestinal barrier dysfunction. For example, severe and persistent diarrhea may be associated with the use of oseltamivir and arborol. Other drugs that can cause gastrointestinal barrier dysfunction include chloroquine phosphate, lopinavir, remdesivir, and some proprietary Chinese medicines, as well as immunosuppressors[96].

CONCLUSION

Gastrointestinal barrier dysfunction in COVID-19 patients is not an independent symptom, but rather a trigger of other diseases. In critically ill patients, gastrointestinal barrier dysfunction, if not treated early, may aggravate primary disease or even cause multi-organ dysfunction syndrome, thus endangering patients' lives. To assess gastrointestinal barrier dysfunction in COVID-19 patients, clinicians should not only consider the effect of the primary disease, but also the pathophysiological situation within the intestine. The pathological mechanisms that cause gastrointestinal barrier damage and dysfunction are complex and various mechanisms are often intertwined, interacting with each other. Therefore, the clinical diagnosis and treatment of gastrointestinal barrier dysfunction should be comprehensive and targeted.

FOOTNOTES

Author contributions: Xue W and Honda M designed the research; Xue W and Honda M performed the research; Xue W, Honda M and Hibi T analyzed the data; Xue W and Honda M wrote the paper.

Conflict-of-interest statement: Authors declare no conflict of interests for this article.

Country/Territory of origin: Japan

ORCID number: Masaki Honda 0000-0001-5526-2591; Taizo Hibi 0000-0002-6867-228X.

S-Editor: Yan JP
L-Editor: A
P-Editor: Cai YX

REFERENCES

1 **Bartoszko JJ**, Siemieniuk RAC, Kum E, Qasim A, Zeraatkar D, Ge L, Han MA, Sadeghirad B, Agarwal A, Agoritsas T, Chu DK, Couban R, Darzi AJ, Devji T, Ghadimi M, Honarmand K, Izcovich A, Khamis A, Lamontagne F, Loeb M, Marcucci M, McLeod SL, Motaghi S, Murthy S, Mustafa RA, Neary JD, Pardo-Hernandez H, Rada G, Rochwerg B, Switzer C, Tendal B, Thabane L, Vandvik PO, Vernooij RWM, Viteri-García A, Wang Y, Yao L, Ye Z, Guyatt GH,

Brignardello-Petersen R. Prophylaxis against covid-19: living systematic review and network meta-analysis. *BMJ* 2021; **373**: n949 [PMID: 33903131 DOI: 10.1136/bmj.n949]

2 **Hoffmann M**, Kleine-Weber H, Schroeder S, Krüger N, Herrler T, Erichsen S, Schiergens TS, Herrler G, Wu NH, Nitsche A, Müller MA, Drosten C, Pöhlmann S. SARS-CoV-2 Cell Entry Depends on ACE2 and TMPRSS2 and Is Blocked by a Clinically Proven Protease Inhibitor. *Cell* 2020; **181**: 271-280.e8 [PMID: 32142651 DOI: 10.1016/j.cell.2020.02.052]

3 **Hussman JP**. Cellular and Molecular Pathways of COVID-19 and Potential Points of Therapeutic Intervention. *Front Pharmacol* 2020; **11**: 1169 [PMID: 32848776 DOI: 10.3389/fphar.2020.01169]

4 **Wu Z**, McGoogan JM. Characteristics of and Important Lessons From the Coronavirus Disease 2019 (COVID-19) Outbreak in China: Summary of a Report of 72 314 Cases From the Chinese Center for Disease Control and Prevention. *JAMA* 2020; **323**: 1239-1242 [PMID: 32091533 DOI: 10.1001/jama.2020.2648]

5 **Hamming I**, Timens W, Bulthuis ML, Lely AT, Navis G, van Goor H. Tissue distribution of ACE2 protein, the functional receptor for SARS coronavirus. A first step in understanding SARS pathogenesis. *J Pathol* 2004; **203**: 631-637 [PMID: 15141377 DOI: 10.1002/path.1570]

6 **Eckburg PB**, Bik EM, Bernstein CN, Purdom E, Dethlefsen L, Sargent M, Gill SR, Nelson KE, Relman DA. Diversity of the human intestinal microbial flora. *Science* 2005; **308**: 1635-1638 [PMID: 15831718 DOI: 10.1126/science.1110591]

7 **Bouhnik Y**, Alain S, Attar A, Flourié B, Raskine L, Sanson-Le Pors MJ, Rambaud JC. Bacterial populations contaminating the upper gut in patients with small intestinal bacterial overgrowth syndrome. *Am J Gastroenterol* 1999; **94**: 1327-1331 [PMID: 10235214 DOI: 10.1111/j.1572-0241.1999.01016.x]

8 **Camilleri M**, Madsen K, Spiller R, Greenwood-Van Meerveld B, Verne GN. Intestinal barrier function in health and gastrointestinal disease. *Neurogastroenterol Motil* 2012; **24**: 503-512 [PMID: 22583600 DOI: 10.1111/j.1365-2982.2012.01921.x]

9 **Raya-Sandino A**, Luissint AC, Kusters DHM, Narayanan V, Flemming S, Garcia-Hernandez V, Godsel LM, Green KJ, Hagen SJ, Conway DE, Parkos CA, Nusrat A. Regulation of intestinal epithelial intercellular adhesion and barrier function by desmosomal cadherin desmocollin-2. *Mol Biol Cell* 2021; **32**: 753-768 [PMID: 33596089 DOI: 10.1091/mbc.E20-12-0775]

10 **Turner JR**. Molecular basis of epithelial barrier regulation: from basic mechanisms to clinical application. *Am J Pathol* 2006; **169**: 1901-1909 [PMID: 17148655 DOI: 10.2353/ajpath.2006.060681]

11 **González-Mariscal L**, Betanzos A, Nava P, Jaramillo BE. Tight junction proteins. *Prog Biophys Mol Biol* 2003; **81**: 1-44 [PMID: 12475568 DOI: 10.1016/s0079-6107(02)00037-8]

12 **Shen L**, Weber CR, Raleigh DR, Yu D, Turner JR. Tight junction pore and leak pathways: a dynamic duo. *Annu Rev Physiol* 2011; **73**: 283-309 [PMID: 20936941 DOI: 10.1146/annurev-physiol-012110-142150]

13 **Corfield AP**, Myerscough N, Longman R, Sylvester P, Arul S, Pignatelli M. Mucins and mucosal protection in the gastrointestinal tract: new prospects for mucins in the pathology of gastrointestinal disease. *Gut* 2000; **47**: 589-594 [PMID: 10986224 DOI: 10.1136/gut.47.4.589]

14 **Nyström EEL**, Martinez-Abad B, Arike L, Birchenough GMH, Nonnecke EB, Castillo PA, Svensson F, Bevins CL, Hansson GC, Johansson MEV. An intercrypt subpopulation of goblet cells is essential for colonic mucus barrier function. *Science* 2021; **372** [PMID: 33859001 DOI: 10.1126/science.abb1590]

15 **Schneider H**, Pelaseyed T, Svensson F, Johansson MEV. Study of mucin turnover in the small intestine by in vivo labeling. *Sci Rep* 2018; **8**: 5760 [PMID: 29636525 DOI: 10.1038/s41598-018-24148-x]

16 **Johansson ME**, Larsson JM, Hansson GC. The two mucus layers of colon are organized by the MUC2 mucin, whereas the outer layer is a legislator of host-microbial interactions. *Proc Natl Acad Sci U S A* 2011; **108** Suppl 1: 4659-4665 [PMID: 20615996 DOI: 10.1073/pnas.1006451107]

17 **Nowarski R**, Jackson R, Gagliani N, de Zoete MR, Palm NW, Bailis W, Low JS, Harman CC, Graham M, Elinav E, Flavell RA. Epithelial IL-18 Equilibrium Controls Barrier Function in Colitis. *Cell* 2015; **163**: 1444-1456 [PMID: 26638073 DOI: 10.1016/j.cell.2015.10.072]

18 **van der Post S**, Jabbar KS, Birchenough G, Arike L, Akhtar N, Sjovall H, Johansson MEV, Hansson GC. Structural weakening of the colonic mucus barrier is an early event in ulcerative colitis pathogenesis. *Gut* 2019; **68**: 2142-2151 [PMID: 30914450 DOI: 10.1136/gutjnl-2018-317571]

19 **Birchenough GM**, Nyström EE, Johansson ME, Hansson GC. A sentinel goblet cell guards the colonic crypt by triggering Nlrp6-dependent Muc2 secretion. *Science* 2016; **352**: 1535-1542 [PMID: 27339979 DOI: 10.1126/science.aaf7419]

20 **Bel S**, Hooper LV. Secretory autophagy of lysozyme in Paneth cells. *Autophagy* 2018; **14**: 719-721 [PMID: 29388875 DOI: 10.1080/15548627.2018.1430462]

21 **Nakimbugwe D**, Masschalck B, Deckers D, Callewaert L, Aertsen A, Michiels CW. Cell wall substrate specificity of six different lysozymes and lysozyme inhibitory activity of bacterial extracts. *FEMS Microbiol Lett* 2006; **259**: 41-46 [PMID: 16684100 DOI: 10.1111/j.1574-6968.2006.00240.x]

22 **Gadaleta RM**, van Erpecum KJ, Oldenburg B, Willemsen EC, Renooij W, Murzilli S, Klomp LW, Siersema PD, Schipper ME, Danese S, Penna G, Laverny G, Adorini L, Moschetta A, van Mil SW. Farnesoid X receptor activation inhibits inflammation and preserves the intestinal barrier in inflammatory bowel disease. *Gut* 2011; **60**: 463-472 [PMID: 21242261 DOI: 10.1136/gut.2010.212159]

23 **Sonnenburg JL**, Angenent LT, Gordon JI. Getting a grip on things: how do communities of bacterial symbionts become established in our intestine? *Nat Immunol* 2004; **5**: 569-573 [PMID: 15164016 DOI: 10.1038/ni1079]

24 **Kim HJ**, Huh D, Hamilton G, Ingber DE. Human gut-on-a-chip inhabited by microbial flora that experiences intestinal peristalsis-like motions and flow. *Lab Chip* 2012; **12**: 2165-2174 [PMID: 22434367 DOI: 10.1039/c2lc40074j]

25 **Ostaff MJ**, Stange EF, Wehkamp J. Antimicrobial peptides and gut microbiota in homeostasis and pathology. *EMBO Mol Med* 2013; **5**: 1465-1483 [PMID: 24039130 DOI: 10.1002/emmm.201201773]

26 **Kayama H**, Okumura R, Takeda K. Interaction Between the Microbiota, Epithelia, and Immune Cells in the Intestine. *Annu Rev Immunol* 2020; **38**: 23-48 [PMID: 32340570 DOI: 10.1146/annurev-immunol-070119-115104]

27 **Gill SR**, Pop M, Deboy RT, Eckburg PB, Turnbaugh PJ, Samuel BS, Gordon JI, Relman DA, Fraser-Liggett CM, Nelson

KE. Metagenomic analysis of the human distal gut microbiome. *Science* 2006; **312**: 1355-1359 [PMID: 16741115 DOI: 10.1126/science.1124234]

28 **Ferguson A**. Immunological functions of the gut in relation to nutritional state and mode of delivery of nutrients. *Gut* 1994; **35**: S10-S12 [PMID: 8125382 DOI: 10.1136/gut.35.1_suppl.s10]

29 **Nagura H**, Sumi Y. Immunological functions of the gut--role of the mucosal immune system. *Toxicol Pathol* 1988; **16**: 154-164 [PMID: 3055225 DOI: 10.1177/019262338801600208]

30 **Noval Rivas M**, Wakita D, Franklin MK, Carvalho TT, Abolhesn A, Gomez AC, Fishbein MC, Chen S, Lehman TJ, Sato K, Shibuya A, Fasano A, Kiyono H, Abe M, Tatsumoto N, Yamashita M, Crother TR, Shimada K, Arditi M. Intestinal Permeability and IgA Provoke Immune Vasculitis Linked to Cardiovascular Inflammation. *Immunity* 2019; **51**: 508-521.e6 [PMID: 31471109 DOI: 10.1016/j.immuni.2019.05.021]

31 **Nagalingam NA**, Lynch SV. Role of the microbiota in inflammatory bowel diseases. *Inflamm Bowel Dis* 2012; **18**: 968-984 [PMID: 21936031 DOI: 10.1002/ibd.21866]

32 **Honda M**, Surewaard BGJ, Watanabe M, Hedrick CC, Lee WY, Brown K, McCoy KD, Kubes P. Perivascular localization of macrophages in the intestinal mucosa is regulated by Nr4a1 and the microbiome. *Nat Commun* 2020; **11**: 1329 [PMID: 32165624 DOI: 10.1038/s41467-020-15068-4]

33 **Honda M**, Kubes P. Neutrophils and neutrophil extracellular traps in the liver and gastrointestinal system. *Nat Rev Gastroenterol Hepatol* 2018; **15**: 206-221 [PMID: 29382950 DOI: 10.1038/nrgastro.2017.183]

34 **Zhou P**, Yang XL, Wang XG, Hu B, Zhang L, Zhang W, Si HR, Zhu Y, Li B, Huang CL, Chen HD, Chen J, Luo Y, Guo H, Jiang RD, Liu MQ, Chen Y, Shen XR, Wang X, Zheng XS, Zhao K, Chen QJ, Deng F, Liu LL, Yan B, Zhan FX, Wang YY, Xiao GF, Shi ZL. A pneumonia outbreak associated with a new coronavirus of probable bat origin. *Nature* 2020; **579**: 270-273 [PMID: 32015507 DOI: 10.1038/s41586-020-2012-7]

35 **Wan Y**, Shang J, Graham R, Baric RS, Li F. Receptor Recognition by the Novel Coronavirus from Wuhan: an Analysis Based on Decade-Long Structural Studies of SARS Coronavirus. *J Virol* 2020; **94** [PMID: 31996437 DOI: 10.1128/JVI.00127-20]

36 **Chen L**, Li L, Han Y, Lv B, Zou S, Yu Q. Tong-fu-li-fei decoction exerts a protective effect on intestinal barrier of sepsis in rats through upregulating ZO-1/occludin/claudin-1 expression. *J Pharmacol Sci* 2020; **143**: 89-96 [PMID: 32173265 DOI: 10.1016/j.jphs.2020.02.009]

37 **Fernández-Blanco JA**, Estévez J, Shea-Donohue T, Martínez V, Vergara P. Changes in Epithelial Barrier Function in Response to Parasitic Infection: Implications for IBD Pathogenesis. *J Crohns Colitis* 2015; **9**: 463-476 [PMID: 25820018 DOI: 10.1093/ecco-jcc/jjv056]

38 **Sun Z**, Song ZG, Liu C, Tan S, Lin S, Zhu J, Dai FH, Gao J, She JL, Mei Z, Lou T, Zheng JJ, Liu Y, He J, Zheng Y, Ding C, Qian F, Chen YM. Gut microbiome alterations and gut barrier dysfunction are associated with host immune homeostasis in COVID-19 patients. *BMC Med* 2022; **20**: 24 [PMID: 35045853 DOI: 10.1186/s12916-021-02212-0]

39 **Assimakopoulos SF**, Papageorgiou I, Charonis A. Enterocytes' tight junctions: From molecules to diseases. *World J Gastrointest Pathophysiol* 2011; **2**: 123-137 [PMID: 22184542 DOI: 10.4291/wjgp.v2.i6.123]

40 **Assimakopoulos SF**, Mastronikolis S, DE Lastic AL, Aretha D, Papageorgiou D, Chalkidi T, Oikonomou I, Triantos C, Mouzaki A, Marangos M. Intestinal Barrier Biomarker ZO1 and Endotoxin Are Increased in Blood of Patients With COVID-19-associated Pneumonia. *In Vivo* 2021; **35**: 2483-2488 [PMID: 34182534 DOI: 10.21873/invivo.12528]

41 **Hernández-Solis A**, Güemes-González AM, Ruiz-Gómez X, Álvarez-Maldonado P, Castañeda-Casimiro J, Flores-López A, Ramírez-Guerra MA, Muñoz-Miranda O, Madera-Sandoval RL, Arriaga-Pizano LA, Nieto-Patlán A, Estrada-Parra S, Pérez-Tapia SM, Serafín-López J, Chacón-Salinas R, Escobar-Gutiérrez A, Soria-Castro R, Ruiz-Sánchez BP, Wong-Baeza I. IL-6, IL-10, sFas, granulysin and indicators of intestinal permeability as early biomarkers for a fatal outcome in COVID-19. *Immunobiology* 2022; **227**: 152288 [PMID: 36209721 DOI: 10.1016/j.imbio.2022.152288]

42 **Yonker LM**, Swank Z, Gilboa T, Senussi Y, Kenyon V, Papadakis L, Boribong BP, Carroll RW, Walt DR, Fasano A. Zonulin Antagonist, Larazotide (AT1001), As an Adjuvant Treatment for Multisystem Inflammatory Syndrome in Children: A Case Series. *Crit Care Explor* 2022; **10**: e0641 [PMID: 35211683 DOI: 10.1097/CCE.0000000000000641]

43 **Yonker LM**, Gilboa T, Ogata AF, Senussi Y, Lazarovits R, Boribong BP, Bartsch YC, Loiselle M, Rivas MN, Porritt RA, Lima R, Davis JP, Farkas EJ, Burns MD, Young N, Mahajan VS, Hajizadeh S, Lopez XIH, Kreuzer J, Morris R, Martinez EE, Han I, Griswold K Jr, Barry NC, Thompson DB, Church G, Edlow AG, Haas W, Pillai S, Arditi M, Alter G, Walt DR, Fasano A. Multisystem inflammatory syndrome in children is driven by zonulin-dependent loss of gut mucosal barrier. *J Clin Invest* 2021; **131** [PMID: 34032635 DOI: 10.1172/JCI149633]

44 **Lehmann M**, Allers K, Heldt C, Meinhardt J, Schmidt F, Rodriguez-Sillke Y, Kunkel D, Schumann M, Böttcher C, Stahl-Hennig C, Elezkurtaj S, Bojarski C, Radbruch H, Corman VM, Schneider T, Loddenkemper C, Moos V, Weidinger C, Kühl AA, Siegmund B. Human small intestinal infection by SARS-CoV-2 is characterized by a mucosal infiltration with activated CD8(+) T cells. *Mucosal Immunol* 2021; **14**: 1381-1392 [PMID: 34420043 DOI: 10.1038/s41385-021-00437-z]

45 **Huang C**, Wang Y, Li X, Ren L, Zhao J, Hu Y, Zhang L, Fan G, Xu J, Gu X, Cheng Z, Yu T, Xia J, Wei Y, Wu W, Xie X, Yin W, Li H, Liu M, Xiao Y, Gao H, Guo L, Xie J, Wang G, Jiang R, Gao Z, Jin Q, Wang J, Cao B. Clinical features of patients infected with 2019 novel coronavirus in Wuhan, China. *Lancet* 2020; **395**: 497-506 [PMID: 31986264 DOI: 10.1016/S0140-6736(20)30183-5]

46 **Yamada S**, Noda T, Okabe K, Yanagida S, Nishida M, Kanda Y. SARS-CoV-2 induces barrier damage and inflammatory responses in the human iPSC-derived intestinal epithelium. *J Pharmacol Sci* 2022; **149**: 139-146 [PMID: 35641026 DOI: 10.1016/j.jphs.2022.04.010]

47 **Li J**, Langkamp-Henken B, Suzuki K, Stahlgren LH. Glutamine prevents parenteral nutrition-induced increases in intestinal permeability. *JPEN J Parenter Enteral Nutr* 1994; **18**: 303-307 [PMID: 7933435 DOI: 10.1177/014860719401800404]

48 **Iiboshi Y**, Nezu R, Kennedy M, Fujii M, Wasa M, Fukuzawa M, Kamata S, Takagi Y, Okada A. Total parenteral nutrition decreases luminal mucous gel and increases permeability of small intestine. *JPEN J Parenter Enteral Nutr* 1994; **18**: 346-350 [PMID: 7523742 DOI: 10.1177/014860719401800412]

49 **Hadfield RJ**, Sinclair DG, Houldsworth PE, Evans TW. Effects of enteral and parenteral nutrition on gut mucosal

permeability in the critically ill. *Am J Respir Crit Care Med* 1995; **152**: 1545-1548 [PMID: 7582291 DOI: 10.1164/ajrccm.152.5.7582291]

50 **Buchman AL**, Moukarzel AA, Bhuta S, Belle M, Ament ME, Eckhert CD, Hollander D, Gornbein J, Kopple JD, Vijayaroghavan SR. Parenteral nutrition is associated with intestinal morphologic and functional changes in humans. *JPEN J Parenter Enteral Nutr* 1995; **19**: 453-460 [PMID: 8748359 DOI: 10.1177/0148607195019006453]

51 **Xia H**, Lazartigues E. Angiotensin-converting enzyme 2 in the brain: properties and future directions. *J Neurochem* 2008; **107**: 1482-1494 [PMID: 19014390 DOI: 10.1111/j.1471-4159.2008.05723.x]

52 **Mao L**, Jin H, Wang M, Hu Y, Chen S, He Q, Chang J, Hong C, Zhou Y, Wang D, Miao X, Li Y, Hu B. Neurologic Manifestations of Hospitalized Patients With Coronavirus Disease 2019 in Wuhan, China. *JAMA Neurol* 2020; **77**: 683-690 [PMID: 32275288 DOI: 10.1001/jamaneurol.2020.1127]

53 **Pourbadie HG**, Sayyah M, Khoshkholgh-Sima B, Choopani S, Nategh M, Motamedi F, Shokrgozar MA. Early minor stimulation of microglial TLR2 and TLR4 receptors attenuates Alzheimer's disease-related cognitive deficit in rats: behavioral, molecular, and electrophysiological evidence. *Neurobiol Aging* 2018; **70**: 203-216 [PMID: 30031930 DOI: 10.1016/j.neurobiolaging.2018.06.020]

54 **Iwasa T**, Matsuzaki T, Tungalagsuvd A, Munkhzaya M, Kawami T, Yamasaki M, Murakami M, Kato T, Kuwahara A, Yasui T, Irahara M. Developmental changes in hypothalamic toll-like-receptor 4 mRNA expression and the effects of lipopolysaccharide on such changes in female rats. *Int J Dev Neurosci* 2015; **40**: 12-14 [PMID: 25448126 DOI: 10.1016/j.ijdevneu.2014.10.002]

55 **Sabatino ME**, Sosa Ldel V, Petiti JP, Mukdsi JH, Mascanfroni ID, Pellizas CG, Gutiérrez S, Torres AI, De Paul AL. Functional Toll-like receptor 4 expressed in lactotrophs mediates LPS-induced proliferation in experimental pituitary hyperplasia. *Exp Cell Res* 2013; **319**: 3020-3034 [PMID: 23973924 DOI: 10.1016/j.yexcr.2013.08.012]

56 **Lindskog C**, Méar L, Virhammar J, Fällmar D, Kumlien E, Hesselager G, Casar-Borota O, Rostami E. Protein Expression Profile of ACE2 in the Normal and COVID-19-Affected Human Brain. *J Proteome Res* 2022; **21**: 2137-2145 [PMID: 35901083 DOI: 10.1021/acs.jproteome.2c00184]

57 **Saithong S**, Worasilchai N, Saisorn W, Udompornpitak K, Bhunyakarnjanarat T, Chindamporn A, Tovichayathamrong P, Torvorapanit P, Chiewchengchol D, Chancharoenthana W, Leelahavanichkul A. Neutrophil Extracellular Traps in Severe SARS-CoV-2 Infection: A Possible Impact of LPS and (1→3)-β-D-glucan in Blood from Gut Translocation. *Cells* 2022; **11** [PMID: 35406667 DOI: 10.3390/cells11071103]

58 **Smith N**, Goncalves P, Charbit B, Grzelak L, Beretta M, Planchais C, Bruel T, Rouilly V, Bondet V, Hadjadj J, Yatim N, Pere H, Merkling SH, Ghozlane A, Kernéis S, Rieux-Laucat F, Terrier B, Schwartz O, Mouquet H, Duffy D, Di Santo JP. Distinct systemic and mucosal immune responses during acute SARS-CoV-2 infection. *Nat Immunol* 2021; **22**: 1428-1439 [PMID: 34471264 DOI: 10.1038/s41590-021-01028-7]

59 **Mizutani T**, Ishizaka A, Koga M, Ikeuchi K, Saito M, Adachi E, Yamayoshi S, Iwatsuki-Horimoto K, Yasuhara A, Kiyono H, Matano T, Suzuki Y, Tsutsumi T, Kawaoka Y, Yotsuyanagi H. Correlation Analysis between Gut Microbiota Alterations and the Cytokine Response in Patients with Coronavirus Disease during Hospitalization. *Microbiol Spectr* 2022; **10**: e0168921 [PMID: 35254122 DOI: 10.1128/spectrum.01689-21]

60 **Nelson DW**, Granberg T, Andersen P, Jokhadar E, Kåhlin J, Granström A, Hallinder H, Schening A, Thunborg C, Walles H, Hagman G, Shams-Latifi R, Yu J, Petersson S, Tzortzakakis A, Levak N, Aspö M, Piehl F, Zetterberg H, Kivipelto M, Eriksson LI. The Karolinska NeuroCOVID study protocol: Neurocognitive impairment, biomarkers and advanced imaging in critical care survivors. *Acta Anaesthesiol Scand* 2022; **66**: 759-766 [PMID: 35332517 DOI: 10.1111/aas.14062]

61 **Vodička M**, Ergang P, Hrnčíř T, Mikulecká A, Kvapilová P, Vagnerová K, Šestáková B, Fajstová A, Hermanová P, Hudcovic T, Kozáková H, Pácha J. Microbiota affects the expression of genes involved in HPA axis regulation and local metabolism of glucocorticoids in chronic psychosocial stress. *Brain Behav Immun* 2018; **73**: 615-624 [PMID: 29990567 DOI: 10.1016/j.bbi.2018.07.007]

62 **Konturek PC**, Brzozowski T, Konturek SJ. Stress and the gut: pathophysiology, clinical consequences, diagnostic approach and treatment options. *J Physiol Pharmacol* 2011; **62**: 591-599 [PMID: 22314561]

63 **Sudo N**, Chida Y, Aiba Y, Sonoda J, Oyama N, Yu XN, Kubo C, Koga Y. Postnatal microbial colonization programs the hypothalamic-pituitary-adrenal system for stress response in mice. *J Physiol* 2004; **558**: 263-275 [PMID: 15133062 DOI: 10.1113/jphysiol.2004.063388]

64 **Zuo T**, Zhang F, Lui GCY, Yeoh YK, Li AYL, Zhan H, Wan Y, Chung ACK, Cheung CP, Chen N, Lai CKC, Chen Z, Tso EYK, Fung KSC, Chan V, Ling L, Joynt G, Hui DSC, Chan FKL, Chan PKS, Ng SC. Alterations in Gut Microbiota of Patients With COVID-19 During Time of Hospitalization. *Gastroenterology* 2020; **159**: 944-955.e8 [PMID: 32442562 DOI: 10.1053/j.gastro.2020.05.048]

65 **Wang XD**, Ar'Rajab A, Andersson R, Soltesz V, Wang W, Svensson M, Bengmark S. The influence of surgically induced acute liver failure on the intestine in the rat. *Scand J Gastroenterol* 1993; **28**: 31-40 [PMID: 8430272 DOI: 10.3109/00365529309096042]

66 **Diebel LN**, Liberati DM, Diglio CA, Dulchavsky SA, Brown WJ. Synergistic effects of Candida and Escherichia coli on gut barrier function. *J Trauma* 1999; **47**: 1045-50; discussion 1050 [PMID: 10608531 DOI: 10.1097/00005373-199912000-00009]

67 **Gaibani P**, D'Amico F, Bartoletti M, Lombardo D, Rampelli S, Fornaro G, Coladonato S, Siniscalchi A, Re MC, Viale P, Brigidi P, Turroni S, Giannella M. The Gut Microbiota of Critically Ill Patients With COVID-19. *Front Cell Infect Microbiol* 2021; **11**: 670424 [PMID: 34268136 DOI: 10.3389/fcimb.2021.670424]

68 **Cao J**, Wang C, Zhang Y, Lei G, Xu K, Zhao N, Lu J, Meng F, Yu L, Yan J, Bai C, Zhang S, Zhang N, Gong Y, Bi Y, Shi Y, Chen Z, Dai L, Wang J, Yang P. Integrated gut virome and bacteriome dynamics in COVID-19 patients. *Gut Microbes* 2021; **13**: 1-21 [PMID: 33678150 DOI: 10.1080/19490976.2021.1887722]

69 **Yin YS**, Minacapelli CD, Parmar V, Catalano CC, Bhurwal A, Gupta K, Rustgi VK, Blaser MJ. Alterations of the fecal microbiota in relation to acute COVID-19 infection and recovery. *Mol Biomed* 2022; **3**: 36 [PMID: 36437420 DOI: 10.1186/s43556-022-00103-1]

70 **Prasad R**, Patton MJ, Floyd JL, Fortmann S, DuPont M, Harbour A, Wright J, Lamendella R, Stevens BR, Oudit GY,

Grant MB. Plasma Microbiome in COVID-19 Subjects: An Indicator of Gut Barrier Defects and Dysbiosis. *Int J Mol Sci* 2022; **23** [PMID: 36012406 DOI: 10.3390/ijms23169141]

71 **Hashimoto T**, Perlot T, Rehman A, Trichereau J, Ishiguro H, Paolino M, Sigl V, Hanada T, Hanada R, Lipinski S, Wild B, Camargo SM, Singer D, Richter A, Kuba K, Fukamizu A, Schreiber S, Clevers H, Verrey F, Rosenstiel P, Penninger JM. ACE2 links amino acid malnutrition to microbial ecology and intestinal inflammation. *Nature* 2012; **487**: 477-481 [PMID: 22837003 DOI: 10.1038/nature11228]

72 **Yacouba A**, Olowo-Okere A, Yunusa I. Repurposing of antibiotics for clinical management of COVID-19: a narrative review. *Ann Clin Microbiol Antimicrob* 2021; **20**: 37 [PMID: 34020659 DOI: 10.1186/s12941-021-00444-9]

73 **Echeverría-Esnal D**, Martin-Ontiyuelo C, Navarrete-Rouco ME, De-Antonio Cuscó M, Ferrández O, Horcajada JP, Grau S. Azithromycin in the treatment of COVID-19: a review. *Expert Rev Anti Infect Ther* 2021; **19**: 147-163 [PMID: 32853038 DOI: 10.1080/14787210.2020.1813024]

74 **Bernard-Raichon L**, Venzon M, Klein J, Axelrad JE, Zhang C, Sullivan AP, Hussey GA, Casanovas-Massana A, Noval MG, Valero-Jimenez AM, Gago J, Putzel G, Pironti A, Wilder E; Yale IMPACT Research Team, Thorpe LE, Littman DR, Dittmann M, Stapleford KA, Shopsin B, Torres VJ, Ko AI, Iwasaki A, Cadwell K, Schluter J. Gut microbiome dysbiosis in antibiotic-treated COVID-19 patients is associated with microbial translocation and bacteremia. *Nat Commun* 2022; **13**: 5926 [PMID: 36319618 DOI: 10.1038/s41467-022-33395-6]

75 **Wu LH**, Ye ZN, Peng P, Xie WR, Xu JT, Zhang XY, Xia HH, He XX. Efficacy and Safety of Washed Microbiota Transplantation to Treat Patients with Mild-to-Severe COVID-19 and Suspected of Having Gut Microbiota Dysbiosis: Study Protocol for a Randomized Controlled Trial. *Curr Med Sci* 2021; **41**: 1087-1095 [PMID: 34846698 DOI: 10.1007/s11596-021-2475-2]

76 **Sefik E**, Qu R, Junqueira C, Kaffe E, Mirza H, Zhao J, Brewer JR, Han A, Steach HR, Israelow B, Blackburn HN, Velazquez SE, Chen YG, Halene S, Iwasaki A, Meffre E, Nussenzweig M, Lieberman J, Wilen CB, Kluger Y, Flavell RA. Inflammasome activation in infected macrophages drives COVID-19 pathology. *Nature* 2022; **606**: 585-593 [PMID: 35483404 DOI: 10.1038/s41586-022-04802-1]

77 **Liang W**, Feng Z, Rao S, Xiao C, Xue X, Lin Z, Zhang Q, Qi W. Diarrhoea may be underestimated: a missing link in 2019 novel coronavirus. *Gut* 2020; **69**: 1141-1143 [PMID: 32102928 DOI: 10.1136/gutjnl-2020-320832]

78 **Yang JY**, Kim MS, Kim E, Cheon JH, Lee YS, Kim Y, Lee SH, Seo SU, Shin SH, Choi SS, Kim B, Chang SY, Ko HJ, Bae JW, Kweon MN. Enteric Viruses Ameliorate Gut Inflammation *via* Toll-like Receptor 3 and Toll-like Receptor 7-Mediated Interferon-β Production. *Immunity* 2016; **44**: 889-900 [PMID: 27084119 DOI: 10.1016/j.immuni.2016.03.009]

79 **Jiao L**, Li H, Xu J, Yang M, Ma C, Li J, Zhao S, Wang H, Yang Y, Yu W, Wang J, Yang J, Long H, Gao J, Ding K, Wu D, Kuang D, Zhao Y, Liu J, Lu S, Liu H, Peng X. The Gastrointestinal Tract Is an Alternative Route for SARS-CoV-2 Infection in a Nonhuman Primate Model. *Gastroenterology* 2021; **160**: 1647-1661 [PMID: 33307034 DOI: 10.1053/j.gastro.2020.12.001]

80 **Zhang F**, Mears JR, Shakib L, Beynor JI, Shanaj S, Korsunsky I, Nathan A; Accelerating Medicines Partnership Rheumatoid Arthritis and Systemic Lupus Erythematosus (AMP RA/SLE) Consortium, Donlin LT, Raychaudhuri S. IFN-γ and TNF-α drive a CXCL10+ CCL2+ macrophage phenotype expanded in severe COVID-19 lungs and inflammatory diseases with tissue inflammation. *Genome Med* 2021; **13**: 64 [PMID: 33879239 DOI: 10.1186/s13073-021-00881-3]

81 **Mills CD**, Kincaid K, Alt JM, Heilman MJ, Hill AM. M-1/M-2 macrophages and the Th1/Th2 paradigm. *J Immunol* 2000; **164**: 6166-6173 [PMID: 10843666 DOI: 10.4049/jimmunol.164.12.6166]

82 **Walrath T**, Malizia RA, Zhu X, Sharp SP, D'Souza SS, Lopez-Soler R, Parr B, Kartchner B, Lee EC, Stain SC, Iwakura Y, O'Connor W Jr. IFN-γ and IL-17A regulate intestinal crypt production of CXCL10 in the healthy and inflamed colon. *Am J Physiol Gastrointest Liver Physiol* 2020; **318**: G479-G489 [PMID: 31790273 DOI: 10.1152/ajpgi.00208.2019]

83 **Farin HF**, Karthaus WR, Kujala P, Rakhshandehroo M, Schwank G, Vries RG, Kalkhoven E, Nieuwenhuis EE, Clevers H. Paneth cell extrusion and release of antimicrobial products is directly controlled by immune cell-derived IFN-γ. *J Exp Med* 2014; **211**: 1393-1405 [PMID: 24980747 DOI: 10.1084/jem.20130753]

84 **Grant RA**, Morales-Nebreda L, Markov NS, Swaminathan S, Querrey M, Guzman ER, Abbott DA, Donnelly HK, Donayre A, Goldberg IA, Klug ZM, Borkowski N, Lu Z, Kihshen H, Politanska Y, Sichizya L, Kang M, Shilatifard A, Qi C, Lomasney JW, Argento AC, Kruser JM, Malsin ES, Pickens CO, Smith SB, Walter JM, Pawlowski AE, Schneider D, Nannapaneni P, Abdala-Valencia H, Bharat A, Gottardi CJ, Budinger GRS, Misharin AV, Singer BD, Wunderink RG; NU SCRIPT Study Investigators. Circuits between infected macrophages and T cells in SARS-CoV-2 pneumonia. *Nature* 2021; **590**: 635-641 [PMID: 33429418 DOI: 10.1038/s41586-020-03148-w]

85 **Zhou R**, To KK, Wong YC, Liu L, Zhou B, Li X, Huang H, Mo Y, Luk TY, Lau TT, Yeung P, Chan WM, Wu AK, Lung KC, Tsang OT, Leung WS, Hung IF, Yuen KY, Chen Z. Acute SARS-CoV-2 Infection Impairs Dendritic Cell and T Cell Responses. *Immunity* 2020; **53**: 864-877.e5 [PMID: 32791036 DOI: 10.1016/j.immuni.2020.07.026]

86 **Ouyang Y**, Yin J, Wang W, Shi H, Shi Y, Xu B, Qiao L, Feng Y, Pang L, Wei F, Guo X, Jin R, Chen D. Downregulated Gene Expression Spectrum and Immune Responses Changed During the Disease Progression in Patients With COVID-19. *Clin Infect Dis* 2020; **71**: 2052-2060 [PMID: 32307550 DOI: 10.1093/cid/ciaa462]

87 **Cheung KS**, Hung IFN, Chan PPY, Lung KC, Tso E, Liu R, Ng YY, Chu MY, Chung TWH, Tam AR, Yip CCY, Leung KH, Fung AY, Zhang RR, Lin Y, Cheng HM, Zhang AJX, To KKW, Chan KH, Yuen KY, Leung WK. Gastrointestinal Manifestations of SARS-CoV-2 Infection and Virus Load in Fecal Samples From a Hong Kong Cohort: Systematic Review and Meta-analysis. *Gastroenterology* 2020; **159**: 81-95 [PMID: 32251668 DOI: 10.1053/j.gastro.2020.03.065]

88 **Wang J**, Li F, Wei H, Lian ZX, Sun R, Tian Z. Respiratory influenza virus infection induces intestinal immune injury *via* microbiota-mediated Th17 cell-dependent inflammation. *J Exp Med* 2014; **211**: 2397-2410 [PMID: 25366965 DOI: 10.1084/jem.20140625]

89 **Papadakis KA**, Prehn J, Nelson V, Cheng L, Binder SW, Ponath PD, Andrew DP, Targan SR. The role of thymus-expressed chemokine and its receptor CCR9 on lymphocytes in the regional specialization of the mucosal immune system. *J Immunol* 2000; **165**: 5069-5076 [PMID: 11046037 DOI: 10.4049/jimmunol.165.9.5069]

90 **Miyake Y**, Yamamoto K. Role of gut microbiota in liver diseases. *Hepatol Res* 2013; **43**: 139-146 [PMID: 22970713 DOI: 10.1111/j.1872-034X.2012.01088.x]

91 **Filliol A**, Piquet-Pellorce C, Raguénès-Nicol C, Dion S, Farooq M, Lucas-Clerc C, Vandenabeele P, Bertrand MJM, Le Seyec J, Samson M. RIPK1 protects hepatocytes from Kupffer cells-mediated TNF-induced apoptosis in mouse models of PAMP-induced hepatitis. *J Hepatol* 2017; **66**: 1205-1213 [PMID: 28088582 DOI: 10.1016/j.jhep.2017.01.005]

92 **Zhu L**, Baker SS, Gill C, Liu W, Alkhouri R, Baker RD, Gill SR. Characterization of gut microbiomes in nonalcoholic steatohepatitis (NASH) patients: a connection between endogenous alcohol and NASH. *Hepatology* 2013; **57**: 601-609 [PMID: 23055155 DOI: 10.1002/hep.26093]

93 **Ni YH**, Huo LJ, Li TT. [Effect of interleukin-22 on proliferation and activation of hepatic stellate cells induced by acetaldehyde and related mechanism]. *Zhonghua Gan Zang Bing Za Zhi* 2017; **25**: 9-14 [PMID: 28297772 DOI: 10.3760/cma.j.issn.1007-3418.2017.01.004]

94 **Wu X**, Wang Y, Wang S, Xu R, Lv X. Purinergic P2X7 receptor mediates acetaldehyde-induced hepatic stellate cells activation *via* PKC-dependent GSK3β pathway. *Int Immunopharmacol* 2017; **43**: 164-171 [PMID: 28061416 DOI: 10.1016/j.intimp.2016.12.017]

95 **Tripathi A**, Debelius J, Brenner DA, Karin M, Loomba R, Schnabl B, Knight R. The gut-liver axis and the intersection with the microbiome. *Nat Rev Gastroenterol Hepatol* 2018; **15**: 397-411 [PMID: 29748586 DOI: 10.1038/s41575-018-0011-z]

96 **Ye Q**, Wang B, Zhang T, Xu J, Shang S. The mechanism and treatment of gastrointestinal symptoms in patients with COVID-19. *Am J Physiol Gastrointest Liver Physiol* 2020; **319**: G245-G252 [PMID: 32639848 DOI: 10.1152/ajpgi.00148.2020]

World Journal of Gastroenterology

Submit a Manuscript: https://www.f6publishing.com

World J Gastroenterol 2023 April 21; 29(15): 2294-2309

DOI: 10.3748/wjg.v29.i15.2294

ISSN 1007-9327 (print) ISSN 2219-2840 (online)

ORIGINAL ARTICLE

Basic Study

Ferroptosis inhibition attenuates inflammatory response in mice with acute hypertriglyceridemic pancreatitis

Yi-Teng Meng, Yi Zhou, Pei-Yu Han, Hong-Bo Ren

Specialty type: Gastroenterology and hepatology

Provenance and peer review: Unsolicited article; Externally peer reviewed.

Peer-review model: Single blind

Peer-review report's scientific quality classification

Grade A (Excellent): 0
Grade B (Very good): B
Grade C (Good): 0
Grade D (Fair): D
Grade E (Poor): 0

P-Reviewer: Bezawork-Geleta A, Australia; Wang G, China

Received: December 6, 2022
Peer-review started: December 6, 2022
First decision: January 22, 2023
Revised: February 20, 2023
Accepted: March 21, 2023
Article in press: March 21, 2023
Published online: April 21, 2023

Yi-Teng Meng, Department of Gastroenterology, Shenzhen People's Hospital (The Second Clinical Medical College, Jinan University; The First Affiliated Hospital, Southern University of Science and Technology), Shenzhen 518020, Guangdong Province, China

Yi Zhou, Pei-Yu Han, Wuxi School of Medicine, Jiangnan University, Wuxi 214000, Jiangsu Province, China

Hong-Bo Ren, Department of Gastroenterology, Qilu Hospital, Jinan 250012, Shandong Province, China

Corresponding author: Hong-Bo Ren, PhD, Professor, Department of Gastroenterology, Qilu Hospital, No. 107 Wenhuaxi Road, Jinan 250012, Shandong Province, China.
rhb2229@163.com

Abstract

BACKGROUND

Ferroptosis is involved in developing inflammatory diseases; yet, its role in acute hypertriglyceridemic pancreatitis (HTGP) remains unclear.

AIM

To explore whether ferroptosis is involved in the process of HTGP and elucidate its potential mechanisms.

METHODS

An HTGP mouse model was induced using intraperitoneal injection of P-407 and caerulein (CAE). Then, pancreatic tissues from the model animals were subjected to proteome sequencing analysis. The pathological changes and scores of the pancreas, lung, and kidney were determined using hematoxylin-eosin staining. The levels of serum amylase (AMY), triglyceride, and total cholesterol were measured with an automatic blood cell analyzer. Additionally, the serum levels of tumor necrosis factor (TNF)-α, interleukin (IL)-6, and IL-1β were determined by enzyme linked immunosorbent assay. Malonaldehyde (MDA), glutathione (GSH), and Fe^{2+} were detected in the pancreas. Finally, immunohistochemistry was performed to assess the expression of ferroptosis-related proteins.

RESULTS

Proteome sequencing revealed that ferroptosis was involved in the process of HTGP and that NADPH oxidase (NOX) 2 may participate in ferroptosis

regulation. Moreover, the levels of serum AMY, TNF-α, IL-6, and IL-1β were significantly increased, MDA and Fe^{2+} were upregulated, GSH and ferroptosis-related proteins were reduced, and the injury of the pancreas, lung, and kidney were aggravated in the P407 + CAE group compared to CAE and wild type groups (all $P < 0.05$). Notably, the inhibition of ferroptosis and NOX2 attenuated the pathological damage and the release of TNF-α, IL-6, and IL-1β in the serum of the mice.

CONCLUSION

Ferroptosis was found to have an important role in HTGP and may be considered a potential target for clinical treatment.

Key Words: Ferroptosis; Acute hypertriglyceridemic pancreatitis; NADPH oxidase 2; Ferrostatin-1; Vas2870

Core Tip: Ferroptosis is involved in the development of inflammatory diseases, but its relationship with acute hypertriglyceridemic pancreatitis (HTGP) remains unclear. This study discoverd ferroptosis is involved in the process of HTGP and therefore a potential target for clinical treatment.

Citation: Meng YT, Zhou Y, Han PY, Ren HB. Ferroptosis inhibition attenuates inflammatory response in mice with acute hypertriglyceridemic pancreatitis. *World J Gastroenterol* 2023; 29(15): 2294-2309
URL: https://www.wjgnet.com/1007-9327/full/v29/i15/2294.htm
DOI: https://dx.doi.org/10.3748/wjg.v29.i15.2294

INTRODUCTION

Hypertriglyceridemia is one of the leading causes of acute pancreatitis (AP). In China, the incidence rate of acute hypertriglyceridemic pancreatitis (HTGP) has increased from 13% in 2009 to 25.6% in 2013, and it is currently considered a second predominant type of AP[1-3]. Compared with AP caused by other causes, HTGP is associated with multiple organ dysfunction syndrome (MODS) and higher mortality[1, 4]. However, the underlying mechanisms of HTGP remain clear, and no effective treatments are available. Therefore, exploring the pathogenesis of HTGP and seeking more accurate therapeutic targets are of critical importance.

It is generally believed that excessive triglyceride (TG), which is hydrolyzed by pancreatic lipase, results in the release of damage-inducing free fatty acids (FFA), which then directly damage the pancreatic function and induce and amplify inflammatory responses through oxidative stress, aggravating multiple organ damage and leading to MODS[5-8]. In 2020, Rawla *et al*[9] found that when serum TG levels were higher than 1000 mg/dL, the incidence of AP was 5%, but when TG was over 2000 mg/dL, the incidence of AP increased to 10%-20%[9].

Previous studies have also revealed that various forms of regulated cell death (RCD), such as apoptosis and autophagy, are involved in the pathogenesis of AP[10-12]. Yet, the role of ferroptosis in HGAP is still not fully understood. Ferroptosis, as an iron-dependent form of non-apoptotic cell death first reported in 2012, is induced by excessive accumulation of peroxidized lipids and strictly regulated by glutathione peroxidase 4 (GPX4) and acyl-CoA synthetase long-chain family member 4[13-16]. Existing evidence suggests that the development of many diseases, including cancer, neurological diseases, ischemia-reperfusion injury, kidney injury, and cardiovascular diseases, is driven by ferroptosis[17-21]. In addition to altered iron homeostasis, the excessive production of reactive oxygen species (ROS) has also been reported as a key factor in ferroptosis induction[22].

Abnormal lipid metabolism is also considered to have an important role in the process of HTGP[4]. Meanwhile, FFA has been found to induce the excessive release of ROS and accumulation in the body [5]. Therefore, since abnormal lipid metabolism and ROS accumulation occur in both ferroptosis and HTGP, we hypothesized that ferroptosis might also participate in the process of HTGP. In the present study, we assessed the role of ferroptosis in HTGP through proteome sequencing. Then, we investigated the possible pathways and verified our results using animal experiments. This study provides new insides into the mechanism and treatment of HTGP.

MATERIALS AND METHODS

Materials and reagents

P-407 and caerulein (CAE) were purchased from Sigma Chemical (St. Louis, MO, United States). Ferrostatin-1 (Fer-1) and Vas2870 (Vas) were obtained from MedChemExpress (MCE, Monmouth Junction, NJ, United States). P-407 was solubilized in phosphate buffer solution (PBS) and stored at 4 °C. CAE, Fer-1, and Vas were solubilized in dimethyl sulfoxide and stored at 20 °C. Enzyme linked immunosorbent assay (ELISA) kits were obtained from Solarbio (Beijing, China).

Animals and modeling

Adult male C57BL/6 mice (25-30 g, 8-wk) were housed in a ventilated environment with a temperature of 22 ± 1 °C, relative humidity of 50% ± 1%, and a light/dark cycle of 12/12 hr and given water and food ad libitum. After acclimatization, mice were randomly categorized into 4 groups (n = 4 per group): Control, P-407, AP (CAE), and HTGP (P-407 + CAE). The P-407 exposure group was intraperitoneally injected with a dosage of 0.6 g/kg body weight (bw) P-407[1,23]. Eight hours later, the AP group was intraperitoneally injected with a dosage of 100 μg/kg bw CAE 8 times (once every hour)[1,24]. The control group was injected with the same volume of PBS. After the last injection, all mice were alive. The animals were sacrificed and pancreas, lung, and kidney tissues were excised.

Serum assays

After the mice fasted for 16 h, Roche blood glucose meter was used to detect fasting blood glucose, and the collected blood from eyeballs was centrifuged at 4 °C, 3000 g for 10 min. The activities of the serum α-amylase (AMY), total cholesterol (TC), TG, aspartate transaminase (AST), and alanine aminotransferase (ALT) in blood samples were measured by an automatic blood cell analyzer (Mindray, Shenzhen, China). Malonaldehyde (MDA), tumor necrosis factor (TNF)-α, interleukin (IL)-6, and IL-1β were detected by specific ELISA kits (Solarbio Science & Technology Co., Ltd, Beijing, China), following the manufacturer's instructions. The concentrations were expressed as pg/mL. The serum fasting insulin (FINS) levels were detected by a specific ELISA kit (Proteintech, Wuhan, China). The homeostasis model assessment insulin resistance index (HOMA-IR) = fasting blood glucose (FBG, mmol/L) × Fasting insulin (FINS, mIU/L)/22.5.

Glutathione detection

The Micro Reduced glutathione (GSH) Assay Kit was from Solarbio (Solarbio Science & Technology Co., Ltd, Beijing, China). Continuously dilute the standard product according to the corresponding concentration, and make the standard curve. Then, the supernatant of pancreas samples and total glutathione test solution were added into the 96-well plate successively, mixed, and incubated at 25 °C or room temperature for 5 min. 50 μL 0.5 mg/mL NADPH solution was added to per hole and mixed. The absorbance of each hole was measured immediately with an enzyme marker (λ = 412 nm). The total GSH content of each pore was obtained according to absorbance and standard curve. The sample is processed with GSH scavenger and GSH scavenger assistant in the kit to remove GSH, and the content of oxidized glutathione disulfide (GSSG) is measured, finally the content of reduced GSH is subtracted by total GSH and GSSG.

Fe^{2+} detection

Fe^{2+} in pancreas was detected according to the instructions in the Ferrous Ion Content Assay Kit (Solarbio Science & Technology Co., Ltd, Beijing, China). The absorbance was measured immediately with an enzyme marker (λ = 593 nm). The content of Fe^{2+} was obtained according to the concentration of standard substance and absorbance.

Malondialdehyde detection

MDA in pancreas was detected according to the instructions of MDA Content Assay Kit (Solarbio Science & Technology Co., Ltd, Beijing, China). After pretreatment, appropriate amount of supernatant was taken, and the absorbance of each group was measured at 532 nm. MDA content was obtained according to absorbance.

Histology and immunohistochemistry analyses

The tissue sections (pancreas, lung, and kidney) were cut into continuous slices. Hematoxylin–eosin (HE) staining was performed according to the Solarbio kit guidelines, and immunohistochemistry (IHC) analysis was conducted according to the Kangwei kit instructions. Images were acquired by Pannoramic MIDI (3DHISTECH). Brown-stained areas indicated immunoreactivity. Tissue sections were blindly evaluated by two pathologists based on previously reported criteria: The pathological injury of the pancreas was scored according to the edema, inflammation, hemorrhage, and necrosis of the pancreas [25]; the pathological score of the lung was measured on the basis of edema, neutrophil infiltration, and hemorrhage[26]; the pathological renal score was evaluated by the degree of tubulointerstitial injury

based on previously reported criteria[27].

Ferroptosis-related proteins (the light chain subunit solute carrier family 7 member 11 (SLC7A11) and GPX4 were determined by IHC analysis. Image J was used to quantify the expression of SLC7A11 and GPX4.

Protein extraction

The sample was ground with liquid nitrogen into cell powder and then transferred to a 5-mL centrifuge tube. After that, four volumes of lysis buffer (8 M urea, 1% protease inhibitor cocktail) were added to the cell powder, followed by sonication three times on ice using a high-intensity ultrasonic processor (Scientz). Next, the remaining debris was removed by centrifugation at 12000 g at 4 °C for 10 min. Finally, the supernatant was collected, and the protein concentration was determined with a Bicinchoninic Acid Assay kit according to the manufacturer's instructions.

Trypsin digestion

For digestion, the protein solution was reduced by 5 mmol/L dithiothreitol for 30 min at 56 °C and alkylated with 11 mmol/L iodoacetamide for 15 min at room temperature in darkness. The protein sample was then diluted by adding 100 mmol/L tetraethyl ammonium bromide to urea concentration < 2 M. Finally, trypsin was added at 1:50 trypsin-to-protein mass ratio for the first digestion overnight and 1:100 trypsin-to-protein mass ratio for a second 4 h digestion. Finally, the peptides were desalted using the C18 SPE column.

4D mass spectrometer

The tryptic peptides were dissolved in solvent A (0.1% formic acid, 2% acetonitrile/in water) and directly loaded onto a homemade reversed-phase analytical column (25 cm length, 75/100 μm inside diameter). Peptides were separated with a gradient from 6% to 24% solvent B (0.1% formic acid in acetonitrile) over 70 min, 24% to 35% in 14 min, and climbing to 80% in 3 min, then holding at 80% for the last 3 min, all at a constant flow rate of 450 nL/min on a nanoElute UHPLC system (Bruker Daltonics).

The peptides were subjected to a capillary source followed by the timsTOF Pro (Bruker Daltonics) mass spectrometry. The electrospray voltage applied was 1.60 kV. Precursors and fragments were analyzed at the TOF detector, with an MS/MS scan ranging from 100 to 1700 m/z. The timsTOF Pro was operated in parallel accumulation serial fragmentation (PASEF) mode. Precursors with charge states 0 to 5 were selected for fragmentation, and 10 PASEF-MS/MS scans were acquired per cycle. The dynamic exclusion was set to 30 s.

Database search

The resulting MS/MS data were processed using the MaxQuant search engine (v.1.6.15.0). Tandem mass spectra were searched against the mouse SwissProt database (17089 entries) concatenated with the reverse decoy database. Trypsin/P was specified as a cleavage enzyme allowing up to 2 missing cleavages. The mass tolerance for precursor ions was set as 20 ppm in the first search and 5 ppm in the main search, and the mass tolerance for fragment ions was set as 0.02 Da. Carbamidomethyl on Cys was specified as a fixed modification, and acetylation on protein N-terminal and oxidation on Met were specified as variable modifications. The false discovery rate was adjusted to < 1%. The data base is UniProt, the species-specific protein library is Mus_musculus_10090_SP_2021072. fasta. The proteomic analysis was performed by PTM Biolabs.

Principle component analysis

Principle component analysis (PCA) was conducted using R packages 'gmodels', 'ggplot2', and 'ggrepel'. The protein quantitative principal component (PC) analysis results of all samples were calculated. The degree of aggregation between samples in the figure represents the difference between samples.

Differentially expressed proteins analysis

The samples to be compared were selected, and the relative quantitative values of each protein in the repeated samples were taken as the difference multiple (fold change, FC). In order to judge the significance of the difference, the relative quantitative value of each protein in the samples of the comparison group was subjected to a *t*-test. The corresponding *P* value was calculated as the significance index. The default *P* value was < 0.05.

Gene Ontology enrichment analysis

Gene Ontology (GO) is used to express various properties of genes and gene products. GO annotations are divided into three categories: Biological Process, Cellular Component, and Molecular Function, which aim to explain the biological role of proteins from different perspectives. We performed differential protein enrichment analysis on a biological process in GO classification.

Kyoto Encyclopedia of Genes and Genomes pathway analysis

Kyoto Encyclopedia of Genes and Genomes (KEGG)[28] analysis was conducted using the 'clusterProfiler' package[29] of R software. A previously described method was used[30].

Cluster analysis

According to Fisher's exact test obtained by the enrichment analysis, the related functions in different comparison groups were clustered using the hierarchical clustering method, and heatmaps were drawn. In the heatmaps, the horizontal direction of the heatmap represents different comparison groups, and the vertical direction indicates related functions enriched by differentially expressed proteins in different comparison groups. The color patches corresponding to the functional description of the enrichment of the differentially expressed proteins in different comparison groups indicate the degree of enrichment. Red color represents strong enrichment, and blue represents weak enrichment.

Statistical analysis

All data are expressed as mean ± SD. The statistical analyses were conducted using SPSS version 18.0 software, and the differences in data among the groups were analyzed using the unpaired Student *t*-test of variance test. $P < 0.05$ (2-tailed) was considered to indicate a statistically significant difference.

RESULTS

P-407 and CAE were successfully used to develop the mouse model of HTGP

The exposure of mice to P-407 and CAE for 48 h resulted in much higher TC and TG in the P-407 (model for hyperlipidemia) and P-407 + CAE (model for HTGP) groups than in the Ctrl and CAE (model for AP) groups (Figure 1A). A slight rise in the AMY level was seen in the CAE group, whereas in the P-407 + CAE group, a significant increase in the AMY level was detected compared to other groups (all $P < 0.05$, Figure 1B). In addition, an increase in AST and ALT levels were seen in the CAE-treated groups, but there was no difference between CAE and P-407 + CAE-treated groups ($P > 0.05$, Figure 1C). There was no change in HOMA-IR among different groups ($P > 0.05$, Figure 1D). Furthermore, in the CAE group, a minor injury was seen in the pancreas and kidney, whereas in the P-407 + CAE group, serious injuries were observed in the pancreas, lung, and kidney, which were detected by HE staining (Figure 1E-G). Also, in the P-407 + CAE group, high levels of serum TNF-α, IL-1β, and IL-6 were detected (Figure 1H). These results proved that P-407 and CAE mice models were successful.

Proteome profiling predicts the role of ferroptosis in P-407 + CAE-induced HTGP rather than AP

Next, proteome sequencing was used to compare the mechanisms of HTGP and AP. Samples of the same group were clustered together from both PCA and clustering analyses (Figure 2A and B). The CAE treatment caused the rightward movement of samples along the PC1, explaining 56.0% of the total variance. The P-407 + CAE treatment upward along PC2 explained 17.5% of the total variance (Figure 2A). Additionally, 190 proteins were downregulated, whereas 272 proteins were upregulated in the pairwise comparisons (CAE *vs* WT). Furthermore, 43 proteins were downregulated and 125 were upregulated when comparing P-407 + CAE and CAE groups (Figure 2C and D). These results suggested that AP and HTGP exert different effects on the pancreas.

GO analyses further showed that the acute inflammatory response was highly enchased in the P-407 + CAE group *vs* CAE group; this difference, however, was not evident when comparing CAE *vs* WT groups, which also confirmed that P-407 + CAE induces more severe pancreas injury than CAE (Figure 2E). Furthermore, KEGG pathway analyses also showed that upregulated proteins were weakly enriched for ferroptosis in the CAE group *vs* WT group but also strongly enriched for ferroptosis in the P-407 + CAE group *vs* CAE group (Figure 2F). These results suggest that ferroptosis occurs specifically in P-407 + CAE-induced HTGP.

Verification of P-407 + CAE-induced ferroptosis in mice

To verify the results of proteome sequencing, we performed IHC staining of mouse pancreatic tissue. The SLC7A11 and GPX4 expression levels were significantly lower in the P-407 + CAE group than in the CAE group (all $P < 0.05$, Figure 3A and B). The MDA (Figure 3C) levels in the P-407 + CAE group were significantly higher than those in the CAE group ($P < 0.05$), while the GSH level in the P-407 + CAE group was significantly lower than that in CAE group ($P < 0.05$) (Figure 3D). The Fe^{2+} (Figure 3E) levels in the P-407 + CAE group were significantly higher than those in the CAE group ($P < 0.05$), too. This data indicates that P-407 + CAE induces ferroptosis in the pancreas of the mice.

HTGP can be attenuated through ferroptosis inhibition in mice

Since we had established that P-407 + CAE specifically induced ferroptosis in the pancreas of the mice, we further aimed to determine the role of ferroptosis in the regulation of HTGP. First, we used Fer-1 to inhibit ferroptosis[7,8]. The expression of GPX4 (Figure 4A) in the P-407 + CAE + Fer-1 group increased

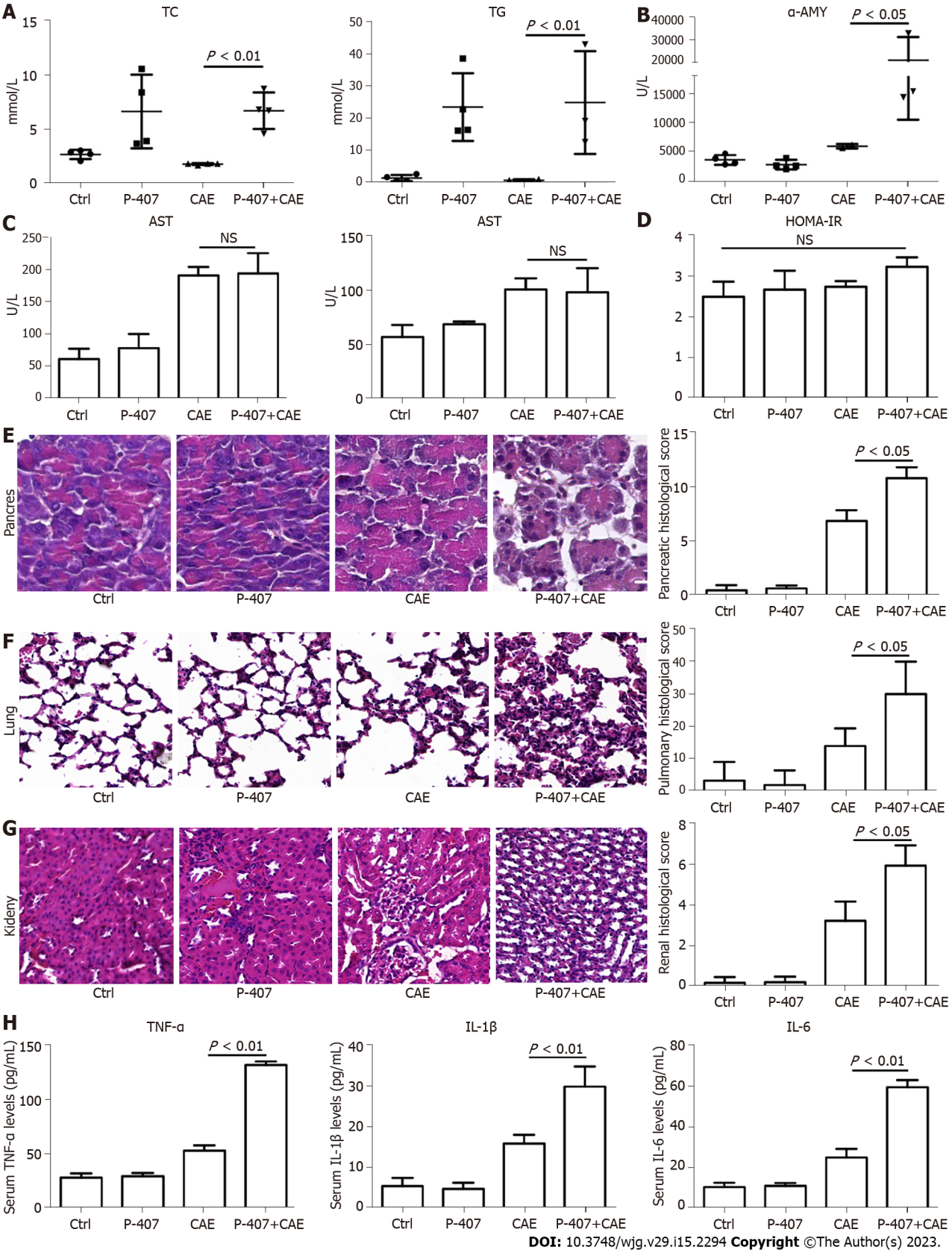

DOI: 10.3748/wjg.v29.i15.2294

Figure 1 P-407 and caerulein-induced hypertriglyceridemic pancreatitis in mice (*n* = 4). A: Serum total cholesterol and triglyceride levels; B: Serum amylase; C: Alanine aminotransferase and Alanine aminotransferase levels; D: Homeostasis model assessment insulin resistance index levels in mice exposed to P-407 and caerulein (CAE); E: Hematoxylin–eosin (HE) staining and histological scores of the pancreas; F: HE staining and histological scores of the lung; G: HE staining and histological scores of the kidney; H: Serum Tumor necrosis factor-α, interleukin (IL)-1β, and IL-6 levels after P-407 and CAE exposure. AST: Aspartate transaminase; ALT: Alanine aminotransferase; HOMA-IR: Homeostasis model assessment insulin resistance index; HE: Hematoxylin–eosin; CAE: Caerulein; AMY: Amylase; TNF: Tumor necrosis factor; IL: Interleukin; NS: Not significant.

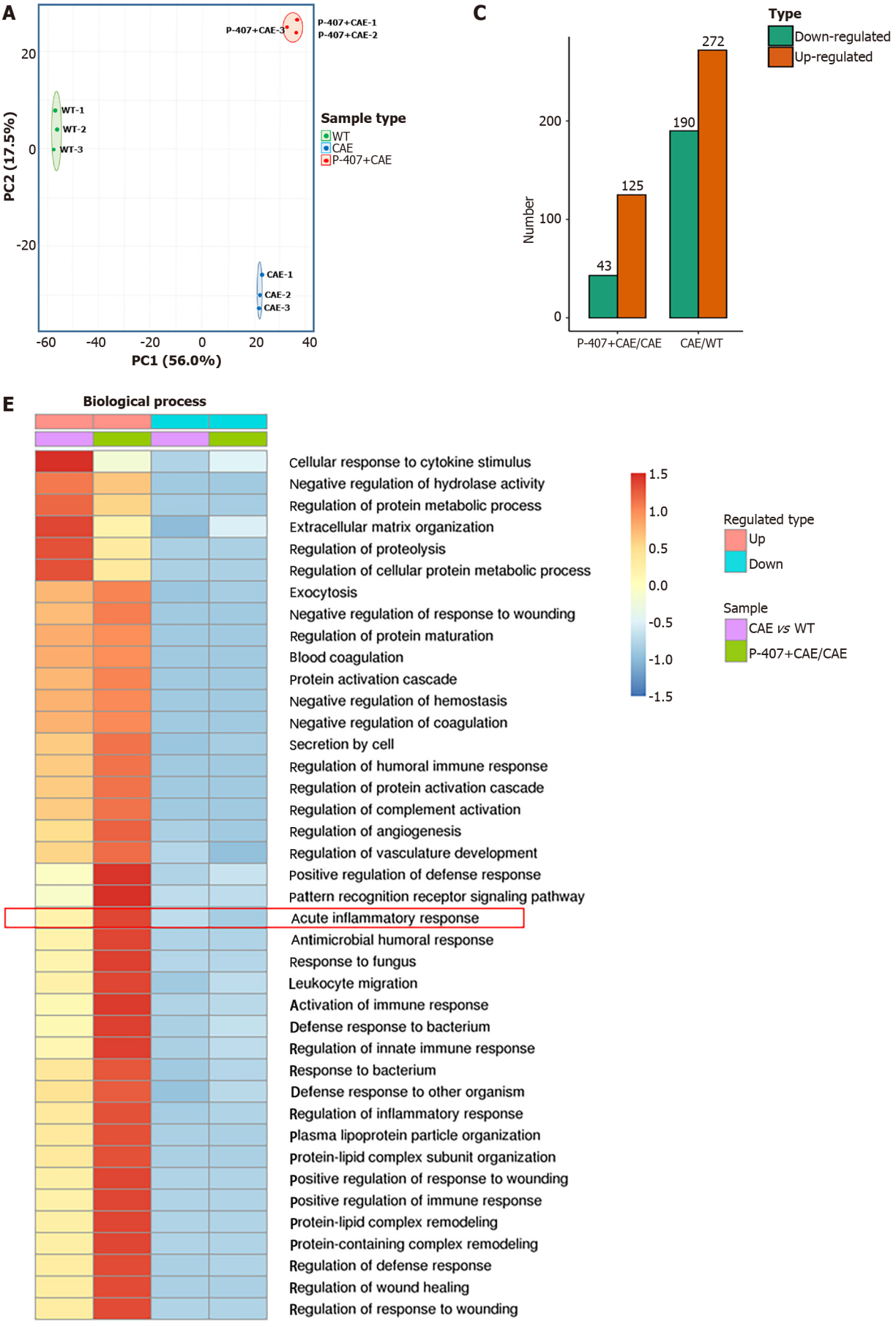
A
P-407+CAE-1
P-407+CAE-2
P-407+CAE-3
WT-1
WT-2
WT-3
CAE-1
CAE-2
CAE-3
Sample type
WT
CAE
P-407+CAE
PC2 (17.5%)
PC1 (56.0%)
C
Type
Down-regulated
Up-regulated
Number
43
125
190
272
P-407+CAE/CAE
CAE/WT
E
Biological process
Cellular response to cytokine stimulus
Negative regulation of hydrolase activity
Regulation of protein metabolic process
Extracellular matrix organization
Regulation of proteolysis
Regulation of cellular protein metabolic process
Exocytosis
Negative regulation of response to wounding
Regulation of protein maturation
Blood coagulation
Protein activation cascade
Negative regulation of hemostasis
Negative regulation of coagulation
Secretion by cell
Regulation of humoral immune response
Regulation of protein activation cascade
Regulation of complement activation
Regulation of angiogenesis
Regulation of vasculature development
Positive regulation of defense response
Pattern recognition receptor signaling pathway
Acute inflammatory response
Antimicrobial humoral response
Response to fungus
Leukocyte migration
Activation of immune response
Defense response to bacterium
Regulation of innate immune response
Response to bacterium
Defense response to other organism
Regulation of inflammatory response
Plasma lipoprotein particle organization
Protein-lipid complex subunit organization
Positive regulation of response to wounding
Positive regulation of immune response
Protein-lipid complex remodeling
Protein-containing complex remodeling
Regulation of defense response
Regulation of wound healing
Regulation of response to wounding
Regulated type
Up
Down
Sample
CAE *vs* WT
P-407+CAE/CAE

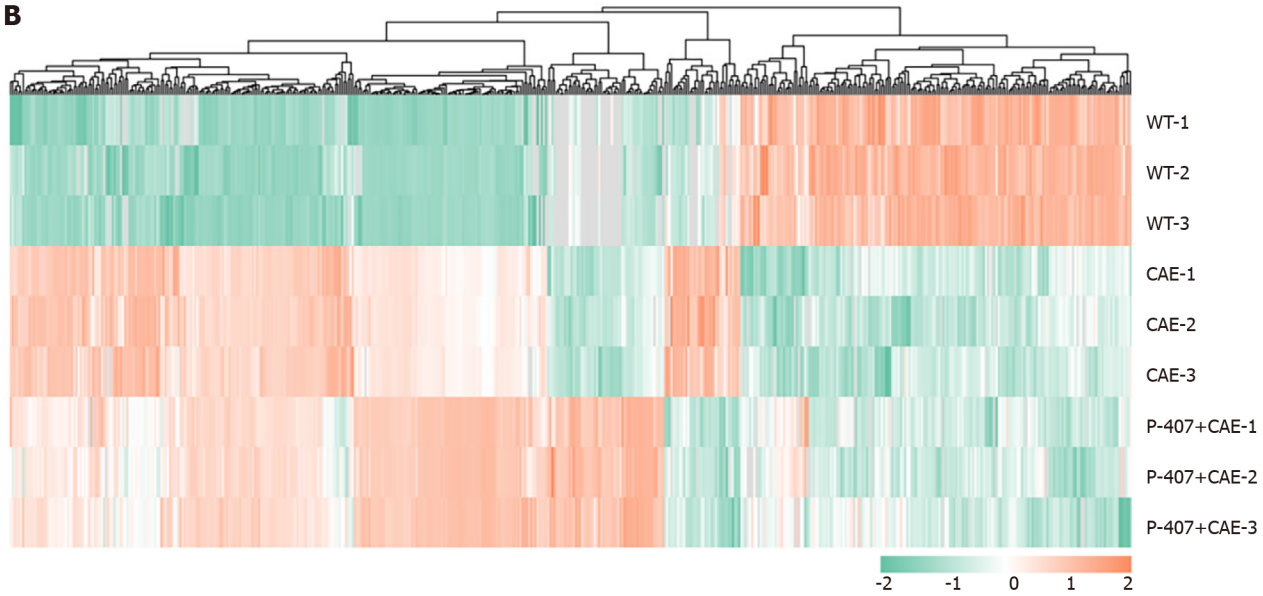
B
WT-1
WT-2
WT-3
CAE-1
CAE-2
CAE-3
P-407+CAE-1
P-407+CAE-2
P-407+CAE-3
-2
-1
0
1
2

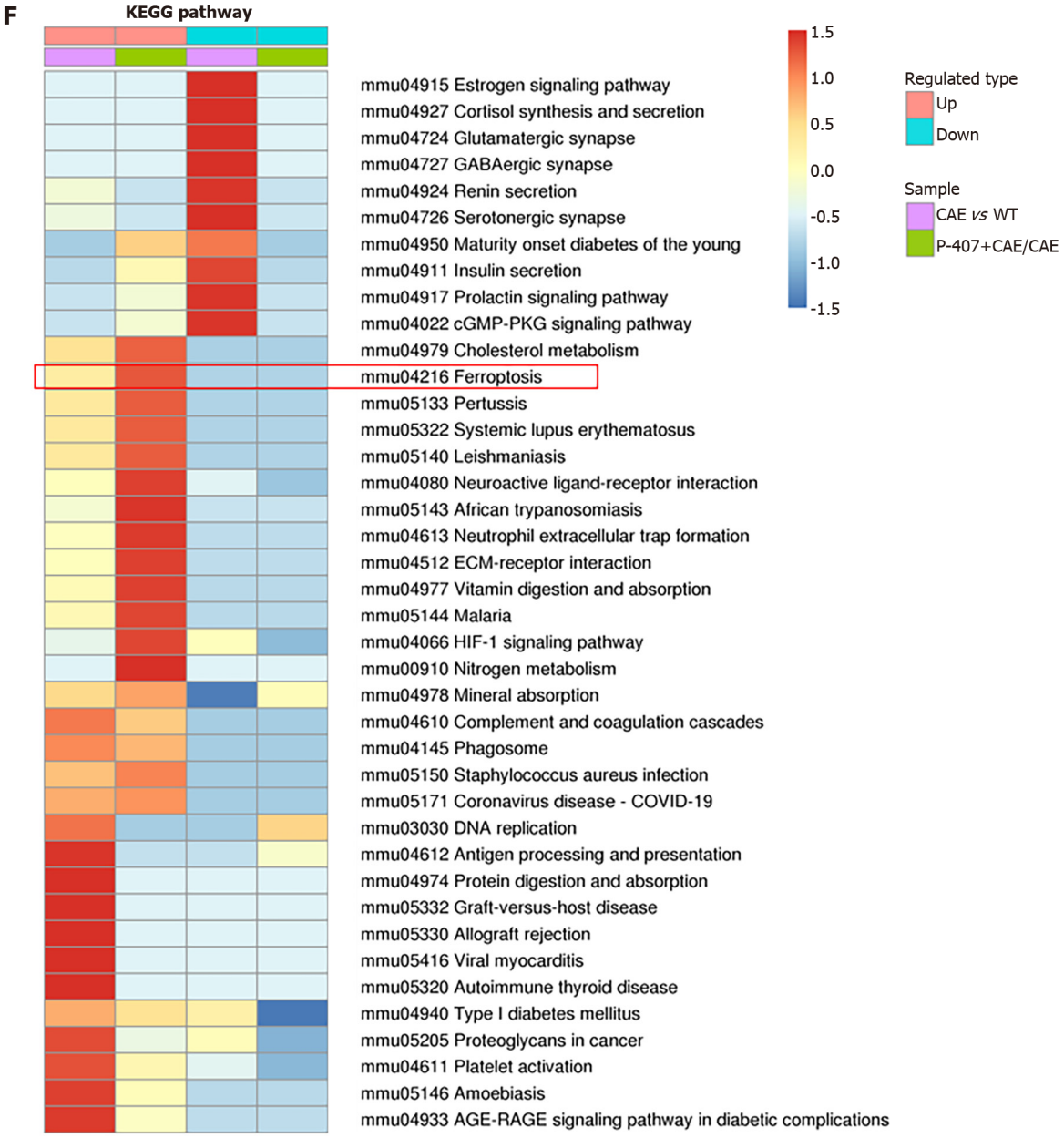
F
KEGG pathway
mmu04915 Estrogen signaling pathway
mmu04927 Cortisol synthesis and secretion
mmu04724 Glutamatergic synapse
mmu04727 GABAergic synapse
mmu04924 Renin secretion
mmu04726 Serotonergic synapse
mmu04950 Maturity onset diabetes of the young
mmu04911 Insulin secretion
mmu04917 Prolactin signaling pathway
mmu04022 cGMP-PKG signaling pathway
mmu04979 Cholesterol metabolism
mmu04216 Ferroptosis
mmu05133 Pertussis
mmu05322 Systemic lupus erythematosus
mmu05140 Leishmaniasis
mmu04080 Neuroactive ligand-receptor interaction
mmu05143 African trypanosomiasis
mmu04613 Neutrophil extracellular trap formation
mmu04512 ECM-receptor interaction
mmu04977 Vitamin digestion and absorption
mmu05144 Malaria
mmu04066 HIF-1 signaling pathway
mmu00910 Nitrogen metabolism
mmu04978 Mineral absorption
mmu04610 Complement and coagulation cascades
mmu04145 Phagosome
mmu05150 Staphylococcus aureus infection
mmu05171 Coronavirus disease - COVID-19
mmu03030 DNA replication
mmu04612 Antigen processing and presentation
mmu04974 Protein digestion and absorption
mmu05332 Graft-versus-host disease
mmu05330 Allograft rejection
mmu05416 Viral myocarditis
mmu05320 Autoimmune thyroid disease
mmu04940 Type I diabetes mellitus
mmu05205 Proteoglycans in cancer
mmu04611 Platelet activation
mmu05146 Amoebiasis
mmu04933 AGE-RAGE signaling pathway in diabetic complications
1.5
1.0
0.5
0.0
-0.5
-1.0
-1.5
Regulated type
Up
Down
Sample
CAE *vs* WT
P-407+CAE/CAE

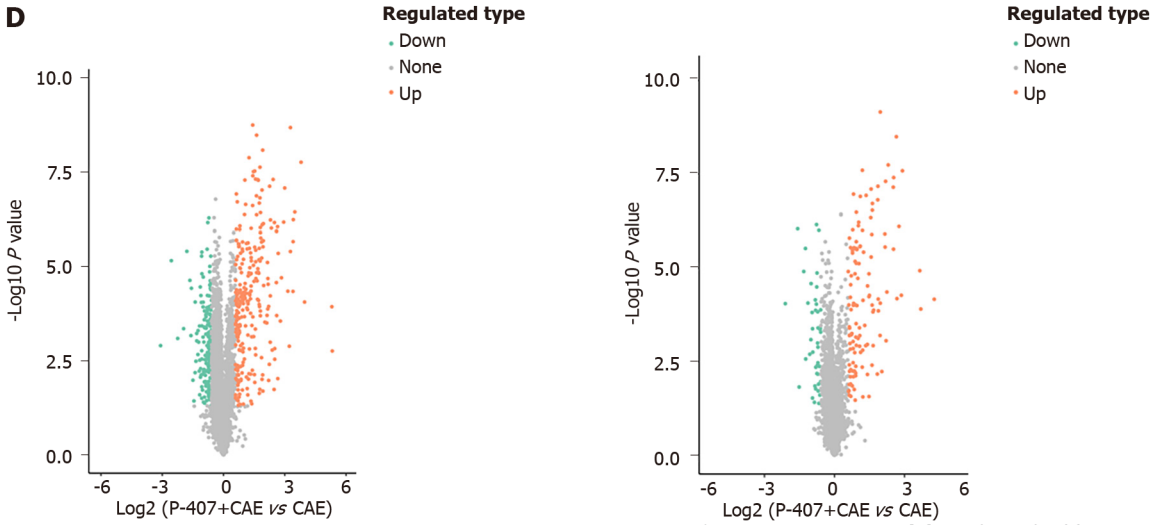

DOI: 10.3748/wjg.v29.i15.2294 **Copyright** ©The Author(s) 2023.

Figure 2 Effects of P-407 and caerulein on the pancreas revealed by proteome sequencing (*n* = 3). A: Principal component analysis; B: Heatmap showing relationships among different sample groups; C: Exhibition of changed protein numbers among the sample groups; D: Volcano plots showing proteins differentially expressed between sample groups; E: Biological process; F: Kyoto Encyclopedia of Genes and Genomes pathways enriched with proteins differentially expressed in pair-wise comparisons of 'CAE group' *vs* WT group'' and 'P-407 + CAE group' *vs* CAE group'. CAE: Caerulein; WT: Wide type; PC: Principal component.

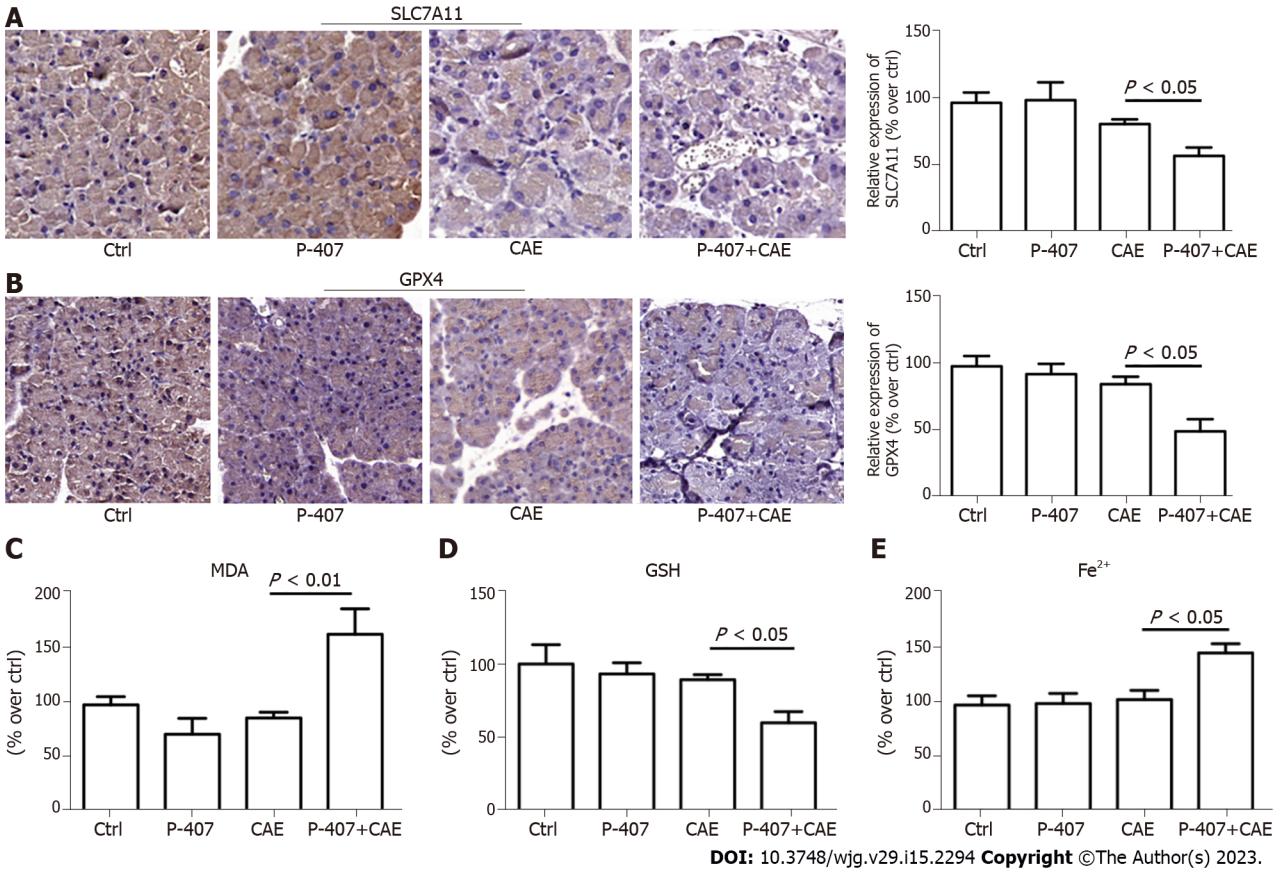

DOI: 10.3748/wjg.v29.i15.2294 **Copyright** ©The Author(s) 2023.

Figure 3 P-407 + Caerulein-induced pancreas ferroptosis in mice as established by immunohistochemistry (*n* = 4). A: Solute carrier family 7 member 11 in the pancreas tissues of the P-407 + Caerulein (CAE) group; B: Glutathione peroxidase 4 in the pancreas tissues of the P-407 + CAE group. The scale bar represents 50 mm; C: Malonaldehyde levels; D: Glutathione levels; E: Fe^{2+} levels in the pancreases of the mice in the P-407 + CAE group. CAE: Caerulein; SLC7A11: Solute carrier family 7 member 11; MDA: Malonaldehyde; GSH: Glutathione; GPX4: Glutathione peroxidase 4.

compared to P-407 + CAE group, while the MDA (Figure 4B) decreased to their normal range (all $P < 0.05$). The GSH level (Figure 4C) in the P-407 + CAE + Fer-1 group increased compared to P-407 + CAE group, while the Fe^{2+} (Figure 4D) decreased to their normal range (all $P < 0.05$). The histological scores of the pancreas, lung, and kidney in the P-407 + CAE + Fer-1 group were lower than those in the P-407 + CAE group (Figure 4E-G). The serum TNF-α, IL-1β, and IL-6 Levels in the P-407 + CAE + Fer-1 group were also lower than those in the P-407 + CAE group (all $P < 0.05$, Figure 4H). These results indicate that the inhibition of ferroptosis can attenuate the inflammatory response in mice with HTGP.

Inhibition of NADPH oxidase 2 can attenuate the inflammatory response in mice with HTGP through ferroptosis suppression

KEGG pathway analyses revealed overexpression of NADPH oxidase (NOX)2 in the enriched ferroptosis pathway in the P-407 + CAE group compared to the CAE group (Figure 5A and B). Next, we determined the role of NOX2 in regulating ferroptosis using Vas, an inhibitor of NOX2[7]. The expression of NOX2 was higher in the P-407 + CAE group than in the Ctrl group, while Vas significantly decreased the NOX2 expression level ($P < 0.05$, Figure 5C). In addition, MDA (Figure 5D) level decreased, GSH level increased (Figure 5E), Fe^{2+} (Figure 5F) level decreased and expression of GPX4 (Figure 5G) rebounded in the P-407 + CAE + Vas group compared to those in the P-407 + CAE group ($P < 0.05$). The histological scores of the pancreas, lung, and kidney in the P-407 + CAE + Vas group were lower than those in the P-407 + CAE group (all $P < 0.05$, Figure 5H-J). The serum TNF-α, IL-1β, and IL-6 Levels in the P-407 + CAE + Vas group were also lower than those in the P-407 + CAE group (all $P < 0.05$, Figure 5K). These results indicate that inhibition of NOX2 can attenuate the inflammatory response in mice with HTGP through attenuation of ferroptosis.

DISCUSSION

The early phase of HTGP is generally believed to be an unregulated inflammatory response or a cytokine storm that results in organ damage and death[31,32]. Pro-inflammatory cytokines, such as TNF-α, IL-6, and IL-1β, are considered pivotal mediators for initiating, amplifying, and perpetuating organ injury[33-35]. Therefore, timely blocking of the inflammatory response is considered critical for successful treatment.

As iron-dependent oxidative stress and lipid peroxidation are common features of ferroptosis and inflammatory diseases, ferroptosis, as a recognized form of RCD, has been reported to participate in the progression of inflammations[36]. Yet, its relationship with HTGP remains unclear. In the process of HTGP, abnormal lipid metabolism is also considered to have an important role, and FFA has been shown to induce the excessive release of ROS and accumulate in the body[4,5]. Previous studies have shown that the excessive production of ROS is a key factor for ferroptosis induction[22]. Therefore, we hypothesized that ferroptosis might also participate in the process of HTGP.

In this study, we found for the first time that ferroptosis has an important role in the process of HTGP, and its inhibition can attenuate the inflammatory response and improve prognosis in mice. To investigate these mechanisms, we induced a mouse model of HTGP by intraperitoneal injection of P-407 and CAE. Then, proteome sequencing predicted that ferroptosis is involved in the process of HTGP. To verify the results of proteome sequencing, we performed IHC staining of mouse pancreatic tissue. GSH, SLC7A11, and GPX4 expression levels were much lower in the P-407 + CAE group than in the AP group. Additionally, the MDA and Fe^{2+} level in the P-407 + CAE group was significantly higher than in the AP group. To further verify whether ferroptosis has a key role in regulating HTGP, we used Fer-1 to inhibit ferroptosis. The histological scores of pancreas and serum TNF-α, IL-1β, and IL-6 Levels in the P-407 + CAE + Fer-1 group were all significantly lower than those in the P-407 + CAE group.

Ma *et al*[21] found that the inhibition of ferroptosis attenuated acute kidney injury in rats with severe AP (SAP), suggesting that ferroptosis may participate in SAP, but there was no distinction between the types of SAP[21]. Furthermore, our KEGG pathway analyses revealed that the upregulated proteins were strongly enriched for ferroptosis in the P-407 + CAE group compared to the CAE group, implying that ferroptosis occurs specifically in the P-407 + CAE group. Based on this finding, we speculate that in the process of HTGP, abnormal lipid metabolism produces excessive ROS, which induces ferroptosis and aggravates damage to the pancreas and other organs.

NOX is a ROS-generating transmembrane flavoprotein enzyme that is widely distributed in pancreas and kidney tissues[37,38]. Studies have shown that excessive ROS produced by NOX can activate the NF-κB pathway, aggravate cell death, and regulate inflammation[39]. Yang *et al*[40] suggested that NOX could have an important role in HTGP-associated kidney injury through the Akt/GSK-3β pathway[40]. Moreover, Wang *et al*[41] found that NOX2 is activated in an AMPK-dependent manner to promote oxidative stress in a diabetic rat model, which in turn led to ferroptosis and aggravated myocardial ischemia-reperfusion injury[41]. Our KEGG pathway analyses also revealed overexpression of NOX2 in the enriched ferroptosis pathway in in the P-407 + CAE group compared to the CAE group. Next, we verified whether NOX2 has a key role in the regulation of ferroptosis using Vas, an inhibitor of NOX2. We found that the serum MDA level decreased, and the expression of GPX4 in the P-407 + CAE + Vas

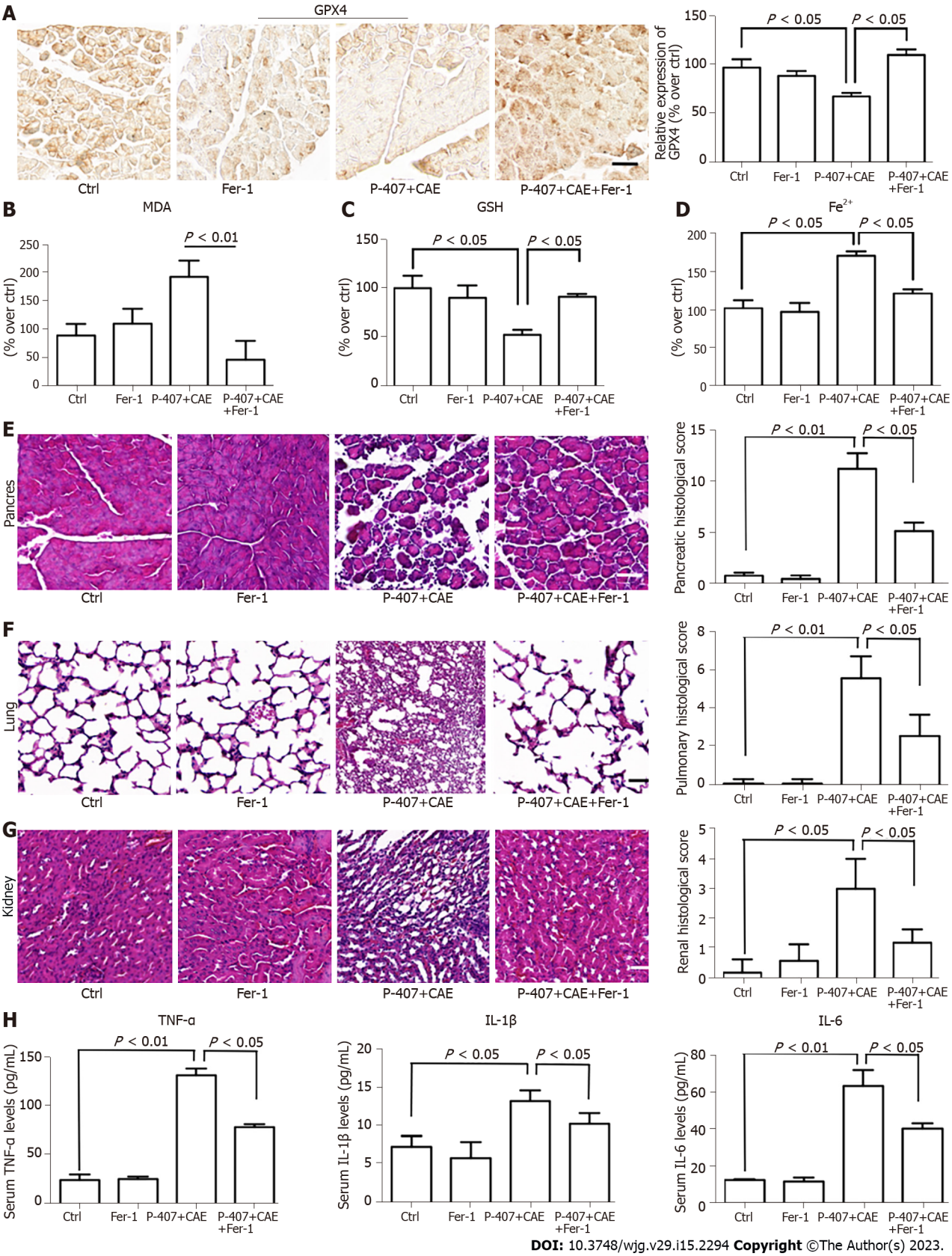

DOI: 10.3748/wjg.v29.i15.2294

Figure 4 The inhibition of ferroptosis attenuated P-407 + Caerulein-induced hypertriglyceridemic pancreatitis in mice (*n* = 4). A: Immunohistochemistry for Glutathione peroxidase 4 in the pancreas tissues of the P-407 + Caerulein (CAE) and P-407 + CAE + Ferrostatin-1 (Fer-1) groups; B: The malonaldehyde levels; C: The glutathione levels; D: Fe^{2+} levels in pancreases of P-407 + CAE and P-407 + CAE + Fer-1 groups; E: Hematoxylin–eosin (HE) staining and histological scores of the pancreas; F: HE staining and histological scores of the lung; G: HE staining and histological scores of the kidney; H: Serum tumor necrosis factor-α, interleukin (IL)-1β, and IL-6 levels of the P-407 + CAE and P-407 + CAE + Fer-1 groups. NOX: NADPH oxidase; ROS: Reactive oxygen species; CAE: Caerulein; MDA: Malonaldehyde; Fer-1: Ferrostatin-1; GSH: Glutathione; GPX4: Glutathione peroxidase 4; TNF: Tumor necrosis factor; IL: Interleukin.

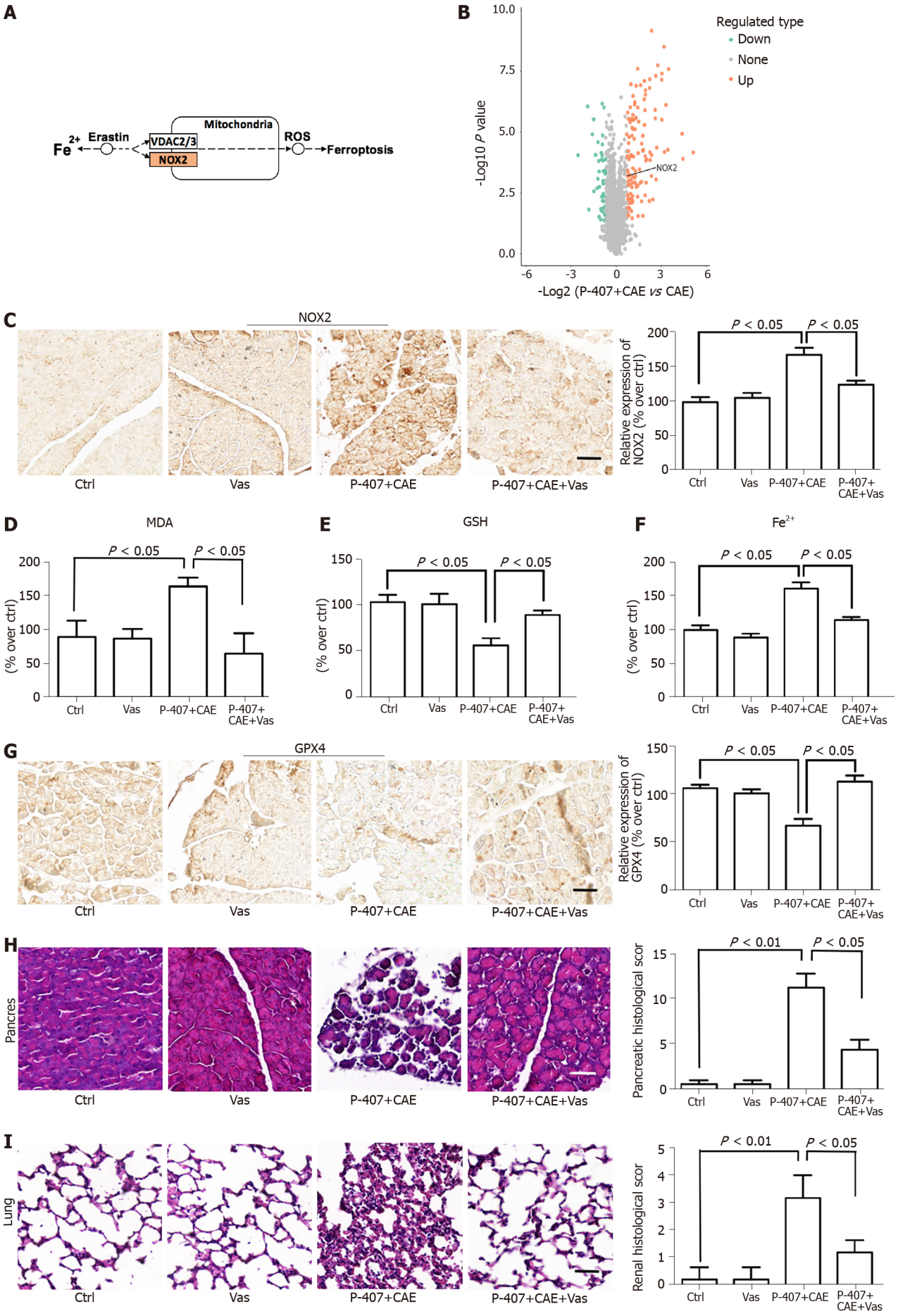
A
Fe 2+
Erastin
Mitochondria
VDAC2/3
NOX2
ROS
Ferroptosis
B
Regulated type
Down
None
Up
-Log10 P value
-Log2 (P-407+CAE vs CAE)
NOX2
C
NOX2
Ctrl
Vas
P-407+CAE
P-407+CAE+Vas
Relative expression of NOX2 (% over ctrl)
P < 0.05
P < 0.05
D
MDA
(% over ctrl)
E
GSH
F
Fe2+
G
GPX4
Relative expression of GPX4 (% over ctrl)
H
Pancres
Pancreatic histological scor
P < 0.01
P < 0.05
I
Lung
Renal histological scor

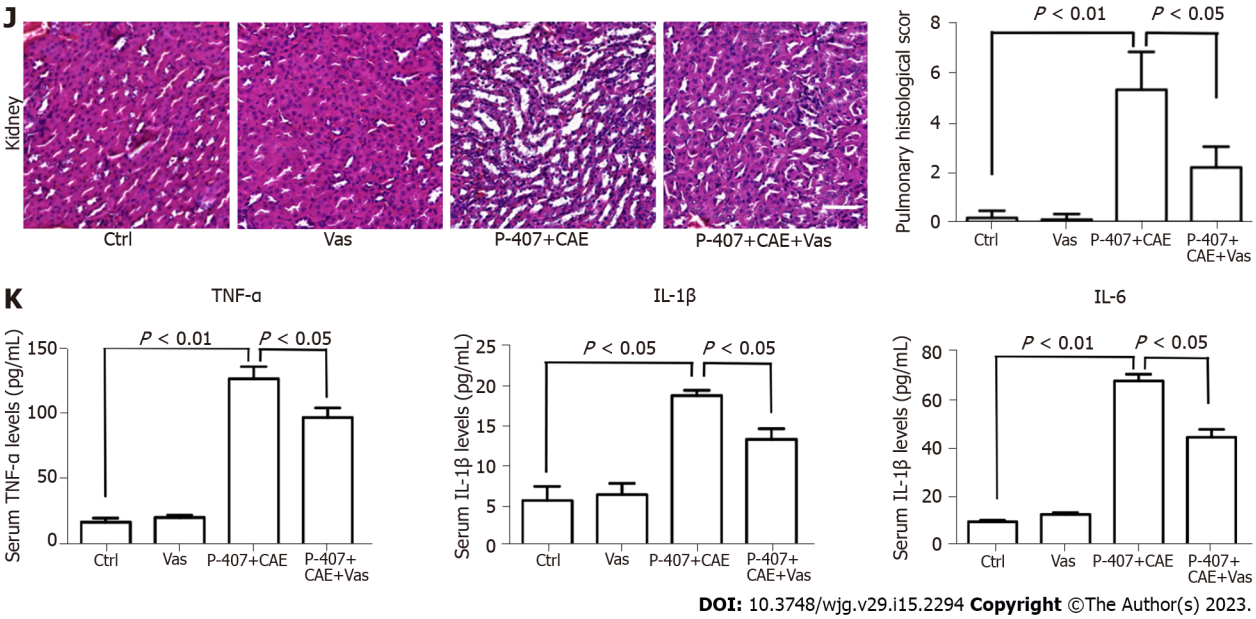

DOI: 10.3748/wjg.v29.i15.2294

Figure 5 The inhibition of NADPH oxidase 2 attenuated hypertriglyceridemic pancreatitis through a ferroptosis reduction in mice (*n* = 4). A: Kyoto Encyclopedia of Genes and Genomes pathways enriched with protein NADPH oxidase (NOX) 2 in comparison of P-407 + caerulein (CAE) group *vs* CAE group; B: Volcano plot showing the location of NOX2 in comparison of P-407 + CAE group *vs* CAE group; C: Immunohistochemistry (IHC) for NOX2 in the pancreas tissues of the P-407 + CAE and P-407 + CAE + Vas2870 (Vas) groups; D: The malonaldehyde levels; E: The glutathione levels; F: Fe^{2+} levels in the pancreases of the mice in the P-407 + CAE and P-407 + CAE + Vas groups; G: IHC for GPX4 in the pancreas tissues of the P-407 + CAE and P-407 + CAE + Vas groups; H: Hematoxylin–eosin (HE) staining and histological scores of the pancreas; I: HE staining and histological scores of the lung; J: HE staining and histological scores of the kidney; K: Serum TNF-α, IL-1β, and IL-6 levels of the P-407 + CAE and P-407 + CAE + Vas groups. The scale bar represents 50 mm. NOX: NADPH oxidase; ROS: Reactive oxygen species; CAE: Caerulein; Vas: Vas2870; MDA: Malonaldehyde; GSH: Glutathione; GPX4: Glutathione peroxidase 4; TNF: Tumor necrosis factor; IL: Interleukin.

group rebounded compared to the P-407 + CAE group. Meanwhile, the histological scores of the pancreas and the serum TNF-α, IL-1β, and IL-6 Levels in the P-407 + CAE + Vas group were significantly lower than those in the P-407 + CAE group. These results indicate that the inhibition of NOX2 attenuated HTGP through suppression of ferroptosis.

CONCLUSION

In summary, these data provide strong evidence that ferroptosis is involved in the process of HTGP and that NOX2 is a key point in the regulation of ferroptosis. The inhibition of ferroptosis and NOX2 attenuates the inflammatory response to improve patient outcomes. This discovery provides new insights into a better understanding of the pathogenesis of HTGP, which may be used as a novel therapeutic target in the future.

ARTICLE HIGHLIGHTS

Research background

Ferroptosis is involved in the development of inflammatory diseases, but its relationship with acute hypertriglyceridemic pancreatitis (HTGP) remains unclear.

Research motivation

HTGP has serious morbidity and high mortality. At present, there is no more effective method except symptomatic treatment. Therefore, exploring the pathogenesis of HTGP and seeking more accurate therapeutic targets are of critical importance.

Research objectives

This study aimed to explore whether ferroptosis is involved in the process of HTGP and elucidate its potential mechanisms in a mouse model.

Research methods

Pancreatic tissues from the model animals were subjected to proteome sequencing analysis. The pathological changes and scores of the pancreas, lung, and kidney were determined using hematoxylin–eosin staining. The levels of serum amylase, triglyceride, and total cholesterol were measured with an automatic blood cell analyzer. Additionally, the serum levels of tumor necrosis factor-α, interleukin (IL)-6, and IL-1β were determined by enzyme linked immunosorbent assay. Malonaldehyde, glutathione, and Fe^{2+} were detected in the pancreas. Finally, immunohistochemistry was performed to assess the expression of ferroptosis-related proteins.

Research results

Proteome sequencing revealed that ferroptosis was involved in the process of HTGP and that NADPH oxidase 2 may participate in ferroptosis regulation.

Research conclusions

Ferroptosis was found to have an important role in HTGP and may be considered a potential target for clinical treatment.

Research perspectives

This discovery provides new insights into a better understanding of the pathogenesis of HTGP, which may be used as a novel therapeutic target. However, the regulatory mechanism needs to be further explored in the future.

FOOTNOTES

Author contributions: Meng YT, Zhou Y, Han PY, and Ren HB designed the study; Meng YT, Zhou Y and Han PY participated in data collection and wrote the paper; Ren HB and Han PY were responsible for revising the manuscript, contributing the same to the paper; All the listed authors have contributed and approved the final manuscript.

Supported by the National Natural Science Foundation of Shandong Province, No. ZR2021MH032.

Institutional animal care and use committee statement: This study was approved by the Ethics Committee of Scientific Research of Jinan University Application for Laboratory Animal Ethical Review, No. 20210303-06.

Conflict-of-interest statement: All the authors report no relevant conflicts of interest for this article.

Data sharing statement: No additional data are available.

Country/Territory of origin: China

ORCID number: Yi-Teng Meng 0000-0002-0413-9048; Pei-Yu Han 0000-0002-8753-2426; Hong-Bo Ren 0000-0002-7667-535X.

S-Editor: Li L
L-Editor: A
P-Editor: Yu HG

REFERENCES

1 **Yang AL**, McNabb-Baltar J. Hypertriglyceridemia and acute pancreatitis. *Pancreatology* 2020; **20**: 795-800 [PMID: 32571534 DOI: 10.1016/j.pan.2020.06.005]

2 **Jin M**, Bai X, Chen X, Zhang H, Lu B, Li Y, Lai Y, Qian J, Yang H. A 16-year trend of etiology in acute pancreatitis: The increasing proportion of hypertriglyceridemia-associated acute pancreatitis and its adverse effect on prognosis. *J Clin Lipidol* 2019; **13**: 947-953.e1 [PMID: 31735687 DOI: 10.1016/j.jacl.2019.09.005]

3 **Yin G**, Cang X, Yu G, Hu G, Ni J, Xiong J, Hu Y, Xing M, Chen C, Huang Y, Tang M, Zhao Y, Cheng G, Wan R, Wang S, Wang X. Different Clinical Presentations of Hyperlipidemic Acute Pancreatitis: A Retrospective Study. *Pancreas* 2015; **44**: 1105-1110 [PMID: 26348469 DOI: 10.1097/MPA.0000000000000403]

4 **Guo YY**, Li HX, Zhang Y, He WH. Hypertriglyceridemia-induced acute pancreatitis: progress on disease mechanisms and treatment modalities. *Discov Med* 2019; **27**: 101-109 [PMID: 30939294 DOI: 10.5114/pg.2014.45412]

5 **Wan J**, He W, Zhu Y, Zeng H, Liu P, Xia L, Lu N. Stratified analysis and clinical significance of elevated serum triglyceride levels in early acute pancreatitis: a retrospective study. *Lipids Health Dis* 2017; **16**: 124 [PMID: 28655321 DOI: 10.1186/s12944-017-0517-3]

6 **Schönfeld P**, Wieckowski MR, Lebiedzińska M, Wojtczak L. Mitochondrial fatty acid oxidation and oxidative stress: lack of reverse electron transfer-associated production of reactive oxygen species. *Biochim Biophys Acta* 2010; **1797**: 929-938 [PMID: 20085746 DOI: 10.1016/j.bbabio.2010.01.010]

7 **Criddle DN**, Murphy J, Fistetto G, Barrow S, Tepikin AV, Neoptolemos JP, Sutton R, Petersen OH. Fatty acid ethyl esters cause pancreatic calcium toxicity *via* inositol trisphosphate receptors and loss of ATP synthesis. *Gastroenterology* 2006; **130**: 781-793 [PMID: 16530519 DOI: 10.1053/j.gastro.2005.12.031]

8 **Maléth J**, Rakonczay Z Jr, Venglovecz V, Dolman NJ, Hegyi P. Central role of mitochondrial injury in the pathogenesis of acute pancreatitis. *Acta Physiol (Oxf)* 2013; **207**: 226-235 [PMID: 23167280 DOI: 10.1111/apha.12037]

9 **Rawla P**, Sunkara T, Thandra KC, Gaduputi V. Hypertriglyceridemia-induced pancreatitis: updated review of current treatment and preventive strategies. *Clin J Gastroenterol* 2018; **11**: 441-448 [PMID: 29923163 DOI: 10.1007/s12328-018-0881-1]

10 **Tan JH**, Cao RC, Zhou L, Zhou ZT, Chen HJ, Xu J, Chen XM, Jin YC, Lin JY, Qi ZC, Zeng JL, Li SJ, Luo M, Hu GD, Jin J, Zhang GW. EMC6 regulates acinar apoptosis *via* APAF1 in acute and chronic pancreatitis. *Cell Death Dis* 2020; **11**: 966 [PMID: 33177505 DOI: 10.1038/s41419-020-03177-3]

11 **Tang GX**, Yang MS, Xiang KM, Yang BC, Liu ZL, Zhao SP. MiR-20b-5p modulates inflammation, apoptosis and angiogenesis in severe acute pancreatitis through autophagy by targeting AKT3. *Autoimmunity* 2021; **54**: 460-470 [PMID: 34402705 DOI: 10.1080/08916934.2021.1953484]

12 **Gukovskaya AS**, Gukovsky I, Algül H, Habtezion A. Autophagy, Inflammation, and Immune Dysfunction in the Pathogenesis of Pancreatitis. *Gastroenterology* 2017; **153**: 1212-1226 [PMID: 28918190 DOI: 10.1053/j.gastro.2017.08.071]

13 **Dixon SJ**, Lemberg KM, Lamprecht MR, Skouta R, Zaitsev EM, Gleason CE, Patel DN, Bauer AJ, Cantley AM, Yang WS, Morrison B 3rd, Stockwell BR. Ferroptosis: an iron-dependent form of nonapoptotic cell death. *Cell* 2012; **149**: 1060-1072 [PMID: 22632970 DOI: 10.1016/j.cell.2012.03.042]

14 **Yang WS**, SriRamaratnam R, Welsch ME, Shimada K, Skouta R, Viswanathan VS, Cheah JH, Clemons PA, Shamji AF, Clish CB, Brown LM, Girotti AW, Cornish VW, Schreiber SL, Stockwell BR. Regulation of ferroptotic cancer cell death by GPX4. *Cell* 2014; **156**: 317-331 [PMID: 24439385 DOI: 10.1016/j.cell.2013.12.010]

15 **Doll S**, Proneth B, Tyurina YY, Panzilius E, Kobayashi S, Ingold I, Irmler M, Beckers J, Aichler M, Walch A, Prokisch H, Trümbach D, Mao G, Qu F, Bayir H, Füllekrug J, Scheel CH, Wurst W, Schick JA, Kagan VE, Angeli JP, Conrad M. ACSL4 dictates ferroptosis sensitivity by shaping cellular lipid composition. *Nat Chem Biol* 2017; **13**: 91-98 [PMID: 27842070 DOI: 10.1038/nchembio.2239]

16 **Black FO**. Response to Stockwell CW. Vestibular testing: Past, present, future. Br J Audiol 1997; 31: 387-398. *Br J Audiol* 1998; **32**: 255-257 [PMID: 9923988 DOI: 10.3109/03005364000000073]

17 **Lachaier E**, Louandre C, Godin C, Saidak Z, Baert M, Diouf M, Chauffert B, Galmiche A. Sorafenib induces ferroptosis in human cancer cell lines originating from different solid tumors. *Anticancer Res* 2014; **34**: 6417-6422 [PMID: 25368241]

18 **Masaldan S**, Bush AI, Devos D, Rolland AS, Moreau C. Striking while the iron is hot: Iron metabolism and ferroptosis in neurodegeneration. *Free Radic Biol Med* 2019; **133**: 221-233 [PMID: 30266679 DOI: 10.1016/j.freeradbiomed.2018.09.033]

19 **Tuo QZ**, Lei P, Jackman KA, Li XL, Xiong H, Liuyang ZY, Roisman L, Zhang ST, Ayton S, Wang Q, Crouch PJ, Ganio K, Wang XC, Pei L, Adlard PA, Lu YM, Cappai R, Wang JZ, Liu R, Bush AI. Tau-mediated iron export prevents ferroptotic damage after ischemic stroke. *Mol Psychiatry* 2017; **22**: 1520-1530 [PMID: 28886009 DOI: 10.1038/mp.2017.171]

20 **Fang X**, Ardehali H, Min J, Wang F. The molecular and metabolic landscape of iron and ferroptosis in cardiovascular disease. *Nat Rev Cardiol* 2023; **20**: 7-23 [PMID: 35788564 DOI: 10.1038/s41569-022-00735-4]

21 **Ma D**, Li C, Jiang P, Jiang Y, Wang J, Zhang D. Inhibition of Ferroptosis Attenuates Acute Kidney Injury in Rats with Severe Acute Pancreatitis. *Dig Dis Sci* 2021; **66**: 483-492 [PMID: 32219613 DOI: 10.1007/s10620-020-06225-2]

22 **Imai H**, Matsuoka M, Kumagai T, Sakamoto T, Koumura T. Lipid Peroxidation-Dependent Cell Death Regulated by GPx4 and Ferroptosis. *Curr Top Microbiol Immunol* 2017; **403**: 143-170 [PMID: 28204974 DOI: 10.1007/82_2016_508]

23 **Dai J**, Jiang M, Hu Y, Xiao J, Hu B, Xu J, Han X, Shen S, Li B, Wu Z, He Y, Ren Y, Wen L, Wang X, Hu G. Dysregulated SREBP1c/miR-153 signaling induced by hypertriglyceridemia worsens acute pancreatitis and delays tissue repair. *JCI Insight* 2021; **6** [PMID: 33491670 DOI: 10.1172/jci.insight.138584]

24 **Silva-Vaz P**, Abrantes AM, Castelo-Branco M, Gouveia A, Botelho MF, Tralhão JG. Murine Models of Acute Pancreatitis: A Critical Appraisal of Clinical Relevance. *Int J Mol Sci* 2019; **20** [PMID: 31181644 DOI: 10.3390/ijms20112794]

25 **Schmidt J**, Rattner DW, Lewandrowski K, Compton CC, Mandavilli U, Knoefel WT, Warshaw AL. A better model of acute pancreatitis for evaluating therapy. *Ann Surg* 1992; **215**: 44-56 [PMID: 1731649 DOI: 10.1097/00000658-199201000-00007]

26 **Matute-Bello G**, Winn RK, Jonas M, Chi EY, Martin TR, Liles WC. Fas (CD95) induces alveolar epithelial cell apoptosis in vivo: implications for acute pulmonary inflammation. *Am J Pathol* 2001; **158**: 153-161 [PMID: 11141488 DOI: 10.1016/s0002-9440(10)63953-3]

27 **Wu C**, Zou L, Shi S, Tong Z, Shen X, Yang D, Ke L, Li W, Li J. The role of hypertriglyceridemia for acute kidney injury in the course of acute pancreatitis and an animal model. *Pancreatology* 2017; **17**: 561-566 [PMID: 28647101 DOI: 10.1016/j.pan.2017.06.006]

28 **Kanehisa M**, Goto S. KEGG: kyoto encyclopedia of genes and genomes. *Nucleic Acids Res* 2000; **28**: 27-30 [PMID: 10592173 DOI: 10.1093/nar/28.1.27]

29 **Yu G**, Wang LG, Han Y, He QY. clusterProfiler: an R package for comparing biological themes among gene clusters. *OMICS* 2012; **16**: 284-287 [PMID: 22455463 DOI: 10.1089/omi.2011.0118]

30 **Han P**, Shen L, Nan N, Zhou R, Li T, Dai X. Cold Atmospheric Plasma Boosts Virus Multiplication *via* EGFR(Tyr1068) Phosphorylation-Mediated Control on Cell Mitophagy. *Int J Biol Sci* 2022; **18**: 3405-3420 [PMID: 35637956 DOI: 10.7150/ijbs.71983]

31 **Yao W**, Liao H, Pang M, Pan L, Guan Y, Huang X, Hei Z, Luo C, Ge M. Inhibition of the NADPH Oxidase Pathway Reduces Ferroptosis during Septic Renal Injury in Diabetic Mice. *Oxid Med Cell Longev* 2022; **2022**: 1193734 [PMID: 35265258 DOI: 10.1155/2022/1193734]

32 **Deng F**, Zhao BC, Yang X, Lin ZB, Sun QS, Wang YF, Yan ZZ, Liu WF, Li C, Hu JJ, Liu KX. The gut microbiota metabolite capsiate promotes Gpx4 expression by activating TRPV1 to inhibit intestinal ischemia reperfusion-induced ferroptosis. *Gut Microbes* 2021; **13**: 1-21 [PMID: 33779497 DOI: 10.1080/19490976.2021.1902719]

33 **Forsmark CE**, Vege SS, Wilcox CM. Acute Pancreatitis. *N Engl J Med* 2016; **375**: 1972-1981 [PMID: 27959604 DOI: 10.1056/nejmra1505202]

34 **Meng Y**, Sha S, Yang J, Ren H. Effects of Tec Tyrosine Kinase Inhibition on the Inflammatory Response of Severe Acute Pancreatitis-Associated Acute Lung Injury in Mice. *Dig Dis Sci* 2019; **64**: 2167-2176 [PMID: 30761473 DOI: 10.1007/s10620-019-05524-7]

35 **Yu QH**, Guo JF, Chen Y, Guo XR, Du YQ, Li ZS. Captopril pretreatment protects the lung against severe acute pancreatitis induced injury *via* inhibiting angiotensin II production and suppressing Rho/ROCK pathway. *Kaohsiung J Med Sci* 2016; **32**: 439-445 [PMID: 27638402 DOI: 10.1016/j.kjms.2016.07.008]

36 **Mao H**, Zhao Y, Li H, Lei L. Ferroptosis as an emerging target in inflammatory diseases. *Prog Biophys Mol Biol* 2020; **155**: 20-28 [PMID: 32311424 DOI: 10.1016/j.pbiomolbio.2020.04.001]

37 **Vermot A**, Petit-Härtlein I, Smith SME, Fieschi F. NADPH Oxidases (NOX): An Overview from Discovery, Molecular Mechanisms to Physiology and Pathology. *Antioxidants (Basel)* 2021; **10** [PMID: 34205998 DOI: 10.3390/antiox10060890]

38 **Elumalai S**, Karunakaran U, Moon JS, Won KC. NADPH Oxidase (NOX) Targeting in Diabetes: A Special Emphasis on Pancreatic β-Cell Dysfunction. *Cells* 2021; **10** [PMID: 34206537 DOI: 10.3390/cells10071573]

39 **Cao WL**, Xiang XH, Chen K, Xu W, Xia SH. Potential role of NADPH oxidase in pathogenesis of pancreatitis. *World J Gastrointest Pathophysiol* 2014; **5**: 169-177 [PMID: 25133019 DOI: 10.4291/wjgp.v5.i3.169]

40 **Yang X**, Zhao K, Deng W, Zhao L, Jin H, Mei F, Zhou Y, Li M, Wang W. Apocynin Attenuates Acute Kidney Injury and Inflammation in Rats with Acute Hypertriglyceridemic Pancreatitis. *Dig Dis Sci* 2020; **65**: 1735-1747 [PMID: 31617131 DOI: 10.1007/s10620-019-05892-0]

41 **Wang C**, Zhu L, Yuan W, Sun L, Xia Z, Zhang Z, Yao W. Diabetes aggravates myocardial ischaemia reperfusion injury *via* activating Nox2-related programmed cell death in an AMPK-dependent manner. *J Cell Mol Med* 2020; **24**: 6670-6679 [PMID: 32351005 DOI: 10.1111/jcmm.15318]

World Journal of Gastroenterology

Submit a Manuscript: https://www.f6publishing.com

World J Gastroenterol 2023 April 21; 29(15): 2310-2321

DOI: 10.3748/wjg.v29.i15.2310

ISSN 1007-9327 (print) ISSN 2219-2840 (online)

ORIGINAL ARTICLE

Case Control Study

Can visceral fat parameters based on computed tomography be used to predict occult peritoneal metastasis in gastric cancer?

Li-Ming Li, Lei-Yu Feng, Chen-Chen Liu, Wen-Peng Huang, Yang Yu, Peng-Yun Cheng, Jian-Bo Gao

Specialty type: Gastroenterology and hepatology

Provenance and peer review: Unsolicited article; Externally peer reviewed.

Peer-review model: Single blind

Peer-review report's scientific quality classification

Grade A (Excellent): 0
Grade B (Very good): B, B
Grade C (Good): C
Grade D (Fair): D
Grade E (Poor): 0

P-Reviewer: Hori T, Japan; Koganti SB, United States; Sun D, China; Tanabe H, Japan

Received: November 4, 2022
Peer-review started: November 4, 2022
First decision: January 3, 2023
Revised: January 21, 2023
Accepted: March 20, 2023
Article in press: March 20, 2023
Published online: April 21, 2023

Li-Ming Li, Jian-Bo Gao, Department of Radiology, Henan Key Laboratory of Imaging Diagnosis and Treatment for Digestive system Tumor, The First Affiliated Hospital of Zhengzhou University, Zhengzhou 450052, Henan Province, China

Lei-Yu Feng, Department of Cardiology, The First Affiliated Hospital of Zhengzhou University, Zhengzhou 450052, Henan Province, China

Chen-Chen Liu, Department of Radiology, The First Affiliated Hospital of Zhengzhou University, Zhengzhou 450052, Henan Province, China

Wen-Peng Huang, Department of Nuclear Medicine, Peking University First Hospital, Beijing 100034, China

Yang Yu, Peng-Yun Cheng, Beijing Branch, Siemens Healthineers Ltd., Shenyang 110011, Liaoning Province, China

Corresponding author: Jian-Bo Gao, Doctor, Professor, Department of Radiology, Henan Key Laboratory of Imaging Diagnosis and Treatment for Digestive system Tumor, The First Affiliated Hospital of Zhengzhou University, No. 1 East Jianshe Road, Zhengzhou 450052, Henan Province, China. jianbogaochina@163.com

Abstract

BACKGROUND

The preoperative prediction of peritoneal metastasis (PM) in gastric cancer would prevent unnecessary surgery and promptly indicate an appropriate treatment plan.

AIM

To explore the predictive value of visceral fat (VF) parameters obtained from preoperative computed tomography (CT) images for occult PM and to develop an individualized model for predicting occult PM in patients with gastric carcinoma (GC).

METHODS

A total of 128 confirmed GC cases (84 male and 44 female patients) that underwent CT scans were analyzed and categorized into PM-positive (n = 43) and PM-negative (n = 85) groups. The clinical characteristics and VF parameters of two regions of interest (ROIs) were collected. Univariate and stratified analyses

based on VF volume were performed to screen for predictive characteristics for occult PM. Prediction models with and without VF parameters were established by multivariable logistic regression analysis.

RESULTS

The mean attenuations of $VF_{ROI\,1}$ and $VF_{ROI\,2}$ varied significantly between the PM-positive and PM-negative groups (P = 0.044 and 0.001, respectively). The areas under the receiver operating characteristic curves (AUCs) of $VF_{ROI\,1}$ and $VF_{ROI\,2}$ were 0.599 and 0.657, respectively. The mean attenuation of $VF_{ROI\,2}$ was included in the final prediction combined model, but not an independent risk factor of PM (P = 0.068). No significant difference was observed between the models with and without mean attenuation of VF (AUC: 0.749 *vs* 0.730, P = 0.339).

CONCLUSION

The mean attenuation of VF is a potential auxiliary parameter for predicting occult PM in patients with GC.

Key Words: Gastric carcinoma; Peritoneal metastasis; Visceral fat; Tomography; X-ray computed; Prediction; Individualized model

Core Tip: The preoperative prediction of peritoneal metastasis (PM) in gastric cancer would prevent unnecessary surgery and promptly indicate an appropriate treatment plan. We therefore aimed to explore the predictive value of visceral fat (VF) parameters obtained from preoperative computed tomography images for occult PM and to develop an individualized model for predicting occult PM in patients with gastric carcinoma (GC). Consequently, mean attenuation of VF is a potential auxiliary parameter to predict occult PM in patients with GC.

Citation: Li LM, Feng LY, Liu CC, Huang WP, Yu Y, Cheng PY, Gao JB. Can visceral fat parameters based on computed tomography be used to predict occult peritoneal metastasis in gastric cancer? *World J Gastroenterol* 2023; 29(15): 2310-2321

URL: https://www.wjgnet.com/1007-9327/full/v29/i15/2310.htm

DOI: https://dx.doi.org/10.3748/wjg.v29.i15.2310

INTRODUCTION

Peritoneal metastasis (PM) is the major cause of postoperative distant metastasis and occurs in more than 10% of patients with newly diagnosed gastric cancer[1]. Gastric carcinoma (GC) is the third leading cause of cancer-related deaths worldwide. In gastric cancer with PM, the survival time is only a few months[2]. Many recent studies[3] have shown that the combination of complete cell reduction and intraperitoneal thermal perfusion chemotherapy can significantly prolong the median survival time in gastric cancer with PM. Thus, the preoperative prediction of PM in gastric cancer would prevent unnecessary surgery and promptly indicate an appropriate treatment plan. For example, laparoscopic exploration may be the preferred choice. Additionally, intraperitoneal hyperthermic chemotherapy may be prepared, and open exploration may be the final choice for a patient with occult PM.

Traditional preoperative imaging methods, such as computed tomography (CT) and magnetic resonance imaging, demonstrate high specificity and low sensitivity in the detection of PM[4]. Therefore, occult PM has attracted extensive attention; it refers to metastasis not indicated on preoperative CT imaging but detected during surgery and pathologic examination[5]. In the last few years, many studies have demonstrated the great potential of radiomics in the prediction of occult PM in gastric cancer[6]. However, most studies have used manual delineation of regions of interest (ROIs) in PM, which reduces repeatability and increases subjective dependence. Therefore, the urgent exploration for new parameters for predicting occult PM is warranted.

Tumor infiltration of the peritoneum alters the characteristics of the surrounding visceral fat (VF) on CT, and these changes have been investigated in previous radiomics studies[7]. In addition, the feature referred to as "smudge-like ground-glass opacity" in the abdominal cavity, which presents an increased CT attenuation of VF, is a common but easily overlooked sign of early-stage omental metastasis[8]. In addition, the adipose microenvironment has a subtle relationship with tumor progression[9].

We therefore aimed to explore the predictive value of VF parameters based on preoperative CT imaging for occult PM in GC and to develop an individualized model for predicting occult PM preoperatively.

MATERIALS AND METHODS

Patients

This retrospective study was approved by the local institutional review board, and the requirement for informed consent was waived.

Patients at our hospital who met the inclusion/exclusion criteria were consecutively enrolled between July 2012 and July 2021. The inclusion criteria were as follows: (1) Diagnosis of gastric cancer by endoscopy and biopsy, with complete biopsy information; (2) Diagnosis of cT3 and cT4 gastric cancer by CT without obvious PM characteristics; and (3) PM status confirmed by exploratory surgery and pathological biopsy. The exclusion criteria were follows: (1) A history of abdominal tumors, cirrhosis, or other inflammatory diseases; (2) A history of abdominal surgery; (3) An interval between CT and surgical exploration longer than 2 wk; and (4) The presence of artifacts that affect the evaluation of VF parameters.

Clinical patient data (*e.g.*, sex and age), blood test information [*e.g.*, carcinoembryonic antigen (CEA), carbohydrate antigen 199 (CA199), and carbohydrate antigen 125 (CA125)], and biopsy information (*e.g.*, pathological type and differentiation) were collected for further analysis.

CT examination

CT examinations were performed using SOMATOM Definition Flash CT or SOMATOM Force (Siemens, Germany). All patients fasted for 6 h, and drank 800-1000 mL water 5-15 min before CT examination. Following an unenhanced scan, dual-phase enhanced CT images were obtained at 30- and 70-s delays. Approximately 1.3 mL/kg iodinated contrast agent (Ultravist 370, Bayer Schering Pharma) was injected intravenously at a rate of 3.0 mL/s. The parameters of the unenhanced scan were as follows: 120 kV tube voltage, 250–350 mAs, and 5 mm slice thickness and slice interval. The parameters of the enhanced scan were as follows: 120 kV tube voltage, automatic tube current modulation techniques, and 5- or 1.25-mm slice thickness and slice interval.

Fat assessment

The volume and mean CT attenuation of VF and subcutaneous fat (SF) were measured using unenhanced scan CT images on a workstation (MM Research Frontier SyngoVia, VB2.0, Siemens Healthineers, Forchheim, Germany). VF was defined as fat within the abdominal cavity, whereas SF was defined as fat below the skin. ROIs were manually drawn by tracing the medial edge of the abdominal muscle using a semiautomated technique, starting from the maximal axial section of the tumor and extending 15 mm (ROI 1) and 25 mm (ROI 2) downward. The contour of each layer can be adjusted manually as necessary. A primary radiologist (with 6 years of experience) was responsible for outlining, while another senior radiologist (with 25 years of experience) was responsible for supervising each operation (Figure 1). Twenty cases were randomly chosen for outlining by another radiologist (with 3 years of experience) to verify the consistency.

CT attenuation between −150 and −50 Hounsfield units (HU) was performed to evaluate voxels containing adipose tissue[10]. Adipose tissue volume was measured in cubic centimeters (cm^3), while mean CT attenuation was measured in HU. The mean CT attenuation and volume of VF were obtained directly on the workstation simultaneously with a table including the CT attenuation of each voxel. The 10^{th}, 30^{th}, 50^{th}, 70^{th}, 90^{th}, 25^{th}, and 75^{th} percentiles of CT attenuation were obtained during postprocessing and calculation.

Analysis of CT images

Two radiologists blinded to the pathologic data analyzed the CT characteristics. When disagreements occurred, a senior radiologist made the final decision. The cT and cN stages were analyzed according to the 8th American Joint Committee staging classification[11,12]. Mild ascites refers to ascites that could not be clearly determined to be caused by metastasis[5]. The GC thickness was measured at the maximal axial section[13].

Statistical analysis

Statistical analyses were conducted using SPSS software (version 22.0) and MedCalc software (version 15.2). Interobserver reliability was assessed using the intraclass correlation coefficient (ICC), where ICC ≥ 0.80 is excellent, 0.61-0.80 is good, and < 0.60 is the difference. The discrimination capability of various VF characteristics was evaluated using the receiver operating characteristic (ROC) curve and compared using Delong's test. The relationship between volume and mean attenuation was evaluated using Pearson correlation analysis. Stratified analysis based on VF volume was performed. The differences in

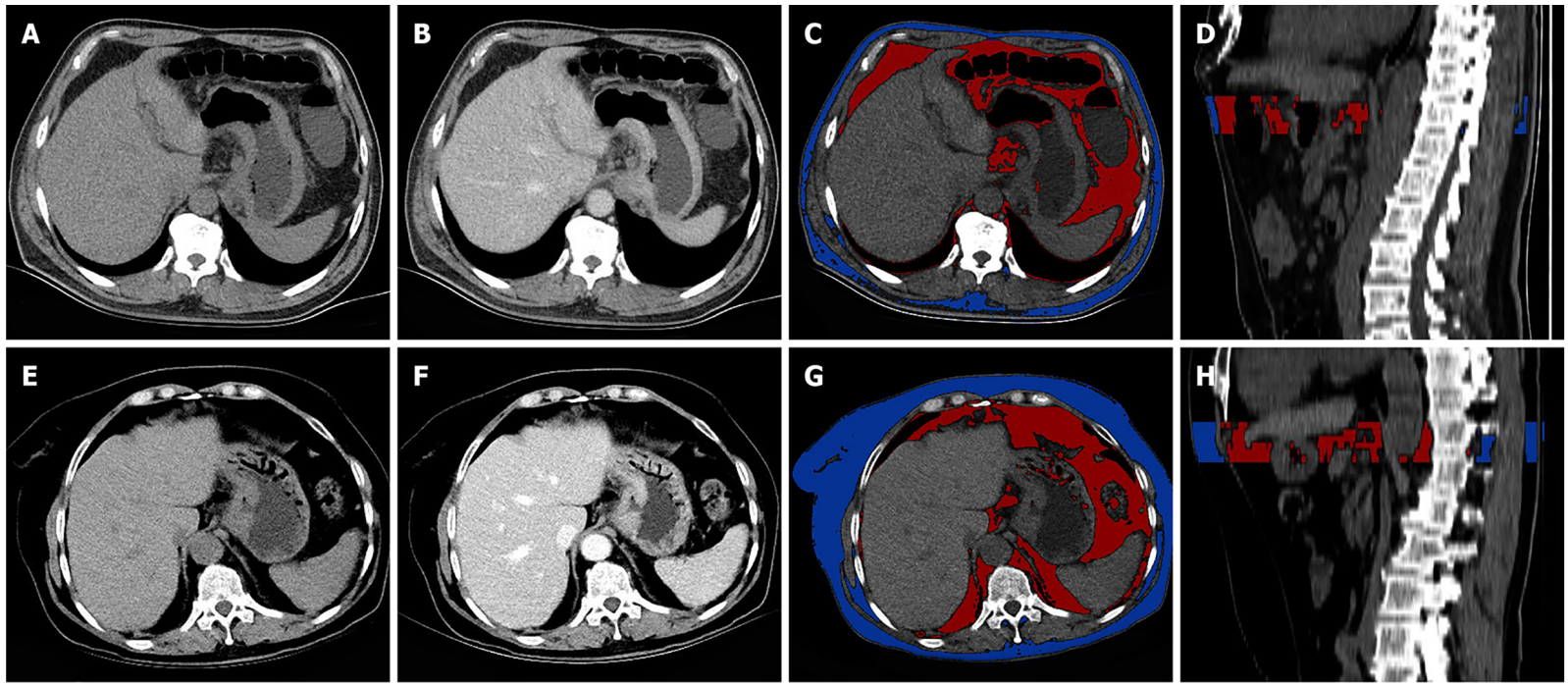

DOI: 10.3748/wjg.v29.i15.2310

Figure 1 Determination of visceral fat parameters. A-D: Detection of visceral fat (VF) parameters in a 54-year-old male patient with gastric cancer with peritoneal metastasis (PM); A and B: Axial unenhanced and venous computed tomography (CT) images showing wall thickening in the cardia and the lesser and greater curvatures of the stomach; C: Regions of interest (ROI) were drawn using a semiautomated technique. The red area represents VF, while the blue area represents subcutaneous fat (SF); D: Sagittal image showing a three-dimensional (3D) ROI, delineated starting from the maximal axial section of the tumor and extending 25 mm; E-H: Determination of VF parameters in a 66-year-old female patient with gastric cancer without PM; E and F: Axial unenhanced and venous CT images showing irregular wall thickening and a mass in the cardia of the stomach; G and H: A 3D ROI drawn with a 25-mm height using a semiautomated technique. The red area represents VF, while the blue area represents SF.

continuous variables were compared using the two-tailed *t* test, Mann–Whitney *U* test, Kruskal-Wallis *H* test, and one-way ANOVA. The differences in categorical variables were compared using the χ^2 test. Significant variables were analyzed using multifactorial logistic regression analysis (backward: Conditional). $P < 0.05$ was considered to suggest a statistically significant difference.

RESULTS

Patient characteristics

A total of 43 PM-positive patients were included in the study, and 85 PM-negative patients treated

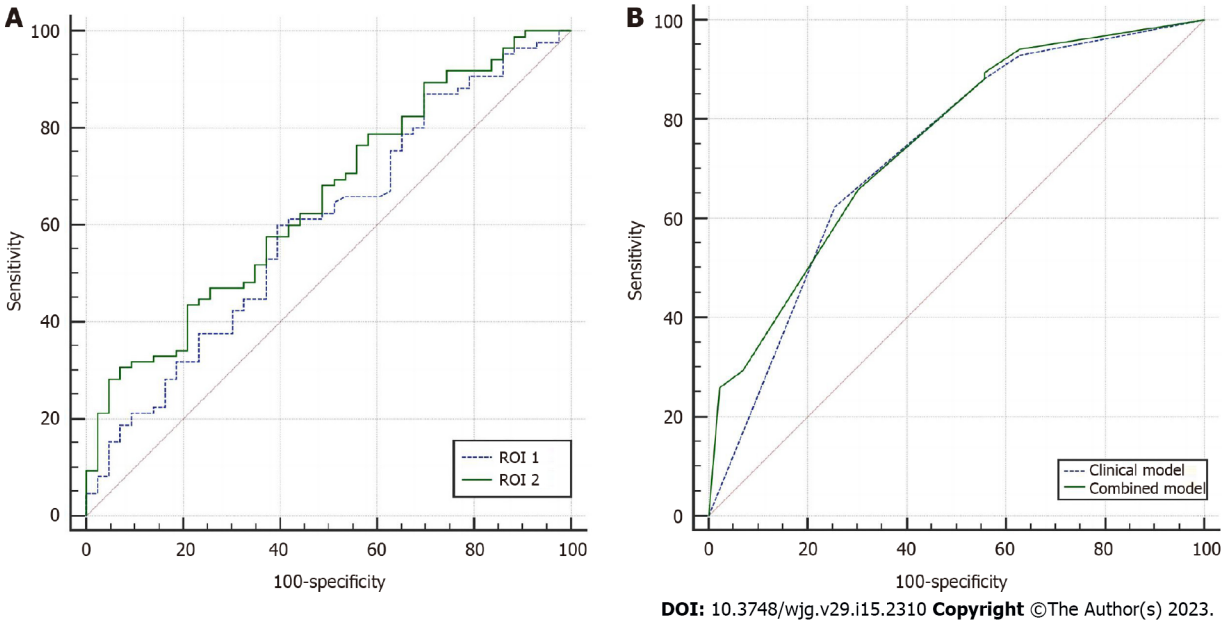

DOI: 10.3748/wjg.v29.i15.2310

Figure 2 Predictive performance of computed tomography attenuations for visceral fat in two regions of interest and two models for predicting peritoneal metastasis in gastric cancer. A: Receiving operator characteristic (ROC) curves of the visceral fat (VF) computed tomography (CT) attenuations on ROIs 1 and 2. The VF CT attenuations on ROI 2 [area under the curve (AUC): 0.657, sensitivity 93.0%, specificity 30.6%] showed a better predictive performance than those on ROI 1 (AUC: 0.599, sensitivity 60.0%, specificity 60.0%); B: ROC curves of the clinical and combined models. The two models showed comparable predictive performance for peritoneal metastasis in gastric cancer (AUC: 0.730 *vs* 0.749, $P = 0.399$)

between January 2021 and July 2021 were included as control subjects. Significant differences in age, CA125, tumor location, thickness, mild ascites, and cT ($P < 0.05$ for all) were found between the PM-positive and PM-negative groups (Table 1). No significant differences were found for sex, pathological type, differentiation, CEA, CA199, or cN stage ($P > 0.05$ for all).

VF characteristics

Significant differences in the mean attenuations of $VF_{ROI\,1}$ and $VF_{ROI\,2}$ ($P = 0.044$ and 0.001, respectively) were found between the PM-positive and PM-negative groups (Table 2). No significant differences were found for the mean attenuations of $SF_{ROI\,1}$ and $SF_{ROI\,2}$, the volumes of $VF_{ROI\,1}$, $VF_{ROI\,2}$, $SF_{ROI\,1}$, and $SF_{ROI\,2}$, or the volume ratio VF/SF ($P > 0.05$ for all).

The areas under the receiver operating characteristic curves (AUCs) of $VF_{ROI\,1}$ and $VF_{ROI\,2}$ for predicting PM in GC were 0.599 [95% confidence interval (CI): 0.509-0.685] and 0.657 (95%CI: 0.568-0.738), respectively (Figure 2A). The comparison of the ROC curves of the VF characteristics suggested that $VF_{ROI\,2}$ significantly outperformed $VF_{ROI\,1}$ ($P = 0.002$). Most of the interobserver agreements between the two operators were excellent (Table 2).

Significant differences in the 30th, 50th, 70th, 25th, and 75th percentiles of CT attenuation of $VF_{ROI\,2}$ were found between the PM-positive and PM-negative groups (Supplementary Table 1). The AUCs of the 10th, 30th, 50th, 70th, 90th, 25th, and 75th percentiles of CT attenuation for predicting PM in GC were 0.612, 0.642, 0.641, 0.619, 0.608, 0.629, and 0.619, respectively. The comparison of ROC curves suggested no significant difference between the 30th percentile and the mean CT attenuation of $VF_{ROI\,2}$ ($P = 0.664$) (Supplementary Figure 1).

Relationship between VF and clinical characteristics

Significant differences in the mean attenuation of $VF_{ROI\,2}$ were observed between the different cN and cT stage classifications ($P = 0.030$ and 0.003, respectively). The mean attenuation of $VF_{ROI\,2}$ in patients with elevated CA125, elevated CA199, and mild ascites was significantly higher than that in normal conditions ($P = 0.002$, 0.039, and 0.001, respectively) (Table 3).

Stratified analysis

The mean attenuation was negatively correlated with the volume of $VF_{ROI\,2}$ (Pearson correlation coefficient = -0.688; $P = 0.001$) (Supplementary Figure 2). Patients were divided into two groups according to the median volume of $VF_{ROI\,2}$ (median = 141.58 cm^3). Stratified analysis suggested that the mean attenuation of $VF_{ROI\,2}$ was more effective in predicting occult PM in the high-volume group than in the low-volume group (Table 4, Figure 3).

Table 1 Comparison of clinical and computed tomography characteristics between two groups, *n* (%)

Variable		PM (-) (*n* = 85)	PM (+) (*n* = 43)	*P* value
Sex	Male	60 (70.6)	24 (55.8)	0.096
	Female	25 (29.4)	19 (44.2)	
Age (yr) (mean ± SD)		56.44±12.63	61.25±11.11	0.029[1]
Pathological type	Adenocarcinoma	83 (97.6)	38 (88.4)	0.077
	Non-adenocarcinoma	2 (2.4)	5 (11.6)	
Differentiation	Poorly differentiated	50 (58.8)	30 (69.8)	0.227
	Moderately and well differentiated	35 (41.2)	13 (30.2)	
CEA	Normal	74 (87.1)	37 (86.0)	0.873
	Elevated	11 (12.9)	6 (14.0)	
CA199	Normal	74 (87.1)	32 (74.4)	0.073
	Elevated	11 (12.9)	11 (25.6)	
CA125	Normal	83 (97.6)	37 (86.0)	0.030[1]
	Elevated	2 (2.4)	6 (14.0)	
Location	Cardia	44 (51.8)	7 (16.3)	0.001[1]
	Body	12 (14.1)	14 (32.6)	
	Antrum	20 (23.5)	13 (30.2)	
	≥ 2 parts	9 (10.6)	9 (20.9)	
Mild ascites	(-)	75 (88.2)	24 (55.8)	0.001[1]
	(+)	10 (11.8)	29 (44.2)	
cN stage	N0	26 (30.6)	11 (25.6)	0.150
	N1-2	41 (48.2)	16 (37.2)	
	N3-4	18 (21.2)	16 (37.2)	
cT stage	≤ T3	57 (67.1)	14 (32.6)	0.001[1]
	≥ T4	28 (32.9)	29 (67.4)	
Thickness (mm), median (IQR)		15.11 (13.02, 18.85)	13.43 (11.28, 17.83)	0.023[1]

[1]$P < 0.05$.

PM: Peritoneal metastasis; CEA: Carcinoembryonic antigen; CA199: Carbohydrate antigen 199; CA125: Carbohydrate antigen 199; IQR: Interquartile range.

Risk factors for occult PM

Multiple logistic regression analysis based on clinical characteristics showed that mild ascites and cT stage (≥ T4) were independent risk factors for occult PM (P = 0.003 and 0.010, respectively) (Table 5). The Hosmer-Lemeshow test revealed that the model had a good fit (P = 0.977). Furthermore, the clinical model showed a moderate prediction performance (AUC = 0.730, 95%CI: 0.644-0.804).

Multiple logistic regression analyses of both clinical characteristics and VF parameters showed that the mean attenuation of $VF_{ROI\,2}$, mild ascites, and cT stage (≥ T_4) were included in the final prediction combined model, but the mean attenuation of $VF_{ROI\,2}$ was not an independent risk factor for PM (P = 0.068) (Table 5). The Hosmer-Lemeshow test indicated that the model had a good fit (P = 0.523). The combined model showed a moderate prediction performance (AUC = 0.749, 95%CI: 0.665-0.821). No significant difference was found between the prediction performance of the two models (P = 0.339) (Figure 2B).

DISCUSSION

We explored the value of VF parameters in predicting occult PM in GC and subsequently developed a preoperative prediction model based on clinical features and VF parameters. A significant difference in the mean attenuation of VF was found between the PM-positive and PM-negative groups. The mean

Table 2 Comparison of visceral fat characteristics between the two lesions

Variable	PM (+) (*n* = 43)	PM (-) (*n* = 85)	*P* value	ICC
$VF_{ROI\ 1}$				
Volume (cc)	84.45 (36.70, 161.04)	87.92 (49.89, 160.75)	0.412	0.913
Mean attenuation (HU)	-82.07 ± 6.06	-85.33 ± 5.89	0.044[1]	0.810
SD attenuation (HU)	18.82 (17.78, 21.25)	19.51 (18.63, 21.11)	0.133	0.926
$SF_{ROI\ 1}$				
Volume (cc)	108.79 (55.10, 170.90)	115.96 (62.70, 178.72)	0.760	0.979
Mean attenuation (HU)	-85.33 ± 5.89	-86.05 ± 8.23	0.934	0.955
SD attenuation (HU)	17.94 (16.60, 19.37)	18.58 (17.27, 20.16)	0.180	0.981
$VF_{ROI\ 2}$				
Volume (cc)	132.63 (58.85, 273.65)	145.48 (82.58, 277.42)	0.302	0.932
Mean attenuation (HU)	-82.19 ± 5.35	-85.70 ± 5.65	0.001[1]	0.974
SD attenuation (HU)	19.86 (17.58, 20.46)	19.13 (18.47, 20.66)	0.317	0.950
$SF_{ROI\ 2}$				
Volume (cc)	163.24 (82.57, 261.17)	175.86 (97.86, 267.52)	0.76	0.991
Mean attenuation (HU)	-86.28 ± 8.61	-86.41 ± 8.08	0.938	0.980
SD attenuation (HU)	17.80 (16.42, 19.33)	18.45 (17.29, 19.91)	0.124	0.993
Volume ratio				
$VF/SF_{ROI\ 1}$	0.92 (0.44, 1.50)	1.00 (0.61, 1.65)	0.317	0.804
$VF/SF_{ROI\ 2}$	0.98 (0.47, 1.41)	1.00 (0.63, 1.68)	0.279	0.884

[1]$P < 0.05$.

PM: Peritoneal metastasis; ICC: Intraclass correlation coefficient; VF: Visceral fat; SF: Subcutaneous fat; SD: Standard deviation; ROI: Region of interest; HU: Hounsfield units; ROIs 1 and 2: Regions of interest starting at the largest axial level of the tumor and extending down 15 mm and 25 mm, respectively.

attenuation of VF was included in the final prediction combined model but was not an independent predictor of occult PM in GC.

Previous studies on VF have mostly focused on the effect of volume or area on postoperative prognosis, and few studies have investigated the CT attenuation of VF[14,15]. CT attenuation of pericoronary adipose tissue has been shown to be strongly correlated with cardiovascular disease[16]. Xiang *et al*[9] investigated the relationship between adipocytes and gastric cancer cells and found that adipocytes may promote cancer cell invasion through a specific signaling pathway. CT attenuation is an index reflecting changes in the VF microenvironment, and its increase may be closely related to tumor progression[17]. Given all of that, we believe that certain changes occur in VF with PM. The indicators used to quantify such changes in our study included the mean attenuation, volume, and volume ratio. Previous studies[5,18] have suggested that the radiomics features of the adjacent peritoneum are helpful in predicting PM in GC. Therefore, two nearby ROIs that delineated from the maximal axial section of the tumor were adopted in our study, and these ROIs were considered to be the most likely sites of metastasis.

The regression analysis indicated that the mean attenuation of $VF_{ROI\ 2}$ was not an independent risk factor for PM, and it had a lower predictive ability than ascites and cT stage. The changes in the adipose microenvironment and the increase in the mean attenuation of VF may be mainly concentrated around the tumor, and the ROI of VF on the whole axial level may dilute this change and reduce the predictive sensitivity. However, the results confirmed that the mean attenuation of VF was significantly different between the PM-positive and PM-negative groups in both ROI 1 and ROI 2. The 30^{th}, 50^{th}, 70^{th}, 25^{th}, and 75^{th} percentiles of attenuation of $VF_{ROI\ 2}$ were also significantly different between the two groups. Moreover, the mean attenuation of VF was related to clinical features representing tumor invasiveness. Therefore, we have reasons to believe that the mean attenuation of VF is a potential auxiliary parameter for predicting occult PM in patients with GC, especially for those with only nonenhanced CT images or upper abdominal CT images.

The mean attenuation was negatively correlated with the volume of VF; however, noticeably, no significant difference in the VF volume was found between the PM-positive and PM-negative groups. Considering the relationship between the mean attenuation and volume of VF, volume-stratified

Table 3 Comparison of attenuations of visceral fat between different clinical characteristic classifications

Variable		Mean attenuation of VF ROI 2	*P* value
Sex	Male	-84.90 ± 6.19	0.306
	Female	-83.83 ± 4.88	
Age (yr)	≤ 61	-84.48 ± 5.11	0.937
	> 61	-84.46 ± 5.14	
Pathological type	Adenocarcinoma	-84.64 ± 5.81	0.339
	Non-adenocarcinoma	-82.49 ± 4.99	
Differentiation	Poorly differentiated	-84.18 ± 5.91	0.377
	Moderately and well differentiated	-85.11 ± 5.56	
CEA	Normal	-84.64 ± 5.92	0.583
	Elevated	-83.81 ± 4.86	
CA199	Normal	-85.04 ± 6.04	0.002[1]
	Elevated	-82.07 ± 3.40	
CA125	Normal	-84.80 ± 5.81	0.039[1]
	Elevated	-80.46 ± 3.41	
Location	Cardia/Body/Antrum	-84.93 ± 5.86	0.049[1]
	≥ 2 parts	-82.05 ± 4.67	
Mild ascites	(-)	-85.41 ± 5.79	0.001[1]
	(+)	-81.52 ± 4.69	
cN stage	N0	-85.48 (-89.85, -82.95)	0.030[1]
	N1-2	-83.08 (-86.68, -79.43)	
	N3-4	-84.54 (-87.51, -80.60)	
cT stage	≤ T3	-85.88 ± 5.83	0.003[1]
	≥ T4	-82.84 ± 5.29	
Thickness (mm)	≤ 14.5	-84.82 ± 6.36	0.517
	> 14.5	-84.15 ± 4.98	

[1]$P < 0.05$.

CEA: Carcinoembryonic antigen; CA199: Carbohydrate antigen 199; CA125: Carbohydrate antigen 199; VF: Visceral fat; ROI 2: Regions of interest starting at the largest axial level of the tumor and extending down 25 mm.

Table 4 Stratified analysis of volume

	PM (-)	PM (+)	*P* value	AUC (95%CI)
Volume > median				
No	45	19		
Mean attenuation (HU)	-89.08 ± 5.31	-85.44 ± 3.93	0.009[1]	0.726 (0.59-0.854)
Volume ≤ median				
No	40	24		
Mean attenuation (HU)	-81.92 ± 3.01	-79.61 ± 4.94	0.046[1]	0.639 (0.490-0.787)

[1]$P < 0.05$.

PM: Peritoneal metastasis; No: Number; AUC: Area under the curve; HU: Hounsfield units.

Table 5 Variables and coefficients of multiple regression logistic analysis

Variable	OR	95%CI	*P* value
Based on all characteristics			
Mild ascites (+ *vs* -)	3.552	(1.375-9.175)	0.009[1]
Mean attenuations of $VF_{ROI\,2}$	3.437	(0.914-12.914)	0.068
cT stage (≥ T4 *vs* ≤ T3)	2.631	(1.126-6.144)	0.025[1]
Intercept	0.009		0.001[1]
Based on clinical characteristics			
Mild ascites (+ *vs* -)	4.188	(1.636-10.722)	0.003[1]
cT stage (≥ T4 *vs* ≤ T3)	2.992	(1.301-6.881)	0.010[1]
Intercept	0.068		0.001[1]

[1]$P < 0.05$.

VF: Visceral fat; ROI: Region of interest; OR: Odds ratio; CI: Confidence interval.

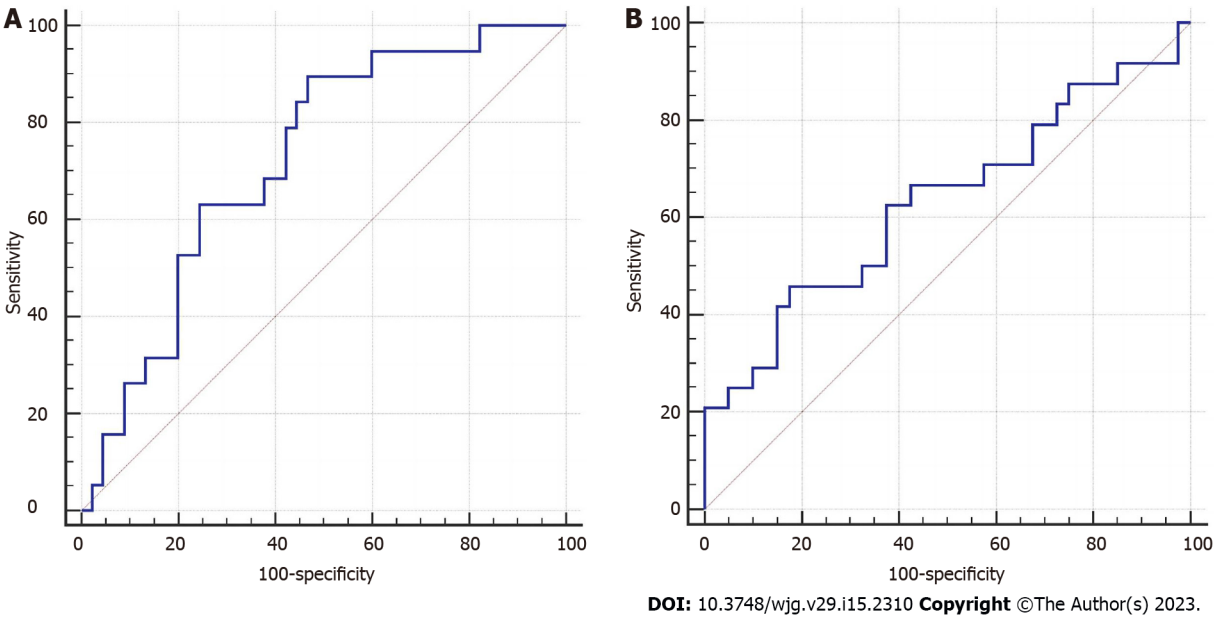

DOI: 10.3748/wjg.v29.i15.2310

Figure 3 Performance of computed tomography attenuations for visceral fat in predicting peritoneal metastasis in gastric cancer. A: High-volume group; B: Low-volume group.

analysis was applied to minimize the deviations in volume variation. The mean attenuation of $VF_{ROI\,2}$ showed a higher predictive potential in the high-volume group than in the low-volume group. This result suggests that patients with high-volume VF may have more hypoxic or disordered adipocytes that secrete proinflammatory cytokines and angiogenic factors and promote tumor metastasis than patients with low-volume VF[19]. The attenuation of VF was significantly correlated with cT stage, cN stage, CA125, and CA199, indicating that increased VF attenuation is highly correlated with tumor progression.

Mild ascites and cT stage are independent predictive factors for occult PM. Liu *et al*[7] reported that cT stage was significantly correlated with occult PM, which reflects tumor aggressiveness. Mild ascites was also incorporated into a clinical model for predicting occult PM in a multicenter study[5]. Significant differences were observed in the mean attenuations of VF between the different ascites statuses and cT stages.

Compared with previous radiomics studies, the extraction of VF parameters in our study was based on unenhanced CT images through semiautomated sketching technology, which would reduce the selection differences between operators. The consistency between the operators of VF parameters was excellent. The ROIs in the peritoneum used in most previous studies on occult PM were manually sketched[5,18]. Thus, evaluating the consistency among different operators in defining the location and area of ROIs selected was difficult. In addition, three-dimensional ROIs were defined in our study,

which remain applicable in patients with lesser VF.

This study has certain limitations. First, the VF parameters were measured using data obtained from a single center with a small sample size, and multicenter studies with a large sample size are thus needed to validate the results. Second, the parameters used to quantify VF changes were obtained only from unenhanced CT images, which warrants the need to consider more parameters from multiphase enhanced images.

CONCLUSION

In conclusion, our study demonstrates the great potential of VF parameters in predicting occult PM in GC and presents a noninvasive preoperative model that combines the mean attenuation of VF and clinical factors for predicting occult PM in GC.

ARTICLE HIGHLIGHTS

Research background

The preoperative prediction of peritoneal metastasis (PM) in gastric cancer (GC) would prevent unnecessary surgery and promptly indicate an appropriate treatment plan.

Research motivation

Tumor infiltration of the peritoneum alters the characteristics of the surrounding VF on computed tomography (CT), and these changes have been investigated in previous studies.

Research objectives

We therefore aimed to explore the predictive value of VF parameters obtained from preoperative CT images for occult PM and to develop an individualized model for predicting occult PM in patients with GC.

Research methods

A total of 128 confirmed GC cases that underwent CT scans were analyzed and categorized into PM-positive and PM-negative groups. The clinical characteristics and VF parameters of two regions of interest (ROIs) were collected. Univariate and stratified analyses based on VF volume were performed to screen for predictive characteristics for occult PM. Prediction models with and without VF parameters were established by multivariable logistic regression analysis.

Research results

The mean attenuations of $VF_{ROI\,1}$ and $VF_{ROI\,2}$ varied significantly between the PM-positive and PM-negative groups (P = 0.044 and 0.001, respectively). The mean attenuation of $VF_{ROI\,2}$ was included in the final prediction combined model, but not an independent risk factor of PM (P = 0.068). No significant difference was observed between the models with and without mean attenuation of VF (area under the curve: 0.749 *vs* 0.730, P = 0.339).

Research conclusions

The mean attenuation of VF is a potential auxiliary parameter for predicting occult PM in patients with GC.

Research perspectives

Our study demonstrates the great potential of VF parameters in predicting occult PM in GC and presents a noninvasive preoperative model that combines the mean attenuation of VF and clinical factors for predicting occult PM in GC.

FOOTNOTES

Author contributions: Li LM, Huang WP, and Gao JB designed the research study; Huang WP, Li LM, and Gao JB performed the research; Yu Y and Cheng PY contributed analytic tools; Li LM, Feng LY, and Liu CC analyzed the data and wrote the manuscript; all authors have read and approved the final manuscript.

Supported by Henan Province 2023 Scientific Research Projects Focused on Higher Education Project, China, No. 23A320059.

Institutional review board statement: The study was reviewed and approved by the First Affiliated Hospital of Zhengzhou University Institutional Review Board (Approval No. 2021-KY-1070-002).

Informed consent statement: Patients were not required to give informed consent to the study because the analysis used anonymous clinical data that were obtained after each patient agreed to treatment by written consent.

Conflict-of-interest statement: All the authors report no relevant conflicts of interest for this article.

Data sharing statement: Dataset available from the corresponding author at jianbogaochina@163.com.

Country/Territory of origin: China

ORCID number: Li-Ming Li 0000-0002-2910-9742; Chen-Chen Liu 0000-0001-5026-3288; Wen-Peng Huang 0000-0002-9104-1494; Jian-Bo Gao 0000-0003-2621-3701.

S-Editor: Liu GL
L-Editor: Wang TQ
P-Editor: Liu GL

REFERENCES

1 **Maehara Y**, Hasuda S, Koga T, Tokunaga E, Kakeji Y, Sugimachi K. Postoperative outcome and sites of recurrence in patients following curative resection of gastric cancer. *Br J Surg* 2000; **87**: 353-357 [PMID: 10718807 DOI: 10.1046/j.1365-2168.2000.01358.x]
2 GLOBOCAN 2012: Stomach cancer: estimated incidence, mortality and prevalence worldwide in 2012. [Internet] [accessed 5 November 2021]. Available from: http://globocan.iarc.fr/old/FactSheets/cancers/stomach-new.asp
3 **Rau B**, Brandl A, Piso P, Pelz J, Busch P, Demtröder C, Schüle S, Schlitt HJ, Roitman M, Tepel J, Sulkowski U, Uzunoglu F, Hünerbein M, Hörbelt R, Ströhlein M, Beckert S, Königsrainer I, Königsrainer A; Peritoneum Surface Oncology Group and members of the StuDoQ|Peritoneum Registry of the German Society for General and Visceral Surgery (DGAV). Peritoneal metastasis in gastric cancer: results from the German database. *Gastric Cancer* 2020; **23**: 11-22 [PMID: 31228044 DOI: 10.1007/s10120-019-00978-0]
4 **Kim SJ**, Kim HH, Kim YH, Hwang SH, Lee HS, Park DJ, Kim SY, Lee KH. Peritoneal metastasis: detection with 16- or 64-detector row CT in patients undergoing surgery for gastric cancer. *Radiology* 2009; **253**: 407-415 [PMID: 19789243 DOI: 10.1148/radiol.2532082272]
5 **Dong D**, Tang L, Li ZY, Fang MJ, Gao JB, Shan XH, Ying XJ, Sun YS, Fu J, Wang XX, Li LM, Li ZH, Zhang DF, Zhang Y, Li ZM, Shan F, Bu ZD, Tian J, Ji JF. Development and validation of an individualized nomogram to identify occult peritoneal metastasis in patients with advanced gastric cancer. *Ann Oncol* 2019; **30**: 431-438 [PMID: 30689702 DOI: 10.1093/annonc/mdz001]
6 **Huang W**, Zhou K, Jiang Y, Chen C, Yuan Q, Han Z, Xie J, Yu S, Sun Z, Hu Y, Yu J, Liu H, Xiao R, Xu Y, Zhou Z, Li G. Radiomics Nomogram for Prediction of Peritoneal Metastasis in Patients With Gastric Cancer. *Front Oncol* 2020; **10**: 1416 [PMID: 32974149 DOI: 10.3389/fonc.2020.01416]
7 **Liu S**, He J, Liu S, Ji C, Guan W, Chen L, Guan Y, Yang X, Zhou Z. Radiomics analysis using contrast-enhanced CT for preoperative prediction of occult peritoneal metastasis in advanced gastric cancer. *Eur Radiol* 2020; **30**: 239-246 [PMID: 31385045 DOI: 10.1007/s00330-019-06368-5]
8 **Li ZY**, Tang L, Li ZM, Li YL, Fu J, Zhang Y, Li XT, Ying XJ, Ji JF. Four-Point Computed Tomography Scores for Evaluation of Occult Peritoneal Metastasis in Patients with Gastric Cancer: A Region-to-Region Comparison with Staging Laparoscopy. *Ann Surg Oncol* 2020; **27**: 1103-1109 [PMID: 31965376 DOI: 10.1245/s10434-019-07812-y]
9 **Xiang F**, Wu K, Liu Y, Shi L, Wang D, Li G, Tao K, Wang G. Omental adipocytes enhance the invasiveness of gastric cancer cells by oleic acid-induced activation of the PI3K-Akt signaling pathway. *Int J Biochem Cell Biol* 2017; **84**: 14-21 [PMID: 27956048 DOI: 10.1016/j.biocel.2016.12.002]
10 **Chen Y**, Xi W, Yao W, Wang L, Xu Z, Wels M, Yuan F, Yan C, Zhang H. Dual-Energy Computed Tomography-Based Radiomics to Predict Peritoneal Metastasis in Gastric Cancer. *Front Oncol* 2021; **11**: 659981 [PMID: 34055627 DOI: 10.3389/fonc.2021.659981]
11 **Tsoukalas N**, Tsapakidis K, Kamposioras K. AJCC-8 TNM Staging System for Gastric Cancer. Is There a Scope for Improvement? *J Invest Surg* 2020; **33**: 939-940 [PMID: 30892116 DOI: 10.1080/08941939.2019.1579280]
12 **Marano L**, D'Ignazio A, Cammillini F, Angotti R, Messina M, Marrelli D, Roviello F. Comparison between 7th and 8th edition of AJCC TNM staging system for gastric cancer: old problems and new perspectives. *Transl Gastroenterol Hepatol* 2019; **4**: 22 [PMID: 31143843 DOI: 10.21037/tgh.2019.03.09]
13 **Li J**, Fang M, Wang R, Dong D, Tian J, Liang P, Liu J, Gao J. Diagnostic accuracy of dual-energy CT-based nomograms to predict lymph node metastasis in gastric cancer. *Eur Radiol* 2018; **28**: 5241-5249 [PMID: 29869176 DOI:

10.1007/s00330-018-5483-2]

14 **Lin YC**, Lin G, Yeh TS. Visceral-to-subcutaneous fat ratio independently predicts the prognosis of locally advanced gastric cancer-----highlighting the role of adiponectin receptors and PPARα, β/δ, ɤ. *Eur J Surg Oncol* 2021; **47**: 3064-3073 [PMID: 33941417 DOI: 10.1016/j.ejso.2021.04.028]

15 **Taniguchi Y**, Kurokawa Y, Takahashi T, Saito T, Yamashita K, Tanaka K, Makino T, Yamasaki M, Nakajima K, Eguchi H, Doki Y. Impacts of Preoperative Psoas Muscle Mass and Visceral Fat Area on Postoperative Short- and Long-Term Outcomes in Patients with Gastric Cancer. *World J Surg* 2021; **45**: 815-821 [PMID: 33179125 DOI: 10.1007/s00268-020-05857-9]

16 **Ichikawa K**, Miyoshi T, Osawa K, Nakashima M, Miki T, Nishihara T, Toda H, Yoshida M, Ito H. High pericoronary adipose tissue attenuation on computed tomography angiography predicts cardiovascular events in patients with type 2 diabetes mellitus: post-hoc analysis from a prospective cohort study. *Cardiovasc Diabetol* 2022; **21**: 44 [PMID: 35303857 DOI: 10.1186/s12933-022-01478-9]

17 **Lee JW**, Son MW, Chung IK, Cho YS, Lee MS, Lee SM. Significance of CT attenuation and F-18 fluorodeoxyglucose uptake of visceral adipose tissue for predicting survival in gastric cancer patients after curative surgical resection. *Gastric Cancer* 2020; **23**: 273-284 [PMID: 31485803 DOI: 10.1007/s10120-019-01001-2]

18 **Kim HY**, Kim YH, Yun G, Chang W, Lee YJ, Kim B. Could texture features from preoperative CT image be used for predicting occult peritoneal carcinomatosis in patients with advanced gastric cancer? *PLoS One* 2018; **13**: e0194755 [PMID: 29596522 DOI: 10.1371/journal.pone.0194755]

19 **Divella R**, De Luca R, Abbate I, Naglieri E, Daniele A. Obesity and cancer: the role of adipose tissue and adipo-cytokines-induced chronic inflammation. *J Cancer* 2016; **7**: 2346-2359 [PMID: 27994674 DOI: 10.7150/jca.16884]

World Journal of Gastroenterology

Submit a Manuscript: https://www.f6publishing.com

World J Gastroenterol 2023 April 21; 29(15): 2322-2335

DOI: 10.3748/wjg.v29.i15.2322

ISSN 1007-9327 (print) ISSN 2219-2840 (online)

ORIGINAL ARTICLE

Retrospective Study

Value of red blood cell distribution width in prediction of diastolic dysfunction in cirrhotic cardiomyopathy

Yan-Ling Chen, Zi-Wen Zhao, Shu-Mei Li, Yong-Zhe Guo

Specialty type: Gastroenterology and hepatology

Provenance and peer review: Unsolicited article; Externally peer reviewed.

Peer-review model: Single blind

Peer-review report's scientific quality classification

Grade A (Excellent): 0
Grade B (Very good): B
Grade C (Good): 0
Grade D (Fair): D
Grade E (Poor): 0

P-Reviewer: Papazafiropoulou A, Greece; Razpotnik M, Austria

Received: October 14, 2022
Peer-review started: October 14, 2022
First decision: January 3, 2023
Revised: January 27, 2023
Accepted: March 15, 2023
Article in press: March 15, 2023
Published online: April 21, 2023

Yan-Ling Chen, Department of Gastroenterology, Fujian Medical University Union Hospital, Fuzhou 350001, Fujian Province, China

Zi-Wen Zhao, Shu-Mei Li, Yong-Zhe Guo, Department of Cardiology, Fujian Medical University Union Hospital, Fuzhou 350001, Fujian Province, China

Corresponding author: Yong-Zhe Guo, Doctor, Attending Doctor, Department of Cardiology, Fujian Medical University Union Hospital, No. 29 Xin-Quan Road, Fuzhou 350001, Fujian Province, China. 13705935398@163.com

Abstract

BACKGROUND

Clinical diagnosis of cirrhotic cardiomyopathy (CCM) often encounters challenges of lack of timeliness and disease severity, with the commonly positive indicator usually associated with advanced heart failure.

AIM

To explore suitable biomarkers for early CCM prediction.

METHODS

A total of 505 eligible patients were enrolled in this study and divided into four groups according to Child-Pugh classification: Group I, Class A without CCM (105 cases); Group II, Class A with CCM (175 cases); Group III, Class B with CCM (139 cases); and Group IV, Class C with CCM (86 cases). Logistic regression and receiver operating characteristic (ROC) curve analyses were performed to determine whether red blood cell distribution width (RDW) was an independent risk factor for CCM risk. The relationships between RDW and Child-Pugh scores, Model for End-Stage Liver Disease (MELD) scores, and N-terminal pro-brain natriuretic peptide (NT-proBNP) were analyzed by Pearson correlation analysis.

RESULTS

A constant RDW increase was evident from Group I to Group IV (12.54 ± 0.85, 13.29 ± 1.19, 14.30 ± 1.96, and 16.25 ± 2.13, respectively). Pearson correlation analysis showed that RDW was positively correlated with Child-Pugh scores (r = 0.642, P < 0.001), MELD scores (r = 0.592, P < 0.001), and NT-proBNP (r = 0.715, P < 0.001). Furthermore, between Group I and Group II, RDW was the only significant index (odds ratio: 2.175, 95% confidence interval [CI]: 1.549-3.054, P < 0.001), and it reached statistical significance when examined by ROC curve

analysis (area under the curve: 0.686, 95%CI: 0.624-0.748, $P < 0.001$).

CONCLUSION
RDW can serve as an effective and accessible clinical indicator for the prediction of diastolic dysfunction in CCM, in which a numerical value of more than 13.05% may indicate an increasing CCM risk.

Key Words: Cirrhotic cardiomyopathy; Child-Pugh; Diagnosis; N-terminal pro-brain natriuretic peptide; Red blood cell distribution width

Core Tip: Diastolic dysfunction is usually an early stage of cirrhotic cardiomyopathy (CCM). This study found that red blood cell distribution width would have an advantage over N-Terminal pro-brain natriuretic peptide in indicating diastolic dysfunction in such patients, which is of great significance for the early diagnosis and treatment of CCM.

Citation: Chen YL, Zhao ZW, Li SM, Guo YZ. Value of red blood cell distribution width in prediction of diastolic dysfunction in cirrhotic cardiomyopathy. *World J Gastroenterol* 2023; 29(15): 2322-2335
URL: https://www.wjgnet.com/1007-9327/full/v29/i15/2322.htm
DOI: https://dx.doi.org/10.3748/wjg.v29.i15.2322

INTRODUCTION

As a manifestation of unnoticeable cardiac dysfunction, cirrhotic cardiomyopathy (CCM) features diastolic dysfunction, chronotropic dysfunction, electrophysiological abnormalities, and compromised myocardial contractility in the absence of other cardiac diseases. In such a setting, liver cirrhosis-induced hyperdynamic circulation may even result in structural cardiac abnormalities[1,2]. Available literature evidences that CCM-associated diastolic dysfunction can pose very adverse clinical implications[3], including severe liver diseases, hepatorenal syndrome, ascites[4,5], and death[6]. The current clinical diagnosis of CCM-related diastolic dysfunction mainly relies on transthoracic echocardiography (TTE)[7], with N-terminal pro-brain natriuretic peptide (NT-proBNP) and other indicators playing a supportive role[8,9]. However, studies contend that NT-proBNP level is not an optimal biomarker for CCM screening and cannot serve as an independent diagnostic tool for such a condition, though increased NT-proBNP level in liver cirrhosis has been found to be positively associated with echocardiographic measures of left ventricular diastolic dysfunction (LVDD) and may be indicative of CCM[10]. Therefore, an urgent need remains regarding a more objective indicator for CCM screening in patients with LVDD, especially in the early stages of the disease.

Of all the other potential candidate indicators, red blood cell distribution width (RDW), a common blood laboratory parameter, has been closely associated with cardiac function and/or the disease severity of heart failure (HF), including the natriuretic peptides[11], left ventricular end diastolic pressure[12], and left ventricular deformation[13,14]. Meanwhile, RDW levels are more or less correlated with various liver diseases[15-18]. Studies have demonstrated that the assessment of RDW may improve risk stratification of patients with acute decompensation of cirrhosis[19]. Other studies have documented RDW as a novel inflammatory marker in various conditions, including cardiovascular diseases[20], functional bowel conditions[21], autoimmune diseases[22,23], degenerative vertebral conditions[24], malignancy[25], and even COVID-19[26]. Taken together, these findings evidence that RDW may be altered in cirrhosis patients comorbid with cardiac diastolic dysfunction and may serve as a promising objective indicator for CCM screening. Therefore, this study attempted to probe into the value of RDW in the prediction of LVDD in CCM patients.

MATERIALS AND METHODS

Patient recruitment

A single-center, retrospective study was designed to evaluate the correlation between RDW levels and liver cirrhosis with diastolic dysfunction. The clinical data of 5205 patients diagnosed with cirrhosis of various etiologies were collected between June 2017 and May 2022, and a total of 505 cases were selected and included in this study. All these patients were referred to Fujian Medical University Union Hospital

(Fuzhou, Fujian Province, China). For patients hospitalized more than once, data from the first admission were used. The following items were set to support a diagnosis of liver cirrhosis[27,28]: (1) Imaging by ultrasonography, computed tomography, or magnetic resonance imaging indicating irregular liver surface and heterogeneous liver parenchyma; (2) impaired liver synthetic function: Albumin level less than 35.0 g/L without other identifiable causes of hypoalbuminemia such as renal loss or gastrointestinal loss; and (3) evidence of portal hypertension (variceal hemorrhage, refractory ascites, or splenomegaly) or life-threatening complications such as spontaneous bacterial peritonitis or hepatic encephalopathy. Liver cirrhosis was defined as conditions meeting criteria (1) and (2) or (1) and (3).

The inclusion criteria were: (1) Age over 18 years; (2) diagnosis of cirrhosis confirmed as above mentioned; (3) severity of liver cirrhosis evaluated by Child-Pugh classification and Model for End-Stage Liver Disease (MELD) score; and (4) LVDD confirmed by TTE (controls without LVDD). The exclusion criteria were: (1) Known cardiac diseases (such as valvular heart disease, rhythm or conduction disorders, congenital heart disease, coronary artery disease, non-ischemic cardiopathy, and pulmonary arterial hypertension); (2) TTE-confirmed systolic dysfunction only; (3) other causes of liver insufficiency (such as septicaemia and toxic liver disease); (4) RDW increase-related pre-existing conditions such as thalassemia, hemolytic anemia, hereditary spherocytosis, sickle cell disease, myelodysplastic syndrome, or aplastic anemia; and (5) other underlying conditions including gastric or duodenal ulcer, pregnancy, active malignancy other than liver cancer, and recent transfusion or use of iron or erythropoietin (within past 3 mo).

In particular, this study not only explored the changes of RDW in patients with CCM, but more importantly, revealed the value of RDW in predicting early CCM by comparing the differences of RDW in cirrhotic patients with or without cardiomyopathy. As a result, we set a group consisting of Child-Pugh A cirrhotic patients without CCM as the control group.

Measurements of baseline variables

Upon admission, blood samples were collected at 6 a.m. and processed immediately at the clinical laboratory of Fujian Medical University Union Hospital. The reference range of RDW was 11.5%-15.0%. Cardiac function was measured by TTE (Philips iE33, Philips Medical Systems, Andover, MA, United States). According to the latest CCM guidelines [2019 Cirrhotic Cardiomyopathy Consortium (CCC)][7], LVDD in CCM was diagnosed when three of the following conditions were present: E/e' ≥ 15 [early diastolic transmitral and myocardial velocity on Doppler tissue imaging ratio], peak tricuspid regurgitation velocity > 2.8 m/s, septal e' velocity < 7 cm/s (early diastolic myocardial velocity on TDI), and left atrial volume index > 34 mL/m^2.

Spontaneous bacterial peritonitis (SBP) was defined as a bacterial infection of the ascitic fluid in the absence of a secondary intra-abdominal focus and determined by ascitic fluid polymorphonuclear (PMN) count, in which PMN count ≥ 250 cells/mm^3 was diagnosed as SBP[29]. Refractory ascites was defined as ascites that cannot be mobilized or the early recurrence of which (after a large volume paracentesis) cannot be prevented by medical therapy[30]. At last, hepatic encephalopathy (HE) was defined as brain dysfunction in patients with liver failure and/or portosystemic shunts presenting cognitive alterations and personality and mental disorders[31].

Statistical analysis

The data were analyzed with SPSS version 26.0 (IBM, Somers, NY, United States). The normality of the data was evaluated by Kolmogorov-Smirnov test. For normally-distributed continuous variables, the data are presented as the mean ± SD; inter-group comparison was performed by one-way analysis of variance (ANOVA) and pairwise comparison by least significant difference *T* test (LSD-T). For abnormally-distributed continuous variables, data are presented as the median (interquartile range); inter-group and pairwise comparisons were analyzed by Kruskal-Wallis test and Bonferroni correction, respectively. The count data are presented as percentages (%). The proportions were measured by Chi-square test and Fisher's exact test was applied if the expected frequency was < 5. The potential association between RDW and CCM was examined by multivariate logistic regression analysis. The discriminatory power was evaluated by the area under the receiver operating characteristic (ROC) curve (AUC) with its 95% confidence interval (CI). The statistical significance was set at a two-sided probability value of $P < 0.05$. Simultaneously, Pearson correlation analysis was used to compare the relationships between RDW and Child-Pugh scores, MELD scores, and NT-proBNP.

RESULTS

Demographic features

In addition to the 400 cases diagnosed with CCM, we matched 105 patients with early cirrhosis without cardiomyopathy. According to Child-Pugh classification[9], all 505 eligible patients were divided into four groups: Group I, Class A without CCM (control group); Group II, Class A with CCM; Group III, Class B with CCM; Group IV, Class C with CCM. The baseline demographic and clinical characteristics

of the patient cohort are shown in Table 1. Patients with more serious Child-Pugh rating featured a significantly high incidence rate of hyperlipidemia and atrial fibrillation, though no statistical significance was found for age, gender, body mass index, smokers, and other demographic information among the groups.

Clinical information

The clinical symptoms, laboratory parameters, and medications of the enrolled patients are summarized in Table 2. Generally, with the worsening disease severity, more obvious complications were evident from Group I to Group IV, such as haematemesis (5.7%, 6.9%, 11.5%, and 18.6%, respectively, $P = 0.009$), edema (1.9%, 6.9%, 14.4%, and 38.4%, respectively, $P < 0.001$), SBP (1%, 2.3%, 7.9%, and 15.1%, respectively, $P < 0.001$), hyponatremia (2.9%, 12%, 22.3%, and 36%, respectively, $P < 0.001$), HE (4.8%, 5.7%, 10.1%, and 22.1%, respectively, $P < 0.001$), refractory ascites (1.9%, 2.3%, 10.8%, and 24.4%, respectively, $P < 0.001$), and jaundice (11.4%, 7.4%, 23.3%, and 24.4%, respectively, $P = 0.003$). Along with the presence of these indicators, MELD score also increased in the four groups (8.74 ± 1.54, 8.64 ± 1.57, 17.04 ± 1.96, and 25.19 ± 2.15, respectively, $P < 0.001$). Except for alkaline phosphatase (ALP), regardless of the increase or decrease along with the rise of Child-Pugh level, a statistical difference was found in other laboratory indicators, such as total bilirubin (TBIL), alanine transaminase (ALT), aspartic transaminase (AST), γ-glutamyl transferase (γ-GT), albumin, white blood cell (WBC) count, hemoglobin, platelet count, international normalized ratio (INR), and estimated glomerular filtration rate (eGFR) ($P < 0.050$ for all). The frequency of administration of diuretics, anti-ventricular remodeling agents, and β-blocker increased apparently with the progression of cirrhosis ($P \leq 0.001$ for all). The clinical manifestations, laboratory indicators, and CCM medications listed in Table 2 were basically consistent with the clinical practice.

RDW as an independent diagnostic indicator for CCM

The pairwise comparison of the four groups revealed a significant difference for the RDW value that rose constantly with the increasing severity of cirrhosis (12.54 ± 0.85, 13.29 ± 1.19, 14.30 ± 1.96, and 16.25 ± 2.13, $P < 0.001$) (Table 2). All indexes with $P < 0.05$ in Tables 1 and 2 are summarized in Table 3. Multivariate logistics regression analysis was divided into three parts, with the first, second, and third parts corresponding to risk factor analysis of Group II, Group III, and Group IV (Group I as the control group), respectively. Part I reported statistical significance in RDW (odds ratio [OR]: 2.175, 95%CI: 1.549-3.054, $P < 0.001$) between Group II and the control group, with no significant differences in other indicators, which suggests RDW as an independent risk factor in Part I. Part II revealed a marked difference in RDW (OR: 2.447, 95%CI: 1.375-4.354, $P = 0.002$), ALB, ALT, AST, γ-GT, WBC count, hemoglobin, platelet count, INR, NT-proBNP, and eGFR ($P < 0.05$, respectively). Further multivariate logistic regression reported significant differences in RDW (OR: 4.863, 95%CI: 2.493-9.483, $P < 0.001$), ALB, ALT, AST, WBC count, hemoglobin, platelet count, INR, NT-proBNP, and edema ($P < 0.05$, respectively), which were considered as independent risk factors in Part III. Besides, as shown in Table 4, the linear regression analysis showed a positive correlation between RDW and Child-Pugh scores ($r = 0.642$, $P < 0.001$) (Figure 1A) and between RDW and MELD scores ($r = 0.592$, $P < 0.001$) (Figure 1B).

A strong correlation between RDW and different Child-Pugh levels

In Table 2, due to the distribution abnormality in the data of NT-proBNP, the independent sample Kruskal-Wallis test was employed for analysis. The results showed no significant increase in NT-proBNP when the cardiomyopathy cases (Group II) were compared with the non-cardiomyopathy cases (Group I) [76 (61, 98) *vs* 72 (61, 84), $P > 0.05$] but huge differences for both Group III and Group IV ($P < 0.001$ for both). Similarly, the multivariate logistic regression reported no significant difference in NT-proBNP between Group I and Group II (OR: 1.001, 95%CI: 0.997-1.005, $P = 0.518$). The linear regression analysis (Figure 1C) further revealed a positive correlation between RDW and NT-proBNP ($r = 0.715$, $P < 0.001$) (Table 4). Finally, the ROC curve analysis was performed to determine the critical value of continuous variables (RDW and NT-proBNP) for identifying diastolic dysfunction of cardiomyopathy in cirrhosis. The criterion for the selection of optimal cut-off points was comprehensive optimization results of sensitivity and specificity. An obvious difference of P values was found for RDW and NT-proBNP (Figure 2), with a respective AUC of 0.686 (95%CI: 0.624-0.748, $P < 0.001$) and 0.556 (95%CI: 0.490-0.623, $P > 0.050$). The threshold value in ROC curves indicated that LVDD in CCM was more likely to occur if RDW was above 13.05%, with a sensitivity and specificity of 56.0% and 71.4%, respectively (Table 5).

DISCUSSION

As a chronic cardiac dysfunction, CCM is prevalent in 30%-70% of patients with cirrhosis in recent years [32,33] and features a blunted contractile response to stress and altered diastolic relaxation[34]. CCM manifests a complex progression, which depends on the systemic changes resulting from cirrhosis[35].

Table 1 Comparison of demographic and medical records in the study groups, *n* (%)

Variable	Group I (*n* = 105)	Group II (*n* = 175)	Group III (*n* = 139)	Group IV (*n* = 86)	F/χ^2	*P*
Demographics						
Age (yr)	66.20 ± 7.93	67.94 ± 7.41	67.74 ± 7.84	68.00 ± 7.86	1.344	0.259
Male	65 (61.9)	95 (54.3)	82 (59.0)	56 (65.1)	3.304	0.347
Smokers	29 (27.6)	49 (28.0)	51 (36.7)	32 (37.2)	4.697	0.195
Body-mass index (kg/m^2)	23.11 ± 2.37	23.23 ± 3.95	23.75 ± 3.24	24.27 ± 3.52	2.520	0.057
Medical history						
Hypertension	20 (19.0)	32 (18.3)	35 (25.2)	26 (30.2)	6.041	0.110
Hyperlipidemia	20 (19.0)	50 (28.6)	68 (48.9)	40 (46.5)	31.658	< 0.001
Diabetes mellitus	23 (21.9)	35 (20.0)	37 (26.6)	26 (30.2)	4.146	0.246
Atrial fibrillation	8 (7.6)	36 (20.6)	52 (37.4)	34 (39.5)	38.947	< 0.001
Stroke	3 (2.9)	5 (2.9)	4 (2.9)	4 (4.7)	0.908[1]	0.864
Cirrhosis etiology						
Fatty liver	17 (16.2)	22 (12.6)	17 (12.2)	17 (19.8)	3.277	0.351
Alcoholic liver	18 (17.1)	38 (21.7)	32 (23)	26 (30.2)	4.748	0.191
Viral hepatitis	53 (50.5)	100 (57.1)	75 (54)	36 (41.9)	5.695	0.127
Autoimmune liver disease	16 (15.2)	15 (8.6)	14 (10.1)	9 (10.5)	3.157	0.368
Liver cancer	5 (4.8)	8 (4.6)	7 (5)	4 (4.7)	0.151[1]	1.000

[1]Fisher's exact test.

Meanwhile, different criteria may indicate a distinct prevalence. A comparison between the 2005 Montreal criteria and 2019 CCC criteria[3,7] reports a higher prevalence of diastolic dysfunction by the Montreal criteria (64.8% *vs* 7.4%) and a higher proportion of cases with systolic dysfunction by the CCC criteria (16.4% *vs* 53.3%). These cases with systolic dysfunction can only be detected by echocardiography in the presence of stress[36-38]. Unlike systolic dysfunction, diastolic dysfunction appears early and can be detected at the baseline and most patients with cirrhosis display a certain degree of diastolic dysfunction[1,3,37]. Therefore, it is imminent to pinpoint some objective biomarkers before the condition deteriorates into HF.

As a traditional biomarker for the diagnosis and prognostic evaluation of HF, the clinical application of NT-proBNP is quite limited due to multiple factors[39], such as an advanced age and renal dysfunction[40]. Its effectiveness is further compromised in cases of HF with preserved ejection fraction (HFpEF), due to the impact from the clinical characteristics of HFpEF, including obesity, atrial fibrillation, and renal impairment[41]. Moreover, NT-proBNP levels may appear normal in the HFpEF patients, thereby impacting the accuracy of risk assessment[42]. Therefore, it is of great significance to find new biomarkers for the early detection of CCM.

As a hematological parameter, RDW indicates the level of anisocytosis *in vivo*. It can be assessed rapidly and economically. In acute HF patients in the emergency department (ED)[43], advanced HF patients immediately before orthotopic heart transplantation[44], and LVDD in patients with advanced stage of chronic kidney disease (CKD)[45], RDW has always been regarded as an independent predictor. Furthermore, growing evidence has confirmed an inextricable link between RDW and various types of liver-related disorders. Studies have reported the predictive value of RDW for the histological severity of primary biliary cholangitis[15] and its positive correlations with chronic hepatitis B virus infection[16,46-48], non-alcoholic fatty liver disease[49,50], and autoimmune hepatitis[17]. Altogether, these findings lend strong support to our speculation that RDW has unique value in the diagnosis of cirrhosis.

In the current study, the regression analysis showed that RDW was the only significant indicator when Group I was compared with Group II (Table 3, Part I), which highlights that RDW is the only abnormal index in the early stage of CCM. Further linear regression analysis revealed a strong positive correlation between RDW and Child-Pugh (Figure 1A) and MELD scores (Figure 1B), indicating that RDW can serve as an evaluation index for the progression of cirrhosis. As a routine parameter of blood laboratory results, RDW is closely related to HF[11,44,51]. Although the exact underlying mechanism remains controversial, several pathophysiological mechanisms of RDW increase in HF have been proposed, such as inflammation, oxidative stress, adrenergic stimulation, undernutrition, ineffective erythropoiesis, and reduced iron mobilization[51]. Studies have speculated about the link between

Table 2 Comparison of clinical data among groups, *n* (%)

Variable	Group I (*n* = 105)	Group II (*n* = 175)	Group III (*n* = 139)	Group IV (*n* = 86)	F/χ^2	*P*
Clinical feature						
Haematemesis	6 (5.7)	12 (6.9)	16 (11.5)	16 (18.6)	11.588	0.009
Edema	2 (1.9)	12 (6.9)	20 (14.4)	33 (38.4)	65.284	< 0.001
SBP	1 (1.0)	4 (2.3)	11 (7.9)	13 (15.1)	23.486	< 0.001
Hyponatremia	3 (2.9)	21 (12.0)	31 (22.3)	31 (36.0)	42.806	< 0.001
Hepatic encephalopathy	5 (4.8)	10 (5.7)	14 (10.1)	19 (22.1)	21.565	< 0.001
Refractory ascites	2 (1.9)	4 (2.3)	15 (10.8)	21 (24.4)	44.367	< 0.001
Jaundice	12 (11.4)	13 (7.4)	15 (10.8)	20 (23.3)	14.120	0.003
MELD score	8.74 ± 1.54	8.64 ± 1.57	17.04 ± 1.96[a,b]	25.19 ± 2.15[a,b,c]	2081.425	< 0.001
Laboratory index						
RDW (%)	12.54 ± 0.85	13.29 ± 1.19[a]	14.3 ± 1.96[a,b]	16.25 ± 2.13[a,b,c]	101.958	< 0.001
TBIL (μmol/L)	12.3 (10.9, 13.45)	11.5 (9.8, 14.5)	12.8 (10.7, 17.5)[b]	16.3 (13.18,24.95)[a,b,c]	57.344	< 0.001
ALB (g/L)	45.91 ± 3.83	44.92 ± 5.19[a]	37.85 ± 4.71[a,b]	33.50 ± 5.65[a,b,c]	159.072	< 0.001
ALT (IU/L)	24 (18, 32)	27 (21, 34)[a]	32 (23, 37)[a,b]	35 (26, 75)[a,b,c]	40.591	< 0.001
AST (IU/L)	26 (19.5, 33)	28 (21, 35)	30 (22, 36)[a]	34 (25, 62)[a,b]	25.257	< 0.001
γ-GT (IU/L)	32 (20, 44)	30 (22, 41)	35 (26, 43)	37 (26, 47)[a,b]	14.96	0.002
ALP (IU/L)	65 (52, 84)	74 (53, 88)	69 (54, 87)	69 (58, 84)	3.535	0.316
WBC count (× 10^9/L)	5.64 ± 1.51	5.36 ± 1.40	5.76 ± 1.16[b]	6.10 ± 1.55[a,b]	5.695	0.001
Hemoglobin (g/L)	122.86 ± 15.53	121.10 ± 15.30	107.92 ± 16.33[a,b]	99.28 ± 18.15[a,b,c]	52.186	< 0.001
Platelet count (× 10^9/L)	190.15 ± 62.47	174.98 ± 41.71[a]	101.09 ± 27.46[a,b]	90.38 ± 32.33[a,b]	165.715	< 0.001
INR	0.91 (0.59, 1.27)	1.21 (0.61, 1.80)[a]	1.58 (0.86, 2.41)[a,b]	1.37 (1.17, 2.22)[a,b]	57.797	< 0.001
NT-proBNP (pg/mL)	72 (61, 84)	76 (61, 98)	354 (127, 653)[a,b]	647 (364, 1430)[a,b,c]	242.974	< 0.001
eGFR (ml/min/1.73 m^2)	62.35 ± 11.09	60.87 ± 13.52	59.07 ± 15.94	43.31 ± 11.39[a,b,c]	40.691	< 0.001
Drug information						
Diuretic	3 (2.9)	7 (4)	20 (14.4)	32 (37.2)	69.996	< 0.001
Spirolactone	3 (2.9)	7 (4)	17 (12.2)	26 (30.2)	50.491	< 0.001
ACEI/ARB	7 (6.7)	23 (13.1)	22 (15.8)	23 (26.7)	15.690	0.001
β-blocker	6 (5.7)	13 (7.4)	23 (16.5)	22 (25.6)	23.776	< 0.001

[a]*P* < 0.05 when compared with Group I.
[b]*P* < 0.05 when compared with Group II.
[c]*P* < 0.05 when compared with Group III.
ACEI: Angiotensin converting enzyme inhibitor; ALB: Albumin; ALP: Alkaline phosphatase; ALT: Alanine transaminase; ARB: Angiotensin receptor blocker; AST: Aspartic transaminase; eGFR: Estimated glomerular filtration rate; INR: International normalized ratio; NT-proBNP: N-terminal pro-brain natriuretic peptide; RDW: Red blood cell distribution width; SBP: Spontaneous bacterial peritonitis; TBIL: Total bilirubin; WBC: White blood cell; γ-GT: γ-glutamyl transferase.

impaired hematopoiesis and cardiac dysfunction, given the concurrent presence of increased heterogeneity of erythrocyte volume in HF patients and the contributing role of anisocytosis in the HF deterioration[52]. Meanwhile, studies have also suggested NT-proBNP as an important index for the diagnosis and evaluation of HF[39]. In the current study, the comparison of NT-proBNP between groups II, III, and IV in Table 2 showed that HFpEF deteriorated with the worsening severity of cirrhosis, which was similar to the increasing tendency of RDW in the aggravating Child-Pugh levels. Nevertheless, unlike RDW, NT-proBNP was not a percipient of cardiomyopathy in patients with Child-Pugh Class A cirrhosis, which was verified by the multiple logistic regression analysis in the first part of Table 3. In order to further expound the relationship between the two indicators, the linear regression analysis was performed between RDW and NT-proBNP (Figure 1C, Table 4), which showed that they

Table 3 Multiple logistics regression analysis for each group and the control group

Part	Variable	B	SE	Wald	*P*	OR (95%CI)
Part I	RDW (%)	0.777	0.173	20.141	< 0.001	2.175 (1.549, 3.054)
	TBIL (μmol/L)	-0.086	0.051	2.810	0.094	0.918 (0.83, 1.015)
	ALB (g/L)	-0.060	0.035	2.973	0.085	0.942 (0.879, 1.008)
	ALT (IU/L)	0.122	0.067	3.350	0.067	1.129 (0.991, 1.287)
	AST (IU/L)	-0.108	0.060	3.178	0.075	0.898 (0.798, 1.011)
	γ-GT (IU/L)	0.004	0.011	0.117	0.733	1.004 (0.982, 1.026)
	WBC count (× 10^9/L)	0.026	0.107	0.059	0.808	1.026 (0.832, 1.265)
	Hemoglobin (g/L)	0.012	0.010	1.294	0.255	1.012 (0.992, 1.032)
	Platelet count (× 10^9/L)	-0.006	0.003	3.638	0.056	0.994 (0.988, 1.000)
	INR	0.418	0.290	2.074	0.150	1.519 (0.86, 2.683)
	NT-proBNP (pg/mL)	0.001	0.002	0.417	0.518	1.001 (0.997, 1.005)
	eGFR (mL/min/1.73 m^2)	-0.009	0.012	0.598	0.439	0.991 (0.967, 1.015)
	Hyperlipidemia	-0.074	0.346	0.046	0.831	0.929 (0.471, 1.830)
	Atrial fibrillation	-0.402	0.602	0.448	0.503	0.669 (0.206, 2.174)
	Haematemesis	-0.730	0.711	1.054	0.305	0.482 (0.12, 1.942)
	Edema	0.105	1.196	0.008	0.930	1.111 (0.107, 11.580)
	SBP	1.623	2.242	0.524	0.469	5.07 (0.063, 410.934)
	Hyponatremia	-1.682	0.934	3.243	0.072	0.186 (0.030, 1.16)
	Hepatic encephalopathy	-0.161	0.804	0.040	0.842	0.852 (0.176, 4.119)
	Jaundice	-1.044	1.264	0.683	0.409	0.352 (0.030, 4.188)
	Refractory ascites	0.256	1.498	0.029	0.864	1.292 (0.069, 24.324)
Part II	RDW (%)	0.895	0.294	9.265	0.002	2.447 (1.375, 4.354)
	TBIL (μmol/L)	-0.028	0.083	0.116	0.733	0.972 (0.825, 1.145)
	ALB (g/L)	-0.723	0.140	26.552	< 0.001	0.485 (0.369, 0.639)
	ALT (IU/L)	0.337	0.087	15.167	< 0.001	1.401 (1.182, 1.660)
	AST (IU/L)	-0.390	0.087	19.883	< 0.001	0.677 (0.571, 0.804)
	γ-GT (IU/L)	0.037	0.018	4.313	0.038	1.037 (1.002, 1.074)
	WBC count (× 10^9/L)	0.592	0.253	5.464	0.019	1.807 (1.100, 2.969)
	Hemoglobin (g/L)	-0.057	0.026	4.929	0.026	0.944 (0.898, 0.993)
	Platelet count (× 10^9/L)	-0.055	0.010	32.104	< 0.001	0.947 (0.929, 0.965)
	INR	1.894	0.563	11.321	0.001	6.643 (2.205, 20.018)
	NT-proBNP (pg/mL)	0.008	0.003	8.203	0.004	1.008 (1.003, 1.014)
	eGFR (mL/min/1.73 m^2)	0.062	0.027	5.365	0.021	1.064 (1.010, 1.121)
	Hyperlipidemia	-1.173	0.658	3.174	0.075	0.309 (0.085, 1.125)
	Atrial fibrillation	0.365	1.006	0.132	0.717	1.441 (0.201, 10.345)
	Haematemesis	2.282	1.499	2.318	0.128	9.792 (0.519, 184.678)
	Edema	3.004	1.778	2.855	0.091	20.159 (0.618, 657.095)
	SBP	4.715	4.750	0.985	0.321	111.572 (0.010, 1231574.165)
	Hyponatremia	-0.424	1.259	0.113	0.736	0.655 (0.055, 7.724)
	Hepatic encephalopathy	-1.850	1.290	2.057	0.151	0.157 (0.013, 1.970)

	Jaundice	1.862	2.392	0.606	0.436	6.437 (0.059, 699.588)
	Refractory ascites	-1.431	3.819	0.140	0.708	0.239 (0, 425.671)
Part III	RDW (%)	1.582	0.341	21.541	< 0.001	4.863 (2.493, 9.483)
	TBIL (μmol/L)	-0.080	0.090	0.787	0.375	0.923 (0.774, 1.101)
	ALB (g/L)	-0.910	0.150	37.020	< 0.001	0.402 (0.300, 0.539)
	ALT (IU/L)	0.350	0.087	16.273	< 0.001	1.419 (1.197, 1.682)
	AST (IU/L)	-0.410	0.088	21.725	< 0.001	0.664 (0.559, 0.789)
	γ-GT (IU/L)	0.032	0.018	3.226	0.072	1.033 (0.997, 1.070)
	WBC count (× 10^9/L)	0.763	0.292	6.798	0.009	2.144 (1.208, 3.803)
	Hemoglobin (g/L)	-0.070	0.029	5.697	0.017	0.932 (0.880, 0.988)
	Platelet count (× 10^9/L)	-0.077	0.013	35.070	< 0.001	0.926 (0.902, 0.950)
	INR	1.828	0.621	8.661	0.003	6.224 (1.842, 21.031)
	NT-proBNP (pg/mL)	0.008	0.003	7.937	0.005	1.008 (1.002, 1.014)
	eGFR (mL/min/1.73 m^2)	-0.005	0.033	0.018	0.892	0.995 (0.932, 1.063)
	Hyperlipidemia	-0.404	0.764	0.280	0.597	0.667 (0.149, 2.986)
	Atrial fibrillation	0.417	1.132	0.135	0.713	1.517 (0.165, 13.954)
	Haematemesis	3.164	1.693	3.493	0.062	23.67 (0.857, 653.530)
	Edema	3.826	1.882	4.132	0.042	45.891 (1.147, 1836.043)
	SBP	5.570	4.815	1.339	0.247	262.503 (0.021, 3291299.144)
	Hyponatremia	-0.376	1.364	0.076	0.783	0.687 (0.047, 9.940)
	Hepatic encephalopathy	-1.949	1.468	1.763	0.184	0.142 (0.008, 2.530)
	Jaundice	0.527	2.529	0.043	0.835	1.694 (0.012, 240.821)
	Refractory ascites	-0.538	3.896	0.019	0.890	0.584 (0, 1210.714)

The multiple logistics regression reference group was Group I. Child-Pugh group assignment: Group I = 0, Group II = 1, Group III = 2, Group IV = 3. Every count indicator was set to 0 if unavailable and 1 if available. ALB: Albumin; ALT: Alanine transaminase; AST: Aspartic transaminase; eGFR: Estimated glomerular filtration rate; INR: International normalized ratio; NT-proBNP: N-Terminal pro-brain natriuretic peptide; RDW: Red blood cell distribution width; SBP: Spontaneous bacterial peritonitis; TBIL: Total bilirubin; WBC: White blood cell; γ-GT: γ-glutamyl transferase.

Table 4 Pearson correlation analysis between red blood cell distribution width and each index

		Child-Pugh score	MELD score	NT-proBNP
RDW	*r* value	0.642	0.592	0.715
	P value	< 0.001	< 0.001	< 0.001

MELD score: Model for End-Stage Liver Disease score; NT-proBNP: N-terminal pro-brain natriuretic peptide; RDW: Red blood cell distribution width.

Table 5 Receiver operating characteristic curve analysis of key indexes among groups

Variable	AUC (95%CI)	SE	*P*	Critical value	Sensitivity	Specificity	Youden index
RDW	0.686 (0.624, 0.748)	0.032	< 0.001	13.05	56.0%	71.4%	0.274
NTproBNP	0.556 (0.490, 0.623)	0.034	0.114	95.50	28.0%	89.5%	0.175

AUC: Area under the curve; CI: Confidence interval; NT-proBNP: N-terminal pro-brain natriuretic peptide; RDW: Red blood cell distribution width.

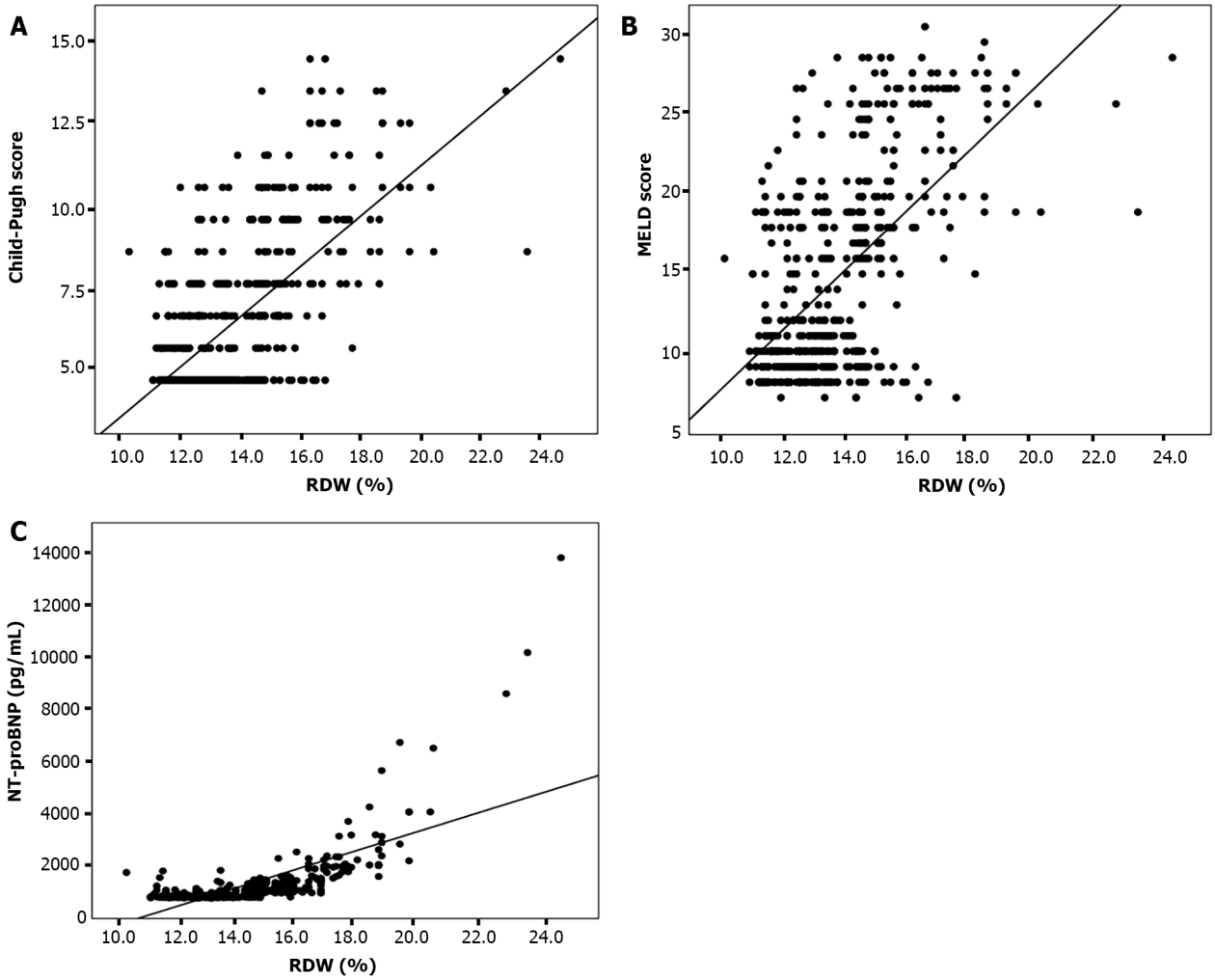

DOI: 10.3748/wjg.v29.i15.2322

Figure 1 Correlation. A: Correlation between red blood cell distribution width (RDW) and Child-Pugh scores; B: Correlation between RDW and Model for End-Stage Liver Disease scores; C: Correlation between RDW and N-terminal pro-brain natriuretic peptide. RDW: Red blood cell distribution width; NT-proBNP: N-terminal pro-brain natriuretic peptide.

were positively correlated with different slopes. The ROC curve analysis on this basis (Figure 2, Table 5) revealed that for mild cases of cirrhosis, the possibility of cardiomyopathy increased (sensitivity 56.0%, specificity 71.4%) when RDW was greater than 13.05%, while the change of NT-proBNP was not significant (P = 0.114). Taken together, these findings suggest that compared with NT-proBNP, RDW can serve as a more sensitive indicator for the early stage of CCM.

The above finding may be accounted for with the following explanations. First, cirrhosis is a chronic inflammatory disease characterized by gradual necrosis of hepatocytes, which causes a systemic inflammatory response, a slow but irreversible decline in liver function, and the development of portal hypertension[53]. On the one hand, the pathological function of the liver can increase anisocytosis and reduce erythrocyte deformability and oxygen-carrying capacity, which may further result in reduced peripheral and myocardial tissue oxygenation, contributing to HF. On the other hand, inflammatory cytokines that are closely related to cirrhosis also play an important role in the pathogenesis of HF[54], which may affect the maturation and speed of erythrocytes. Moreover, the entry of younger and larger reticulocytes into the peripheral circulation may be potential reasons for increasing RDW[50]. Still, inflammation may impair the bone marrow function, resulting in the release of premature senescent erythrocytes into the circulation and RDW increase[28,51]. Malnutrition, a common complication of liver disease, has been shown to be involved in RDW increase in HF[51]. Finally, portal hypertension due to cirrhosis can cause hemodynamic abnormalities and hypersplenism, thus accelerating the changes in erythrocyte morphology, which is inextricably linked to LVDD[4]. However, the exact mechanism awaits further exploration.

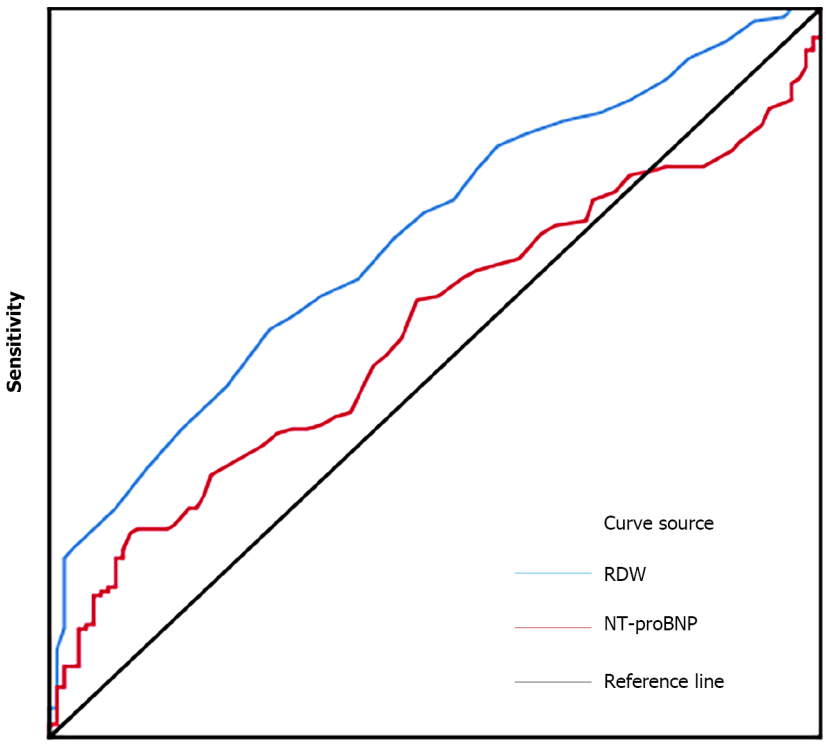

DOI: 10.3748/wjg.v29.i15.2322

Figure 2 Sensitivity and specificity of red blood cell distribution width and N-terminal pro-brain natriuretic peptide assesserd by receiver operating characteristic curve analysis. RDW: Red blood cell distribution width; NT-proBNP: N-terminal pro-brain natriuretic peptide.

CONCLUSION

Compared with NT-proBNP, RDW displays a higher sensitivity in the prediction of LVDD in CCM, especially in forepart hepetocirrhosis. A significant risk of CCM may be indicated if the quantitative RDW value of more than 13.05% is reported.

ARTICLE HIGHLIGHTS

Research background

Cirrhotic cardiomyopathy (CCM) was originally derived from studies of perioperative heart failure (HF) in liver transplant patients. In recent years, more and more researchers have found that not only patients undergoing liver transplantation, but also many patients diagnosed with cirrhosis will have cardiac insufficiency without other organic heart disease. CCM was often found in advanced cirrhosis.

Research motivation

At present, exact diagnostic criteria of echocardiography have been established for CCM. However, in most Chinese hospitals, due to high cost, echocardiography is not a good screening method for cases without clinical manifestations of HF. We are trying to find a proper method to predict CCM in order to achieve early detection and treatment.

Research objectives

To explore suitable biomarkers for early CCM prediction.

Research methods

We adopted the methods of data analysis. Under the premise of clear diagnostic criteria for CCM, risk factors were screened by multivariate regression analysis, and red blood cell distribution width (RDW), Child-Pugh classification, and N-terminal pro-brain natriuretic peptide (NT-proBNP) were analyzed by linear regression, and finally ROC curve analysis was performed to determine the critical value.

Research results

The possibility of cardiomyopathy increased (sensitivity 56.0%, specificity 71.4%) when RDW was greater than 13.05%, while the change of NT-proBNP was not significant (P = 0.114). Taken together, these findings suggest that compared with NT-proBNP, RDW can serve as a more sensitive indicator for the early stage of CCM.

Research conclusions

RDW can serve as an effective and accessible clinical indicator for the prediction of diastolic dysfunction in CCM, in which a numerical value of more than 13.05% may indicate an increasing CCM risk.

Research perspectives

First, large-scale and multi-center studies are needed to reduce the deviation error. Second, continuous hemodynamic monitoring is necessary to further analyze the hemodynamic changes in early cirrhosis.

ACKNOWLEDGEMENTS

The authors express their gratitude to the medical and technical staff of the departments of gastroenterology and cardiology who participated in this program.

FOOTNOTES

Author contributions: Guo YZ contributed to study conception and design; Chen YL contributed to data collection; Zhao ZW and Li SM contributed to data analysis; Chen YL contributed to first draft writing; Guo YZ contributed to paper review and editing.

Supported by the Fujian Provincial Education and Scientific Research Project, No. JAT200121; and Fujian Provincial Health Technology Project, No. 2021QNA021.

Institutional review board statement: All procedures involving animals were reviewed and approved by the Ethics Committee of Fujian Medical University Union Hospital (Approval No. 2022KY176).

Informed consent statement: All study participants, or their legal guardian, provided informed written consent prior to study enrollment.

Conflict-of-interest statement: There are no conflicts of interest to report.

Data sharing statement: The datasets generated during and/or analyzed during the current study are available from the corresponding author on reasonable request.

Country/Territory of origin: China

ORCID number: Yong-Zhe Guo 0000-0003-0414-3925.

S-Editor: Chen YL
L-Editor: Wang TQ
P-Editor: Chen YL

REFERENCES

1 **Stundiene I**, Sarnelyte J, Norkute A, Aidietiene S, Liakina V, Masalaite L, Valantinas J. Liver cirrhosis and left ventricle diastolic dysfunction: Systematic review. *World J Gastroenterol* 2019; **25**: 4779-4795 [PMID: 31528101 DOI: 10.3748/wjg.v25.i32.4779]
2 **Møller S**, Bernardi M. Interactions of the heart and the liver. *Eur Heart J* 2013; **34**: 2804-2811 [PMID: 23853073 DOI: 10.1093/eurheartj/eht246]
3 **Chahal D**, Liu H, Shamatutu C, Sidhu H, Lee SS, Marquez V. Review article: comprehensive analysis of cirrhotic cardiomyopathy. *Aliment Pharmacol Ther* 2021; **53**: 985-998 [PMID: 33689169 DOI: 10.1111/apt.16305]

4 **Ruíz-del-Árbol L**, Achécar L, Serradilla R, Rodríguez-Gandía MÁ, Rivero M, Garrido E, Natcher JJ. Diastolic dysfunction is a predictor of poor outcomes in patients with cirrhosis, portal hypertension, and a normal creatinine. *Hepatology* 2013; **58**: 1732-1741 [PMID: 23703953 DOI: 10.1002/hep.26509]

5 **Cholongitas E**, Goulis I, Pagourelias E, Birtsou C, Ioannidou M, Chalevas P, Soulaidopoulos S, Vassilikos V, Akriviadis E. Diastolic dysfunction is associated with low urinary sodium excretion in patients with decompensated cirrhosis. *Ann Hepatol* 2016; **15**: 545-751 [PMID: 27493103 DOI: 10.5604/16652681.1212534]

6 **Karagiannakis DS**, Vlachogiannakos J, Anastasiadis G, Vafiadis-Zouboulis I, Ladas SD. Diastolic cardiac dysfunction is a predictor of dismal prognosis in patients with liver cirrhosis. *Hepatol Int* 2014; **8**: 588-594 [PMID: 26202764 DOI: 10.1007/s12072-014-9544-6]

7 **Izzy M**, VanWagner LB, Lin G, Altieri M, Findlay JY, Oh JK, Watt KD, Lee SS; Cirrhotic Cardiomyopathy Consortium. Redefining Cirrhotic Cardiomyopathy for the Modern Era. *Hepatology* 2020; **71**: 334-345 [PMID: 31342529 DOI: 10.1002/hep.30875]

8 **Møller S**, Lee SS. Cirrhotic cardiomyopathy. *J Hepatol* 2018; **69**: 958-960 [PMID: 29716752 DOI: 10.1016/j.jhep.2018.01.006]

9 **European Association for the Study of the Liver**. EASL Clinical Practice Guidelines for the management of patients with decompensated cirrhosis. *J Hepatol* 2018; **69**: 406-460 [PMID: 29653741 DOI: 10.1016/j.jhep.2018.03.024]

10 **Singh AJ**, Wyawahare M, Sarin K, Rajendiran S, Subrahmanyam DKS, Satheesh S. Association of N- terminal Pro Brain Natriuretic Peptide with Echocardiographic Measures of Diastolic Dysfunction in Cirrhosis. *Adv Biomed Res* 2020; **9**: 55 [PMID: 33457338 DOI: 10.4103/abr.abr_250_19]

11 **Su JL**, Zhang SG, Gao RJ, Han QF, Wang LH, Zhou YH, Li T, Yao HC. Red cell distribution width is a predictor of mortality in patients with chronic heart failure. *Int J Cardiol* 2016; **212**: 79-81 [PMID: 27035607 DOI: 10.1016/j.ijcard.2016.03.064]

12 **Senthong V**, Hudec T, Neale S, Wu Y, Hazen SL, Tang WH. Relation of Red Cell Distribution Width to Left Ventricular End-Diastolic Pressure and Mortality in Patients With and Without Heart Failure. *Am J Cardiol* 2017; **119**: 1421-1427 [PMID: 28285713 DOI: 10.1016/j.amjcard.2017.01.036]

13 **Eroglu E**, Kilicgedik A, Kahveci G, Bakal RB, Kirma C. Red cell distribution width and its relationship with global longitudinal strain in patients with heart failure with reduced ejection fraction: a study using two-dimensional speckle tracking echocardiography. *Kardiol Pol* 2018; **76**: 580-585 [PMID: 29297194 DOI: 10.5603/KP.a2017.0256]

14 **Fang S**, Zhang Z, Wang Y, Jiang F, Yang K, He F, Zhang C. Predictive value of left ventricular myocardial strain by four-dimensional speckle tracking echocardiography combined with red cell distribution width in heart failure with preserved ejection fraction. *Echocardiography* 2019; **36**: 1074-1083 [PMID: 31162738 DOI: 10.1111/echo.14373]

15 **Meng J**, Xu H, Liu X, Wu R, Niu J. Increased red cell width distribution to lymphocyte ratio is a predictor of histologic severity in primary biliary cholangitis. *Medicine (Baltimore)* 2018; **97**: e13431 [PMID: 30508955 DOI: 10.1097/MD.0000000000013431]

16 **Wang J**, Huang R, Yan X, Li M, Chen Y, Xia J, Liu Y, Jia B, Zhu L, Zhang Z, Zhu C, Wu C. Red blood cell distribution width: A promising index for evaluating the severity and long-term prognosis of hepatitis B virus-related diseases. *Dig Liver Dis* 2020; **52**: 440-446 [PMID: 32008975 DOI: 10.1016/j.dld.2019.12.144]

17 **Li X**, Xu H, Gao P. Red Blood Cell Distribution Width-to-Platelet Ratio and Other Laboratory Indices Associated with Severity of Histological Hepatic Fibrosis in Patients with Autoimmune Hepatitis: A Retrospective Study at a Single Center. *Med Sci Monit* 2020; **26**: e927946 [PMID: 33180750 DOI: 10.12659/MSM.927946]

18 **Ustaoglu M**, Aktas G, Avcioglu U, Bas B, Bahceci BK. Elevated platelet distribution width and red cell distribution width are associated with autoimmune liver diseases. *Eur J Gastroenterol Hepatol* 2021; **33**: e905-e908 [PMID: 34643621 DOI: 10.1097/MEG.0000000000002296]

19 **Turcato G**, Campagnaro T, Bonora A, Vignola N, Salvagno GL, Cervellin G, Ricci G, Maccagnani A, Lippi G. Red blood cell distribution width independently predicts 1-month mortality in acute decompensation of cirrhotic patients admitted to emergency department. *Eur J Gastroenterol Hepatol* 2018; **30**: 33-38 [PMID: 29064853 DOI: 10.1097/MEG.0000000000000993]

20 **Danese E**, Lippi G, Montagnana M. Red blood cell distribution width and cardiovascular diseases. *J Thorac Dis* 2015; **7**: E402-E411 [PMID: 26623117 DOI: 10.3978/j.issn.2072-1439.2015.10.04]

21 **Aktas G**, Alcelik A, Tekce BK, Tekelioglu V, Sit M, Savli H. Red cell distribution width and mean platelet volume in patients with irritable bowel syndrome. *Prz Gastroenterol* 2014; **9**: 160-163 [PMID: 25097713 DOI: 10.5114/pg.2014.43578]

22 **Aktas G**, Sit M, Dikbas O, Tekce BK, Savli H, Tekce H, Alcelik A. Could red cell distribution width be a marker in Hashimoto's thyroiditis? *Exp Clin Endocrinol Diabetes* 2014; **122**: 572-574 [PMID: 25380549 DOI: 10.1055/s-0034-1383564]

23 **Cakır L**, Aktas G, Mercimek OB, Enginyurt O, Kaya Y, Mercimek K. Are Red Cell Distribution Width and Mean Platelet Volume associated with Rheumatoid Arthritis? *Bio Res* 2016; **27**: 292-294 [DOI: 10.9734/bjmmr/2014/12040]

24 **Dagistan Y**, Dagistan E, Gezici AR, Halicioglu S, Akar S, Özkan N, Gulali A. Could red cell distribution width and mean platelet volume be a predictor for lumbar disc hernias? *Ideggyogy Sz* 2016; **69**: 411-414 [PMID: 29733559 DOI: 10.18071/isz.69.0411]

25 **Aktas G**, Sit M, Karagoz I, Erkus E, Ozer B, Kocak MZ, Yaman S, Keyif F, Altinordu R, Erkol H, Savli H. Could Red Cell Distribution Width be a Marker of Thyroid Cancer? *J Coll Physicians Surg Pak* 2017; **27**: 556-558 [PMID: 29017671]

26 **Sousa Filho LF**, Santos MMB, da Silva Júnior WM. COVID-19 pandemic information on Brazilian websites: credibility, coverage, and agreement with World Health Organization. Quality of COVID-19 online information in Brazil. *Rev Assoc Med Bras (1992)* 2021; **67** Suppl 1: 57-62 [PMID: 34259766 DOI: 10.1590/1806-9282.67.Suppl1.20200721]

27 **Yoshiji H**, Nagoshi S, Akahane T, Asaoka Y, Ueno Y, Ogawa K, Kawaguchi T, Kurosaki M, Sakaida I, Shimizu M, Taniai M, Terai S, Nishikawa H, Hiasa Y, Hidaka H, Miwa H, Chayama K, Enomoto N, Shimosegawa T, Takehara T, Koike K. Evidence-based clinical practice guidelines for Liver Cirrhosis 2020. *J Gastroenterol* 2021; **56**: 593-619 [PMID:

34231046 DOI: 10.1007/s00535-021-01788-x]
28 **Hullin R**, Barras N, Abdurashidova T, Monney P, Regamey J. Red cell distribution width and prognosis in acute heart failure: ready for prime time! *Intern Emerg Med* 2019; **14**: 195-197 [PMID: 30547345 DOI: 10.1007/s11739-018-1995-7]
29 **Ratnasekera IU**, Johnson A, Powell EE, Henderson A, Irvine KM, Valery PC. Epidemiology of ascites fluid infections in patients with cirrhosis in Queensland, Australia from 2008 to 2017: A population-based study. *Medicine (Baltimore)* 2022; **101**: e29217 [PMID: 35608422 DOI: 10.1097/MD.0000000000029217]
30 **Salerno F**, Guevara M, Bernardi M, Moreau R, Wong F, Angeli P, Garcia-Tsao G, Lee SS. Refractory ascites: pathogenesis, definition and therapy of a severe complication in patients with cirrhosis. *Liver Int* 2010; **30**: 937-947 [PMID: 20492521 DOI: 10.1111/j.1478-3231.2010.02272.x]
31 **Vilstrup H**, Amodio P, Bajaj J, Cordoba J, Ferenci P, Mullen KD, Weissenborn K, Wong P. Hepatic encephalopathy in chronic liver disease: 2014 Practice Guideline by the American Association for the Study of Liver Diseases and the European Association for the Study of the Liver. *Hepatology* 2014; **60**: 715-735 [PMID: 25042402 DOI: 10.1002/hep.27210]
32 **Premkumar M**, Devurgowda D, Vyas T, Shasthry SM, Khumuckham JS, Goyal R, Thomas SS, Kumar G. Left Ventricular Diastolic Dysfunction is Associated with Renal Dysfunction, Poor Survival and Low Health Related Quality of Life in Cirrhosis. *J Clin Exp Hepatol* 2019; **9**: 324-333 [PMID: 31360025 DOI: 10.1016/j.jceh.2018.08.008]
33 **Razpotnik M**, Bota S, Wimmer P, Hackl M. Factors associated with the presence of cirrhotic cardiomyopathy defined according to the new multidisciplinary diagnostic criteria J Hepatol 2020; 73: S739-S740 [DOI: 10.1016/s0168-8278(20)31929-2]
34 **Wiese S**, Hove JD, Bendtsen F, Møller S. Cirrhotic cardiomyopathy: pathogenesis and clinical relevance. *Nat Rev Gastroenterol Hepatol* 2014; **11**: 177-186 [PMID: 24217347 DOI: 10.1038/nrgastro.2013.210]
35 **Wong F**. Cirrhotic cardiomyopathy. *Hepatol Int* 2009; **3**: 294-304 [PMID: 19669380 DOI: 10.1007/s12072-008-9109-7]
36 **Koshy AN**, Farouque O, Cailes B, Testro A, Ramchand J, Sajeev JK, Han HC, Srivastava PM, Jones EF, Salehi H, Teh AW, Lim HS, Calafiore P, Gow PJ. Impaired Cardiac Reserve on Dobutamine Stress Echocardiography Predicts the Development of Hepatorenal Syndrome. *Am J Gastroenterol* 2020; **115**: 388-397 [PMID: 31738284 DOI: 10.14309/ajg.0000000000000462]
37 **Lee RF**, Glenn TK, Lee SS. Cardiac dysfunction in cirrhosis. *Best Pract Res Clin Gastroenterol* 2007; **21**: 125-140 [PMID: 17223501 DOI: 10.1016/j.bpg.2006.06.003]
38 **Møller S**, Henriksen JH. Cardiovascular dysfunction in cirrhosis. Pathophysiological evidence of a cirrhotic cardiomyopathy. *Scand J Gastroenterol* 2001; **36**: 785-794 [PMID: 11495071 DOI: 10.1080/003655201750313289]
39 **Suzuki S**, Sugiyama S. The Molar Ratio of N-terminal pro-B-type Natriuretic Peptide/B-type Natriuretic Peptide for Heart Failure-related Events in Stable Outpatients with Cardiovascular Risk Factors. *Intern Med* 2018; **57**: 2621-2630 [PMID: 29709934 DOI: 10.2169/internalmedicine.0471-17]
40 **Ibrahim NE**, Januzzi JL Jr. Established and Emerging Roles of Biomarkers in Heart Failure. *Circ Res* 2018; **123**: 614-629 [PMID: 30355136 DOI: 10.1161/CIRCRESAHA.118.312706]
41 **Liang L**, Huang L, Zhao X, Zhao L, Tian P, Huang B, Feng J, Zhang J, Zhang Y. Prognostic value of RDW alone and in combination with NT-proBNP in patients with heart failure. *Clin Cardiol* 2022; **45**: 802-813 [PMID: 35621296 DOI: 10.1002/clc.23850]
42 **Januzzi JL Jr**, Myhre PL. The Challenges of NT-proBNP Testing in HFpEF: Shooting Arrows in the Wind. *JACC Heart Fail* 2020; **8**: 382-385 [PMID: 32241618 DOI: 10.1016/j.jchf.2020.03.003]
43 **Turcato G**, Cervellin G, Bonora A, Prati D, Zorzi E, Ricci G, Salvagno GL, Maccagnani A, Lippi G. Red Blood Cell Distribution Width Improves Reclassification of Patients Admitted to the Emergency Department with Acute Decompensated Heart Failure. *J Med Biochem* 2018; **37**: 299-306 [PMID: 30598626 DOI: 10.1515/jomb-2017-0054]
44 **Szygula-Jurkiewicz B**, Szczurek W, Skrzypek M, Nadziakiewicz P, Siedlecki L, Zakliczynski M, Gasior M, Zembala M. Red Blood Cell Distribution Width in End-Stage Heart Failure Patients Is Independently Associated With All-Cause Mortality After Orthotopic Heart Transplantation. *Transplant Proc* 2018; **50**: 2095-2099 [PMID: 30177116 DOI: 10.1016/j.transproceed.2018.02.141]
45 **Gromadziński L**, Januszko-Giergielewicz B, Pruszczyk P. Red cell distribution width is an independent factor for left ventricular diastolic dysfunction in patients with chronic kidney disease. *Clin Exp Nephrol* 2015; **19**: 616-625 [PMID: 25248504 DOI: 10.1007/s10157-014-1033-7]
46 **Xu WS**, Qiu XM, Ou QS, Liu C, Lin JP, Chen HJ, Lin S, Wang WH, Lin SR, Chen J. Red blood cell distribution width levels correlate with liver fibrosis and inflammation: a noninvasive serum marker panel to predict the severity of fibrosis and inflammation in patients with hepatitis B. *Medicine (Baltimore)* 2015; **94**: e612 [PMID: 25761184 DOI: 10.1097/MD.0000000000000612]
47 **Lee HW**, Kang W, Kim BK, Kim SU, Park JY, Kim DY, Ahn SH, Park YN, Han KH. Red cell volume distribution width-to-platelet ratio in assessment of liver fibrosis in patients with chronic hepatitis B. *Liver Int* 2016; **36**: 24-30 [PMID: 25966326 DOI: 10.1111/liv.12868]
48 **Fan X**, Deng H, Wang X, Fu S, Liu Z, Sang J, Zhang X, Li N, Han Q. Association of red blood cell distribution width with severity of hepatitis B virus-related liver diseases. *Clin Chim Acta* 2018; **482**: 155-160 [PMID: 29627486 DOI: 10.1016/j.cca.2018.04.002]
49 **Lou Y**, Wang M, Mao W. Clinical usefulness of measuring red blood cell distribution width in patients with hepatitis B. *PLoS One* 2012; **7**: e37644 [PMID: 22649548 DOI: 10.1371/journal.pone.0037644]
50 **Yang W**, Huang H, Wang Y, Yu X, Yang Z. High red blood cell distribution width is closely associated with nonalcoholic fatty liver disease. *Eur J Gastroenterol Hepatol* 2014; **26**: 174-178 [PMID: 24025980 DOI: 10.1097/MEG.0b013e328365c403]
51 **Xanthopoulos A**, Giamouzis G, Dimos A, Skoularigki E, Starling RC, Skoularigis J, Triposkiadis F. Red Blood Cell Distribution Width in Heart Failure: Pathophysiology, Prognostic Role, Controversies and Dilemmas. *J Clin Med* 2022; **11** [PMID: 35407558 DOI: 10.3390/jcm11071951]
52 **Yunita M**, Hariman H. Comparison of Red Cell Distribution Width (RDW) Value in Congestive Heart Failure (CHF)

Patients with Normal Persons. *Int J Res Rev* 2021; **8**: 27-30 [DOI: 10.52403/ijrr.20210806]

53 **Mehta G**, Gustot T, Mookerjee RP, Garcia-Pagan JC, Fallon MB, Shah VH, Moreau R, Jalan R. Inflammation and portal hypertension - the undiscovered country. *J Hepatol* 2014; **61**: 155-163 [PMID: 24657399 DOI: 10.1016/j.jhep.2014.03.014]

54 **Allen LA**, Felker GM, Mehra MR, Chiong JR, Dunlap SH, Ghali JK, Lenihan DJ, Oren RM, Wagoner LE, Schwartz TA, Adams KF Jr. Validation and potential mechanisms of red cell distribution width as a prognostic marker in heart failure. *J Card Fail* 2010; **16**: 230-238 [PMID: 20206898 DOI: 10.1016/j.cardfail.2009.11.003]

World Journal of Gastroenterology

Submit a Manuscript: https://www.f6publishing.com

World J Gastroenterol 2023 April 21; 29(15): 2336-2348

DOI: 10.3748/wjg.v29.i15.2336

ISSN 1007-9327 (print) ISSN 2219-2840 (online)

ORIGINAL ARTICLE

Retrospective Study

Reduction of portosystemic gradient during transjugular intrahepatic portosystemic shunt achieves good outcome and reduces complications

Shi-Hua Luo, Mi-Mi Zhou, Ming-Jin Cai, Shao-Lei Han, Xue-Qiang Zhang, Jian-Guo Chu

Specialty type: Gastroenterology and hepatology

Provenance and peer review: Unsolicited article; Externally peer reviewed.

Peer-review model: Single blind

Peer-review report's scientific quality classification

Grade A (Excellent): 0
Grade B (Very good): B, B
Grade C (Good): 0
Grade D (Fair): 0
Grade E (Poor): 0

P-Reviewer: Garbuzenko DV, Russia; Mahmoud MZ, Saudi Arabia

Received: December 9, 2022
Peer-review started: December 9, 2022
First decision: January 3, 2023
Revised: January 15, 2023
Accepted: March 23, 2023
Article in press: March 23, 2023
Published online: April 21, 2023

Shi-Hua Luo, Mi-Mi Zhou, Ming-Jin Cai, Department of Interventional Radiology, The Third Affiliated Hospital of Guangzhou Medical University, Guangzhou 510150, Guangdong Province, China

Shao-Lei Han, Department of Liver Disease, Jinan Infectious Disease Hospital, Shandong University School of Medicine, Jinan 250021, Shandong Province, China

Xue-Qiang Zhang, Department of Gastroenterology, The Second Hospital of Hebei Medical University, Shijiazhuang 050000, Hebei Province, China

Jian-Guo Chu, Department of Gastroenterology, Air Force Medical Center of PLA, Beijing 100142, China

Corresponding author: Jian-Guo Chu, MD, Professor, Department of Gastroenterology, Air Force Medical Center of PLA, No. 30 Fucheng Road, Haidian District, Beijing 100142, China. cjgchina@126.com

Abstract

BACKGROUND

Transjugular intrahepatic portosystemic shunt (TIPS) is placed important role in the therapy of complications of portal hypertension, there is still no suitable criterion for a reduction in portosystemic gradient (PSG), which can both reduce PSG and maximize clinical results and minimize hepatic encephalopathy (HE).

AIM

To compare the clinical outcomes and incidence of HE after one-third PSG reduction during TIPS in patients with variceal bleeding and refractory ascites.

METHODS

A total of 1280 patients with portal-hypertension-related complications of refractory ascites or variceal bleeding who underwent TIPS from January 2016 to January 2019 were analyzed retrospectively. Patients were divided into group A (variceal hemorrhage and PSG reduced by one third, n = 479); group B (variceal hemorrhage and PSG reduced to < 12 mmHg, n = 412); group C (refractory ascites and PSG reduced by one third, n = 217); and group D (refractory ascites and PSG reduced to < 12 mmHg of PSG, plus medication, n = 172). The clinical outcomes

were analyzed.

RESULTS

By the endpoint of follow-up, recurrent bleeding was no different between groups A and B (χ^2 = 7.062, P = 0.374), but recurrent ascites did differ significantly between groups C and D (χ^2 = 14.493, P = 0.006). The probability of total hepatic impairment within 3 years was significantly different between groups A and B (χ^2 = 11.352, P = 0.005) and groups C and D (χ^2 = 13.758, P = 0.002). The total incidence of HE differed significantly between groups A and B (χ^2 = 7.932, P = 0.016), groups C and D (χ^2 = 13.637, P = 0.007). There were no differences of survival rate between groups A and B (χ^2 = 3.376, P = 0.369, log-rank test), but did differ significantly between groups C and D (χ^2 = 13.582, P = 0.014, log-rank test).

CONCLUSION

The PSG reduction by one third may reduce the risk of HE, hepatic function damage and achieve good clinical results.

Key Words: Portal hypertension; Transjugular intrahepatic portosystemic shunt; Portosystemic gradient; Liver cirrhosis; Variceal bleeding; Refractory ascites

Core Tip: Patients with cirrhosis who underwent transjugular intrahepatic portosystemic shunt for recurrent variceal bleeding and refractory ascites were evaluated. Reduction in portosystemic gradient (PSG) should be based on the original basal pressure and reduction by one third may reduce the risk of hepatic encephalopathy, hepatic function damage and achieve similar clinical results as for the refractory ascites patients. Appropriate reduction of PSG directly influences the patient prognosis.

Citation: Luo SH, Zhou MM, Cai MJ, Han SL, Zhang XQ, Chu JG. Reduction of portosystemic gradient during transjugular intrahepatic portosystemic shunt achieves good outcome and reduces complications. *World J Gastroenterol* 2023; 29(15): 2336-2348

URL: https://www.wjgnet.com/1007-9327/full/v29/i15/2336.htm

DOI: https://dx.doi.org/10.3748/wjg.v29.i15.2336

INTRODUCTION

Transjugular intrahepatic portosystemic shunt (TIPS) is placed important role in the therapy of complications of portal hypertension[1], It has been progressively recognized as an effective therapeutic option in a growing number of clinical situations[2,3]. Measurement of portosystemic pressure gradient (PSG) is important during the TIPS procedure. Reduction of PSG can achieve good clinical results, but when PSG is too low, TIPS can have many complications, of which, hepatic encephalopathy (HE) and liver function damage are the most frequent[4]. Post-TIPS HE could depend mainly on portocaval pressure gradient and volume of blood shunted through the liver[5].

Several guidelines[6,7] recommend that the PSG should be reduced to 12 mmHg after TIPS creation to achieve a better clinical outcome. In that situation, however, the incidence of HE is higher than in clinical practice. This has prompted many centers to anecdotally adopt the technique of dilation of stent grafts using balloons with a nominal diameter of ≤ 8 mm at TIPS positioning. Recently, a new controlled expansion stent has been introduced in clinical practice (Viatorr Controlled Expansion Endoprosthesis; Gore and Associates, Flagstaff, AZ, United States), which allows lasting diameter control within a range of 8–10 mm during implantation to reach a targeted portal pressure gradient[8].

However, there is still no suitable criterion for a reduction in PSG, which can both reduce PSG and maximize clinical results and minimize HE, and few data are available to calculate an appropriate PSG value[9]. Here, we report our multicenter retrospective study to compare the occurrence of HE and clinical results of one-third reduction of PSG with PSG reduced to < 12 mmHg in patients who required TIPS placement.

MATERIALS AND METHODS

Patient information

This was a multicenter retrospective study. The Ethics Committee approved the study protocol and all procedures were conducted according to the guidelines approved by the Committee. Between January 2016 and January 2019, 1280 patients were referred on an intention-to-treat basis and underwent a TIPS procedure. Indications for stent graft shunt were variceal hemorrhage or refractory ascites. The outcomes of HE, recurrent variceal bleeding and ascites, and mortality were compared between the groups. The patients' medical records and images were reviewed to gather information regarding underlying etiology, clinical presentation, age, sex, and severity of cirrhosis (Table 1).

Study design

This was a multicenter retrospective study that compared the rate of HE and clinical outcomes after TIPS with PSG reduced by one third with PSG reduced to < 12 mmHg in patients who required TIPS placement for portal-hypertension-related complications of ascites or variceal bleeding. The patients were divided into four groups[10]: Group A (variceal hemorrhage and PSG reduced by one third, n = 479); group B (variceal hemorrhage and PSG reduced to < 12 mmHg, n = 412); group C (refractory ascites and PSG reduced by one third, n = 217); and group D (refractory ascites and PSG reduced to < 12 mmHg, plus medication, n = 172). The clinical outcomes were analyzed.

The inclusion criteria were: Recurrent variceal bleeding after a session of variceal sclerotherapy, and refractory ascites that required TIPS placement with portal-hypertension-related complications. Only *de novo* TIPS procedures using Viatorr stent grafts (Gore & Associates) were included. We excluded: TIPS procedures performed with bare stents, TIPS with bare stents followed by revision with Viatorr stent grafts, and TIPS performed with other types of stent grafts; variceal bleeding as an emergency indication; portal vein thrombosis; history of HE; severe right-sided heart failure; severe liver failure (bilirubin > 4 mg/dL), polycystic liver disease, and dilated biliary ducts; age > 75 years; Child–Pugh score > 11; Model of End-Stage Liver Disease (MELD) score > 18; hepatic carcinoma; sepsis spontaneous bacterial peritonitis; and liver transplantation.

TIPS procedure

TIPS was performed under standard local anesthesia as described previously[11]. The entire length of the intrahepatic tract was covered by the stent graft. Hepatic venous pressure gradient and portal venous pressure were measured during the procedure, and the shunts were dilated to an appropriate diameter to reach a target PSG of < 12 mmHg or reduced by one third. To reduce PSG by one third of basal value, the stent was not fully expanded, the diameter was retained, and the pressure was measured several times until it was reduced by one third. Obvious gastroesophageal collateral vessels observed during the TIPS procedure were embolized with coils (Cook Inc., Bloomington, IL, United States; or Interlock Coil, Boston Scientific Corporation, Natikeshi, MA, United States). Subsequent direct portography was performed to evaluate whether the portal venous system was completely patent.

After the TIPS procedure, intravenous Dalteparin Sodium Injection (5000 U/d; VetterPharma-Fertigung, Germany) was administered for 3 d. No patients had portal vein thrombosis, and oral warfarin was not given.

Follow-up

After TIPS deployment, baseline duplex sonography was performed. Shunt velocities were compared with this baseline result during follow-up. Patients were placed into a routine follow-up protocol identical for each group. They were seen as outpatients 1 mo after the procedure and then at 3 and 6 mo and 1 and 3 years, or whenever needed. Each consultation included a clinical examination, blood chemistry, upper abdominal ultrasonography, and assessment of HE.

TIPS angiography was performed in patients with recurrent symptoms or suspected shunt dysfunction. TIPS revision was performed when hemodynamically significant shunt stenosis (> 50%) was present with recurrent variceal bleeding, or recurrent or gradually worsening ascites. HE was defined according to the practice guidelines of the European Association for the Study of the Liver (EASL) and American Association for the Study of Liver Diseases (AASLD)[12,13]. Patients lost to follow-up were censored at the time of the last known imaging of the shunt (duplex ultrasonography or shunt venography).

Statistical analysis

Data measurements results of the four groups were normally distributed, and expressed as mean ±SD, and their differences were determined using t test. Categorical variables were expressed as frequencies and compared using χ^2 test, and their differences among the four groups were determined by one-way ANOVA. A P value of less than 0.05 was considered significant. The statistical analyses were performed with SPSS version 22.0 (SPSS, Armonk, NY, United States).

Table 1 Baseline characteristics

Characteristics	Group A	Group B	*P* value	Group C	Group D	*P* value
Gender, M/F	256/223	237/175	0.369	126/91	93/79	0.319
Age (mean ± SD) (yr)	54.616 ± 17.27	56.39 ± 12.19	0.319	56.24 ± 13.67	58.27 ± 13.25	0.246
Child–Pugh A/B/C	39/342/98	32/318/62	0.187	0/60/157	0/41/131	0.215
MELD score (mean ± SD)	8.42 ± 1.37	9.29 ± 2.16	0.576	13.26 ± 4.56	14.39 ± 5.38	0.472
Viral hepatitis	324	276	0.528	136	107	0.632
Chronic ethanol consumption	102	87	0.317	55	38	0.258
Cryptogenic hepatitis	53	49	0.492	26	27	0.146
Variceal hemorrhage	479	412	0.721	0	0	0
Refractory ascites	0	0	0	217	172	0.562
Laboratory tests						
Alanine transaminase (U/L)	48.36 ± 4.21	53.19 ± 3.27	0.462	62.13 ± 6.48	57.49 ± 7.29	0.368
Aspartate Transaminase (U/L)	54.17 ± 9.25	58.27 ± 12.37	0.361	67.43 ± 15.7	64.28 ± 17.24	0.357
Alkaline phosphatase (U/L)	145.36 ± 23.45	167.18 ± 27.36	0.382	89.67 ± 13.24	92.36 ± 16.58	0.413
γ-Glutamyl transpeptidase (U/L)	278.54 ± 37.47	259.74 ± 46.37	0.463	364.27 ± 58.74	382.17 ± 47.26	0.482
Total bilirubin (mmol/L)	29.45 ± 3.17	32.46 ± 4.28	0.147	37.18 ± 7.69	35.24 ± 8.54	0.367
Albumin (g/L)	31.28 ± 1.47	32.07 ± 1.25	0.106	28.07 ± 1.29	29.36 ± 1.48	0.294
Prothrombin time (s)	14.02 ± 1.35	15.04 ± 1.19	0.236	18.12 ± 2.39	19.23 ± 2.41	0.241
Clinical presentations						
Abdominal distention	89	93	0.261	217	172	0.562
Abdominal pain	48	52	0.273	134	97	0.183
Weakness	364	314	0.148	189	154	0.136
Poor appetite	373	362	0.302	196	153	0.324
Jaundice	28	24	0.532	21	16	0.214
Splenomegaly	264	249	0.357	205	168	0.436
Lower limbs edema	47	62	0.159	189	157	0.327
Ascites paracentesis	0	0	0	217	172	0.562
Endoscopic therapy	453	407	0.372	0	0	0

No difference ($P > 0.05$) could be seen in terms of age, sex, Child–Pugh score, MELD score, laboratory tests, and clinical presentations. MELD: Model of End-Stage Liver Disease; SD: Standard deviation; M: Male; F: Female.

RESULTS

All TIPS procedures showed similar efficacy in all four groups by reducing the PSG before and after TIPS. PSG was reduced after TIPS placement from 24.58 ± 2.41 to 15.72 ± 1.04 mmHg in group A (P = 0.012), 25.37 ± 2.54 to 11.27 ± 2.04 mmHg in group B (P = 0.004), 25.12 ± 3.16 to 16.15 ± 1.37 mmHg in group C (P = 0.016), and 24.48 ± 3.24 to 10.28 ± 1.18 mmHg in group D (P = 0.003) (Table 2). It showed that there were significant differences between groups A and B (P = 0.017) and groups C and D (P = 0.026).

No patient died within 30 d after TIPS, with an early survival of 100%. None of the patients in groups A and B had recurrent bleeding within the first week. The symptoms of ascites in 198 (91.24%) patients in group C and 161 (93.60%) in group D disappeared or were relieved without paracentesis, with no significant differences (P = 0.327).

During 3-years' follow-up, the total primary unassisted patency rates in groups A and B were 86.41% *vs* 87.24% (χ^2 = 4.486, P = 0.257), and in groups C and D were 85.31% *vs* 84.29% (χ^2 = 4.529, P = 0.248), with no significant differences (Figure 1).

Table 2 Portosystemic gradient changes in the two groups

Groups	PSG (mmHg)		*t* value	*P* value
	Before	After		
Group A	24.58 ± 2.41	15.72 ± 1.04	11.48	0.012
Group B	25.37 ± 2.54	11.27 ± 2.04	14.25	0.004
	(*t* value) 0.649	6.382		
	(*P* value) 0.483	0.026		
Group C	25.12 ± 3.16	16.15 ± 1.37	12.43	0.016
Group D	24.48 ± 3.24	10.28 ± 1.18	15.47	0.003
	(*t* value) 0.367	5.734		
	(*P* value) 0.534	0.017		

There are differences before and after transjugular intrahepatic portosystemic shunt in the four groups: group A compared with B, and group C compared with D. PSG: Portosystemic gradient.

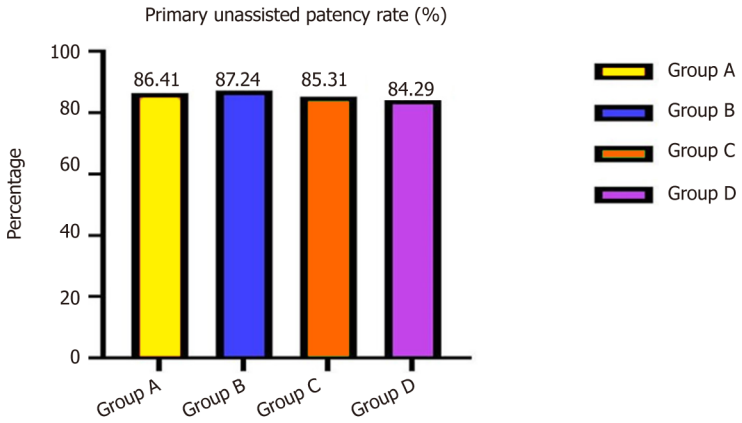

DOI: 10.3748/wjg.v29.i15.2336

Figure 1 Total primary unassisted patency rates of four groups. The total primary unassisted patency rates were not significantly different.

Forty-three (8.97%) patients in group A, 96 (23.30%) in group B, 27 (12.44%) in group C and 63 (36.62%) in group D developed hepatic function compromise after TIPS placement. The probability of total hepatic impairment within 3 years differed significantly between groups A and B (χ^2 = 11.352, *P* = 0.005) and groups C and D (χ^2 = 13.758, *P* = 0.002) (Figure 2). Mean aspartate transaminase, alanine transaminase, and total bilirubin concentrations were elevated, albumin levels decreased, and prothrombin time was prolonged compared with pre-TIPS.

At the end of follow-up, 56 (11.69%) patients in group A and 47 (11.40%) in group B had recurrent variceal bleeding, which was not a significant difference (χ^2 = 7.062, *P* = 0.374) (Figure 3).

Eighty-Nine (41.01%) patients in group C, 126 (73.25%) in group D with recurrent ascites, which was a significant difference (χ^2 = 14.493, *P* = 0.006) (Figure 4).

Of these, 27 (5.63%) patients in group A, 21 (5.09%) in group B, 13 (5.99%) in group C and nine (5.23%) in group D were caused by stent dysfunction, and after stent revision, the symptoms disappeared, and there was no significant difference between the groups (χ^2 = 834, *P* = 0.358; χ^2 = 4.574, *P* = 0.375).

The bleeding in patients in groups A and B that was not caused by stent dysfunction was relieved after medical treatment. However, 76 (35.02%) patients in group C and 117 (68.02%) in group D was not caused by stent graft dysfunction but rather hepatic dysfunction and hypoalbuminemia, which differed significantly between the two groups (χ^2 = 13.356, *P* = 0.006). After medication and albumin supplementation, the symptoms recurred many times (Table 3).

Symptoms of variceal bleeding in groups A and B disappeared within 1 wk, and symptoms of ascites in groups C and D disappeared or were relieved within 1 wk without paracentesis, and total primary unassisted patency rates were not significantly different. The probability of total hepatic impairment and recurrent symptoms was significantly different between the groups.

Table 3 Outcomes of symptoms in the four groups

Symptoms	Group A	Group B	χ^2	*P* value	Group C	Group D	χ^2	*P* value
Ascites within 1 wk	/	/		/	198 (198/217, 91.24%)	161 (161/172, 93.60%)		0.327
Hemorrhage within 1 wk	0	0		0	/	/		/
Primary unassisted patency rate	0.8641	0.8724	4.486	0.257	0.8531	0.8429	4.529	0.248
Hepatic function compromise	43 (43/479, 8.97%)	96 (96/412, 23.30%)	11.352	0.005	27 (27/217, 12.44%)	63 (63/172, 36.62%)	13.758	0.002
Recurrence of hemorrhage	56 (56/479, 11.69%)	47 (47/412, 11.40%)	7.062	0.374	/	/	/	/
Stent dysfunction	27 (27/479, 5.63%)	21 (21/412, 5.09%)	6.834	0.358	/	/	/	/
Non-stent dysfunction	29 (29/479, 6.05%)	26 (26/412, 6.31%)	6.486	0.362	/	/	/	/
Recurrence of ascites	/	/	/	/	89 (89/217, 41.01%)	126 (126/172,73.25%)	14.493	0.006
Stent dysfunction	/	/	/	/	13 (13/217, 5.99%)	9 (9/172, 5.23%)	4.574	0.375
Non-stent dysfunction	/	/	/	/	76 (76/217, 35.02%)	117 (117/172, 68.02%)	13.356	0.006

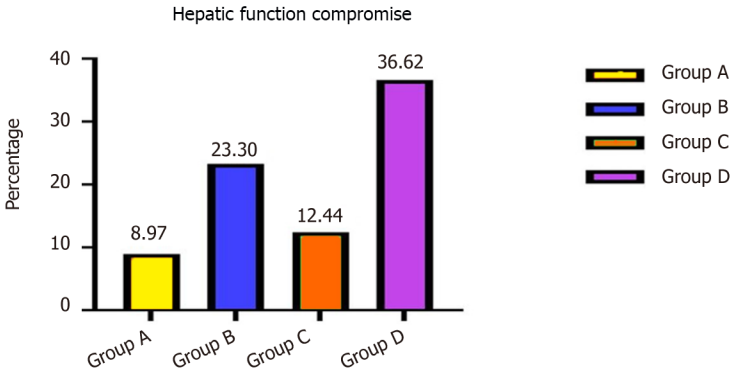

DOI: 10.3748/wjg.v29.i15.2336

Figure 2 Hepatic function compromise after transjugular intrahepatic portosystemic shunt. The probability of total hepatic impairment differed significantly between groups A and B, and C and D.

During the 3-year follow-up period, 46 (9.60%) patients in group A, 67 (16.26%) in group B, 47 (21.65%) in group C and 69 (40.11%) in group D developed HE, and the incidence of HE in group A compared with group B, and group C compared with group D differed significantly (χ^2 = 7.932, *P* = 0.016; χ^2 = 13.637, *P* = 0.007, respectively). There were significant differences in the occurrence of HE between groups A and B at 1 mo (χ^2 = 6.463, *P* = 0.027), 3 mo (χ^2 = 5.0368, *P* = 0.023), 6 mo (χ^2 = 6.473, *P* = 0.017), 1 year (χ^2 = 4.538, *P* = 0.027), 2 years (χ^2 = 5.452, *P* = 0.026) and 3 years (χ^2 = 5.467, *P* = 0.028). There were also significant differences in HE occurrence between groups C and D at 1 mo (χ^2 = 14.673, *P* = 0.014), 3 mo (χ^2 = 17.478, *P* = 0.009), 6 mo (χ^2 = 13.957, *P* = 0.011), 1 year (χ^2 = 14.576, *P* = 0.014), 2 years (χ^2 = 11.476, *P* = 0.013) and 3 years (χ^2 = 8.473, *P* = 0.017) (Figure 5).

The incidence of HE in the four groups showed a downward trend. After drug treatment, the symptoms disappeared in patients with covert and grade II HE. In patients with grade III or IV HE, the symptoms disappeared after shunt reduction, but five patients who underwent shunt reduction still had hepatic myelopathy (Table 4).

During 3 years' follow-up, 262 patients in group A, 234 in group B, 189 in group C and 160 in group D were lost to follow-up. Total survival rates were no different compared groups A with B (χ^2 = 3.376, *P* = 0.369, log-rank test), but there were significant differences between groups C and D (χ^2 =13.582, *P* = 0.014, log-rank test) (Figure 6).

The 3-mo, 6-mo, and 1-, 2-, and 3-year survival rates were different between groups A and B (χ^2 = 5.368, *P* = 0.425; χ^2 = 4.557, *P* = 0.436; χ^2 = 4.562, *P* = 0.427, χ^2 = 5.487, *P* = 0.382, and χ^2 = 4.582, *P* = 0.375, respectively); and significantly different between groups C and D (χ^2 = 13.364, *P* = 0.012; χ^2 = 12.463, *P* = 0.013; χ^2 = 12.568, *P* = 0.016; χ^2 = 11.467, *P* = 0.017, and χ^2 = 10.367, *P* = 0.027, respectively). Four hundred

Table 4 Hepatic encephalopathy occurrence in the four groups

Time	Group	HE occurrence		Occurrence rate (%)	χ^2	*P* value
		Yes	No			
1 mo	A	43	436	8.97	6.463	0.027
	B	67	345	16.26		
	C	27	190	12.44	14.673	0.014
	D	41	131	23.83		
3 mo	A	45	434	9.39	5.368	0.023
	B	79	333	19.17		
	C	39	178	17.97	17.478	0.009
	D	83	89	48.25		
6 mo	A	39	440	8.14	6.473	0.017
	B	72	340	17.47		
	C	31	186	14.28	13.957	0.011
	D	74	98	43.02		
1 year	A	36	443	7.51	4.538	0.027
	B	61	351	14.8		
	C	29	188	13.36	14.576	0.014
	D	69	103	40.11		
2 year	A	34	445	7.09	5.452	0.026
	B	49	363	11.89		
	C	23	194	10.59	11.476	0.013
	D	54	118	31.39		
3 year	A	29	443	6.14	5.467	0.028
	B	43	369	10.43		
	C	17	155	9.88	8.473	0.017
	D	42	130	24.41		
Total HE rate	A	46	433	9.6	7.932	0.016
	B	67	158	16.26		
	C	47	170	21.65	13.637	0.007
	D	69	103	40.11		

There were significant differences in incidence of hepatic encephalopathy in group A compared with groups B–D at 1, 3, 6 and 9 mo, and 1, 2 and 3 years ($P < 0.05$). HE: Hepatic encephalopathy.

and forty-nine patients died of multiorgan failure, 127 of hepatic tumor, and 298 of other causes (Table 5).

DISCUSSION

During the TIPS procedure, measuring PSG is an important step because reducing PSG can achieve good clinical results, in which a conduit is constructed within the liver between the systemic venous and portal systems, with the aim of decreasing portal systemic pressure[14]. However, too low portal pressure can lead to some complications, and to avoid the recurrence of bleeding and uncontrolled ascites induced by excess reduction of portal vein pressure, appropriate PSG levels are required[15].

Most guidelines recommend[16] that the upper threshold of the post-TIPS PSG for a patient with variceal bleeding is < 12 mmHg or 50% of baseline, and the AASLD practice guidelines suggest a

Table 5 Survival at 3 and 6 mo, and 1, 2 and 3 years

Time	Group	Survival		Survival rate (%)	χ^2	*P* value
		Yes	No			
3 mo	A	470	9	98.12	5.368	0.425
	B	401	11	97.33		
	C	184	33	84.79	13.364	0.012
	D	127	45	73.83		
6 mo	A	442	37	92.27	4.557	0.436
	B	381	31	92.47		
	C	162	55	74.65	12.463	0.013
	D	107	65	62.2		
1 year	A	397	82	82.88	4.562	0.427
	B	335	77	81.31		
	C	117	100	53.91	12.568	0.016
	D	65	107	37.79		
2 year	A	293	186	61.16	5.487	0.382
	B	245	167	59.46		
	C	59	158	27.18	11.467	0.017
	D	26	146	15.11		
3 year	A	229	250	47.8	4.582	0.375
	B	193	219	46.84		
	C	32	185	14.74	10.367	0.027
	D	16	156	9.3		
Total survival rate	A	217	262	45.3	3.376	0.369
	B	178	234	43.2		
	C	28	189	12.9	13.582	0.014
	D	12	160	6.97		

Survival rates showed no significant differences between groups A and B ($P > 0.05$), but there were significant differences between groups C and D.

gradient of ≤ 8 mmHg[17]. Most centers presently use the thresholds for TIPS procedures.

The complications of TIPS are classified as related to the TIPS procedure itself, the stent, portosystemic shunting, *etc.*[18]. Among them, HE and deterioration of liver function, as complications related to portosystemic shunting, are associated with reduced PSG. Some of the patients with low PSG after TIPS have complications such as worsening of HE, which causes multiple admissions to hospital and increased liver enzymes and bilirubin, even though they are ultimately medically controlled[19].

This creates a paradoxical dilemma in which low PSG results in complications such as severe HE or liver function failure, and inappropriate reduction of PSG also leads to recurrence of symptoms of portal hypertension, such as variceal bleeding and ascites. The current concept of small balloon expansion is intended to reduce PSG appropriately to reduce portal hypertension without associated serious complications[20].

Self-expandable stents may continue to dilate until achieving their nominal diameter[21]. This means that if PSG is 11 mmHg after dilating a 10-mm stent to only 8 mm, the stent may continue to self-dilate until reaching approximately 10 mm in diameter, leading to a further decrease in PSG and an increased risk of HE. How frequently this spontaneous expansion is clinically relevant is a matter of debate, but certainly represents a limitation. This led to a further technical improvement, the controlled-expansion stents, that cannot spontaneously dilate over preset limits. More crucially, the exact reduction of PSG is unknown.

However, we do not have an answer for simple questions such as how large the shunt should be, or what PSG reduction should be targeted to prevent recurrent bleeding or ascites during TIPS. PSG should be decreased to ≤ 12 mmHg, or by > 50% of baseline (which in most cases means < 12 mmHg) to

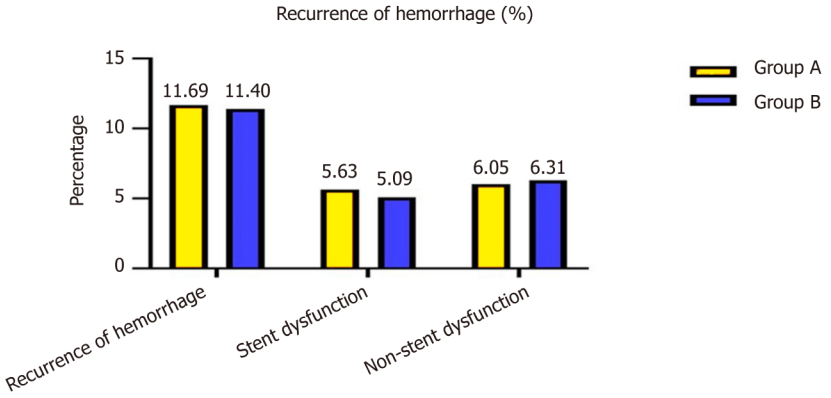

DOI: 10.3748/wjg.v29.i15.2336 **Copyright** ©The Author(s) 2023.

Figure 3 Recurrent variceal bleeding after transjugular intrahepatic portosytemic shunt. Patients in groups A and B had recurrent variceal bleeding, and there was no significant difference between the groups.

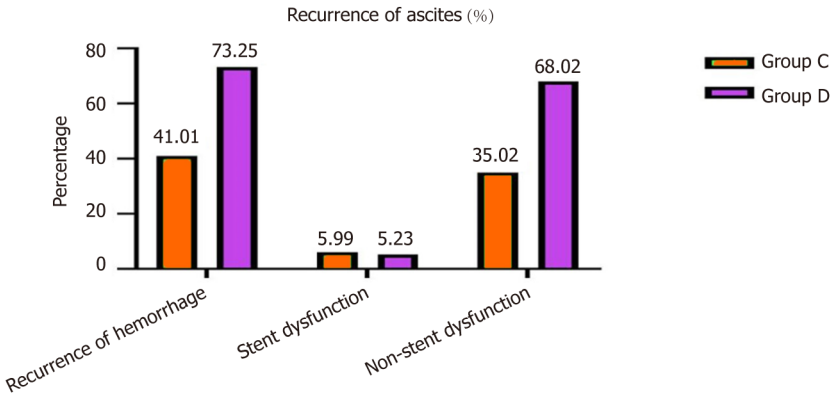

DOI: 10.3748/wjg.v29.i15.2336 **Copyright** ©The Author(s) 2023.

Figure 4 Recurrent ascites after transjugular intrahepatic portosytemic shunt of groups C and D. Patients in groups C and D had recurrent ascites, with a significant difference between the groups.

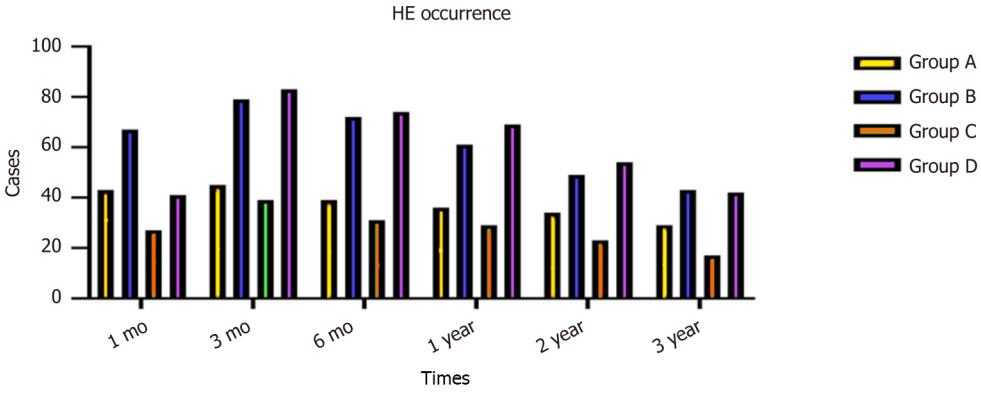

DOI: 10.3748/wjg.v29.i15.2336 **Copyright** ©The Author(s) 2023.

Figure 5 Incidence of hepatic encephalopathy after transjugular intrahepatic portosytemic shunt. The incidence of HE differed significantly in group A compared with group B, and in group C compared with group D at different times. HE: Hepatic encephalopathy.

prevent the complications of portal hypertension[22]. This comes from observations that recurrent bleeding and ascites occurred almost exclusively when patients had a PSG of at least 12 mmHg after TIPS[23].

A study has suggested that despite a traditional PSG reduction to below 12 mmHg or > 50% of baseline, a PSG decrease to 14 mmHg or > 30% of baseline would be appropriate when uncovered stents are used[24]. This goal is achieved in a large proportion of patients with small diameter TIPS such as 7

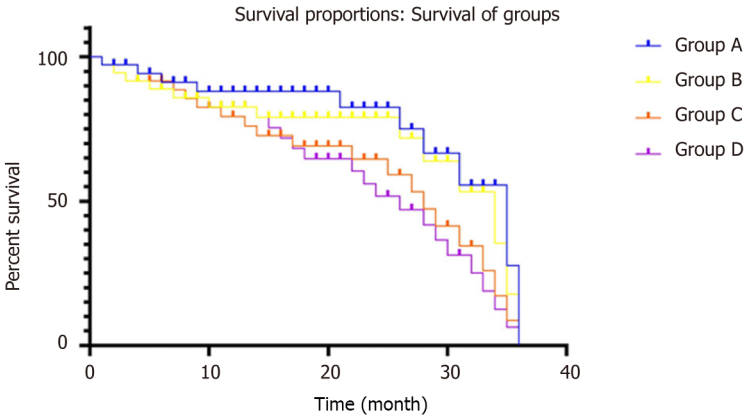

DOI: 10.3748/wjg.v29.i15.2336

Figure 6 The survival rates of four groups. The total survival rates were not different between groups A and B, but differed significantly between groups C and D.

or 6 mm dilated shunts that are likely to result in less worsening of portosystemic shunting and hence a lower likelihood of severe HE and post-TIPS liver failure[25]. Of note, in high-risk situations, such as refractory ascites, the recent EASL guidelines recommended small diameter TIPS, although not as small as 6 mm[15].

It has been shown that complementing a small diameter TIPS with drugs can be converted into a satisfactory one by adding propranolol, even at low doses[26]. The synergistic effect of combining two different mechanisms decreases PSG by bypassing liver resistance to portal flow, and propranolol decreases PSG by reducing splanchnic blood flow. This approach achieves good clinical results and lower incidence of HE. Post-TIPS HE is a complex condition that is determined by TIPS diameter and many nonhemodynamic factors. Age, degree of liver and kidney failure, chronic inflammation, urease-producing intestinal bacteria, bacterial translocation and malnutrition/sarcopenia, are other important factors that can modulate the therapeutic effect[27]. Several of them are associated with post-TIPS HE and survival[28]. Therefore, appropriate reduction of PSG can reduce the occurrence of TIPS-related complications, such as HE. Combined with drugs, if good clinical results are achieved, it is not necessary to reduce PSG too low to produce higher TIPS-related complications.

Based on the above, we hypothesize that for patients with gastrointestinal bleeding and refractory ascites requiring TIPS, one-third reduction of PSG of the baseline is appropriate, which was supplemented by drug-lowering portal pressure therapy. We should reduce portal hypertension as much as possible, achieve good therapeutic results, and minimize complications, especially the incidence of HE and compromise of liver function.

In this study, we divided the patients with gastrointestinal bleeding and refractory ascites who required TIPS into four groups, to make a detailed evaluation of the clinical effects. The results showed that, as for patients with variceal bleeding who required TIPS placement, PSG reduced by one third compared with < 12 mmHg baseline, the two groups had a similar effect on variceal bleeding, but the incidence of HE and compromise of liver function differed. During the TIPS procedure, to achieve the goal of reducing PSG by one third, a small balloon was required for gradual dilatation, slowly from 6 mm to 8 mm, which would also be useful for the controlled expansion stent that has been introduced in clinical practice. During the dilatation process, the operating procedure will be slower, PSG measurement will take approximately 30 min longer, and two more balloons will be used, resulting in increased cost. However, the cost should be worthwhile in comparison to the cost of complications.

For patients with refractory ascites who required TIPS, the incidence of HE and compromise of liver function were obviously different. In the short term, the symptoms of ascites disappear or subside, but in the medium and long term, PSG drops less, ascites still recurs in some cases, and drug therapy is necessary. Post-TIPS HE is a complex condition that is determined by TIPS and many nonhemodynamic factors. The liver function reserve of patients with refractory ascites and survival rate are poor, and the patients are prone to hypoproteinemia and electrolyte disturbances, which are likely to cause recurrence of ascites and require drug treatment[29]. In this circumstance, to reduce TIPS-related complications and liver function damage, it is not necessary to reduce PSG drastically, one-third PSG reduction plus drug therapy would be appropriate.

As a retrospective analysis, our study may manifestaed some limitations. For the one, it maybe need randomized controlled trials to validate the results. Next, to achieve main goal of reducing the PSG by one third, it requires gradual balloon dilatation from 6 mm to 8 mm, the operating procedure will be slower, PSG measurement will take approximately 30 min longer, and two more balloons will be used, resulting in increased cost. Finally, our hypothesis needs to be validated by a comparative study on the results of small balloon dilatation.

CONCLUSION

This multicenter retrospective study showed that patients who underwent TIPS creation with PSG reduced to one third of baseline or to < 12 mmHg or 50% of baseline had similar successful clinical outcomes. However, PSG reduced to < 12 mmHg had a lower rate of HE and liver compromise. Given that the PSG will become more controllable in the future with the advent of controllable stents, we believe that our concept is worthy of clinical application.

ARTICLE HIGHLIGHTS

Research background

Transjugular intrahepatic portosystemic shunt (TIPS) is placed important role in the therapy of complications of liver cirrhosis. Measuring portosystemic pressure gradient (PSG) is important during the TIPS procedure. Reducing PSG can achieve good clinical results, but when PSG is too low, TIPS leads to many complications. Factors associated with post-TIPS complications depend mainly on portocaval pressure gradient and the volume of blood shunted through the liver. Several guidelines recommend that PSG reduced to 12 mmHg after TIPS creation achieves better clinical outcomes. However, in that situation, the incidence of hepatic encephalopathy (HE) was higher in clinical practice. There is still no suitable criterion for a reduction in PSG, which can both reduce PSG and maximize clinical results and minimize HE, and few data are available to calculate an appropriate PSG value.

Research motivation

We report our multicenter retrospective study to compare the rate of HE and clinical results of reducing PSG by one third of baseline with PSG reduction to < 12 mmHg in patients with portal hypertension who required TIPS placement wtih of variceal bleeding and ascites.

Research objectives

The main objective was to establish that patients who underwent TIPS PSG reduced by one third of baseline compared with PSG reduced to < 12 mmHg of baseline were associated with similar successful clinical outcomes.

Research methods

We hypothesized that reducing PSG by one third of baseline compared with < 12 mmHg of baseline would result in a lower rate of HE and liver compromise. The patients were divided into four groups: Group A (variceal hemorrhage and PSG reduced by one third, n = 479); group B (variceal hemorrhage and PSG reduced to < 12 mmHg, n = 412); group C (refractory ascites and PSG reduced by one third, n = 217); and group D (refractory ascites and PSG reduced to < 12 mmHg, plus medication, n = 172). The clinical outcomes were compared and evaluated. Data measurements results of the four groups were normally distributed, and expressed as mean ± standard deviation, and their differences were determined using t-test. The statistical analyses were performed with SPSS version 22.0.

Research results

This study showed that during TIPS placement, when PSG was reduced by one third compared with < 12 mmHg of baseline, recurrent bleeding showed no significant difference, but recurrent ascites did differ significantly. The probability of total hepatic impairment within 3 years was significantly different. During follow-up, the total incidence of HE differed significantly. The total survival rates were no different for the variceal bleeding patients but were significantly different for the patients with refractory ascites.

Research conclusions

We found that patients who underwent TIPS PSG reduced by one third of baseline compared with reduced to < 12 mmHg of baseline were associated with similar successful clinical outcomes, but PSG reduced by one third resulted in a lower rate of HE and liver compromise.

Research perspectives

Measuring PSG is important during the TIPS procedure. Reducing PSG can achieve good clinical results, but when PSG is too low, TIPS leads to many complications. Reduction of PSG by one third of baseline is recommended to decrease the probability of liver function impairment after TIPS, decrease the incidence of HE, and increase survival in patients with refractory ascites.

ACKNOWLEDGEMENTS

We thank all the patients participated in this study, and department of gastroenterology and department of interventional radiology of all the hospital for their contributions to the data collection. We also acknowledge the cooperation of all participating units for the collection and processing of case data.

FOOTNOTES

Author contributions: Chu JG designed the research; Luo SH and Zhou MM performed the research; Han SL, Zhang XQ analyzed the data; Luo SH wrote the paper; Cai MJ revised the paper; All authors have read and approved the final version to be submitted.

Institutional review board statement: This study was reviewed and approved by the Ethics Committee of Air Force Medical Center of PLA, No. AB-22.12/06.

Informed consent statement: This is a retrospective study, and informed written consent was thus waived.

Conflict-of-interest statement: All the authors report no relevant conflicts of interest for this article.

Data sharing statement: No additional data are available.

Country/Territory of origin: China

ORCID number: Shi-Hua Luo 0000-0003-4926-144X; Mi-Mi Zhou 0000-0003-2130-9691; Jian-Guo Chu 0000-0002-4815-1129.

S-Editor: Li L
L-Editor: A
P-Editor: Li L

REFERENCES

1 **Bureau C**, Thabut D, Oberti F, Dharancy S, Carbonell N, Bouvier A, Mathurin P, Otal P, Cabarrou P, Péron JM, Vinel JP. Transjugular Intrahepatic Portosystemic Shunts With Covered Stents Increase Transplant-Free Survival of Patients With Cirrhosis and Recurrent Ascites. *Gastroenterology* 2017; **152**: 157-163 [PMID: 27663604 DOI: 10.1053/j.gastro.2016.09.016]

2 **Philips CA**, Ahamed R, Rajesh S, George T, Mohanan M, Augustine P. Beyond the scope and the glue: update on evaluation and management of gastric varices. *BMC Gastroenterol* 2020; **20**: 361 [PMID: 33126847 DOI: 10.1186/s12876-020-01513-7]

3 **Saab S**, Kim NG, Lee EW. Practical Tips on TIPS: When and When Not to Request It. *Am J Gastroenterol* 2020; **115**: 797-800 [PMID: 32427674 DOI: 10.14309/ajg.0000000000000611]

4 **Cui J**, Smolinski SE, Liu F, Xu D, Dulaimy K, Irani Z. Incrementally Expandable Transjugular Intrahepatic Portosystemic Shunts: Single-Center Experience. *AJR Am J Roentgenol* 2018; **210**: 438-446 [PMID: 29261352 DOI: 10.2214/AJR.17.18222]

5 **Schindler P**, Heinzow H, Trebicka J, Wildgruber M. Shunt-Induced Hepatic Encephalopathy in TIPS: Current Approaches and Clinical Challenges. *J Clin Med* 2020; **9** [PMID: 33238576 DOI: 10.3390/jcm9113784]

6 **Nicoară-Farcău O**, Han G, Rudler M, Angrisani D, Monescillo A, Torres F, Casanovas G, Bosch J, Lv Y, Thabut D, Fan D, Hernández-Gea V, García-Pagán JC; Preemptive TIPS Individual Data Metanalysis, International Variceal Bleeding Study and Baveno Cooperation Study groups. Effects of Early Placement of Transjugular Portosystemic Shunts in Patients With High-Risk Acute Variceal Bleeding: a Meta-analysis of Individual Patient Data. *Gastroenterology* 2021; **160**: 193-205.e10 [PMID: 32980344 DOI: 10.1053/j.gastro.2020.09.026]

7 **Morrison JD**, Mendoza-Elias N, Lipnik AJ, Lokken RP, Bui JT, Ray CE Jr, Gaba RC. Gastric Varices Bleed at Lower Portosystemic Pressure Gradients than Esophageal Varices. *J Vasc Interv Radiol* 2018; **29**: 636-641 [PMID: 29352698 DOI: 10.1016/j.jvir.2017.10.014]

8 **Mollaiyan A**, Bettinger D, Rössle M. The underdilation of nitinol stents at TIPS implantation: Solution or illusion? *Eur J Radiol* 2017; **89**: 123-128 [PMID: 28267527 DOI: 10.1016/j.ejrad.2017.01.032]

9 **Kloster ML**, Ren A, Shah KY, Alqadi MM, Bui JT, Lipnik AJ, Niemeyer MM, Ray CE, Gaba RC. High Incidence of Hepatic Encephalopathy After Viatorr Controlled Expansion Transjugular Intrahepatic Portosystemic Shunt Creation. *Dig*

Dis Sci 2021; **66**: 4058-4062 [PMID: 33236314 DOI: 10.1007/s10620-020-06716-2]
10 **de Franchis R**, Bosch J, Garcia-Tsao G, Reiberger T, Ripoll C; Baveno VII Faculty. Baveno VII - Renewing consensus in portal hypertension. *J Hepatol* 2022; **76**: 959-974 [PMID: 35120736 DOI: 10.1016/j.jhep.2021.12.022]
11 **Luo SH**, Chu JG, Huang H, Yao KC. Effect of initial stent position on patency of transjugular intrahepatic portosystemic shunt. *World J Gastroenterol* 2017; **23**: 4779-4787 [PMID: 28765699 DOI: 10.3748/wjg.v23.i26.4779]
12 **Vilstrup H**, Amodio P, Bajaj J, Cordoba J, Ferenci P, Mullen KD, Weissenborn K, Wong P. Hepatic encephalopathy in chronic liver disease: 2014 Practice Guideline by the American Association for the Study of Liver Diseases and the European Association for the Study of the Liver. *Hepatology* 2014; **60**: 715-735 [PMID: 25042402 DOI: 10.1002/hep.27210]
13 **Chalasani N**, Younossi Z, Lavine JE, Charlton M, Cusi K, Rinella M, Harrison SA, Brunt EM, Sanyal AJ. The diagnosis and management of nonalcoholic fatty liver disease: Practice guidance from the American Association for the Study of Liver Diseases. *Hepatology* 2018; **67**: 328-357 [PMID: 28714183 DOI: 10.1002/hep.29367]
14 **Pieper CC**, Jansen C, Meyer C, Nadal J, Lehmann J, Schild HH, Trebicka J, Thomas D. Prospective Evaluation of Passive Expansion of Partially Dilated Transjugular Intrahepatic Portosystemic Shunt Stent Grafts-A Three-Dimensional Sonography Study. *J Vasc Interv Radiol* 2017; **28**: 117-125 [PMID: 27553918 DOI: 10.1016/j.jvir.2016.06.023]
15 **Bosch J**. Small diameter shunts should lead to safe expansion of the use of TIPS. *J Hepatol* 2021; **74**: 230-234 [PMID: 32987029 DOI: 10.1016/j.jhep.2020.09.018]
16 **Tripathi D**, Stanley AJ, Hayes PC, Travis S, Armstrong MJ, Tsochatzis EA, Rowe IA, Roslund N, Ireland H, Lomax M, Leithead JA, Mehrzad H, Aspinall RJ, McDonagh J, Patch D. Transjugular intrahepatic portosystemic stent-shunt in the management of portal hypertension. *Gut* 2020; **69**: 1173-1192 [PMID: 32114503 DOI: 10.1136/gutjnl-2019-320221]
17 **Northup PG**, Garcia-Pagan JC, Garcia-Tsao G, Intagliata NM, Superina RA, Roberts LN, Lisman T, Valla DC. Vascular Liver Disorders, Portal Vein Thrombosis, and Procedural Bleeding in Patients With Liver Disease: 2020 Practice Guidance by the American Association for the Study of Liver Diseases. *Hepatology* 2021; **73**: 366-413 [PMID: 33219529 DOI: 10.1002/hep.31646]
18 **Khan A**, Maheshwari S, Gupta K, Naseem K, Chowdry M, Singh S. Rate, reasons, predictors, and burden of readmissions after transjugular intrahepatic portosystemic shunt placement. *J Gastroenterol Hepatol* 2021; **36**: 775-781 [PMID: 32710679 DOI: 10.1111/jgh.15194]
19 **Li W**, Duan Y, Liu Z, Lu X, She J, Qing J, Zhang C. Clinical value of hemodynamic changes in diagnosis of hepatic encephalopathy after transjugular intrahepatic portosystemic shunt. *Scand J Gastroenterol* 2022; 1-6 [PMID: 35098853 DOI: 10.1080/00365521.2022.2029938]
20 **Trebicka J**, Bastgen D, Byrtus J, Praktiknjo M, Terstiegen S, Meyer C, Thomas D, Fimmers R, Treitl M, Euringer W, Sauerbruch T, Rössle M. Smaller-Diameter Covered Transjugular Intrahepatic Portosystemic Shunt Stents Are Associated With Increased Survival. *Clin Gastroenterol Hepatol* 2019; **17**: 2793-2799.e1 [PMID: 30940552 DOI: 10.1016/j.cgh.2019.03.042]
21 **Miraglia R**, Maruzzelli L, Di Piazza A, Mamone G, Caruso S, Gentile G, Tuzzolino F, Floridia G, Petridis I, Volpes R, Luca A. Transjugular Intrahepatic Portosystemic Shunt Using the New Gore Viatorr Controlled Expansion Endoprosthesis: Prospective, Single-Center, Preliminary Experience. *Cardiovasc Intervent Radiol* 2019; **42**: 78-86 [PMID: 30073477 DOI: 10.1007/s00270-018-2040-y]
22 **Slowik V**, Monroe EJ, Friedman SD, Hsu EK, Horslen S. Pressure gradients, laboratory changes, and outcomes with transjugular intrahepatic portosystemic shunts in pediatric portal hypertension. *Pediatr Transplant* 2019; **23**: e13387 [PMID: 30932316 DOI: 10.1111/petr.13387]
23 **Zhao D**, Zhang G, Wang M, Zhang C, Li J. Portal pressure gradient and serum albumin: A simple combined parameter associated with the appearance of ascites in decompensated cirrhosis treated with transjugular intrahepatic portosystemic shunt. *Clin Mol Hepatol* 2019; **25**: 210-217 [PMID: 30897897 DOI: 10.3350/cmh.2018.0083]
24 **Perello MP**, Mur JP, Vives MS, Riutort JMM, Artigues AP, Garcia CN, Vidal MLB, Gelabert AE, Garau MV. Long-term follow-up of transjugular intrahepatic portosystemic shunt (TIPS) with stent-graft. *Diagn Interv Radiol* 2019; **25**: 346-352 [PMID: 31322502 DOI: 10.5152/dir.2019.18416]
25 **Huang Z**, Yao Q, Zhu J, He Y, Chen Y, Wu F, Hua T. Efficacy and safety of transjugular intrahepatic portosystemic shunt (TIPS) created using covered stents of different diameters: A systematic review and meta-analysis. *Diagn Interv Imaging* 2021; **102**: 279-285 [PMID: 33303394 DOI: 10.1016/j.diii.2020.11.004]
26 **Bellis L**, Moitinho E, Abraldes JG, Graupera M, García-Pagán JC, Rodés J, Bosch J. Acute propranolol administration effectively decreases portal pressure in patients with TIPS dysfunction. Transjugular intrahepatic portosystemic shunt. *Gut* 2003; **52**: 130-133 [PMID: 12477774 DOI: 10.1136/gut.52.1.130]
27 **García-Pagán JC**, Saffo S, Mandorfer M, Garcia-Tsao G. Where does TIPS fit in the management of patients with cirrhosis? *JHEP Rep* 2020; **2**: 100122 [PMID: 32671331 DOI: 10.1016/j.jhepr.2020.100122]
28 **Horhat A**, Bureau C, Thabut D, Rudler M. Transjugular intrahepatic portosystemic shunt in patients with cirrhosis: Indications and posttransjugular intrahepatic portosystemic shunt complications in 2020. *United European Gastroenterol J* 2021; **9**: 203-208 [PMID: 32819214 DOI: 10.1177/2050640620952637]
29 **Adebayo D**, Neong SF, Wong F. Refractory Ascites in Liver Cirrhosis. *Am J Gastroenterol* 2019; **114**: 40-47 [PMID: 29973706 DOI: 10.1038/s41395-018-0185-6]

World Journal of Gastroenterology

Submit a Manuscript: https://www.f6publishing.com

World J Gastroenterol 2023 April 21; 29(15): 2349-2358

DOI: 10.3748/wjg.v29.i15.2349

ISSN 1007-9327 (print) ISSN 2219-2840 (online)

ORIGINAL ARTICLE

Retrospective Study

Repeat peroral endoscopic myotomy with simultaneous submucosal and muscle dissection as a salvage option for recurrent achalasia

Yun-Juan Lin, Sheng-Zhen Liu, Long-Song Li, Ke Han, Bo-Zong Shao, En-Qiang Linghu, Ning-Li Chai

Specialty type: Gastroenterology and hepatology

Provenance and peer review: Unsolicited article; Externally peer reviewed.

Peer-review model: Single blind

Peer-review report's scientific quality classification

Grade A (Excellent): 0
Grade B (Very good): B, B, B
Grade C (Good): 0
Grade D (Fair): 0
Grade E (Poor): 0

P-Reviewer: Hakimi T, Afghanistan; Herbella FAM, Brazil; Vyshka G, Albania

Received: January 15, 2023
Peer-review started: January 15, 2023
First decision: February 7, 2023
Revised: February 20, 2023
Accepted: March 29, 2023
Article in press: March 29, 2023
Published online: April 21, 2023

Yun-Juan Lin, Department of Gastroenterology and Hepatology, Chinese PLA General Hospital and Chinese PLA Medical School, Beijing 100853, China

Sheng-Zhen Liu, Long-Song Li, Ke Han, Bo-Zong Shao, En-Qiang Linghu, Ning-Li Chai, Department of Gastroenterology and Hepatology, The First Medical Center, Chinese PLA General Hospital, Beijing 100853, China

Corresponding author: Ning-Li Chai, MD, Chief Physician, Professor, Department of Gastroenterology and Hepatology, The First Medical Center, Chinese PLA General Hospital, No. 28 Fuxing Road, Haidian District, Beijing 100853, China. chainingli@vip.163.com

Abstract

BACKGROUND

For recurrent achalasia after initial peroral endoscopic myotomy (POEM) failure, repeat POEM (Re-POEM) has been reported as a treatment option. However, severe esophageal interlayer adhesions caused by previous procedures impede the successful establishment of a submucosal tunnel and lead to aborted Re-POEM procedures. Our team previously described POEM with simultaneous submucosal and muscle dissection (POEM-SSMD) as a feasible solution for achalasia with severe interlayer adhesions.

AIM

To investigate the effectiveness and safety of Re-POEM with simultaneous submucosal and muscle dissection (Re-POEM-SSMD).

METHODS

A total of 1049 patients with achalasia who underwent successful endoscopic myotomy at the Digestive Endoscopic Center of Chinese PLA General Hospital from December 2014 to May 2022 were reviewed. Patients with recurrent achalasia who experienced initial POEM clinical failure were retrospectively included in this study. The primary endpoint was retreatment clinical success, defined as an Eckardt score ≤ 3 during the postretreatment follow-up and no need for additional treatment. Procedure-related adverse events, changes in manometric lower esophageal sphincter (LES) pressure and reflux complications, as well as procedure-related parameters, were recorded.

RESULTS

Sixteen patients underwent Re-POEM (9 patients) or Re-POEM-SSMD (7 patients)

successfully at a median of 45.5 mo (range, 4-95 mo) after initial POEM. During a median follow-up period of 31 mo (range, 7-96 mo), clinical success (Eckardt score ≤ 3) was achieved in 8 (88.9%) and 6 (85.7%) patients after Re-POEM and Re-POEM-SSMD, respectively (P = 0.849). The median Eckardt score dropped from 4 (range, 3-8) at preretreatment to 1 (range, 0-5) at postretreatment in the Re-POEM group (P = 0.025) and from 5 (range, 2-8) to 2 (range, 0-4) in the Re-POEM-SSMD group (P < 0.001). The mean manometric LES pressure decreased from 23.78 ± 9.04 mmHg to 11.45 ± 5.37 mmHg after Re-POEM (P < 0.001) and from 26.80 ± 7.48 mmHg to 11.05 ± 4.38 mmHg after Re-POEM-SSMD (P < 0.001). No serious adverse events were recorded in both groups.

CONCLUSION

In conclusion, Re-POEM-SSMD appears to be a safe and effective salvage therapy for recurrent achalasia with severe interlayer adhesions.

Key Words: Esophageal achalasia; Recurrence; Peroral endoscopic myotomy; Simultaneous submucosal and muscle dissection; Interlayer adhesion; Salvage therapy

Core Tip: For recurrent achalasia after initial peroral endoscopic myotomy (POEM) failure, repeat POEM (Re-POEM) has been reported as a potential treatment option. However, severe interlayer adhesions caused by previous procedures impede the successful establishment of a submucosal tunnel. In this study, we retrospectively analyzed the data of patients who had persistent or recurrent symptoms after initial POEM and underwent Re-POEM or Re-POEM with simultaneous submucosal and muscle dissection (Re-POEM-SSMD). The results show that Re-POEM-SSMD could serve as an effective and safe salvage option for patients with recurrent achalasia when conventional POEM procedures are impeded by severe interlayer adhesions.

Citation: Lin YJ, Liu SZ, Li LS, Han K, Shao BZ, Linghu EQ, Chai NL. Repeat peroral endoscopic myotomy with simultaneous submucosal and muscle dissection as a salvage option for recurrent achalasia. *World J Gastroenterol* 2023; 29(15): 2349-2358

URL: https://www.wjgnet.com/1007-9327/full/v29/i15/2349.htm

DOI: https://dx.doi.org/10.3748/wjg.v29.i15.2349

INTRODUCTION

Achalasia is an uncommon esophageal motor disorder estimated to affect 2 to 3 people per 100000 people in the general population and is caused by failure of adequate relaxation of the lower esophageal sphincter (LES) and impaired esophageal peristalsis[1]. Treatment options mainly include endoscopic botulinum toxin injection, laparoscopic Heller's myotomy (LHM), pneumatic dilation (PD) and peroral endoscopic myotomy (POEM) and aim to relax or cause a mechanical disruption of the LES in order to achieve symptom relief and restore quality of life[2].

POEM is a super minimally invasive surgery (SMIS) with transesophageal tunnelling endoscopic myotomy and has been used to treat achalasia since 2010[3]. Because of digestive endoscopic tunnel techniques (DETTs), diseases such as achalasia that were previously treated surgically can now be treated endoscopically by creating a submucosal tunnel as a surgical space[4]. Based on results from a multitude of retrospective studies, the clinical success rate of POEM for achalasia treatment exceeds 90%, with only approximately 5%-10% of patients remaining symptomatic postoperatively[5-7].

Recently, repeat POEM (Re-POEM) has been reported as an endoscopic therapeutic option for patients with persistent or recurrent symptoms of achalasia after POEM[8,9]. However, severe interlayer adhesions in the submucosa caused by previous POEM could hinder the establishment of a submucosal tunnel and therefore increase the procedural difficulty of RE-POEM. Coincidentally, we previously reported POEM with simultaneous submucosal and muscle dissection (POEM-SSMD) as a treatment option for patients with achalasia and severe interlayer adhesions[10]. Herein, we retrospectively compared Re-POEM and Re-POEM with simultaneous submucosal and muscle dissection (Re-POEM-SSMD) as a salvage therapy for patients with prior failed POEM procedures in terms of clinical efficacy and safety.

MATERIALS AND METHODS

Patients

We reviewed 1049 patients with achalasia who underwent successful endoscopic myotomy (POEM, Re-POEM and Re-POEM-SSMD) at the Digestive Endoscopic Center of Chinese PLA General Hospital from December 2014 to May 2022. Patients with recurrent acha-lasia who experienced initial POEM clinical failure were retrospectively included in this study. Post-POEM clinical failure was defined as having persistent or recurrent symptoms for at least 3 mo. The diagnosis of recurrent achalasia was based on medical history, clinical symptoms, esophagogastroduodenoscopy (EGD), barium swallow and manometry. Patients who had undergone surgical therapy for achalasia or had previous surgery of the esophagus were excluded. Patient demographics, baseline clinical status and preprocedural evaluation were recorded. The esophageal symptoms and clinical status were quantified using the Eckardt score [11]. The study was reviewed and approved by the Ethics Committee of Chinese PLA General Hospital (Approval No. S2021-207-01). All study participants signed a written informed consent form.

Interventions

The standard endoscopic procedures were performed by two senior endoscopists with sufficient experience in therapeutic endoscopy as previously described[12]. Patients were kept in the supine position with the right shoulder elevated. Re-POEM or Re-POEM-SSMD was performed using a single-channel high-definition gastroscope and carbon dioxide (CO_2) gas for insufflation during the procedure.

During the Re-POEM procedure, the scarred area was avoided in the opposite orientation of the initial POEM site to allow the establishment of a new submucosal tunnel. When severe interlayer adhesions impeded the establishment of new submucosal tunnel, Re-POEM-SSMD was performed to dissect the submucosa and muscle synchronously as we described previously[13].

The sequential steps were generally performed as follows: (1) The submucosal space was created by injecting methylene blue saline solution to create a liquid mat, and then an inverse T incision was made for tunnel entry; (2) the extended submucosal tunnel was terminated at the lesser curvature of the cardia (Re-POEM) or as far as possible due to the interlayer adhesions (RE-POEM-SSMD); (3) a circumferential layer myotomy was performed at the proximal esophagus and a full-thickness myotomy was performed extended to 2-3 cm below the cardia (Re-POEM), or the submucosa and muscle were incised simultaneously and a full-thickness myotomy was performed 2-3 cm below the cardia without impairing the mucosa (RE-POEM-SSMD); and (4) then the mucosal incision site was sealed using endoscopic metal clips after hemostasis was achieved.

All patients were observed for gas-related adverse events such as subcutaneous emphysema, pneumothorax or pneumoperitoneum to confirm the absence of gas leakage. After the procedure, dietary restrictions were enforced, and proton pump inhibitors (PPIs) and antibiotics were routinely administered intravenously. Upon discharge, patients were instructed to continue taking oral PPIs and adhere to a soft diet for at least four weeks.

Outcome measures

The primary endpoint was retreatment clinical success, which was defined as an Eckardt score of ≤ 3 during the postprocedure follow-up and no need for additional treatment. Secondary outcome measures were procedure-related adverse events, changes in manometric LES pressure and Eckardt score, reflux complications after retreatment, and procedure-related parameters such as operative time, tunnel length, myotomy length and length of hospital stay.

High-resolution manometry and Ling classification

LES pressures before and after retreatment were recorded by using a high-resolution manometry (HRM) system at 1-cm intervals with high-fidelity circumferential sensors (ManoScan; Sierra Scientific Instruments Inc, Los Angeles, CA, United States) as we previously described[12]. HRM was performed with patients in a supine position after a minimum of 6 hours of fasting. Pressure data of 10 wet swallows were recorded and analyzed with Mano-View software. Ling classification of achalasia, which is used to describe the endoscopic morphology of the esophageal lumen, was recorded as we previously described[14].

Follow-up

Upper gastrointestinal endoscopic evaluation including monitoring of wound healing and examination of objective signs of reflux esophagitis and HRM were scheduled at 3, 6 and 12 mo post retreatment. Patient-reported outcomes such as Eckardt scores and symptomatic reflux were recorded in the outpatient clinic or by telephone at 3, 6 and 12 mo and then annually thereafter.

Statistical analysis

The results were expressed as the mean with a standard deviation (SD) or median with a range for quantitative data and numbers with percentages for categorical data. Student's *t* test and the Mann–Whitney *U* test were used to compare baseline characteristics (other than sex), operation

Table 1 Demography and clinical profile of patients with recurrent achalasia after initial peroral endoscopic myotomy

	Total (*n* = 16)	Re-POEM (*n* = 9)	Re-POEM-SSMD (*n* = 7)	*P* value
Age, mean ± SD, yr	43.4 ± 16.3	43.0 ± 15.4	43.86 ± 18.7	0.916
Male, *n* (%)	9 (56.3)	4 (44.4)	5 (71.4)	0.008
Duration of dysphagia, median (range), mo	86.5 (16-420)	92 (16-147)	24 (16-420)	0.751
Time symptoms recurred after initial POEM, median (range), mo	15.5 (0-92)	12 (0-92)	7.5 (0-50)	0.414
Interval between initial POEM and Re-POEM, median (range), mo	45.5 (4-95)	64 (14-95)	9 (4-60)	0.013
Achalasia endoscopy type, *n* (%)				
Ling I	2 (12.5)	2 (22.2)	0 (0)	
Ling IIa	5 (31.3)	3 (33.3)	2 (28.6)	
Ling IIb	1 (6.3)	0 (0)	1 (14.3)	
Ling IIc	5 (31.3)	3 (33.3)	2 (28.6)	
Ling IIIr	3 (18.8)	1 (11.1)	2 (28.6)	

The values are expressed as mean ± SD or medians (range) for quantitative data, and *n* (%) for categorical data. SD: Standard deviation; POEM: Peroral endoscopic myotomy; Re-POEM: Repeat peroral endoscopic myotomy; Re-POEM-SSMD: Repeat peroral endoscopic myotomy with simultaneous submucosal and muscle dissection.

parameters, Eckardt score and LES pressure between the Re-POEM and Re-POEM-SSMD groups. Fisher's exact test was used to compare sex, clinical success and reflux complications between the Re-POEM and Re-POEM-SSMD groups. The Friedman Test was used to compare the baseline, preretreatment and postretreatment Eckardt score and Paired Student's *t* test was used to compare preretreatment and postretreatment LES pressure. All reported *P* values were two-tailed, with statistical significance set at $P < 0.05$. Statistical analyses were performed using SPSS software (version 26.0; SPSS, Chicago, IL, United States).

RESULTS

Clinical characteristics of patients

Sixteen patients (9 male, 7 female; mean age 43.4 ± 16.3 years) who experienced initial POEM clinical failure were diagnosed with recurrent achalasia. The median duration of dysphagia was 86.5 mo (range, 16-420 mo). Symptoms of achalasia recurred a median time of 15.5 mo (range, 0-92 mo) after initial POEM. Retreatment procedures were conducted after a mean of 45.5 mo (range, 4-95 mo) following the initial POEM. According to the Ling classification, 2 patients (12.5%), 5 patients (31.3%), 1 patient (6.3%), 5 patients (31.3%) and 3 patients (18.8%) had Ling I, Ling IIa, Ling IIb, Ling IIc and Ling IIIr types, respectively (Table 1).

Procedure-related parameters and adverse events

Re-POEM (9 patients) and Re-POEM-SSMD (7 patients) procedures were conducted successfully in all patients. A representative case of Re-POEM-SSMD is described in Figure 1. The mean operative time was 39.22 ± 15.19 min in the Re-POEM group and 47.86 ± 9.71 min in the Re-POEM-SSMD group ($P = 0.414$). The median lengths of the submucosal tunnel and myotomy were 9 cm (range, 7-13 cm) and 6 cm (range, 4.5-11 cm) in the Re-POEM group and 5 cm (range, 4-12 cm) ($P = 0.012$) and 6 cm (range, 4-11 cm) ($P = 1.000$) in the Re-POEM-SSMD group, respectively. Prophylactic antibiotics were administered for 3 to 6 d after the procedures. The average length of hospital stay was 6.0 ± 1.7 d and 7.1 ± 1.3 d after Re-POEM and Re-POEM-SSMD, respectively ($P = 0.454$). Regarding procedure-related adverse events, computed tomography showed pneumoperitoneum in two patients in the Re-POEM group but no apparent clinical consequence occurred during later follow-up. One patient in the Re-POEM-SSMD group sustained mucosal perforation during submucosal tunnel construction and was treated by endoscopic metal clips, no additional clinical complications were observed (Table 2).

Treatment outcomes and reflux complications

During a median follow-up period of 31 mo (range, 7-96 mo), clinical success (Eckardt score ≤ 3) was achieved in 8 (88.9%) and 6 (85.7%) patients after Re-POEM and Re-POEM-SSMD, respectively ($P =$

Table 2 Operation information and treatment outcomes of patients with recurrent achalasia after initial peroral endoscopic myotomy

	Re-POEM (*n* = 9)	Re-POEM-SSMD (*n* = 7)	*P* value
Operation parameters			
Operative time, mean ± SD, min	39.22 ± 15.19	47.86 ± 9.71	0.414
Submucosal tunnel length, median (range), cm	9 (7-13)	5 (4-12)	0.012
Myotomy length, median (range), cm	6 (4.5-11)	6 (4-11)	1.000
Postoperative hospital stay, mean ± SD, d	6.0 ± 1.7	7.1 ± 1.3	0.454
Adverse events, *n*			
Mucosal injury	0	1	
Subcutaneous emphysema	0	0	
Pneumothorax	0	0	
Pneumoperitoneum	2	0	
Tunnel infection	0	0	
Clinical success during follow-up, *n* (%)	8 (88.9)	6 (85.7)	0.849
Eckardt score, median (range)			
Pre-POEM	6 (2-8)	5 (2-8)	0.892
Preretreatment	4 (3–8)	5 (2-8)	0.425
Postretreatment	1 (0-5)	2 (0-4)	0.416
Lower esophageal sphincter pressure, mean ± SD, mmHg			
Preretreatment	23.78 ± 9.04	26.80 ± 7.48	0.489
Postretreatment	11.45 ± 5.37	11.05 ± 4.38	0.872
Reflux complications			
Symptomatic reflux, *n* (%)	6 (66.7)	0 (0)	0.001
R, *n* (%)	6 (66.7)	3 (42.9)	0.100

SD: Standard deviation; POEM: Peroral endoscopic myotomy; Re-POEM: Repeat peroral endoscopic myotomy; Re-POEM-SSMD: Repeat peroral endoscopic myotomy with simultaneous submucosal and muscle dissection.

0.849). None of the patients underwent balloon dilation, temporary esophageal stent placement, or botulinum toxin injections after POEM or retreatment. One patient in the Re-POEM group had recurrent symptoms of achalasia and chose a follow-up strategy. Reintervention was performed in 1 patient in the Re-POEM-SSMD group for recurrent symptoms (Table 2).

The median Eckardt score dropped from 4 (range, 3-8) at preretreatment to 1 (range, 0-5) at postretreatment in the Re-POEM group ($P = 0.025$) and from 5 (range, 2-8) to 2 (range, 0-4) in the Re-POEM-SSMD group ($P < 0.001$) (Figure 2). The mean manometric LES pressure decreased from 23.78 ± 9.04 mmHg to 11.45 ± 5.37 mmHg after Re-POEM ($P < 0.001$) and from 26.80 ± 7.48 mmHg to 11.05 ± 4.38 mmHg after Re-POEM-SSMD ($P < 0.001$) (Figure 3).

At the follow-up EGD, no severe complications, such as delayed bleeding or mucosal barrier failure, were detected. The overall rate of clinical reflux complications following retreatment was 56.3% (9/16). Six patients developed symptomatic gastroesophageal reflux such as heartburn and reflux after Re-POEM and were treated by intermittent administration of standard-dose PPI. Reflux esophagitis was detected in six patients (Los Angeles classification A, 2; B, 1; C, 3) in the Re-POEM and three (Los Angeles classification B, 1; C, 2) in the Re-POEM-SSMD group ($P = 0.100$).

DISCUSSION

Although POEM is highly effective as a first-line treatment for achalasia, a small percentage of patients remain symptomatic or experience relapse after POEM[15,16]. Inadequate myotomy below the EGJ, premature fusion healing and early myotomy site scarring may be the main causes of recurrent dysphagia in POEM patients. Prior botulinum toxin injections and balloon dilations may also lead to substantial fibrosis, making myotomy more difficult. Consensus on the optimal management strategy

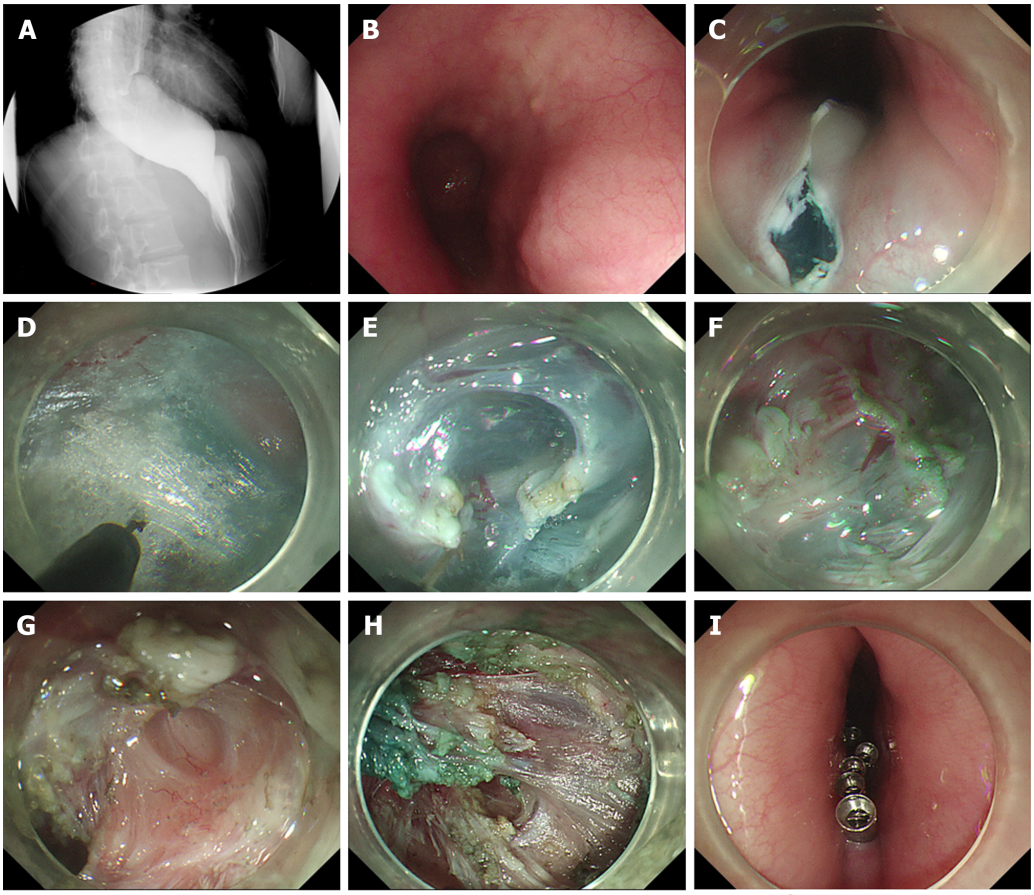

DOI: 10.3748/wjg.v29.i15.2349

Figure 1 Repeat peroral endoscopic myotomy with simultaneous submucosal and muscle dissection in a 28-year-old woman with recurrence of symptoms after previous peroral endoscopic myotomy. A: Radiographic image showing the difficulty of barium to pass through the pipe into the stomach; B: The mucosal scar of previous peroral endoscopic myotomy; C: Reverse T incision of submucosal entry near the scarred area; D: Construction of the submucosal tunnel; E: Obvious submucosal fibrosis disconnected by electrocoagulation forceps; F: Simultaneous submucosal and muscle dissection started from the muscular scar; G: Full-thickness myotomy of the esophagus; H: Exact hemostasis using hemostatic forceps; I: Closure of the mucosal entry point with metal clips.

for patients with recurrent achalasia after initial POEM failure has not yet been reached.

Re-POEM after failed surgical Heller myotomy has been reported to have good short-term results[17,18]. Recently, Re-POEM has also been described as an effective endoscopic therapy for the treatment of achalasia after failed initial POEM procedures with clinical success rates ranging from 63%-100%[8,19]. Moreover, Ichkhanian *et al*[9] reported that when compared with pneumatic dilation and LHM, Re-POEM had a higher clinical success rate in the management of patients with failed initial POEM. As a SMIS, Re-POEM is less invasive compared to Heller myotomy and requires fewer attempts compared to balloon dilation. In this retrospective study, we found that Re-POEM had a clinical success rate of 88.9% for recurrent achalasia after initial POEM failure, which is similar to that reported in previous studies.

In POEM procedures, submucosal tunnel dissection and endoscopic myotomy must extend deep beyond the gastroesophageal junction (at least 2 cm) to guarantee the success of POEM[16]. Re-POEM is technically challenging due to the presence of post-POEM interlayer adhesions and fibrosis and is usually performed using a new submucosal tunnel in a relatively unobstructed area to avoid contact with the previous procedure site. The presence of severe esophageal interlayer adhesions impede the establishment of a new submucosal tunnel. In 2014, our team introduced a novel, modified procedure, entitled POEM-SSMD, to address severe interlayer adhesions[10]. As a result of the procedure, the long-term symptom relief rate was 83% with controllable adverse events for patients with achalasia and severe interlayer adhesions[13]. Interlayer adhesions are more common in patients with recurrent achalasia who underwent initial POEM than in patients with untreated achalasia. Re-POEM-SSMD can be performed in the scar area of an earlier myotomy site without considering the adhesions or fibrosis from the previous operation, which makes it easier for the endoscopist to select the preferred direction of the myotomy. Based on our data, Re-POEM-SSMD had a comparable clinical success rate of 85.7% and could serve as an effective salvage option when conventional endoscopic procedures are impeded by severe interlayer adhesions caused by previous POEM procedures.

The orientation selection of Re-POEM and whether to use SSMD operation depends on the preference of the endoscopists and their own technical levels. Before retreatment, mucosal inflammation and submucosal fibrosis of the esophagus are classified to determine the degree of adhesion[20]. If the initial

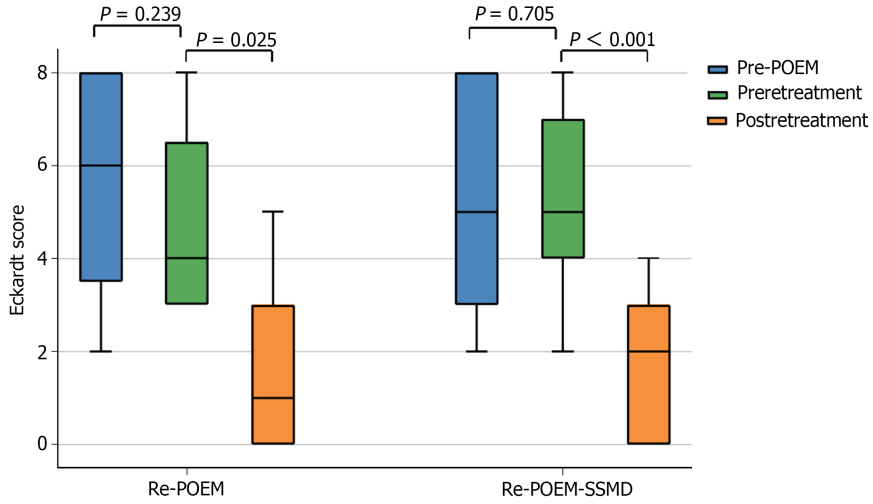

DOI: 10.3748/wjg.v29.i15.2349 **Copyright** ©The Author(s) 2023.

Figure 2 Eckardt score changes in patients with recurrent achalasia. POEM: Peroral endoscopic myotomy; Re-POEM: Repeat peroral endoscopic myotomy; Re-POEM-SSMD: Repeat peroral endoscopic myotomy with simultaneous submucosal and muscle dissection.

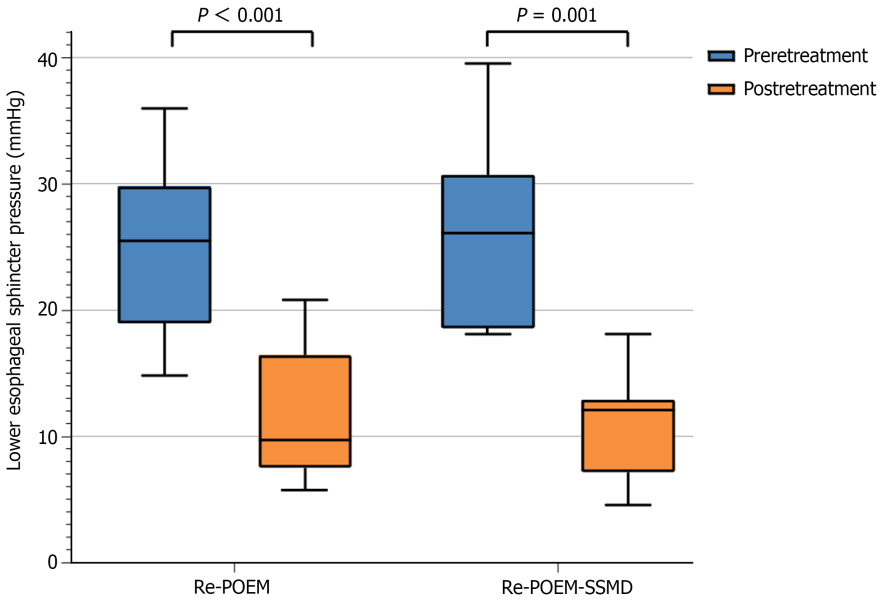

DOI: 10.3748/wjg.v29.i15.2349 **Copyright** ©The Author(s) 2023.

Figure 3 Lower esophageal sphincter pressure changes in patients with recurrent achalasia. Re-POEM: Repeat peroral endoscopic myotomy; Re-POEM-SSMD: Repeat peroral endoscopic myotomy with simultaneous submucosal and muscle dissection.

operative region has obvious adhesions and the rest of esophagus has no or mild adhesions, another tunnel can be created at the contralateral esophagus to improve the success rate of Re-POEM. If the esophagus has severe and extensive adhesions and performing SSMD is necessary, the endoscopist can choose to create a tunnel at the original procedure site, which usually means a relatively comfortable operative orientation and may help to improve the technical success rate.

In the Re-POEM-SSMD group, due to the presence of post-POEM adhesions and fibrosis, the submucosa and muscle layer are cut simultaneously from the adhesion site with aborted intended termination point of the submucosal tunnel, leading to a shorter submucosal tunnel than that created in conventional RE-POEM procedures.

The incidence of major adverse events such as vital-sign instability and intensive care unit stay ranged between 2% and 4% in the published literature[21-23]. No major adverse events were recorded in both groups of our study. A rupture in the mucosa may compromise its integrity and lead to esophageal leakage and secondary infection, which should be managed appropriately once identified. One mucosal injury in the Re-POEM-SSMD group was successfully managed with secure closure and sufficient drainage without the need for surgical repair. The incision made at the tunnel entry site in the mucosa should be tightly clipped after myotomy. CO_2 should be used as the insufflation gas and a lower

flow should be used sparingly once the creation of the submucosal tunnel or SSMD is started. In our study, two cases of pneumoperitoneum in the Re-POEM group were recorded but no apparent clinical consequence occurred during later follow-up. It should be noted that Re-POEM-SSMD should be performed by endoscopists with sufficient experience in therapeutic endoscopy and after preparation for all contingencies.

Gastroesophageal reflux and Barrett's esophagus are usually considered long-term major concerns after POEM with no antireflux procedure[15]. Our study showed that fewer cases of symptomatic reflux occurred in the Re-POEM-SSMD group than in the Re-POEM group. Re-POEM-SSMD was more likely to be performed in the earlier myotomy site, while Re-POEM was usually performed in the opposite direction with a new myotomy site. Therefore, in Re-POEM-SSMD, less damage to the muscular layer may be responsible for less symptomatic reflux. Nevertheless, follow-up EGD showed no difference in postretreatment LES pressure or incidence of esophagitis between the two groups. Therefore, the results should be interpreted with caution and effectiveness of Re-POEM-SSMD in reducing reflux must be verified in prospective studies with large samples.

There are several limitations to the current study. For instance, a small sample of patients were classified into two groups, so a subgroup analysis of the Ling classification could not be performed. Moreover, the retrospective nature of the study and variable duration of follow-up were also limitations. There was also a potential for patient selection bias.

CONCLUSION

In conclusion, Re-POEM-SSMD appears to be a safe and effective salvage option for recurrent achalasia with adhesions or fibrosis caused by previous POEM procedures, thereby broadening the applicability of Re-POEM to patients after failed POEM. We are awaiting the results of the RCT and long-term follow-up.

ARTICLE HIGHLIGHTS

Research background

For recurrent achalasia after initial peroral endoscopic myotomy (POEM) failure, repeat POEM (Re-POEM) has been reported as a treatment option.

Research motivation

Interlayer adhesions caused by previous POEM procedures are common, which could impede the establishment of a submucosal tunnel and even lead to aborted Re-POEM procedures.

Research objectives

This study aimed to evaluate the efficacy and safety of Re-POEM with simultaneous submucosal and muscle dissection (Re-POEM-SSMD) as a salvage therapy for recurrent achalasia with severe esophageal interlayer adhesions after prior failed POEM procedures.

Research methods

Patients diagnosed with recurrent achalasia who underwent Re-POEM or Re-POEM-SSMD in our center were retrospectively analyzed in terms of clinical efficacy, incidence of procedure-related adverse events and reflux complications.

Research results

Clinical success (Eckardt score ≤ 3) was achieved in 8 (88.9%) patients after Re-POEM and 6 (85.7%) patients after Re-POEM-SSMD (P = 0.849). No severe adverse events were recorded in both groups.

Research conclusions

Re-POEM-SSMD could serve as a safe and effective salvage therapy for recurrent achalasia with severe interlayer adhesions.

Research perspectives

Further studies in large-scale patient population and prospective studies are required to verify the efficacy and safety of Re-POEM-SSMD in the management of patients after failed POEM. Further evaluation of the validity of Re-POEM-SSMD in reducing reflux is also awaited.

ACKNOWLEDGEMENTS

We thank our peer reviewers for the insightful and thorough suggestions on this manuscript.

FOOTNOTES

Author contributions: Chai NL was the guarantor and designed the study; Lin YJ and Liu SZ participated in the acquisition, analysis, and interpretation of the data, and drafted the initial manuscript; Li LS, Han K, and Shao BZ revised the article critically for important intellectual content; Linghu EQ and Chai NL were the patient's endoscopists; and all authors read and approved the final version.

Institutional review board statement: The study was reviewed and approved by the Ethics Committee of Chinese PLA General Hospital (Approval No. S2021-207-01).

Informed consent statement: All study participants or their legal guardian provided informed written consent about personal and medical data collection prior to study enrolment.

Conflict-of-interest statement: The authors declare no conflicts of interest for this article.

Data sharing statement: No additional data are available.

Country/Territory of origin: China

ORCID number: Yun-Juan Lin 0000-0002-2140-777x; Sheng-Zhen Liu 0000-0001-9206-8173; Long-Song Li 0000-0002-4000-7501; Ke Han 0000-0002-6243-8193; Bo-Zong Shao 0000-0002-2621-0669; En-Qiang Linghu 0000-0003-4506-7877; Ning-Li Chai 0000-0002-6791-5817.

S-Editor: Yan JP
L-Editor: A
P-Editor: Cai YX

REFERENCES

1 **Boeckxstaens GE**, Zaninotto G, Richter JE. Achalasia. *Lancet* 2014; **383**: 83-93 [PMID: 23871090 DOI: 10.1016/S0140-6736(13)60651-0]
2 **Eckardt AJ**, Eckardt VF. Treatment and surveillance strategies in achalasia: an update. *Nat Rev Gastroenterol Hepatol* 2011; **8**: 311-319 [PMID: 21522116 DOI: 10.1038/nrgastro.2011.68]
3 **Inoue H**, Minami H, Kobayashi Y, Sato Y, Kaga M, Suzuki M, Satodate H, Odaka N, Itoh H, Kudo S. Peroral endoscopic myotomy (POEM) for esophageal achalasia. *Endoscopy* 2010; **42**: 265-271 [PMID: 20354937 DOI: 10.1055/s-0029-1244080]
4 **Chai NL**, Li HK, Linghu EQ, Li ZS, Zhang ST, Bao Y, Chen WG, Chiu PW, Dang T, Gong W, Han ST, Hao JY, He SX, Hu B, Huang XJ, Huang YH, Jin ZD, Khashab MA, Lau J, Li P, Li R, Liu DL, Liu HF, Liu J, Liu XG, Liu ZG, Ma YC, Peng GY, Rong L, Sha WH, Sharma P, Sheng JQ, Shi SS, Seo DW, Sun SY, Wang GQ, Wang W, Wu Q, Xu H, Xu MD, Yang AM, Yao F, Yu HG, Zhou PH, Zhang B, Zhang XF, Zhai YQ. Consensus on the digestive endoscopic tunnel technique. *World J Gastroenterol* 2019; **25**: 744-776 [PMID: 30809078 DOI: 10.3748/wjg.v25.i7.744]
5 **Khashab MA**, El Zein M, Kumbhari V, Besharati S, Ngamruengphong S, Messallam A, Abdelgalil A, Saxena P, Tieu AH, Raja S, Stein E, Dhalla S, Garcia P, Singh VK, Pasricha PJ, Kalloo AN, Clarke JO. Comprehensive analysis of efficacy and safety of peroral endoscopic myotomy performed by a gastroenterologist in the endoscopy unit: a single-center experience. *Gastrointest Endosc* 2016; **83**: 117-125 [PMID: 26212369 DOI: 10.1016/j.gie.2015.06.013]
6 **Rodríguez de Santiago E**, Shimamura Y, Pioche M, Eleftheriadis N, Albéniz E, Bechara R, Yan Chiu PW, Guarner-Argente C, Herreros de Tejada A, Uchima H, Fujiyoshi Y, Ponchon T, González-Gete G, Hew S, Murzi-Pulgar M, Matallana V, Parejo-Carbonell S, Estremera-Arévalo F, Moll F, Onimaru M, Inoue H. Safety and effectiveness of peroral endoscopic myotomy in patients on antiplatelet or anticoagulant therapy: an international multicenter case-control study. *Gastrointest Endosc* 2021; **93**: 839-849 [PMID: 32717366 DOI: 10.1016/j.gie.2020.07.030]
7 **Von Renteln D**, Fuchs KH, Fockens P, Bauerfeind P, Vassiliou MC, Werner YB, Fried G, Breithaupt W, Heinrich H, Bredenoord AJ, Kersten JF, Verlaan T, Trevisonno M, Rösch T. Peroral endoscopic myotomy for the treatment of achalasia: an international prospective multicenter study. *Gastroenterology* 2013; **145**: 309-11.e1 [PMID: 23665071 DOI: 10.1053/j.gastro.2013.04.057]
8 **Li QL**, Yao LQ, Xu XY, Zhu JY, Xu MD, Zhang YQ, Chen WF, Zhou PH. Repeat peroral endoscopic myotomy: a

salvage option for persistent/recurrent symptoms. *Endoscopy* 2016; **48**: 134-140 [PMID: 26349067 DOI: 10.1055/s-0034-1393095]

9 **Ichkhanian Y**, Assis D, Familiari P, Ujiki M, Su B, Khan SR, Pioche M, Draganov PV, Cho JY, Eleftheriadis N, Barret M, Haji A, Velanovich V, Tantau M, Marks JM, Bapaye A, Sedarat A, Albeniz E, Bechara R, Kumta NA, Costamagna G, Perbtani YB, Patel M, Sippey M, Korrapati SK, Jain R, Estremera F, El Zein MH, Brewer Gutierrez OI, Khashab MA. Management of patients after failed peroral endoscopic myotomy: a multicenter study. *Endoscopy* 2021; **53**: 1003-1010 [PMID: 33197943 DOI: 10.1055/a-1312-0496]

10 **Li Y**, LingHu E, Ding H, Zhang X, Li M, Xiong Y, Wang X. Peroral endoscopic myotomy with simultaneous submucosal and muscle dissection for achalasia with severe interlayer adhesions. *Gastrointest Endosc* 2016; **83**: 651-652 [PMID: 26432944 DOI: 10.1016/j.gie.2015.09.030]

11 **Eckardt VF**, Aignherr C, Bernhard G. Predictors of outcome in patients with achalasia treated by pneumatic dilation. *Gastroenterology* 1992; **103**: 1732-1738 [PMID: 1451966 DOI: 10.1016/0016-5085(92)91428-7]

12 **Zhang WG**, Linghu EQ, Chai NL, Li HK. Ling classification describes endoscopic progressive process of achalasia and successful peroral endoscopy myotomy prevents endoscopic progression of achalasia. *World J Gastroenterol* 2017; **23**: 3309-3314 [PMID: 28566891 DOI: 10.3748/wjg.v23.i18.3309]

13 **Feng J**, Chai N, Zhang W, Li L, Tang X, Zou J, Ye L, Linghu E. Long-term outcomes of peroral endoscopic myotomy with simultaneous submucosal and muscle dissection (POEM-SSMD) for achalasia with severe interlayer adhesions. *Chin Med J (Engl)* 2022; **135**: 724-726 [PMID: 35239285 DOI: 10.1097/CM9.0000000000001971]

14 **Li HK**, Linghu EQ. New endoscopic classification of achalasia for selection of candidates for peroral endoscopic myotomy. *World J Gastroenterol* 2013; **19**: 556-560 [PMID: 23382636 DOI: 10.3748/wjg.v19.i4.556]

15 **Werner YB**, Hakanson B, Martinek J, Repici A, von Rahden BHA, Bredenoord AJ, Bisschops R, Messmann H, Vollberg MC, Noder T, Kersten JF, Mann O, Izbicki J, Pazdro A, Fumagalli U, Rosati R, Germer CT, Schijven MP, Emmermann A, von Renteln D, Fockens P, Boeckxstaens G, Rösch T. Endoscopic or Surgical Myotomy in Patients with Idiopathic Achalasia. *N Engl J Med* 2019; **381**: 2219-2229 [PMID: 31800987 DOI: 10.1056/NEJMoa1905380]

16 **NOSCAR POEM White Paper Committee**, Stavropoulos SN, Desilets DJ, Fuchs KH, Gostout CJ, Haber G, Inoue H, Kochman ML, Modayil R, Savides T, Scott DJ, Swanstrom LL, Vassiliou MC. Per-oral endoscopic myotomy white paper summary. *Gastrointest Endosc* 2014; **80**: 1-15 [PMID: 24950639 DOI: 10.1016/j.gie.2014.04.014]

17 **Tyberg A**, Sharaiha RZ, Familiari P, Costamagna G, Casas F, Kumta NA, Barret M, Desai AP, Schnoll-Sussman F, Saxena P, Martínez G, Zamarripa F, Gaidhane M, Bertani H, Draganov PV, Balassone V, Sharata A, Reavis K, Swanstrom L, Invernizzi M, Seewald S, Minami H, Inoue H, Kahaleh M. Peroral endoscopic myotomy as salvation technique post-Heller: International experience. *Dig Endosc* 2018; **30**: 52-56 [PMID: 28691186 DOI: 10.1111/den.12918]

18 **Onimaru M**, Inoue H, Ikeda H, Yoshida A, Santi EG, Sato H, Ito H, Maselli R, Kudo SE. Peroral endoscopic myotomy is a viable option for failed surgical esophagocardiomyotomy instead of redo surgical Heller myotomy: a single center prospective study. *J Am Coll Surg* 2013; **217**: 598-605 [PMID: 23891071 DOI: 10.1016/j.jamcollsurg.2013.05.025]

19 **Tyberg A**, Seewald S, Sharaiha RZ, Martinez G, Desai AP, Kumta NA, Lambroza A, Sethi A, Reavis KM, DeRoche K, Gaidhane M, Talbot M, Saxena P, Zamarripa F, Barret M, Eleftheriadis N, Balassone V, Inoue H, Kahaleh M. A multicenter international registry of redo per-oral endoscopic myotomy (POEM) after failed POEM. *Gastrointest Endosc* 2017; **85**: 1208-1211 [PMID: 27756611 DOI: 10.1016/j.gie.2016.10.015]

20 **Feng X**, Linghu E, Chai N, Ding H. New endoscopic classification of esophageal mucosa in achalasia: A predictor for submucosal fibrosis. *Saudi J Gastroenterol* 2018; **24**: 122-128 [PMID: 29637920 DOI: 10.4103/sjg.SJG_459_17]

21 **Mittal C**, Wagh MS. Technical Advances in Per-Oral Endoscopic Myotomy (POEM). *Am J Gastroenterol* 2017; **112**: 1627-1631 [PMID: 29016561 DOI: 10.1038/ajg.2017.369]

22 **Liu X**, Yao L, Cheng J, Xu M, Chen S, Zhong Y, He M, Chen W, Zhang Y, Qin W, Hu J, Cai M, Zhou P, Li Q. Landscape of Adverse Events Related to Peroral Endoscopic Myotomy in 3135 Patients and a Risk-Scoring System to Predict Major Adverse Events. *Clin Gastroenterol Hepatol* 2021; **19**: 1959-1966.e3 [PMID: 33905769 DOI: 10.1016/j.cgh.2021.04.033]

23 **Gupta S**, Sidhu M, Banh X, Bradbear J, Byth K, Hourigan LF, Raftopoulos S, Bourke MJ. A prospective multicentre study of per-oral endoscopic myotomy (POEM) for achalasia in Australia. *Med J Aust* 2021; **214**: 173-178 [PMID: 33611796 DOI: 10.5694/mja2.50941]

Published by **Baishideng Publishing Group Inc**
7041 Koll Center Parkway, Suite 160, Pleasanton, CA 94566, USA
Telephone: +1-925-3991568
E-mail: bpgoffice@wjgnet.com
Help Desk: https://www.f6publishing.com/helpdesk
https://www.wjgnet.com